



NDOR Sponsoring Agency Contract No. DPU-STWD (94)

EVALUATION OF ENERGY ABSORBERS FOR USE IN A ROADSIDE/MEDIAN BARRIER

Submitted by

Jennifer D. Schmidt, Ph.D., P.E.
Post-Doctoral Research Associate

Tyler Schmidt
Undergraduate Research Assistant

Ronald K. Faller, Ph.D., P.E.,
Research Associate Professor
MwRSF Director

Dean L. Sicking, Ph.D., P.E.
Emeritus Professor

John D. Reid, Ph.D.
Professor

Karla A. Lechtenberg, M.S.M.E., E.I.T.
Research Associate Engineer

Robert W. Bielenberg, M.S.M.E., E.I.T.
Research Associate Engineer

Scott K. Rosenbaugh, M.S.C.E., E.I.T.
Research Associate Engineer

Jim C. Holloway, M.S.C.E., E.I.T.
Test Site Manager

MIDWEST ROADSIDE SAFETY FACILITY

Nebraska Transportation Center
University of Nebraska-Lincoln
130 Whittier Research Center
2200 Vine Street
Lincoln, Nebraska 68583-0853
(402) 472-0965

Submitted to

NEBRASKA DEPARTMENT OF ROADS
1500 Nebraska Highway 2
Lincoln, Nebraska 68502

**FEDERAL HIGHWAY
ADMINISTRATION**
Nebraska Division
100 Centennial Mall North Room 220
Lincoln, Nebraska 68508

MwRSF Research Report No. TRP-03-280-14

February 6, 2014

TECHNICAL REPORT DOCUMENTATION PAGE

1. Report No. TRP-03-280-14	2.	3. Recipient's Accession No.	
4. Title and Subtitle Evaluation of Energy Absorbers for Use in a Roadside/Median Barrier		5. Report Date February 6, 2014	
		6.	
7. Author(s) Schmidt, J.D., Schmidt, T., Faller, R.K., Sicking, D.L., Reid, J.D., Lechtenberg, K.A., Bielenberg, R.W., Rosenbaugh, S.K., and Holloway, J.C.		8. Performing Organization Report No. TRP-03-280-14	
9. Performing Organization Name and Address Midwest Roadside Safety Facility (MwRSF) Nebraska Transportation Center University of Nebraska-Lincoln 130 Whittier Research Center 2200 Vine Street Lincoln, Nebraska 68583-0853		10. Project/Task/Work Unit No.	
		11. Contract © or Grant (G) No. NDOR DPU-STWD (94)	
12. Sponsoring Organization Name and Address Nebraska Department of Roads 1500 Nebraska Highway 2 Lincoln, Nebraska 68502 Federal Highway Administration Nebraska Division 100 Centennial Mall North Room 220 Lincoln, Nebraska 68508		13. Type of Report and Period Covered Final Report: 2010 – 2014	
		14. Sponsoring Agency Code	
15. Supplementary Notes Prepared in cooperation with U.S. Department of Transportation, Federal Highway Administration.			
16. Abstract (Limit: 200 words) Several types of elastomeric energy absorbers were evaluated for use in a <i>Manual for Assessing Safety Hardware</i> (MASH) Test Level 4 (TL-4) energy-absorbing, urban roadside/median barrier. Twelve dynamic bogie tests were conducted on 60- and 80-durometer EPDM rubber cylinders. Five dynamic bogie tests were conducted on marine shear fenders. One dynamic test was conducted on a 27-ft (8.2-m) long installation of 2-in. (51-mm) thick EPDM rubber cylinders spaced at 8 ft (2.4 m) on center and attached to the front face of a 32-in. (813-mm) tall, concrete New Jersey-shaped barrier with a continuous 6-in. x 12-in. (152-mm x 305-mm) steel tubular front rail. One dynamic test was conducted on a 28-ft (8.5-m) long installation of 11 $\frac{5}{8}$ -in. (295-mm) tall marine shear fender posts spaced at 8 ft (2.4 m) on center with a 6 $\frac{3}{4}$ -in. (171-mm) tall, upper timber rail. Both barrier concepts showed promising results. Several static tests were conducted on the marine shear fenders at hot, cold, and room temperatures to evaluate its effect on energy-absorber behavior.			
17. Document Analysis/Descriptors Highway Safety, Crash Test, Roadside Appurtenances, Compliance Test, MASH, Energy-Absorbing Barrier, Elastomers, Rubber, and Restorable		18. Availability Statement No restrictions. Document available from: National Technical Information Services, Springfield, Virginia 22161	
19. Security Class (this report) Unclassified	20. Security Class (this page) Unclassified	21. No. of Pages 173	22. Price

DISCLAIMER STATEMENT

This report was completed with funding from the Federal Highway Administration, U.S. Department of Transportation. The contents of this report reflect the views and opinions of the authors who are responsible for the facts and the accuracy of the data presented herein. The contents do not necessarily reflect the official views or policies of the Nebraska Department of Roads nor the Federal Highway Administration, U.S. Department of Transportation. This report does not constitute a standard, specification, regulation, product endorsement, or an endorsement of manufacturers.

UNCERTAINTY OF MEASUREMENT STATEMENT

The Midwest Roadside Safety Facility (MwRSF) has determined the uncertainty of measurements for several parameters involved in standard full-scale crash testing and non-standard testing of roadside safety features. Information regarding the uncertainty of measurements for critical parameters is available upon request by the sponsor and the Federal Highway Administration. Test nos. EPDM-1 through EPDM-12, HSF14-1 through HSF14-5 SFHC-1, and SFHT-1 were non-compliant component tests that were conducted for research and development purposes only.

ACKNOWLEDGEMENTS

The authors wish to acknowledge several sources that made a contribution to this project:

(1) the Federal Highway Administration and the Nebraska Department of Roads for sponsoring this project; (2) Maritime International, Inc. for donating marine shear fenders for dynamic testing; and (3) MwRSF personnel for constructing the systems and conducting the component tests.

Acknowledgement is also given to the following individuals who made a contribution to the completion of this research project.

Midwest Roadside Safety Facility

A.T. Russell, B.S.B.A., Shop Manager
K.L. Krenk, B.S.M.A., Maintenance Mechanic
S.M. Tighe, Laboratory Mechanic
D.S. Charroin, Laboratory Mechanic
C.S. Stolle, Ph.D., Post-Doctoral Research Associate
Undergraduate and Graduate Research Assistants

Nebraska Department of Roads

Phil TenHulzen, P.E., Design Standards Engineer
Jodi Gibson, Research Coordinator

Federal Highway Administration

John Perry, P.E., Nebraska Division Office
Danny Briggs, Nebraska Division Office

TABLE OF CONTENTS

TECHNICAL REPORT DOCUMENTATION PAGE	i
DISCLAIMER STATEMENT	ii
UNCERTAINTY OF MEASUREMENT STATEMENT	ii
ACKNOWLEDGEMENTS	iii
TABLE OF CONTENTS	iv
LIST OF FIGURES	vi
LIST OF TABLES	ix
1 INTRODUCTION	1
1.1 Problem Statement	1
1.2 Objectives	1
1.3 Scope	1
2 DYNAMIC COMPONENT TESTING CONDITIONS	3
2.1 Equipment and Instrumentation	3
2.1.1 Bogie Vehicle	3
2.1.2 Accelerometers	6
2.1.3 Pressure Tape Switches	8
2.1.4 Optical Speed Trap	8
2.1.5 Digital Cameras	9
2.2 Data Processing	10
2.3 Results	10
3 CYLINDER COMPONENT TESTING	12
3.1 Purpose	12
3.2 Scope	12
3.3 Results	22
3.3.1 Test No. EPDM-1	22
3.3.2 Test No. EPDM-2	24
3.3.3 Test No. EPDM-3	26
3.3.4 Repeatability Test Nos. EPDM-4 through EPDM-12	28
3.4 Discussion	32
4 SHEAR FENDER COMPONENT TESTING	36
4.1 Purpose	36
4.2 Scope	36
4.3 Results	49
4.3.1 Test No. HSF14-1	49
4.3.2 Test No. HSF14-2	52
4.3.3 Test No. HSF14-3	54
4.3.4 Test No. HSF14-4	56

4.3.5 Test No. HSF14-5	59
4.4 Discussion	63
5 RUBBER-CYLINDER RETROFIT SYSTEM - COMPONENT TESTING	70
5.1 Purpose.....	70
5.2 Scope.....	70
5.3 Results.....	80
5.4 Discussion	84
6 SHEAR FENDER POST AND BEAM SYSTEM - COMPONENT TESTING	87
6.1 Purpose.....	87
6.2 Scope.....	87
6.3 Results.....	99
6.4 Discussion	106
7 SHEAR FENDER STATIC LOAD TESTING	109
7.1 Purpose.....	109
7.2 Scope.....	109
7.3 Results.....	113
7.3.1 Test Nos. SFHS-1 through SFHS-3	113
7.3.2 Test No. SFHS-4.....	118
7.3.3 Test Nos. SFHS-5 and SFHS-6.....	120
7.3.4 Test No. SFHS-7	121
7.3.5 Test Nos. SFHS-8 and SFHS-9.....	123
7.3.6 Test No. SFHS-10.....	127
7.4 Discussion	129
8 SUMMARY, CONCLUSIONS, AND RECOMMENDATIONS.....	130
8.1 Rubber Cylinders	130
8.2 Rubber Shear Fenders	132
9 REFERENCES	135
10 APPENDICES	136
Appendix A. Bogie Test Results	137
Appendix B. Material Specifications	166

LIST OF FIGURES

Figure 1. Rigid-Frame Bogie on Guidance Track, Test Nos. EPDM-1 through EPDM-12	4
Figure 2. Rigid-Frame Bogie on Guidance Track, Test Nos. HSF14-1 through HSF14-4	4
Figure 3. Rigid-Frame Bogie on Guidance Track, Test No. HSF14-5	5
Figure 4. Rigid-Frame Bogie on Guidance Track, Test Nos. SFHC-1 and SFHT-1	5
Figure 5. EPDM Rubber Cylinders 1A, 2A, and 3A	13
Figure 6. Bogie Testing Matrix and Setup, Test Nos. EPDM-1 through EPDM-3	14
Figure 7. Plywood Attachment Details, Test Nos. EPDM-1 through EPDM-3	15
Figure 8. Rubber Cylinder Details, Test Nos. EPDM-1 through EPDM-3	16
Figure 9. Impact Head Details, Test Nos. EPDM-1 through EPDM-3	17
Figure 10. Bogie Testing Matrix and Setup, Test Nos. EPDM-4 through EPDM-12	18
Figure 11. Plywood Attachment Details, Test Nos. EPDM-4 through EPDM-12	19
Figure 12. Rubber Cylinder Details, Test Nos. EPDM-4 through EPDM-12	20
Figure 13. Impact Head Details, Test Nos. EPDM-4 through EPDM-12	21
Figure 14. Force vs. Deflection and Energy vs. Deflection, Test No. EPDM-1	22
Figure 15. Time-Sequential Photographs, Test No. EPDM-1	23
Figure 16. Force vs. Deflection and Energy vs. Deflection, Test No. EPDM-2	24
Figure 17. Time-Sequential Photographs, Test No. EPDM-2	25
Figure 18. Force vs. Deflection and Energy vs. Deflection, Test No. EPDM-3	26
Figure 19. Time-Sequential Photographs, Test No. EPDM-3	27
Figure 20. Force vs. Deflection of 9 $\frac{5}{8}$ x 1x10 in. (244x25x254 mm) Cylinders, Test Nos. EPDM-3 through EPDM-12	29
Figure 21. Energy vs. Deflection of 9 $\frac{5}{8}$ x 1x10 in. (244x25x254 mm) Cylinders, Test Nos. EPDM-3 through EPDM-12	30
Figure 22. Energy vs. Velocity, Test Nos. EPDM-3 through EPDM-12	31
Figure 23. Peak Force vs. Deflection, Test Nos. EPDM-3 through EPDM-12	31
Figure 24. Force vs. Deflection of EPDM Cylinders, Test Nos. EPDM-1 through EPDM-3	34
Figure 25. Energy vs. Deflection of EPDM Cylinders, Test Nos. EPDM-1 through EPDM- 3	35
Figure 26. Maritime International, Inc. HSF-14 Marine Shear Fender	36
Figure 27. Bogie Testing Setup – Perpendicular to Hole, Test No. HSF14-1	38
Figure 28. Bogie Testing Setup – Parallel to Hole, Test No. HSF14-2	39
Figure 29. Bogie Testing Setup – Parallel to Hole, Test No. HSF14-3	40
Figure 30. Bogie Testing Setup – Parallel to Hole, Test Nos. HSF14-4	41
Figure 31. Bogie Testing Setup – Parallel to Hole, Test Nos. HSF14-5	42
Figure 32. System Detail Views, Test Nos. HSF14-1 through HSF14-5	43
Figure 33. Impact Assembly Details, Test Nos. HSF14-1 through HSF14-5	44
Figure 34. Shear Fender Details, Test Nos. HSF14-1 through HSF14-5	45
Figure 35. Impact Assembly Components, Test Nos. HSF14-1 through HSF14-5	46
Figure 36. Bill of Materials, Test Nos. HSF14-1 through HSF14-5	47
Figure 37. Bogie Setup, Test No. HSF14-1	48
Figure 38. Bogie Setup, Test Nos. HSF14-2 through HSF14-4	48
Figure 39. Bogie Setup Photograph, Test No. HSF14-5	49
Figure 40. Force vs. Deflection and Energy vs. Deflection, Test No. HSF14-1	50
Figure 41. Time-Sequential Photographs, Test No. HSF14-1	51
Figure 42. Force vs. Deflection and Energy vs. Deflection, Test No. HSF14-2	52
Figure 43. Time-Sequential Photographs, Test No. HSF14-2	53

Figure 44. Force vs. Deflection and Energy vs. Deflection, Test No. HSF14-3	54
Figure 45. Time-Sequential Photographs, Test No. HSF14-3	55
Figure 46. Force vs. Deflection and Energy vs. Deflection, Test No. HSF14-4	57
Figure 47. Time-Sequential Photographs, Test No. HSF14-4	58
Figure 48. Force vs. Deflection and Energy vs. Deflection, Test No. HSF14-5	60
Figure 49. Time-Sequential Photographs, Test No. HSF14-5	61
Figure 50. Post-Impact Damage, Test No. HSF14-5	62
Figure 51. Force vs. Deflection, Test nos. HSF14-1 and HSF14-2	66
Figure 52. Energy vs. Deflection, Test Nos. HSF14-1 and HSF14-2	67
Figure 53. Force vs. Deflection, Test nos. HSF14-2 through HSF14-5	68
Figure 54. Energy vs. Deflection, Test nos. HSF14-2 through HSF14-5	69
Figure 55. Bogie Testing Matrix and Setup, Test No. SFHC-1	71
Figure 56. System Details, Test No. SFHC-1	72
Figure 57. System Detail View, Test No. SFHC-1	73
Figure 58. Rail Section Weld Details, Test No. SFHC-1	74
Figure 59. Rail Component Details, Test No. SFHC-1	75
Figure 60. Cylinder and Splice Components, Test No. SFHC-1	76
Figure 61. Wooden Shim Details, Test No. SFHC-1	77
Figure 62. Bill of Materials, Test No. SFHC-1	78
Figure 63. Bogie Test Setup, Test No. SFHC-1	79
Figure 64. Force vs. Deflection and Energy vs. Deflection, Test No. SFHC-1	80
Figure 65. Time-Sequential Photographs, Test No. SFHC-1	81
Figure 66. Cylinders Post-Impact Damage, Test No. SFHC-1	82
Figure 67. Post-Impact Damage, Test No. SFHC-1	83
Figure 68. Force vs. Deflection – 2-in. (51-mm) Thick Rubber Cylinder	85
Figure 69. Energy vs. Deflection – 2-in. (51-mm) Thick Rubber Cylinder	86
Figure 70. Bogie Testing Matrix and System Layout, Test No. SFHT-1	88
Figure 71. System Details, Test No. SFHT-1	89
Figure 72. System Detail Views, Test No. SFHT-1	90
Figure 73. Shear Fender Details, Test No. SFHT-1	91
Figure 74. Rail Details, Test No. SFHT-1	92
Figure 75. Splice Component Details, Test No. SFHT-1	93
Figure 76. Splice Details, Test No. SFHT-1	94
Figure 77. L-Bracket Details, Test No. SFHT-1	95
Figure 78. L-Bracket and Threaded Rod Details, Test No. SFHT-1	96
Figure 79. Bill of Materials, Test No. SFHT-1	97
Figure 80. Bogie Test Setup, Test No. SFHT-1	98
Figure 81. Force vs. Deflection and Energy vs. Deflection, Test No. SFHT-1	100
Figure 82. Time-Sequential Photographs, Test No. SFHT-1	101
Figure 83. Time-Sequential Photographs, Test No. SFHT-1	102
Figure 84. Time-Sequential Photographs, Test No. SFHT-1	103
Figure 85. Time-Sequential Photographs, Test No. SFHT-1	104
Figure 86. Post-Impact Damage, Test No. SFHT-1	105
Figure 87. Static and Dynamic Energy vs. Deflection – 14-in. (356-mm) Wide Shear Fender	107
Figure 88. Static Force and Energy vs. Deflection – 10-in. (254-mm) Wide Shear Fender	108
Figure 89. Test Setup, Test Nos. SFHS-5 and SFHS-6	111
Figure 90. Component Details, Test Nos. SFHS-5 and SFHS-6	112

Figure 91. Testing Apparatus, Test Nos. SFHS-1 through SFHS-3	114
Figure 92. Example of System Instabilities, Test Nos. SFHS-1 through SFHS-3.....	116
Figure 93. Load vs. Deflection at Subfreezing, Room, and Hot Temperatures.....	117
Figure 94. Test Setup, Test No. SFHS-4	118
Figure 95. System Instabilities, Test No. SFHS-4.....	119
Figure 96. Test Setup, Test No. SFHS-7	122
Figure 97. System Deflection at 7,000-lb (3,175-kg) Load, Test No. SFHS-7	123
Figure 98. Test Setup, Test No. SFHS-8	125
Figure 99. Test Setup, Test No. SFHS-9	126
Figure 100. Test Setup, Test No. SFHS-10	127
Figure 101. System Deflection at 4,994-lb (2,265-kg) Load, Test No. SFHS-10	128
Figure A-1. Results of Test No. EPDM-1 (DTS)	138
Figure A-2. Results of Test No. EPDM-1 (EDR-3).....	139
Figure A-3. Results of Test No. EPDM-2 (DTS)	140
Figure A-4. Results of Test No. EPDM-2 (EDR-3).....	141
Figure A-5. Results of Test No. EPDM-3 (DTS)	142
Figure A-6. Results of Test No. EPDM-3 (EDR-3).....	143
Figure A-7. Results of Test No. EPDM-4 (EDR-3).....	144
Figure A-8. Results of Test No. EPDM-5 (EDR-3).....	145
Figure A-9. Results of Test No. EPDM-6 (EDR-3).....	146
Figure A-10. Results of Test No. EPDM-7 (EDR-3).....	147
Figure A-11. Results of Test No. EPDM-8 (EDR-3).....	148
Figure A-12. Results of Test No. EPDM-9 (EDR-3).....	149
Figure A-13. Results of Test No. EPDM-10 (EDR-3).....	150
Figure A-14. Results of Test No. EPDM-11 (EDR-3).....	151
Figure A-15. Results of Test No. EPDM-12 (EDR-3).....	152
Figure A-16. Results of Test No. HSF14-1 (DTS)	153
Figure A-17. Results of Test No. HSF14-1 (EDR-3)	154
Figure A-18. Results of Test No. HSF14-2 (DTS)	155
Figure A-19. Results of Test No. HSF14-2 (EDR-3)	156
Figure A-20. Results of Test No. HSF14-3 (DTS)	157
Figure A-21. Results of Test No. HSF14-4 (DTS)	158
Figure A-22. Results of Test No. HSF14-4 (EDR-3)	159
Figure A-23. Results of Test No. HSF14-5 (DTS)	160
Figure A-24. Results of Test No. HSF14-5 (EDR-3)	161
Figure A-25. Results of Test No. SFHC-1 (SLICE 6DX)	162
Figure A-26. Results of Test No. SFHC-1 (EDR-3).....	163
Figure A-27. Results of Test No. SFHT-1 (SLICE 6DX)	164
Figure A-28. Results of Test No. SFHT-1 (EDR-3).....	165
Figure B-1. 80-durometer EPDM Rubber Cylinders.....	167
Figure B-2. 80-durometer EPDM Rubber Cylinders.....	168
Figure B-3. 60-durometer EPDM Rubber Cylinders.....	169
Figure B-4. 60-durometer EPDM Rubber Cylinders.....	170
Figure B-5. 14-in. (356-mm) Wide Shear Fender.....	171
Figure B-6. 10-in. (254-mm) Wide Shear Fender.....	172

LIST OF TABLES

Table 1. Bogie Weight for Dynamic Component Tests.....	3
Table 2. Accelerometers for Dynamic Component Tests.....	6
Table 3. Video Cameras and Locations in Dynamic Component Tests	9
Table 4. Rubber Cylinders for EPDM Test Series.....	13
Table 5. Repeatability Dynamic Test Results, Test Nos. EPDM-3 through EPDM-12	32
Table 6. Dynamic Test Results, Test Nos. EPDM-1 through EPDM-12	33
Table 7. Dynamic Testing Results	63
Table 8. Cylinder Deflection and Energy, Test No. SFHC-1	86
Table 9. Cylinder Deflection and Energy Absorption, Test No. SFHT-1	108
Table 10. Static Shear Fender Testing Summary.....	110
Table 11. Static Shear Fender Testing Results	113
Table 12. Shear Fender Loads and Deflections at Subfreezing Temperature, Test No. SFHS-1	115
Table 13. Shear Fender Loads and Deflections at Room Temperature, Test No. SFHS-2	115
Table 14. Shear Fender Loads and Deflections at Hot Temperature, Test No. SFHS-3	116
Table 15. Test No. SFHS-5 Results	120
Table 16. Test No. SFHS-6 Results	121
Table 17. Test No. SFHS-7 Results	122
Table 18. Test No. SFHS-9 Results	124
Table 19. Test No. SFHS-10 Results	128

1 INTRODUCTION

1.1 Problem Statement

There exists a need for an energy-absorbing roadside/median barrier that lowers passenger vehicle accelerations but still has the capacity to contain high-energy impacts with large trucks. Several types of energy absorbers were analyzed for use in a new energy-absorbing roadside/median barrier by Schmidt, et al., and several rubber energy absorbers were selected for dynamic and static component testing [1]. Schmidt, et al. estimated that each energy absorber should dissipate approximately 52.8 k-in. to 211.2 k-in. (6.0 kJ to 23.9 kJ) of kinetic energy, depending on a spacing from 5 ft to 20 ft (1.5 m to 6.1 m), in a new roadside/median barrier for a 30 percent reduction in lateral acceleration as compared to a rigid concrete barrier subjected to a 2270P impact event [1]. The energy absorbers used in the new barrier need to have acceptable deflection limits, be restorable and reusable, have the capacity to contain an American Association of State Highway and Transportation Officials (AASHTO) *Manual for Assessing Safety Hardware* (MASH) TL-4 impact event [2] and sufficiently reduce passenger vehicle accelerations.

1.2 Objectives

The dynamic properties for each energy absorber, including energy, force, and deflection were determined. The change in rubber behavior as a function of temperature was also examined. Barrier design concepts were also evaluated through dynamic testing.

1.3 Scope

The research objectives were achieved through the completion of several tasks. First, component tests were used to determine the dynamic properties of rubber energy absorbers. Twelve dynamic bogie tests were conducted on 10-in. (254-mm) long, axially-loaded, EPDM rubber cylinders. Five dynamic bogie tests were conducted on a 14-in. wide x 16-in. tall x 22-in.

long (356-mm x 406-mm x 559-mm) rubber marine shear fender. One dynamic bogie test was conducted on a 27-ft (8.2-m) long installation of rubber cylinders spaced at 8 ft (2.4 m) on center and attached to the front face of a New Jersey-shaped concrete barrier with a continuous steel tubular front rail. One dynamic bogie test was conducted on a 28-ft (8.5-m) long installation of marine shear fender posts spaced at 8 ft (2.4 m) on center with an upper timber rail.

Ten static compression tests were conducted on the rubber marine shear fenders to determine the rail weight that could be supported at cold, room, and hot temperatures. A relationship between temperature and deflection of the shear fenders was determined. Multiple shear fenders were gradually loaded in various configurations to find an optimal post spacing and beam weight. Finally, conclusions and recommendations were made regarding the viability of the rubber cylinders and shear fenders for use as energy absorbers in a roadside/median barrier.

2 DYNAMIC COMPONENT TESTING CONDITIONS

2.1 Equipment and Instrumentation

Numerous equipment and instrumentation were used to conduct the dynamic component tests reported herein. All dynamic tests were conducted at the MwRSF Proving Grounds in Lincoln, Nebraska. The equipment and instrumentation that was utilized to collect and record data during the dynamic bogie tests included a bogie vehicle, test jigs, accelerometers, pressure tape switches, optical speed system, high-speed and standard-speed digital video, and still cameras.

2.1.1 Bogie Vehicle

Two rigid-frame bogies were used to impact the elastomeric components and simple barrier systems. A variable-height, detachable impact head was used during the dynamic component testing. The fabricated bogie head was constructed of six 6-in. (152-mm) wide x 8-in. (203-mm) deep x 34-in. (864-mm) long timbers covered with plywood. In test no. HSF14-5, an additional 6-in. (152-mm) x 8-in. (203-mm) timber beam was attached horizontally to the impact head. The impact head was bolted to the bogie vehicle, thus creating a large impact face. The bogie weights, including the mountable impact head and accelerometers, are shown in Table 1. The bogie vehicles used in each of the tests are shown in Figures 1 through 4.

Table 1. Bogie Weight for Dynamic Component Tests

Test Nos.	Weight lb (kg)
EPDM-1 through EPDM-3	1,686 (765)
EPDM-4 through EPDM-12	1,689 (766)
HSF14-1 through HSF14-4	1,818 (825)
HSF14-5	4,946 (2,243)
SFHC-1	4,876 (2,212)
SFHT-1	4,871 (2,209)



Figure 1. Rigid-Frame Bogie on Guidance Track, Test Nos. EPDM-1 through EPDM-12



Figure 2. Rigid-Frame Bogie on Guidance Track, Test Nos. HSF14-1 through HSF14-4



Figure 3. Rigid-Frame Bogie on Guidance Track, Test No. HSF14-5

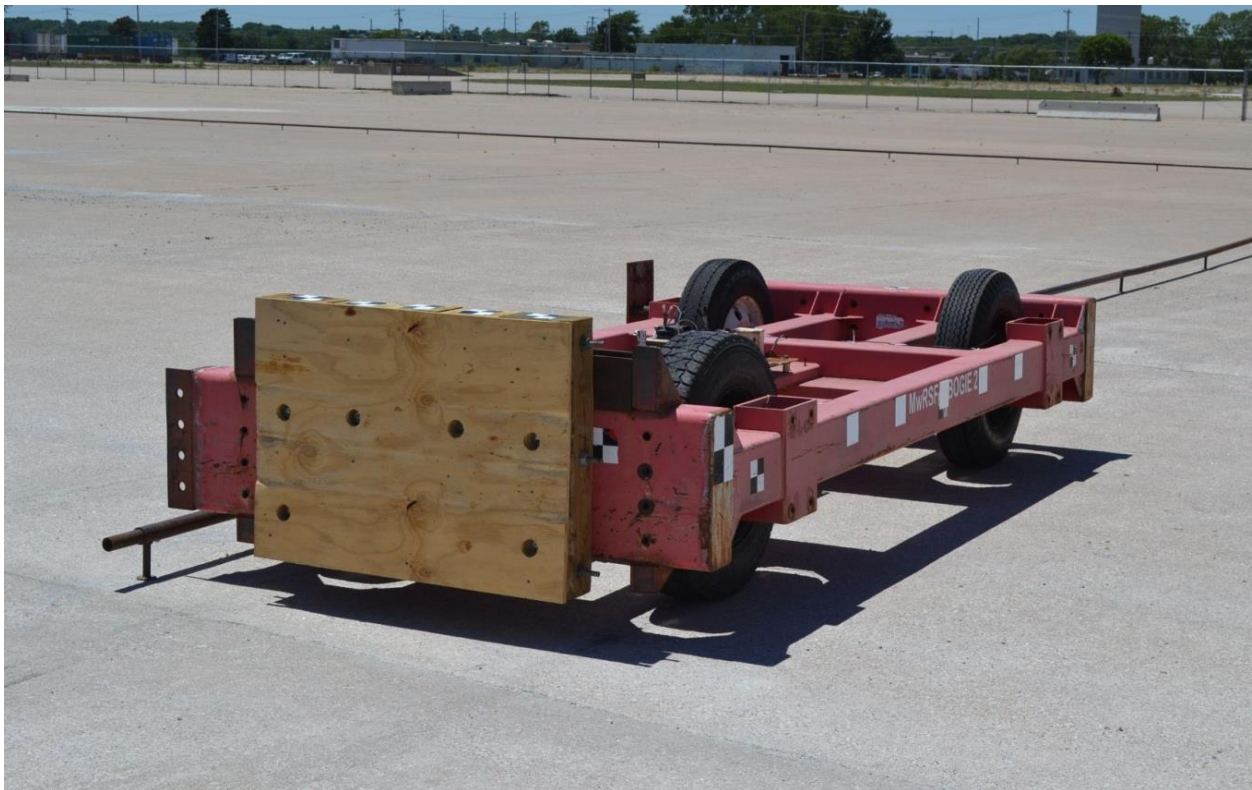


Figure 4. Rigid-Frame Bogie on Guidance Track, Test Nos. SFHC-1 and SFHT-1

A steel corrugated-beam guardrail was used to guide the tires of the bogie vehicle for test nos. EPDM-1 through EPDM-12 and test no. HSF14-5, as shown in Figures 1 and 3. A steel-pipe guidance track was used to guide the bogie vehicle for test nos. HSF14-1 through HSF14-4, SFHC-1, and SFHT-1, as shown in Figures 2 and 4.

A pickup truck was used to push the bogie vehicle to the required impact velocity for test nos. EPDM-1 through EPDM-12 and HSF14-1 through HSF14-4. After reaching the target velocity, the push vehicle braked, allowing the bogie to be free rolling as it came off the track.

A pickup truck with a reverse cable tow system was used to propel the bogie for test nos. HSF14-5, SFHC-1, and SFHT-1. When the bogie approached the end of the guidance system, it was released from the tow cable, allowing it to be free rolling when it impacted the system. A remote braking system was installed on the bogie allowing it to be brought safely to rest after the test.

2.1.2 Accelerometers

Various accelerometer systems were mounted on the bogie vehicle near its center of gravity to measure the acceleration in the longitudinal, lateral, and vertical directions. However, only the longitudinal acceleration was processed and reported. The accelerometer systems used in each test are shown in Table 2.

Table 2. Accelerometers for Dynamic Component Tests

Test Nos.	DTS	SLICE 6DX	EDR-3
EPDM-1 through EPDM-3	X	*	X
EPDM-4 through EPDM-12	*	*	X
HSF14-1 through HSF14-5	X	*	X
SFHC-1	*	X	X
SFHT-1	*	X	X

Note: X – accelerometer system used
* – accelerometer system not used

One accelerometer system, the DTS, was a two-arm piezoresistive accelerometer system manufactured by Endevco of San Juan Capistrano, California. Three accelerometers were used to measure each of the longitudinal, lateral, and vertical accelerations independently at a sample rate of 10,000 Hz. The accelerometers were configured and controlled using a system developed and manufactured by Diversified Technical Systems, Inc. (DTS) of Seal Beach, California. More specifically, data was collected using a DTS Sensor Input Module (SIM), Model TDAS3-SIM-16M. The SIM was configured with 16 MB SRAM and 8 sensor input channels with 250 kB SRAM/channel. The SIM was mounted on a TDAS3-R4 module rack. The module rack was configured with isolated power/event/communications, 10BaseT Ethernet and RS232 communication, and an internal backup battery. Both the SIM and module rack were crashworthy. The “DTS TDAS Control” computer software program and a customized Microsoft Excel worksheet were used to analyze and plot the accelerometer data.

A second system, SLICE 6DX, was a modular data acquisition system manufactured by DTS of Seal Beach, California. The acceleration sensors were mounted inside the body of the custom-built SLICE 6DX event data recorder and recorded data at 10,000 Hz to the onboard microprocessor. The SLICE 6DX was configured with 7 GB of non-volatile flash memory, a range of ± 500 g's, a sample rate of 10,000 Hz, and a 1,650 Hz (CFC 1000) anti-aliasing filter. The “SLICEWare” computer software program and a customized Microsoft Excel worksheet were used to analyze and plot the accelerometer data.

A third system, Model EDR-3, was a triaxial piezoresistive accelerometer system manufactured by Instrumented Sensor Technology, Inc. (IST) of Okemos, Michigan. The EDR-3 was configured with 256 kB of RAM, a range of ± 200 g's, a sample rate of 3,200 Hz, and a 1,120 Hz low-pass filter. The “DynaMax 1 (DM-1)” computer software program and a

customized Microsoft Excel worksheet were used to analyze and plot the accelerometer data. This system did not collect any data for test no. HSF14-3.

2.1.3 Pressure Tape Switches

Three pressure tape switches, spaced at approximately 39³/₈-in. (1-m) intervals and placed near the end of the bogie track, were used to determine the speed of the bogie before impact in test nos. EPDM-1 through EPDM-12 and HSF14-1 through HSF14-5. As the front tire of the bogie passed over each tape switch, a strobe light was fired, sending an electronic timing signal to the data acquisition system. The system recorded the impulses and the time at which each occurred. The speed was then calculated using the spacing between the sensors and the time between the impulses. Strobe lights and high-speed video analysis are used only as a backup in the event that vehicle speeds cannot be determined from the electronic data.

2.1.4 Optical Speed Trap

The retro-reflective optical speed trap was used to determine the speed of the bogie vehicle before impact in test nos. HSF14-1 through HSF14-5, SFHC-1, and SFHT-1. Three retro-reflective targets, spaced at approximately 4-in. (102-mm) intervals, were applied to the side of the bogie vehicle which break the beam of light. When the emitted beam of light was returned to the emitter/receiver, a signal was sent to the optical control box, which in turn sent an impulse to the data computer as well as activated the External LED box. The computer recorded the impulses and the time at which each occurred. The speed was then calculated using the spacing between the retro-reflective targets and the time between the impulses. LED lights and high-speed digital video analysis are only used as a backup in the event that vehicle speeds cannot be determined from the electronic data.

2.1.5 Digital Cameras

At least one AOS high-speed digital video camera and one JVC digital video camera were used to document all dynamic component tests. The AOS high-speed cameras had a frame rate of 500 frames per second and the JVC digital video cameras had a frame rate of 29.97 frames per second. The cameras were placed either overhead or laterally from the energy absorber, with a view perpendicular to the bogie's direction of travel. The cameras used for all component tests are shown in Table 2. A Nikon D50 digital still camera was also used to document pre-test and post-test conditions for all tests.

Table 3. Video Cameras and Locations in Dynamic Component Tests

Test No.	Digital Video Cameras	
	Description	Location
EPDM-1 through EPDM-3	AOS X-PRI	Lateral – Left Side of Bogie
	JVC	Lateral – Left Side of Bogie
	JVC	Lateral – Right Side of Bogie
EPDM-4 through EPDM-12	AOS X-PRI ¹	Lateral – Left Side of Bogie
	JVC ²	Lateral – Left Side of Bogie
HSF14-1 through HSF14-4	AOS X-PRI	Lateral – Left Side of Bogie
	JVC	Lateral – Left Side of Bogie
	JVC	Lateral – Right Side of Bogie
HSF14-5	AOS X-PRI	Lateral – Left Side of Bogie
	AOS X-PRI	Lateral – Left Side of Bogie
	JVC	Lateral – Left Side of Bogie
	JVC	Lateral – Right Side of Bogie
SFHC-1	AOS X-PRI	Lateral – Left Side of Bogie
	AOS X-PRI	Lateral – Right Side of Bogie
	AOS X-PRI	Overhead
	JVC	Lateral – Left Side of Bogie
	JVC	Lateral – Right Side of Bogie
SFHT-1	AOS VITcam	Lateral – Left Side of Bogie
	AOS X-PRI	Lateral – Right Side of Bogie
	AOS X-PRI	Overhead
	JVC	Lateral – Left Side of Bogie
	JVC	Lateral – Right Side of Bogie
	JVC	Overhead

¹camera did not trigger in test no. EPDM-6

²camera did not trigger in test no. EPDM-12

2.2 Data Processing

The electronic accelerometer data obtained in dynamic testing was filtered using the SAE Class 60 Butterworth filter conforming to the SAE J211/1 specifications [3]. The pertinent acceleration signal was extracted from the bulk of the data signals. The processed acceleration data was then multiplied by the mass of the bogie to get the impact force using Newton's Second Law. Next, the acceleration trace was integrated to find the change in velocity versus time. Initial velocity of the bogie, calculated from the optical speed system or pressure tape switch data, was then used to determine the bogie velocity, and the calculated velocity trace was integrated to find the bogie's displacement. This displacement is also the deflection of the energy absorber in most cases. Due to the fact that the rubber rebounded during some tests and the bogie continued moving forward, the deflection from the acceleration trace may not accurately portray the deflection of the energy absorber.

2.3 Results

The information desired from the bogie tests was the force versus deflection behavior of the energy absorber. This data was then used to find total energy (the area under the force versus deflection curve) dissipated during each test.

Although the acceleration data was applied to the impact location, the data came from the center of gravity of the bogie. Error was added to the data; since, the bogie head was not perfectly rigid and sustained vibrations. The bogie may have also rotated during the impact event, thus causing differences in accelerations between the bogie center of mass and the bogie impact head. Since filtering procedures were applied to the data to smooth out vibrations, and the rotations of the bogie during the tests were minor, these issues were deemed minor, and the data was still valid.

Significant pitch angles did develop late in some tests as the bogie overrode the energy absorber. However, these motions occurred after the primary crush of the energy absorber. One useful aspect of using accelerometer data was that it included influences of the energy absorber inertia on the reaction force. This influence was important as the mass of the energy absorber would affect barrier performance as well as test results.

The accelerometer data for each test was processed in order to obtain acceleration, velocity, and deflection curves, as well as force vs. deflection and energy vs. deflection curves. The values described herein were calculated from the DTS or SLICE 6DX data curves when available, because they had a higher data acquisition frequency. The EDR-3 was the only accelerometer used for test nos. EPDM-4 through EPDM-12, so the values for these tests were calculated from the EDR-3 data curves. Test results for all transducers are provided in Appendix A.

3 CYLINDER COMPONENT TESTING

3.1 Purpose

Rubber cylinders have been used successfully in energy-absorbing applications, specifically in roadside safety hardware. One design concept included an axially-loaded rubber energy absorber that was compressed against a rigid concrete wall [1]. Rubber cylinders were chosen for testing and evaluation because they do not require a custom mold. The Ethylene Propylene Diene Monomer (EPDM) rubber has a service temperature that is well beyond extreme temperatures found in the United States, and EPDM has an excellent resistance to important environmental effects, such as oxidations, ozone, sunlight aging, heat aging, weather, and water [4]. EPDM rubber is a common elastomer and has been used in previous crash cushions.

Three different rubber cylinders were manufactured by Eutsler Technical Products, Inc. in Houston, TX. The cylinders were mandrel wrapped. Two 80-durometer, 8 $\frac{1}{8}$ -in. (206-mm) inner diameter, 2-in. (51-mm) thick, and 10-in. (254-mm) long EPDM rubber cylinders were designated 1A and 1B. Two 60-durometer, 8 $\frac{1}{8}$ -in. (206-mm) inner diameter, 2-in. (51-mm) thick, 10-in. (254-mm) long EPDM rubber cylinders were designated 2A and 2B. Two 80-durometer, 9 $\frac{5}{8}$ -in. (244-mm) inner diameter, 1-in. (25-mm) thick, 10-in. (254-mm) long EPDM rubber cylinders were designated 3A and 3B. A series of component tests were conducted to determine the dynamic properties of the cylinders for use in design as well as finite element simulation validation.

3.2 Scope

A total of 12 bogie tests were conducted on axially-loaded, EPDM rubber cylinders, as shown in Table 4. Test no. EPDM-1 was conducted on an 80 durometer, 2-in. (51-mm) thick cylinder. Test no. EPDM-2 was conducted on a 60 durometer, 2-in. (51-mm) thick cylinder. Test

nos. EPDM-3 through EPDM-12 were conducted on an 80 durometer, 1-in. (25-mm) thick cylinder with repeated impact events. The cylinders are shown in Figure 5. The target impact conditions were a speed of 5 mph (8 km/h) and an angle of 0 degrees, axially compressing the cylinders. The cylinders were impacted 22 in. (559 mm) above the groundline, such that the applied force was approximately aligned with the center of gravity (c.g.) height of the bogie. The test matrix and test setup are shown in Figures 6 through 9.

Table 4. Rubber Cylinders for EPDM Test Series

Test No.	Cylinder No.	Durometer	Thickness (T) in. (mm)	Inner Diameter (ID) in. (mm)	Outer Diameter (OD) in. (mm)	Length (L) in. (mm)
EPDM-1	1A	80	2 (51)	8 $\frac{1}{8}$ (206)	12 $\frac{1}{8}$ (308)	10 (254)
EPDM-2	2A	60	2 (51)	8 $\frac{1}{8}$ (206)	12 $\frac{1}{8}$ (308)	10 (254)
EPDM-3 through EPDM-12	3A	80	1 (25)	9 $\frac{5}{8}$ (244)	11 $\frac{5}{8}$ (295)	10 (254)



Figure 5. EPDM Rubber Cylinders 1A, 2A, and 3A

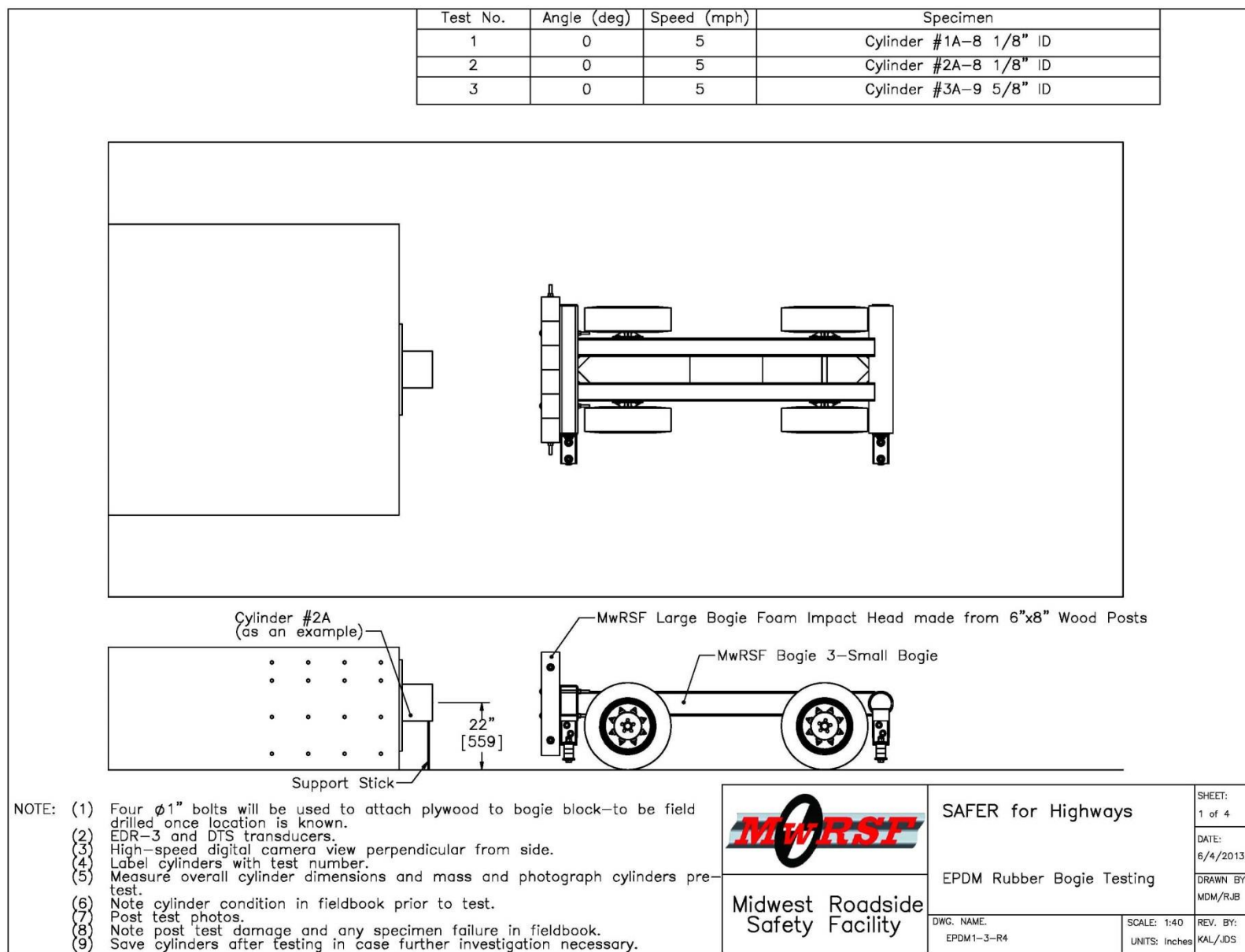


Figure 6. Bogie Testing Matrix and Setup, Test Nos. EPDM-1 through EPDM-3

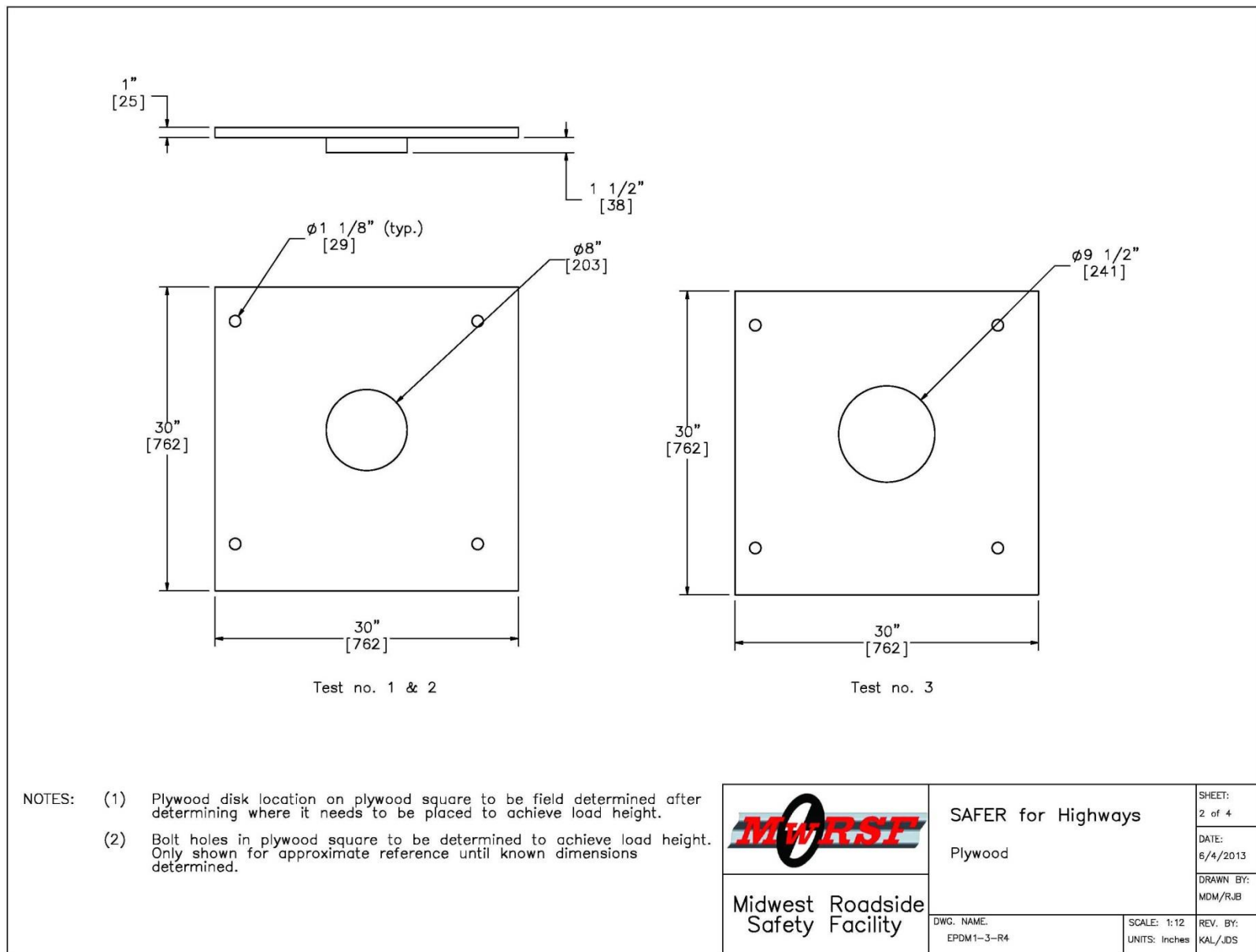


Figure 7. Plywood Attachment Details, Test Nos. EPDM-1 through EPDM-3

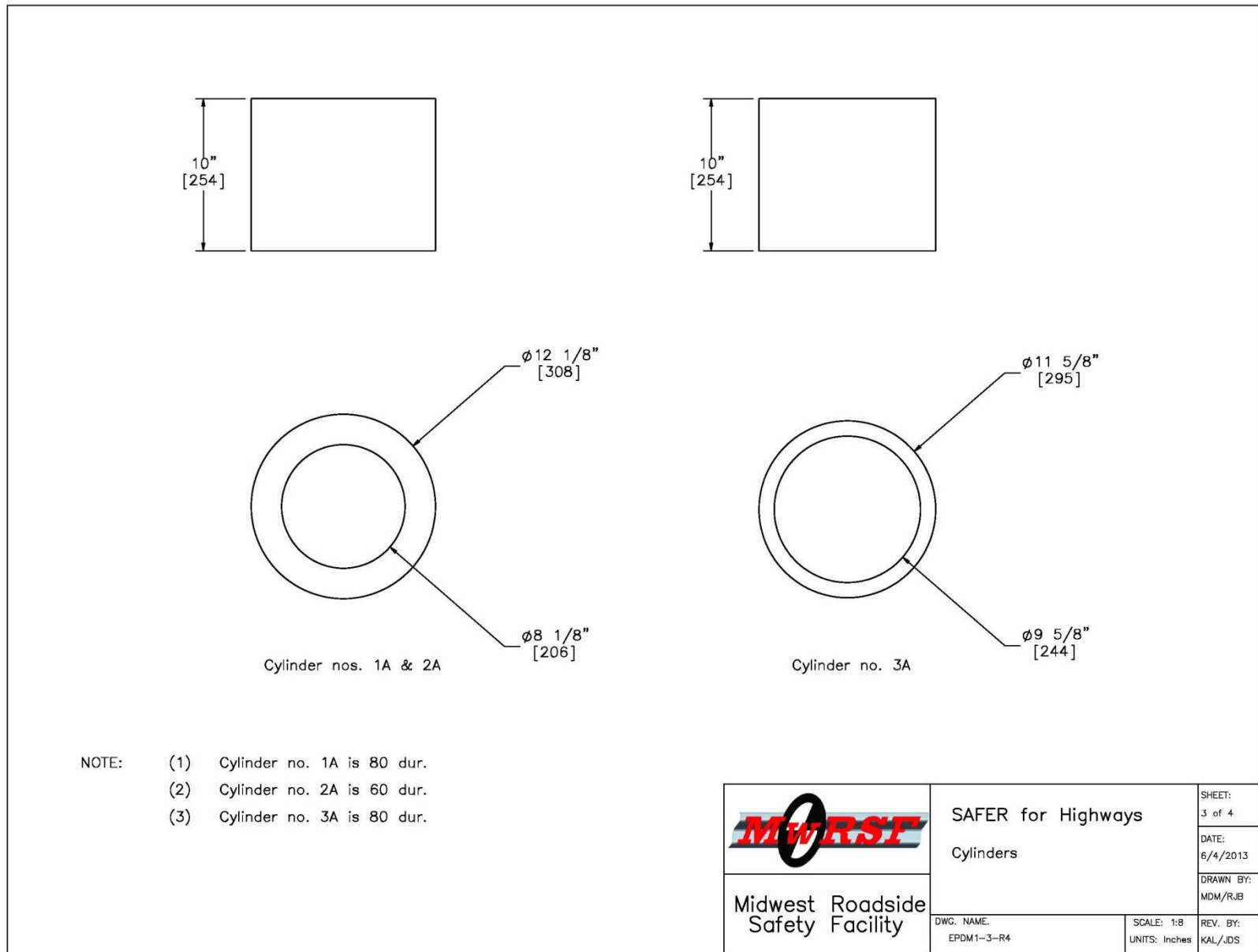


Figure 8. Rubber Cylinder Details, Test Nos. EPDM-1 through EPDM-3

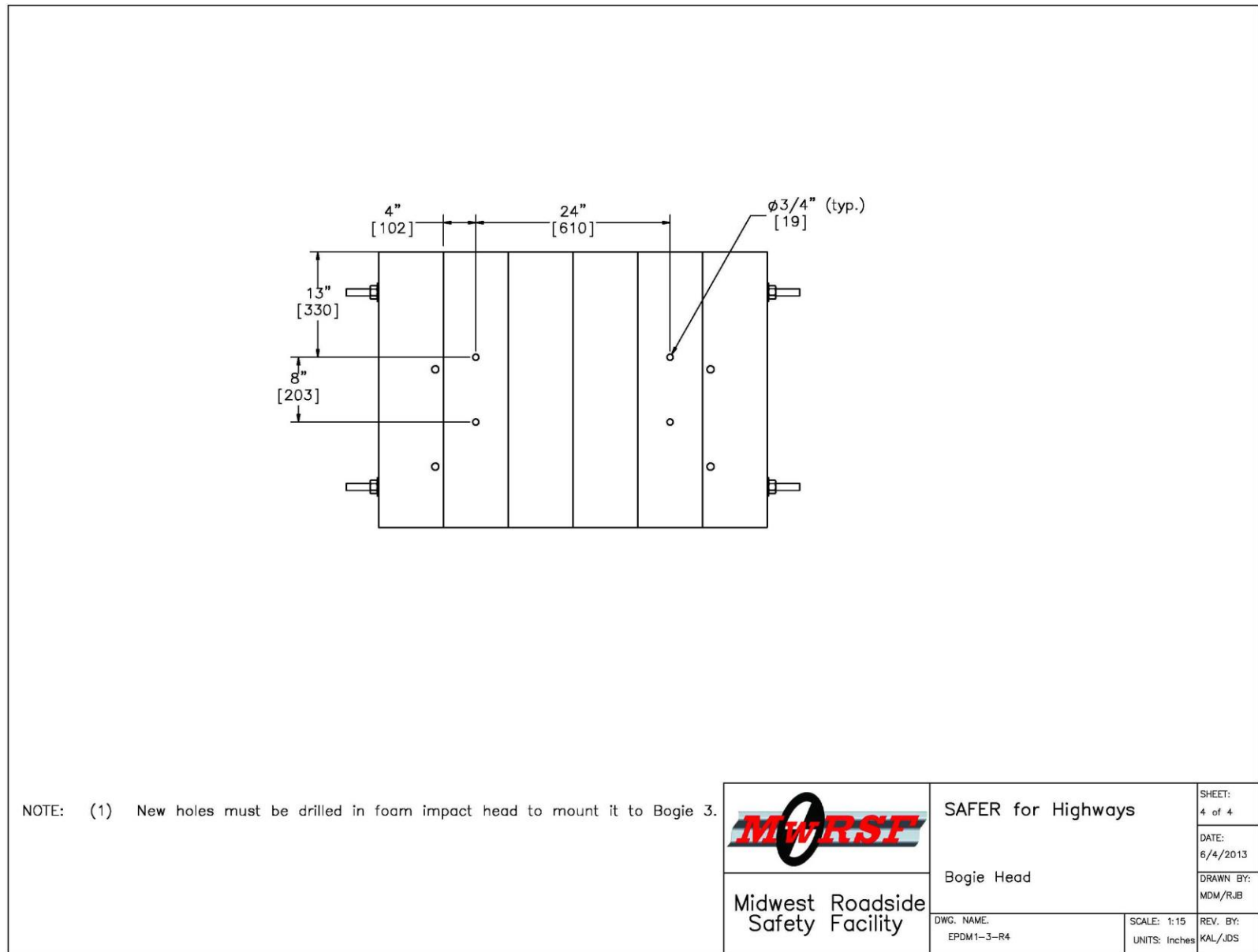


Figure 9. Impact Head Details, Test Nos. EPDM-1 through EPDM-3

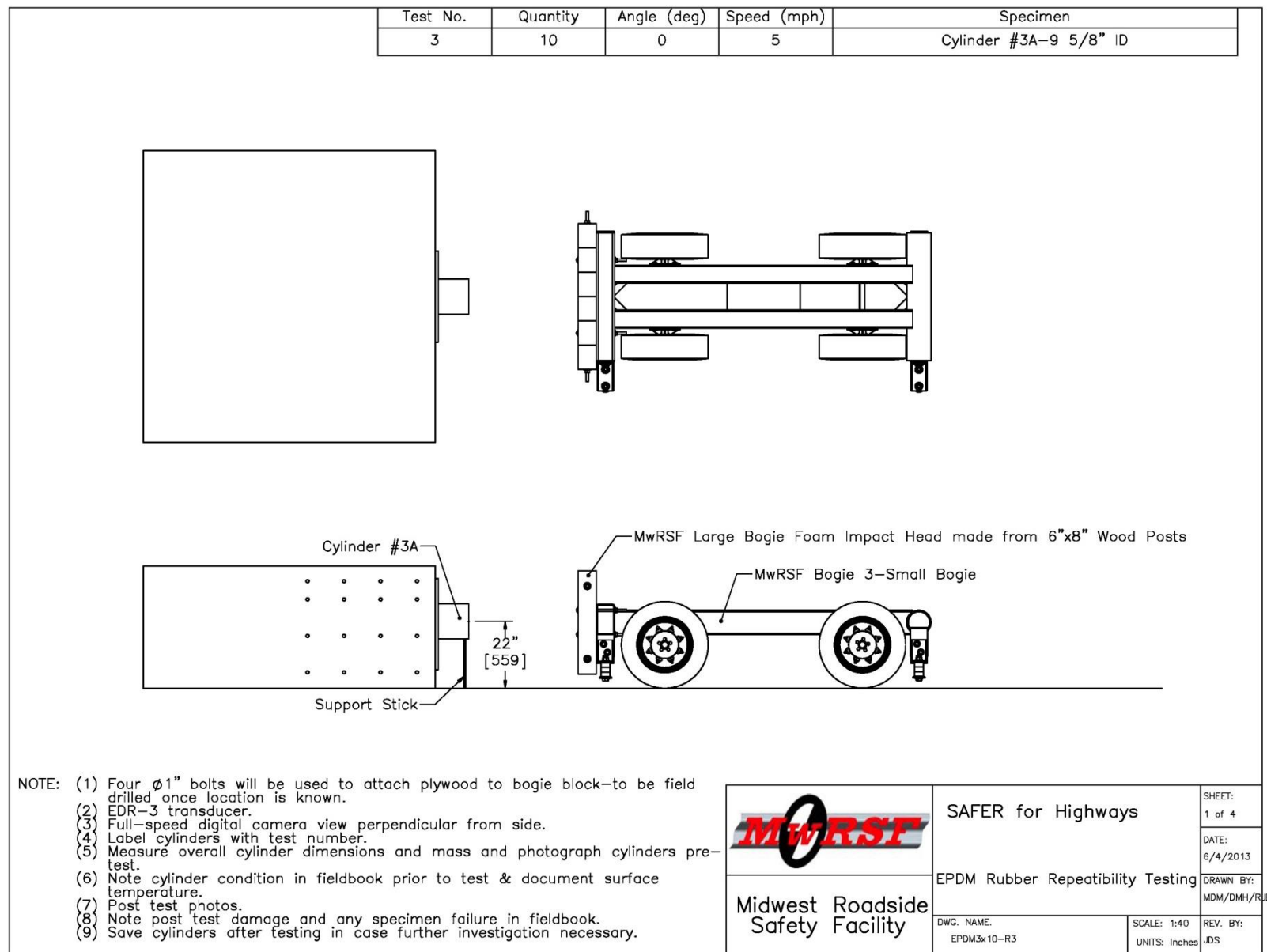


Figure 10. Bogie Testing Matrix and Setup, Test Nos. EPDM-4 through EPDM-12

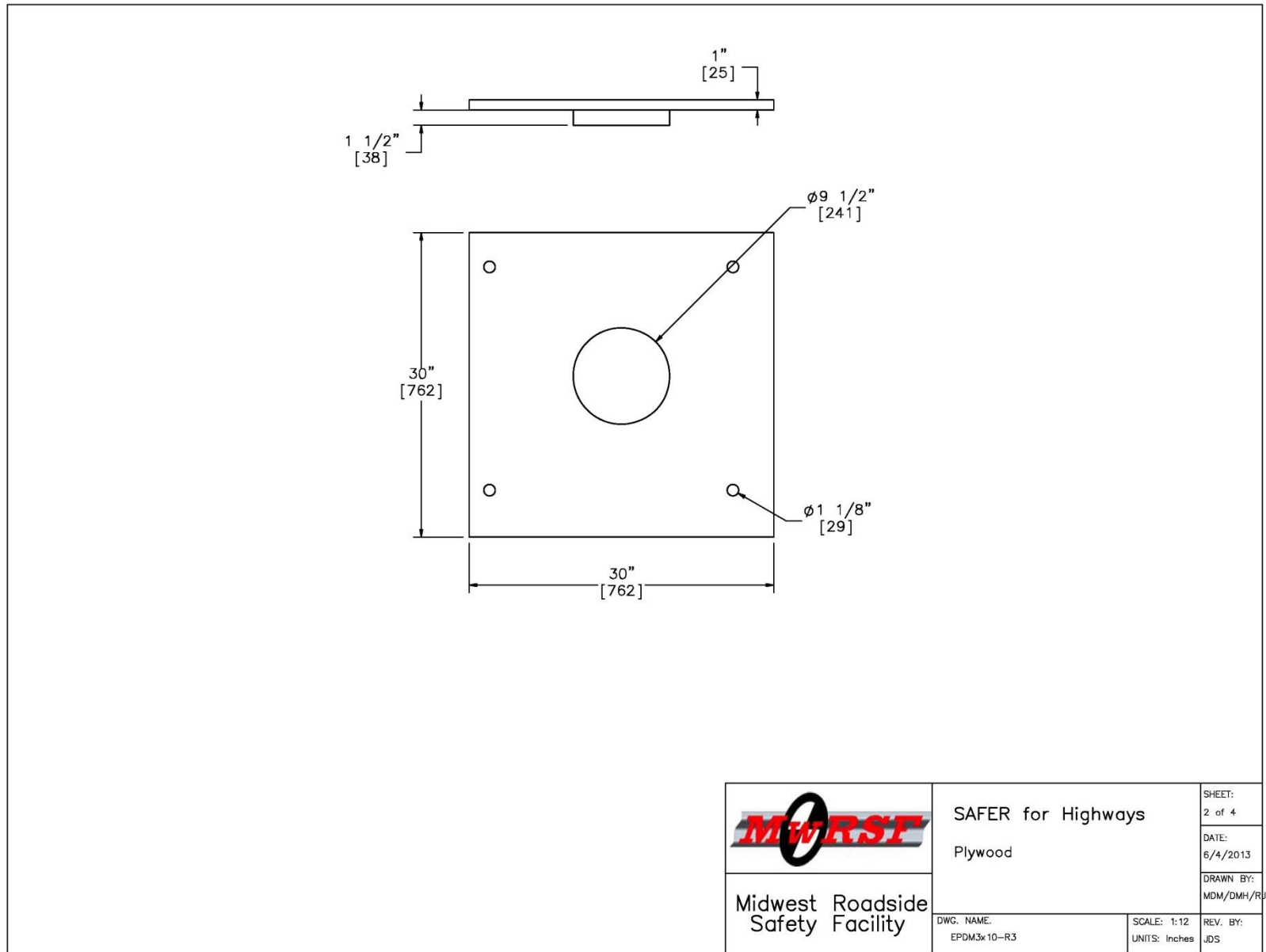


Figure 11. Plywood Attachment Details, Test Nos. EPDM-4 through EPDM-12

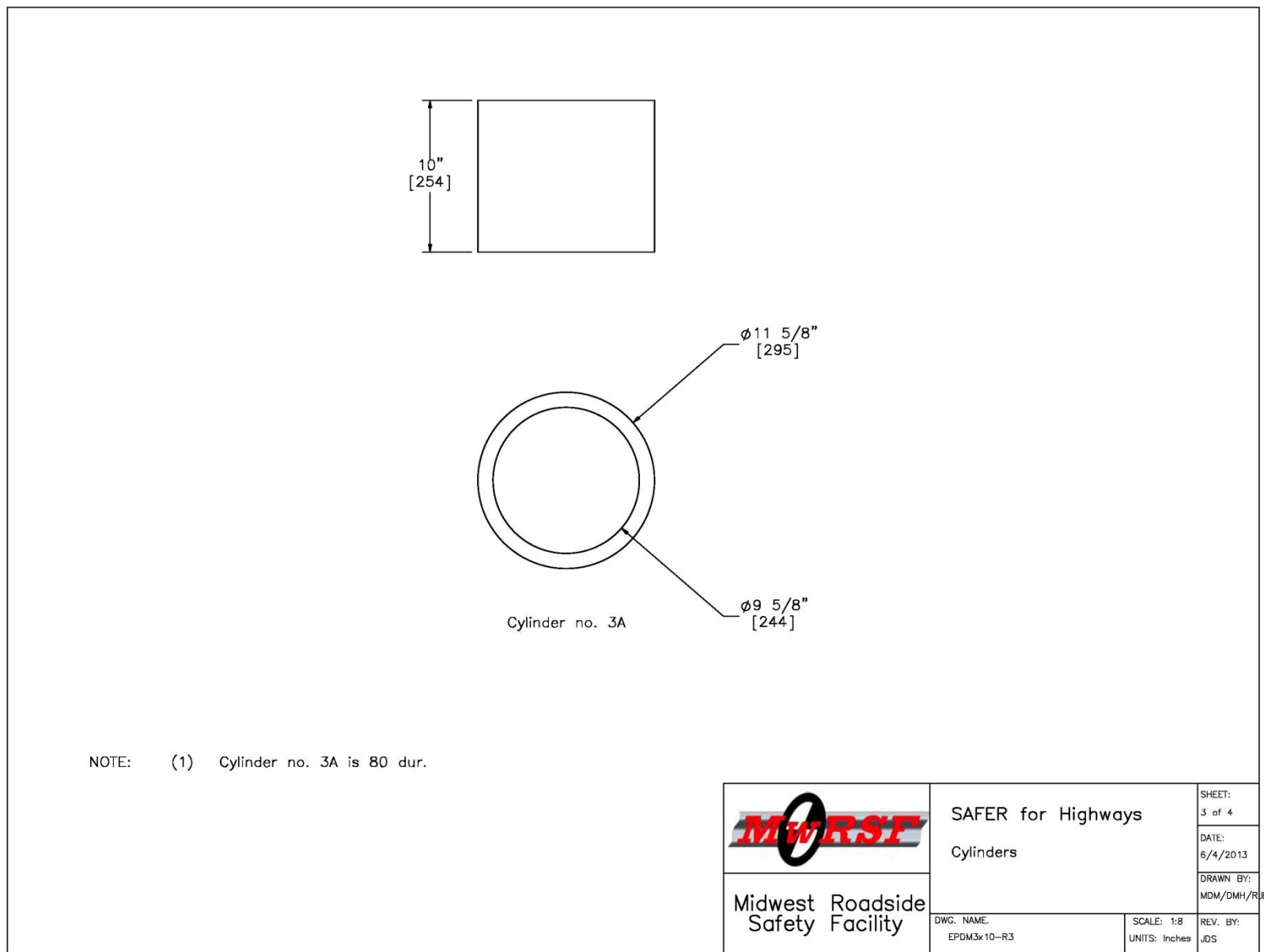


Figure 12. Rubber Cylinder Details, Test Nos. EPDM-4 through EPDM-12

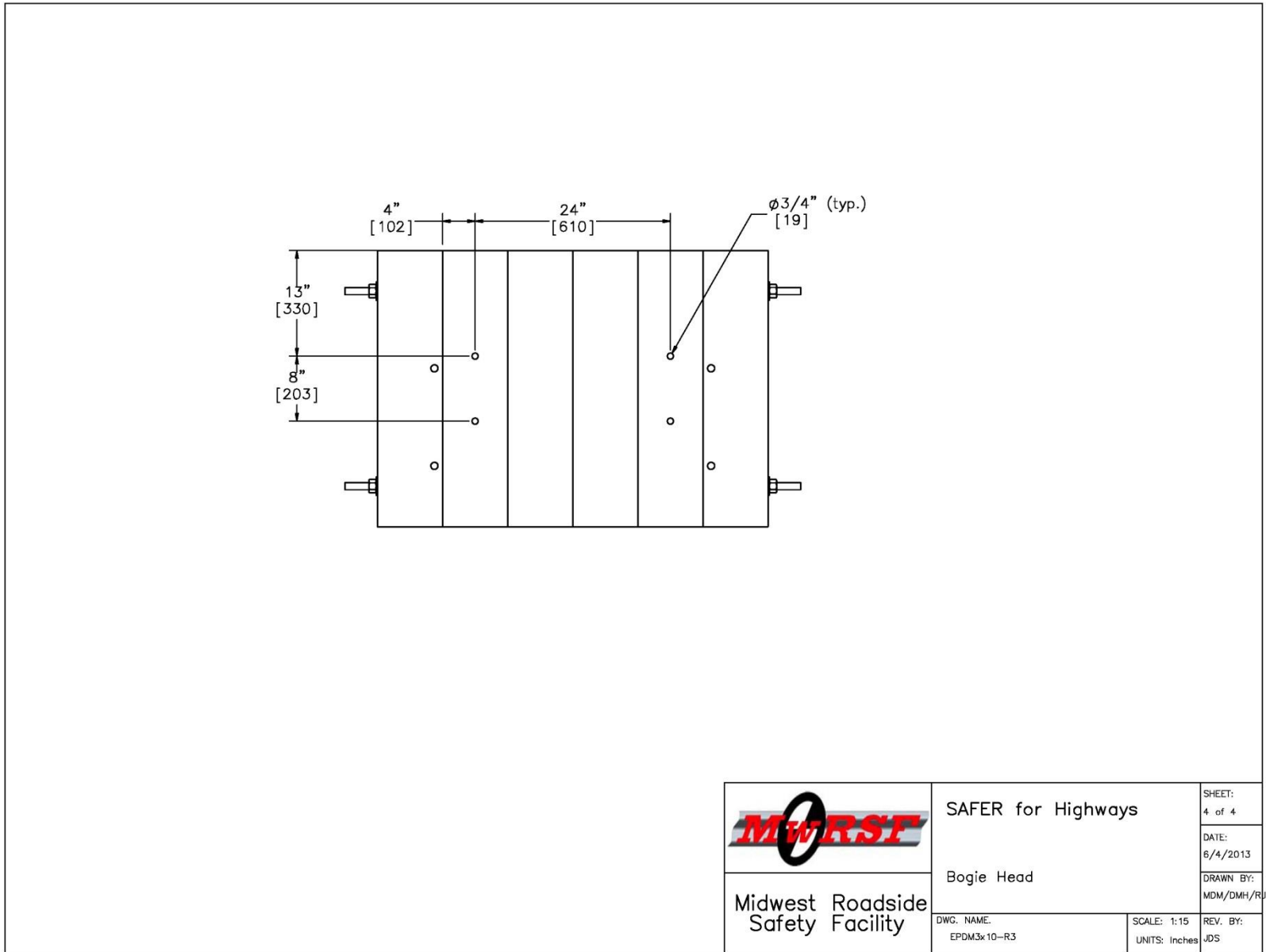


Figure 13. Impact Head Details, Test Nos. EPDM-4 through EPDM-12

3.3 Results

3.3.1 Test No. EPDM-1

The 1,686-lb (765-kg) bogie impacted the 2-in. (51-mm) thick, 80-durometer EPDM cylinder at a speed of 4.3 mph (6.9 km/h) and at an angle of 0 degrees. The cylinder compressed 1.9 in. (48 mm) in 0.040 sec. Upon post-test examination, the cylinder was not damaged and had no permanent set.

Force vs. deflection and energy vs. deflection curves created from the DTS accelerometer data are shown in Figure 14. The peak force of 12.3 k (54.7 kN) occurred at 1.8 in. (46 mm) deflection. The total energy was 12.4 k-in. (1.4 kJ). Sequential photographs are shown in Figure 15.

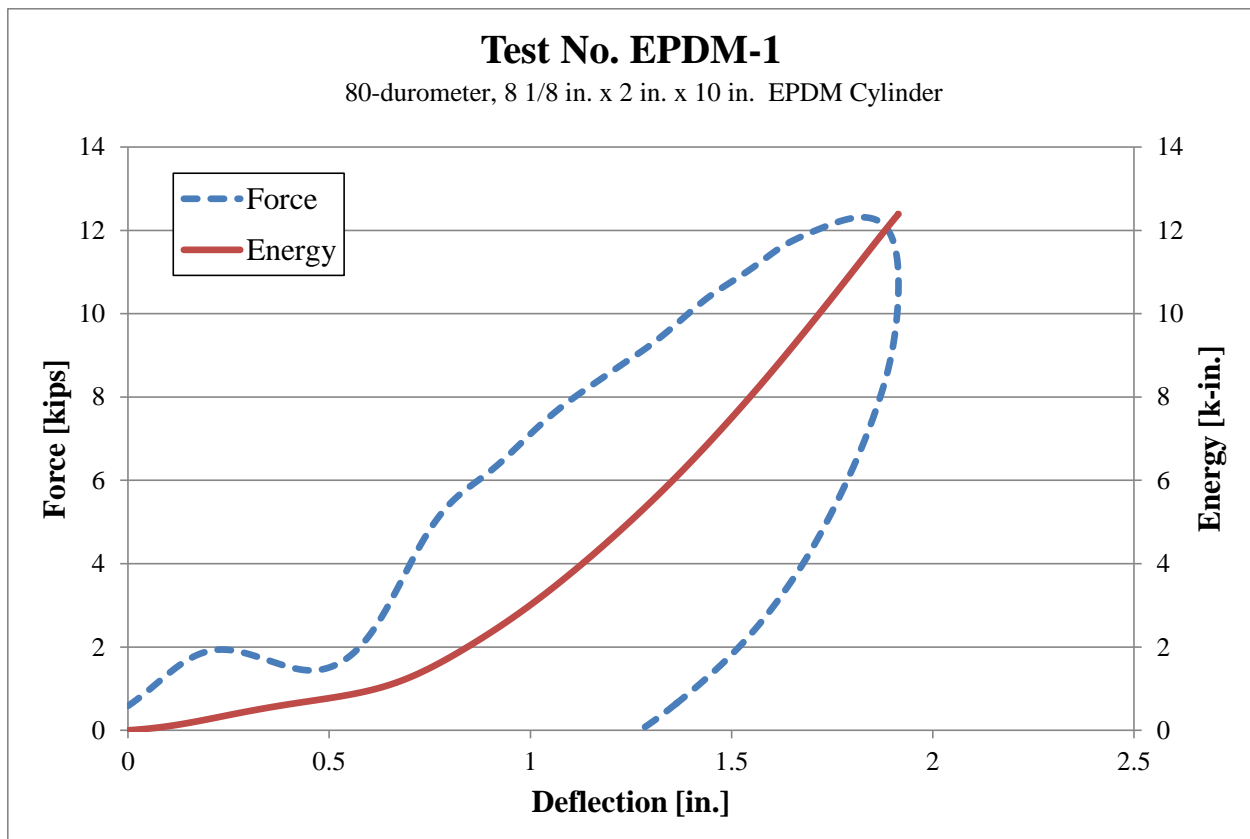


Figure 14. Force vs. Deflection and Energy vs. Deflection, Test No. EPDM-1



Figure 15. Time-Sequential Photographs, Test No. EPDM-1

3.3.2 Test No. EPDM-2

The 1,686-lb (765-kg) bogie impacted the 2-in. (51-mm) thick, 60-durometer EPDM cylinder at a speed of 4.9 mph (7.8 km/h) and at an angle of 0 degrees. The cylinder compressed 2.2 in. (56 mm) in 0.041 sec. Upon post-test examination, the cylinder was not damaged and had no permanent set.

Force vs. deflection and energy vs. deflection curves created from the DTS accelerometer data are shown in Figure 16. The peak force of 12.9 k (57.5 kN) occurred at 2.1 in. (53 mm) deflection. The total energy was 16.1 k-in. (1.8 kJ). Sequential photographs are shown in Figure 17.

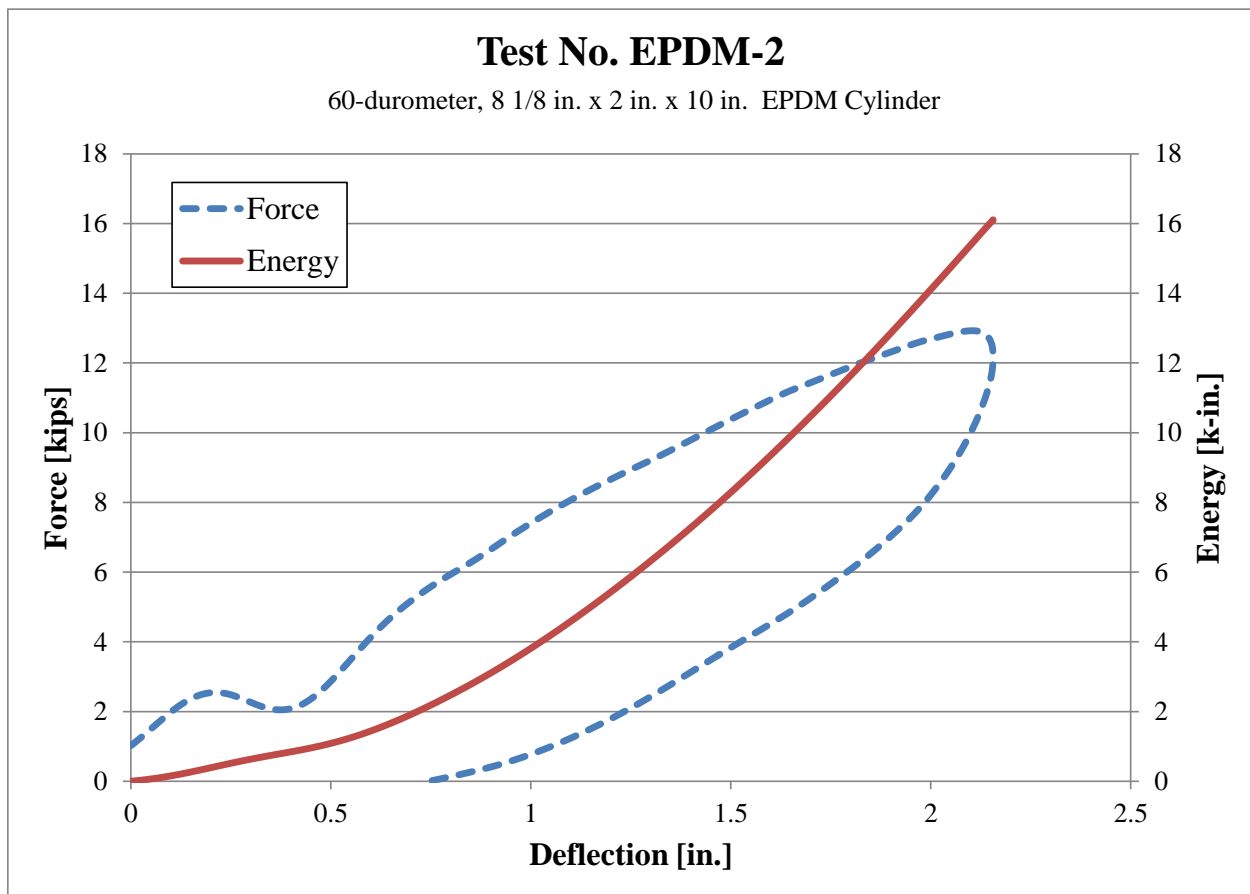


Figure 16. Force vs. Deflection and Energy vs. Deflection, Test No. EPDM-2

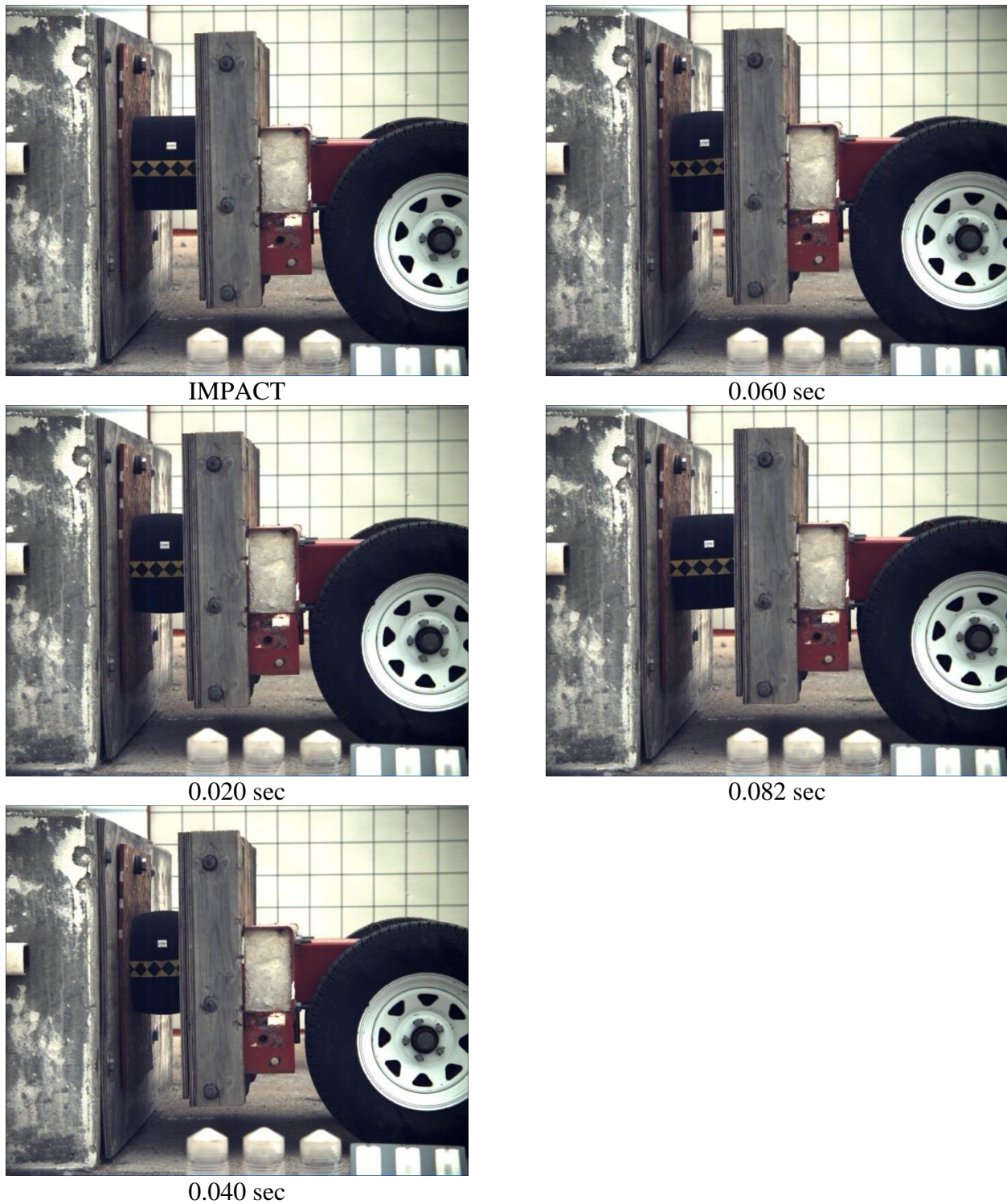


Figure 17. Time-Sequential Photographs, Test No. EPDM-2

3.3.3 Test No. EPDM-3

The 1,686-lb (765-kg) bogie impacted the 1-in. (25-mm) thick, 80-durometer EPDM cylinder at a speed of 6.8 mph (10.9 km/h) and at an angle of 0 degrees. The cylinder compressed 6.2 in. (157 mm) in 0.101 sec. Upon post-test examination, the cylinder was not damaged and had no permanent set.

Force vs. deflection and energy vs. deflection curves created from the DTS accelerometer data are shown in Figure 18. The peak force of 6.7 k (29.8 kN) occurred at 2.4 in. (61 mm) of deflection. The total energy was 30.9 k-in. (3.5 kJ). Sequential photographs are shown in Figure 19.

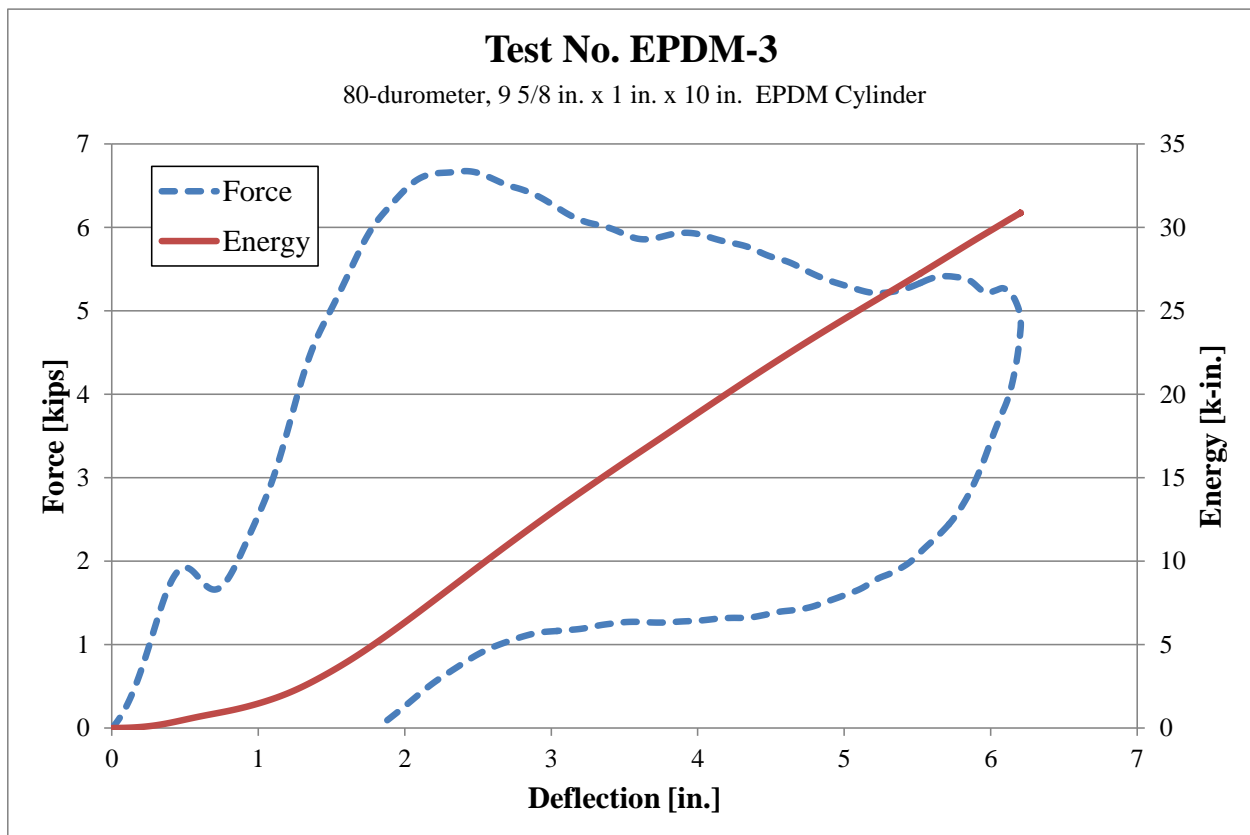


Figure 18. Force vs. Deflection and Energy vs. Deflection, Test No. EPDM-3

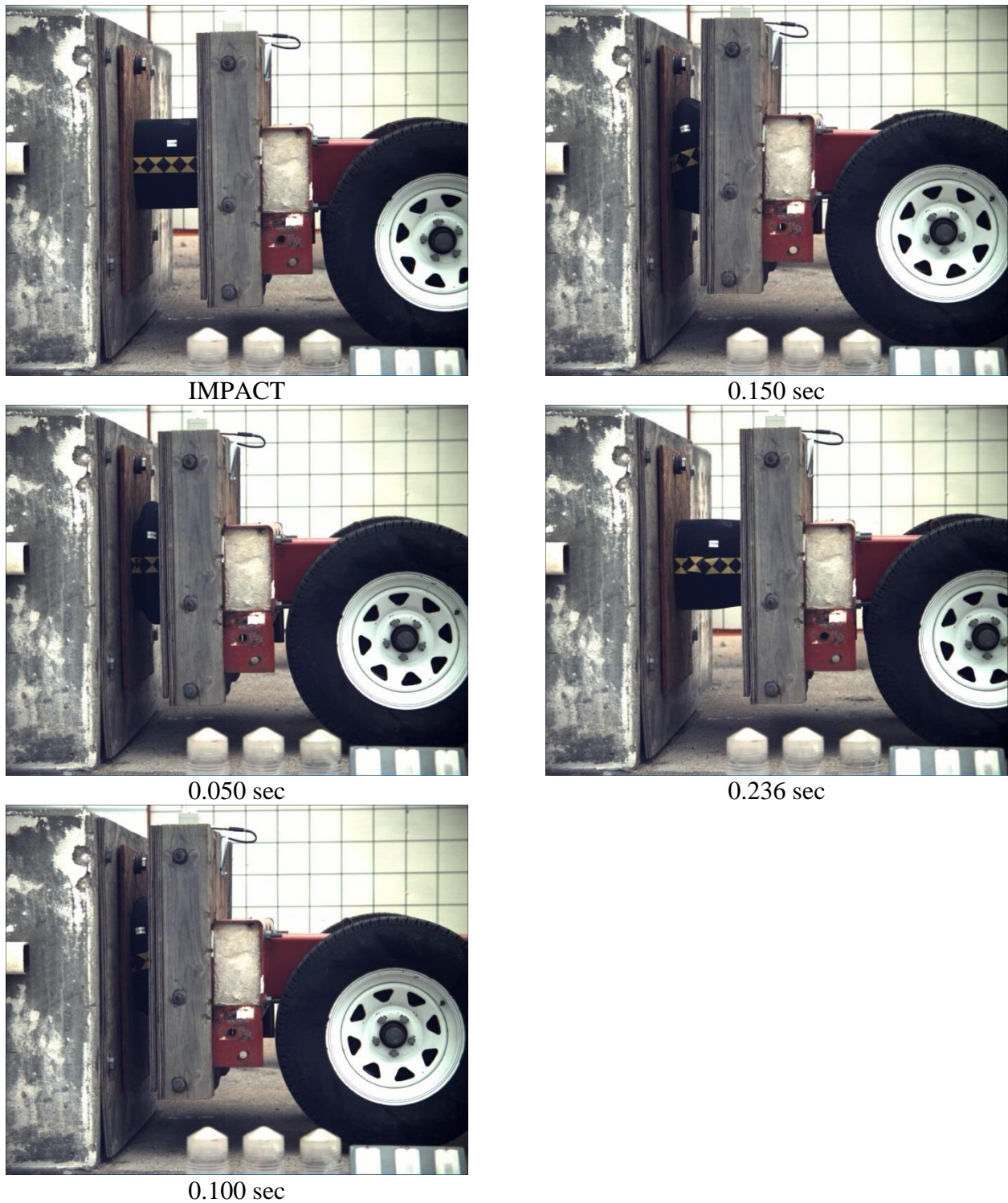


Figure 19. Time-Sequential Photographs, Test No. EPDM-3

3.3.4 Repeatability Test Nos. EPDM-4 through EPDM-12

The 1,689-lb (766-kg) bogie impacted the 1-in. (25-mm) thick, 80-durometer EPDM cylinder at approximately 5 mph (8 km/h) and at an angle of 0 degrees for 9 consecutive tests. With the addition of EPDM-3, a total of 10 component tests were conducted on this cylinder. Upon post-test examination, the cylinder was not damaged and had no permanent set.

Force vs. deflection and energy vs. deflection curves created from the accelerometer data are shown in Figures 20 and 21, respectively. For test nos. EPDM-3 through EPDM-12, the forces and energies are very similar for all tests over the first 2 in. (51 mm) of deflection. Test no. EPDM-3 had an average force of around 5.5 kips (24.5 kN). Test no. EPDM-4 had an average force around 5 kips (22.2 kN). All other tests had an average force around 4 kips (17.8 kN). The reason for this variability could be due to the temperature of the cylinders or due to non-visible permanent strains that remained after unloading. During the first loading cycle, rubber is very stiff, but it softens after the first loading-unloading cycle and is consistent during repeated loading cycles [5]. Also, it was difficult to maintain a constant velocity for all tests, and the velocity of the bogie ranged from 5.3 mph to 7.1 mph (8.5 km/h to 11.4 km/h). Therefore, the peak force, total energy, and deflection varied in each test.

Plots showing the energy vs. velocity and peak force vs. deflection for the 10 tests are shown in Figures 22 through 23, respectively. While the surface temperature of the rubber was taken for each test, there was not a specific trend that could be discerned due to temperature; since, there was not an extreme variation in temperature. The rubber surface temperature, bogie velocity, maximum deflection, peak force, and total energy for test nos. EPDM-3 through EPDM-12 are shown in Table 5.

Force vs. Deflection

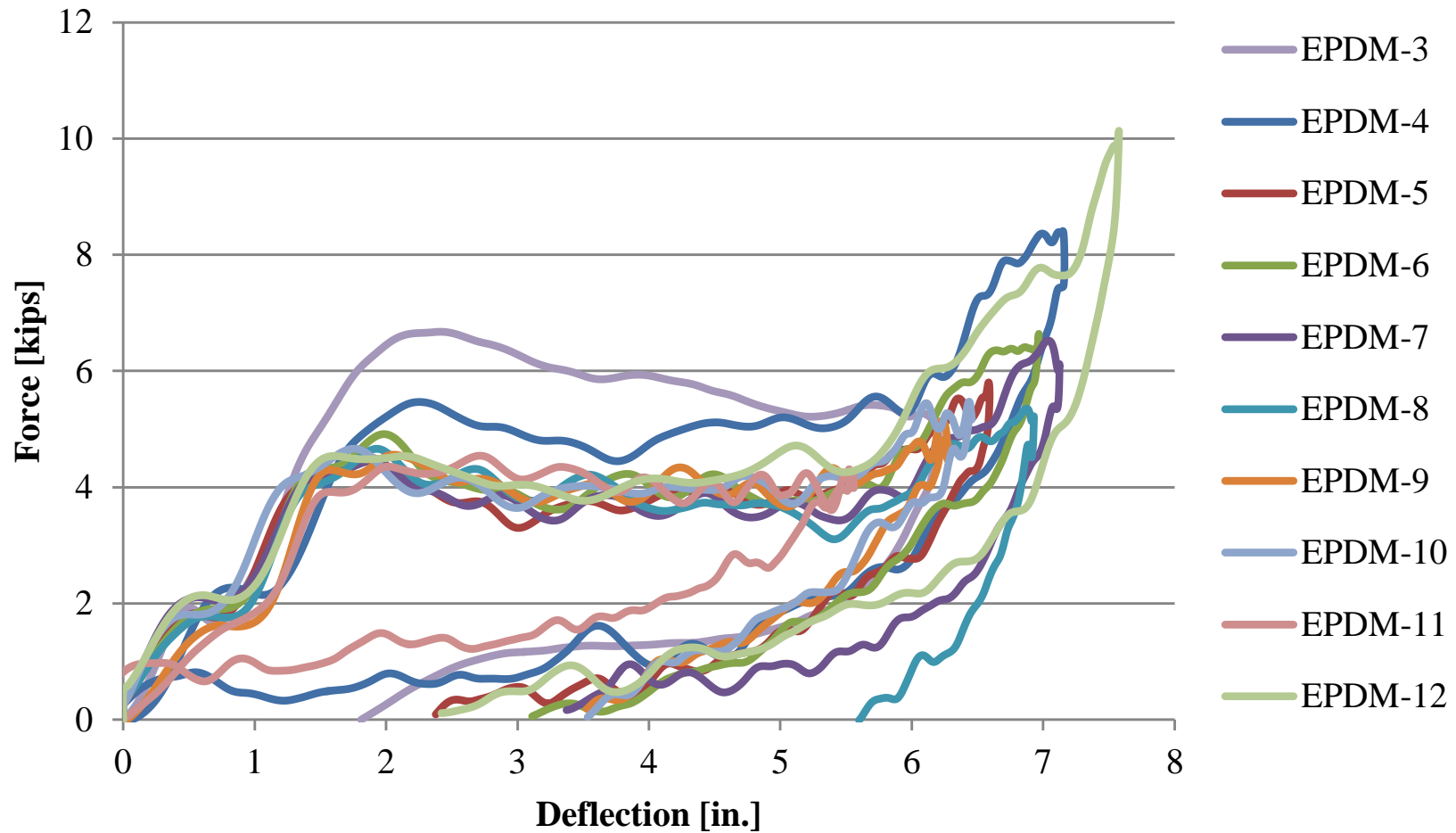


Figure 20. Force vs. Deflection of 9% x 1x10 in. (244x25x254 mm) Cylinders, Test Nos. EPDM-3 through EPDM-12

Energy vs. Deflection

80-durometer, 9 5/8 in. x 1 in. x 10 in. EPDM Cylinder

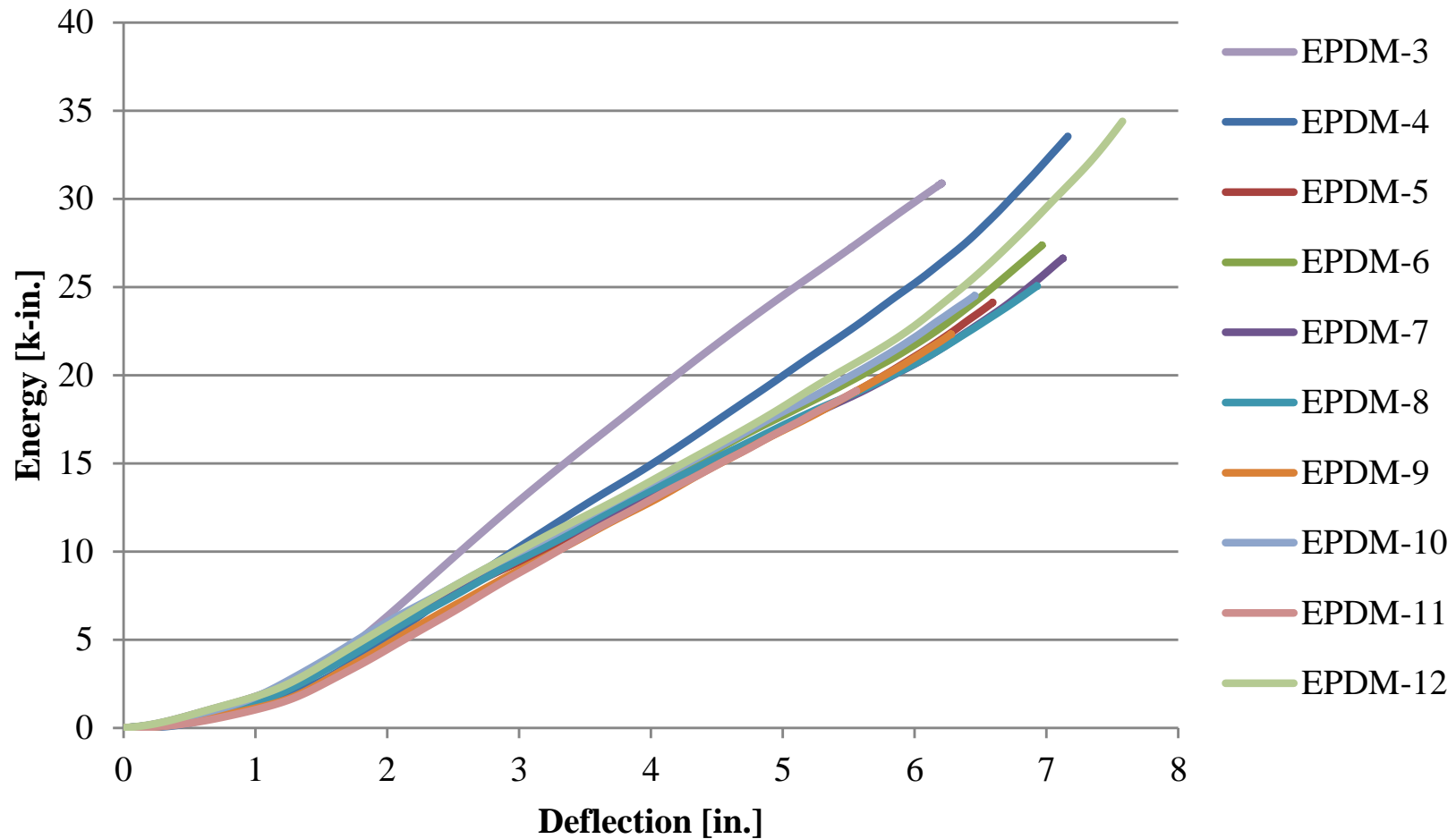


Figure 21. Energy vs. Deflection of 9% x1x10 in. (244x25x254 mm) Cylinders, Test Nos. EPDM-3 through EPDM-12

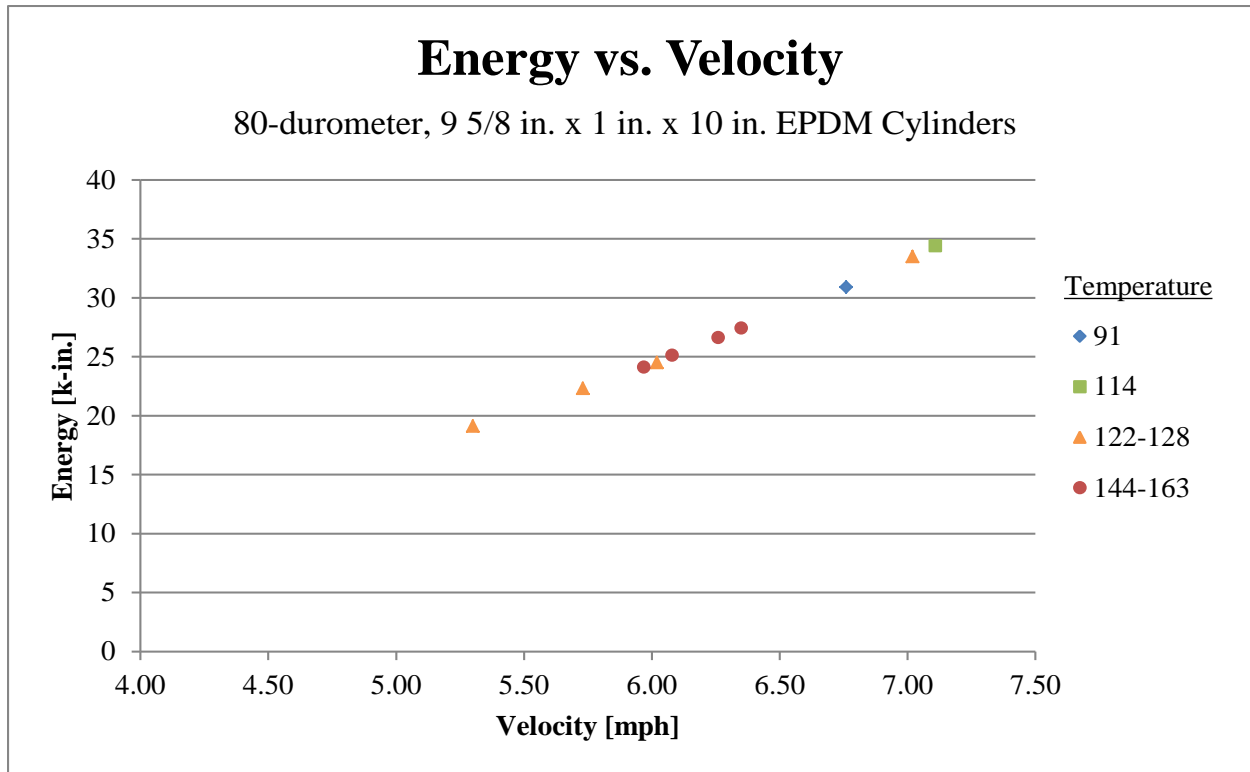


Figure 22. Energy vs. Velocity, Test Nos. EPDM-3 through EPDM-12

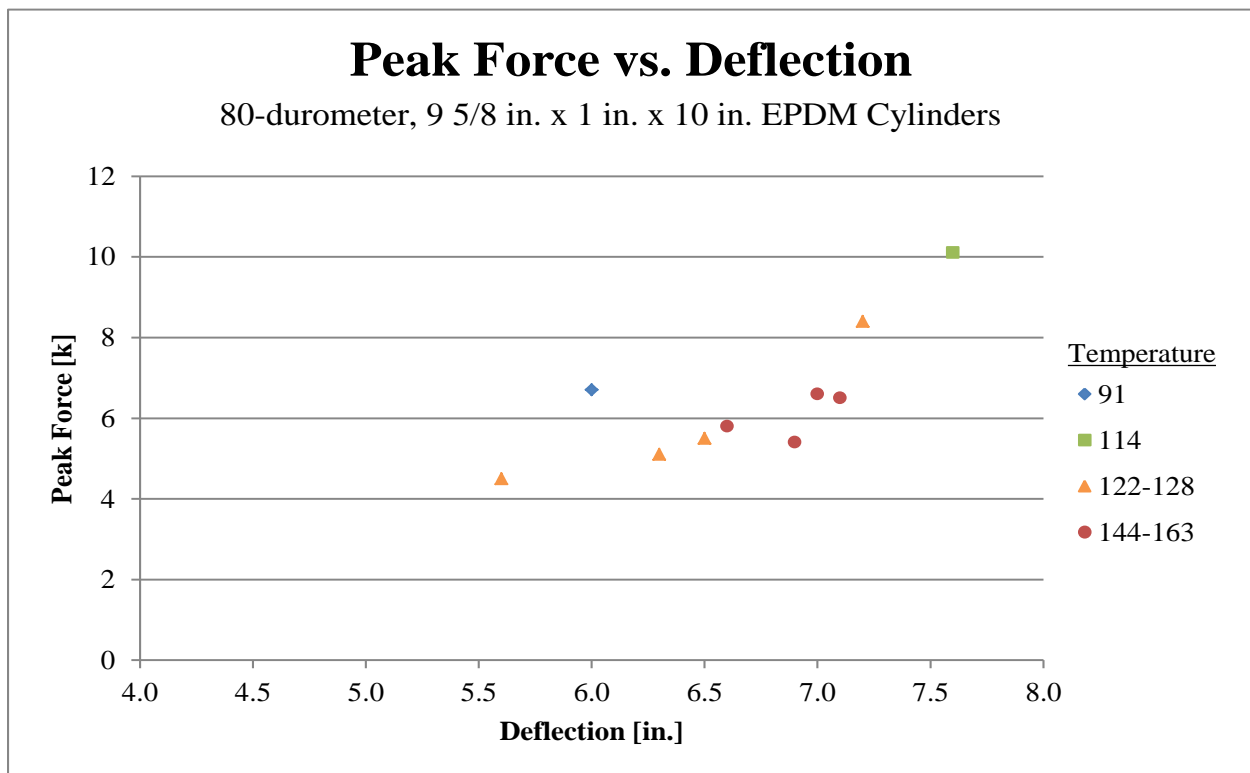


Figure 23. Peak Force vs. Deflection, Test Nos. EPDM-3 through EPDM-12

Table 5. Repeatability Dynamic Test Results, Test Nos. EPDM-3 through EPDM-12

Test No.	Durometer	Dimensions ID x thick x length in. (mm)	Temp. °F (°C)	Impact Velocity mph (km/h)	Max. Deflection in. (mm)	Peak Force kips (kN)	Total Energy k-in. (kJ)
EPDM-3	80	9 ⁵ / ₈ x 1 x 10 (244 x 25 x 254)	91 (32.8)	6.8 (10.9)	6.2 (157)	6.7 (29.8)	30.9 (3.5)
EPDM-4	80	9 ⁵ / ₈ x 1 x 10 (244 x 25 x 254)	125 (51.7)	7.0 (11.3)	7.2 (183)	8.4 (37.4)	33.5 (3.8)
EPDM-5	80	9 ⁵ / ₈ x 1 x 10 (244 x 25 x 254)	159 (70.6)	6.0 (9.6)	6.6 (168)	5.8 (25.8)	24.1 (2.7)
EPDM-6	80	9 ⁵ / ₈ x 1 x 10 (244 x 25 x 254)	163 (72.8)	6.4 (10.2)	7.0 (178)	6.6 (29.4)	27.4 (3.1)
EPDM-7	80	9 ⁵ / ₈ x 1 x 10 (244 x 25 x 254)	150 (65.6)	6.3 (10.1)	7.1 (180)	6.5 (28.9)	26.6 (3.0)
EPDM-8	80	9 ⁵ / ₈ x 1 x 10 (244 x 25 x 254)	144 (62.2)	6.1 (9.8)	6.9 (175)	5.4 (24.0)	25.1 (2.8)
EPDM-9	80	9 ⁵ / ₈ x 1 x 10 (244 x 25 x 254)	128 (53.3)	5.7 (9.2)	6.3 (160)	5.1 (22.7)	22.3 (2.5)
EPDM-10	80	9 ⁵ / ₈ x 1 x 10 (244 x 25 x 254)	124 (51.1)	6.0 (9.7)	6.5 (165)	5.5 (24.5)	24.5 (2.8)
EPDM-11	80	9 ⁵ / ₈ x 1 x 10 (244 x 25 x 254)	122 (50.0)	5.3 (8.5)	5.6 (142)	4.5 (20.0)	19.1 (2.2)
EPDM-12	80	9 ⁵ / ₈ x 1 x 10 (244 x 25 x 254)	114 (45.6)	7.1 (11.4)	7.6 (193)	10.1 (44.9)	34.4 (3.9)

3.4 Discussion

Test nos. EPDM-1 through EPDM-3 were conducted on three different EPDM rubber cylinders: (1) 8¹/₈-in. (206-mm) inner diameter x 2-in. (51-mm) thick x 10-in. (254-mm) long, 80-durometer cylinder; (2) 8¹/₈-in. (206-mm) inner diameter x 2-in. (51-mm) thick x 10-in. (254-mm) long, 60-durometer cylinder; and (3) 9⁵/₈-in. (244-mm) inner diameter x 1-in. (25-mm) thick x 10-in. (254-mm) long, 80-durometer cylinder. The surface temperature was approximately the same for these 3 tests. Thus, conclusions of the energy absorption based on the dimensions and durometer of the EPDM rubber were made. A summary of all bogie testing results is shown in Table 6. Test results for all transducers are provided in Appendix A.

Force vs. deflection and energy vs. deflection were compared for the three different cylinder types, as shown in Figures 24 and 25, respectively. Only a slight difference was observed between the 60 and 80 durometer rubber cylinders (test nos. EPDM-1 and EPDM-2). The 1-in. (25-mm) thick cylinder (test no. EPDM-3) had one-half of the peak force, 2.5 times the total energy, and deflected 3 times as much as the 2-in. (51-mm) thick cylinder (test no. EPDM-1). However, the velocity of test no. EPDM-3 was also approximately 1.5 times greater than test no. EPDM-1. At

such a low impact velocity, it was difficult to maintain the 5 mph (8 km/h) constant velocity. This inconsistency in velocity made it hard to compare the cylinders.

Table 6. Dynamic Test Results, Test Nos. EPDM-1 through EPDM-12

Test No.	Durometer	Dimensions ID x thick x length in. (mm)	Temp. °F (°C)	Impact Velocity mph (km/h)	Max. Deflection in. (mm)	Peak Force kips (kN)	Total Energy k-in. (kJ)
EPDM-1	80	8½ x 2 x 10 (206 x 51 x 254)	97 (36.1)	4.3 (6.9)	1.9 (48)	12.3 (54.7)	12.4 (1.4)
EPDM-2	60	8½ x 2 x 10 (206 x 51 x 254)	91 (32.8)	4.9 (7.9)	2.2 (56)	12.9 (57.4)	16.1 (1.8)
EPDM-3	80	9½ x 1 x 10 (244 x 25 x 254)	91 (32.8)	6.8 (10.9)	6.2 (157)	6.7 (29.8)	30.9 (3.5)
EPDM-4	80	9½ x 1 x 10 (244 x 25 x 254)	125 (51.7)	7.0 (11.3)	7.2 (183)	8.4 (37.4)	33.5 (3.8)
EPDM-5	80	9½ x 1 x 10 (244 x 25 x 254)	159 (70.6)	6.0 (9.6)	6.6 (168)	5.8 (25.8)	24.1 (2.7)
EPDM-6	80	9½ x 1 x 10 (244 x 25 x 254)	163 (72.8)	6.4 (10.2)	7.0 (178)	6.6 (29.4)	27.4 (3.1)
EPDM-7	80	9½ x 1 x 10 (244 x 25 x 254)	150 (65.6)	6.3 (10.1)	7.1 (180)	6.5 (28.9)	26.6 (3.0)
EPDM-8	80	9½ x 1 x 10 (244 x 25 x 254)	144 (62.2)	6.1 (9.8)	6.9 (175)	5.4 (24.0)	25.1 (2.8)
EPDM-9	80	9½ x 1 x 10 (244 x 25 x 254)	128 (53.3)	5.7 (9.2)	6.3 (160)	5.1 (22.7)	22.3 (2.5)
EPDM-10	80	9½ x 1 x 10 (244 x 25 x 254)	124 (51.1)	6.0 (9.7)	6.5 (165)	5.5 (24.5)	24.5 (2.8)
EPDM-11	80	9½ x 1 x 10 (244 x 25 x 254)	122 (50.0)	5.3 (8.5)	5.6 (142)	4.5 (20.0)	19.1 (2.2)
EPDM-12	80	9½ x 1 x 10 (244 x 25 x 254)	114 (45.6)	7.1 (11.4)	7.6 (193)	10.1 (44.9)	34.4 (3.9)

Schmidt, et al. estimated that each energy absorber would need to absorb 52.8 k-in. to 211.2 k-in. (6.0 kJ to 23.9 kJ) of kinetic energy when placed in a roadside/median barrier that was intended to provide a 30 percent reduction in lateral acceleration for 2270P crash events at a velocity of 62 mph (100 km/h) and at an angle of 25 degrees [1]. All of the rubber cylinders absorbed less energy than what was desired. In test no. EPDM-3, the cylinder was loaded very close to its maximum deflection, and it did not absorb adequate energy for the new barrier. Thus, it was not recommended for use in its current configuration. The 2-in. (51-mm) rubber cylinders were not loaded to their maximum deflection, and they were expected to absorb significantly more energy if impacted with a larger load. The rubber cylinders also could be optimized for further energy absorption. The 2-in. (51-mm) thick EPDM rubber cylinders were recommended for further evaluation. In addition, the energy absorption of the EPDM rubber did not appear to change after multiple impact events.

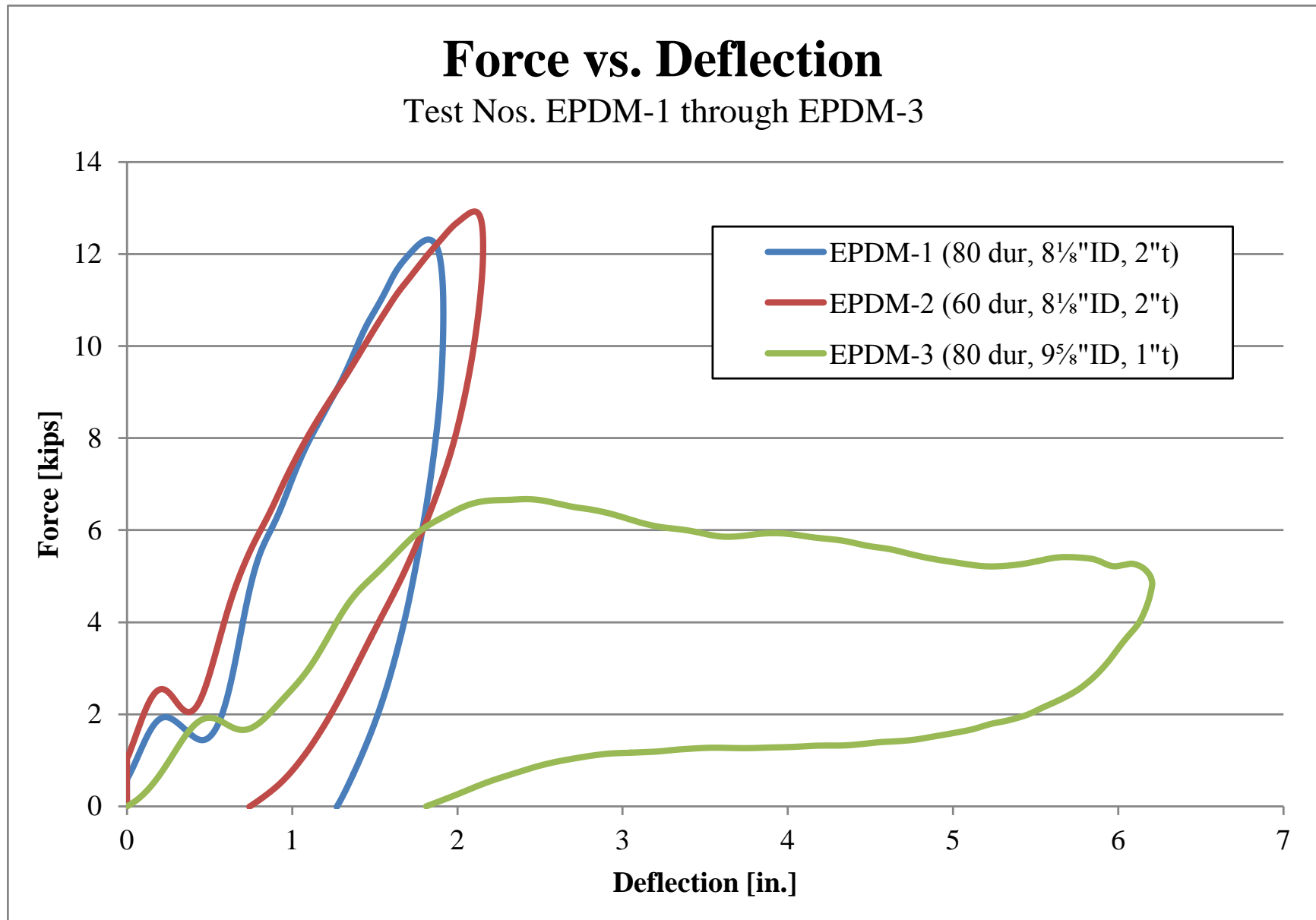


Figure 24. Force vs. Deflection of EPDM Cylinders, Test Nos. EPDM-1 through EPDM-3

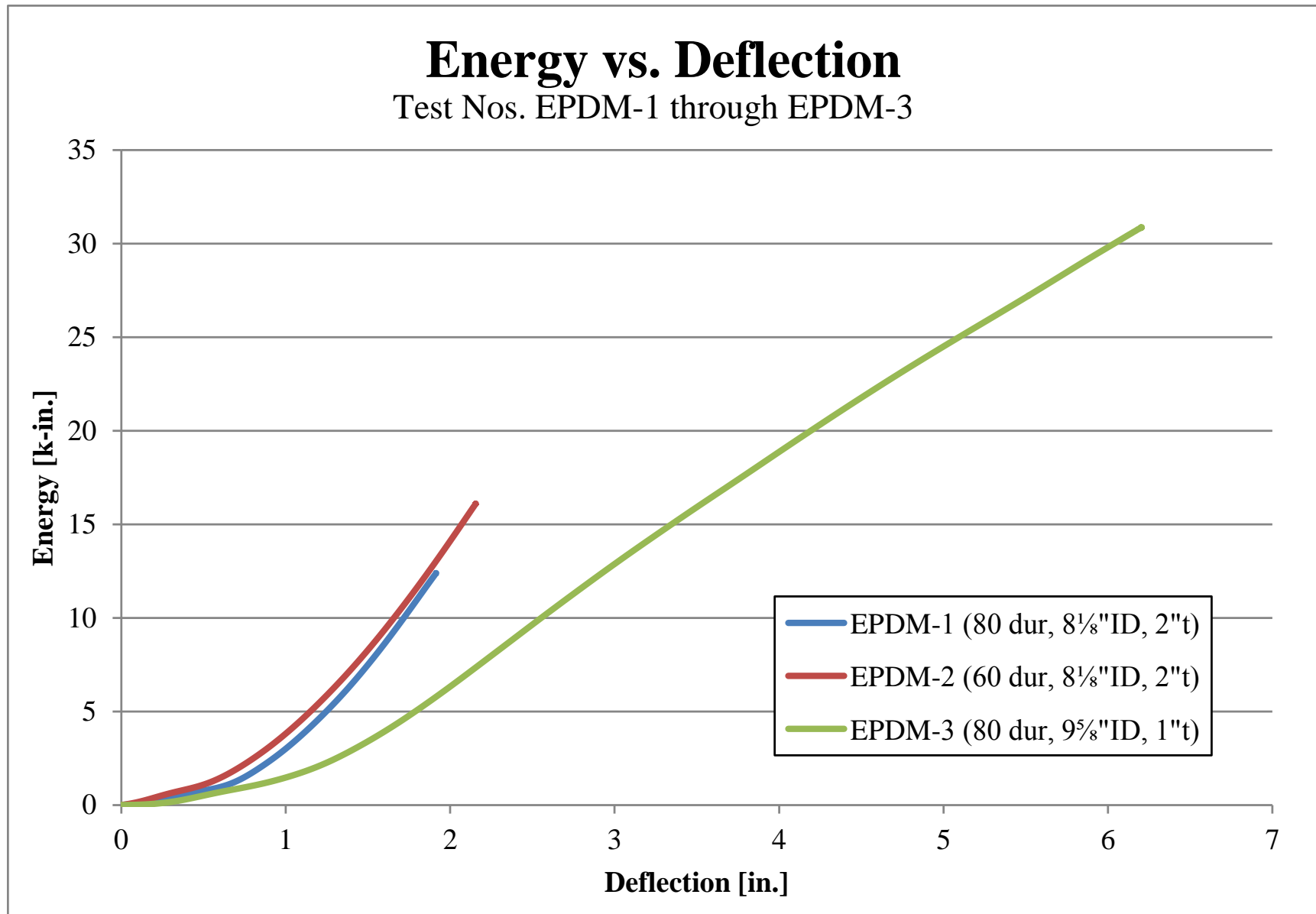


Figure 25. Energy vs. Deflection of EPDM Cylinders, Test Nos. EPDM-1 through EPDM-3

4 SHEAR FENDER COMPONENT TESTING

4.1 Purpose

Another design concept included energy-absorbing posts in conjunction with a continuous top rail. Maritime International, Inc. from Broussard, LA donated two HSF-14 marine shear fenders for evaluation in an energy-absorbing barrier. An example of a HSF-14 marine shear fender is shown in Figure 26.



Figure 26. Maritime International, Inc. HSF-14 Marine Shear Fender

4.2 Scope

A total of five dynamic bogie tests were conducted on a HSF-14 shear fender with dimensions of 16 in. (406 mm) high x 14 in. (356 mm) wide x 22 in. (559 mm) long with a 6-in. (152-mm) diameter hole lengthwise through the shear fender. One bogie test was conducted with the shear fender loaded laterally, which is perpendicular to the length of hole. Four bogie tests

were conducted with the shear fender loaded longitudinally, which is parallel to the length of the hole.

The target impact speeds included 5 mph (8 km/h) for test nos. HSF14-1 and HSF14-2, 10 mph (16 km/h) for test nos. HSF14-3 and HSF14-5, and 15 mph (24 km/h) for test no. HSF14-4. An 1,818-lb (825-kg) bogie was used for test nos. HSF14-1 through HSF14-4, and a 4,946-lb (2,243-kg) bogie was used for test no. HSF14-5. The impact height was 17¾ in. (451 mm) above the ground line. A steel-frame structure was bolted to the top of the shear fender. The bottom of the shear fender was attached to the ground with threaded rods that were epoxied into a concrete tarmac. The test matrix and test setup are shown in Figures 27 through 36. Test setup photographs are shown in Figures 37 through 39.

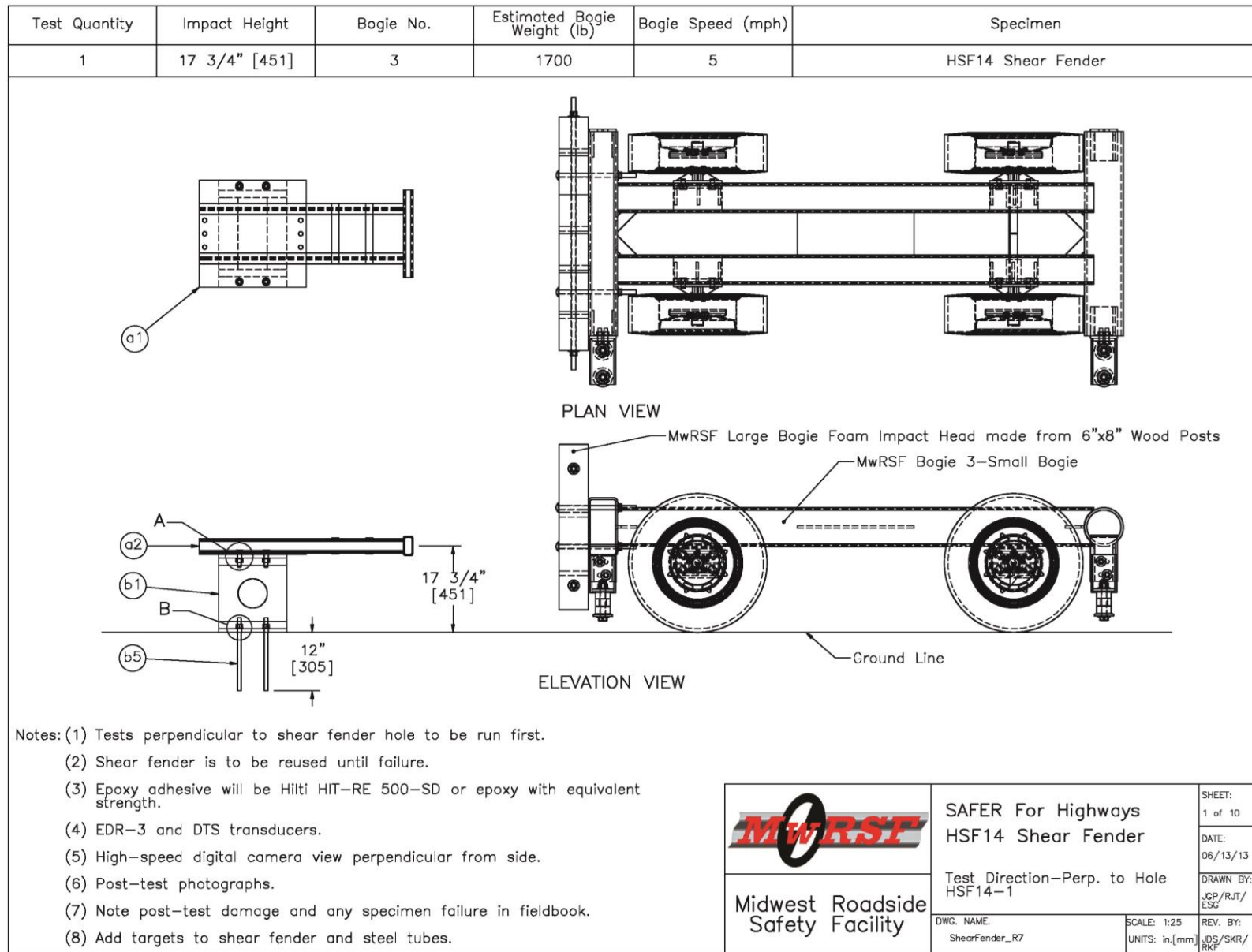


Figure 27. Bogie Testing Setup – Perpendicular to Hole, Test No. HSF14-1

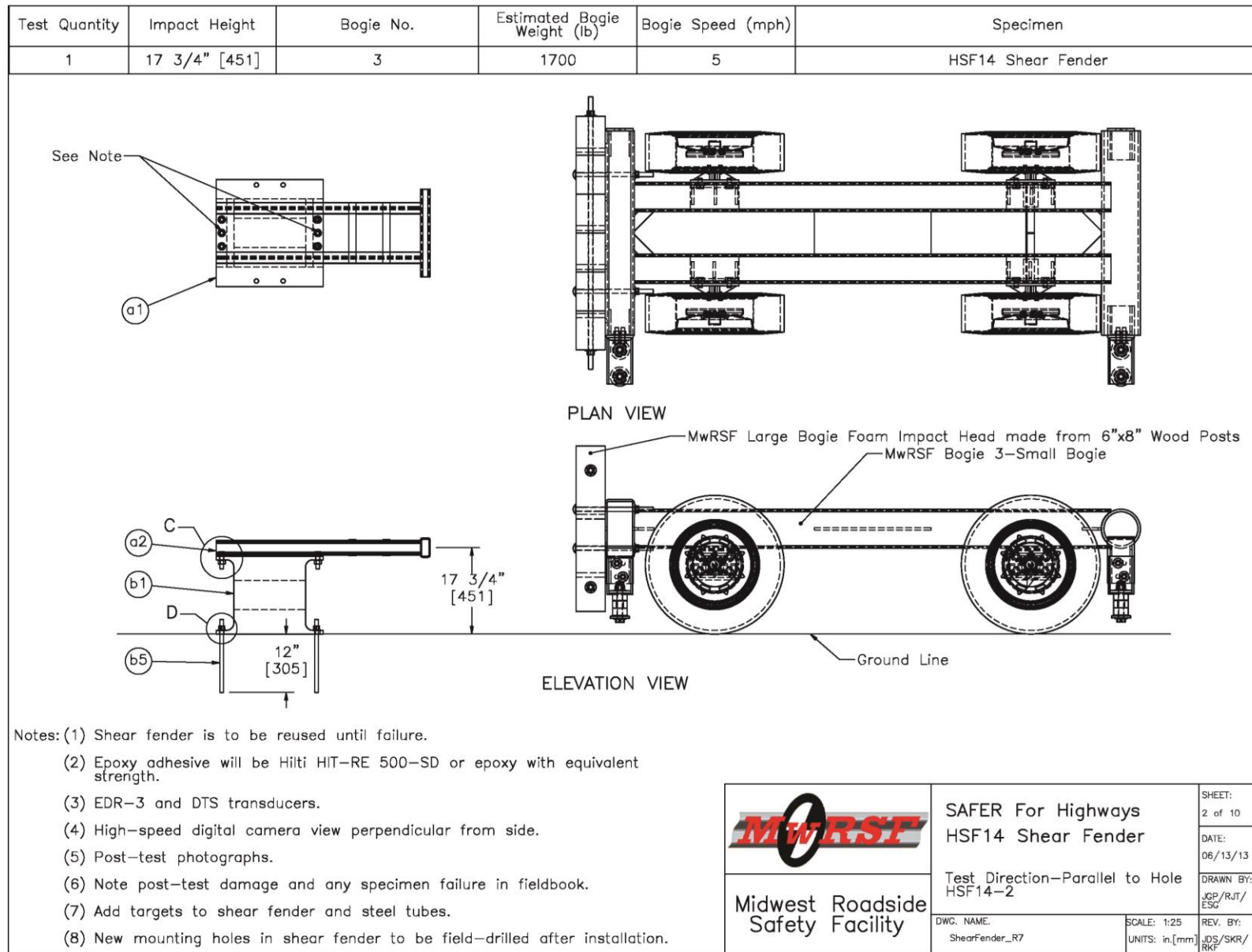


Figure 28. Bogie Testing Setup – Parallel to Hole, Test No. HSF14-2

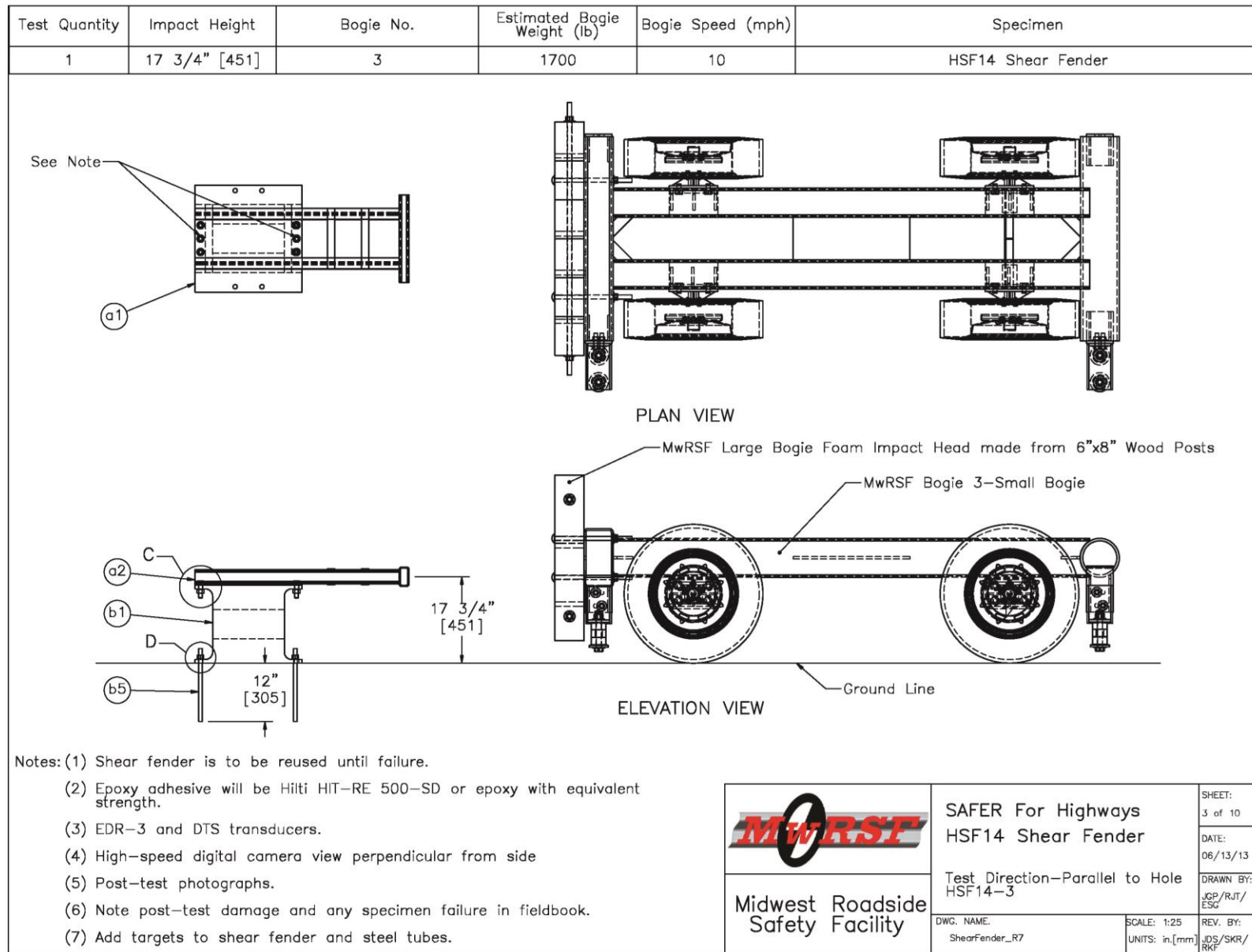


Figure 29. Bogie Testing Setup – Parallel to Hole, Test No. HSF14-3

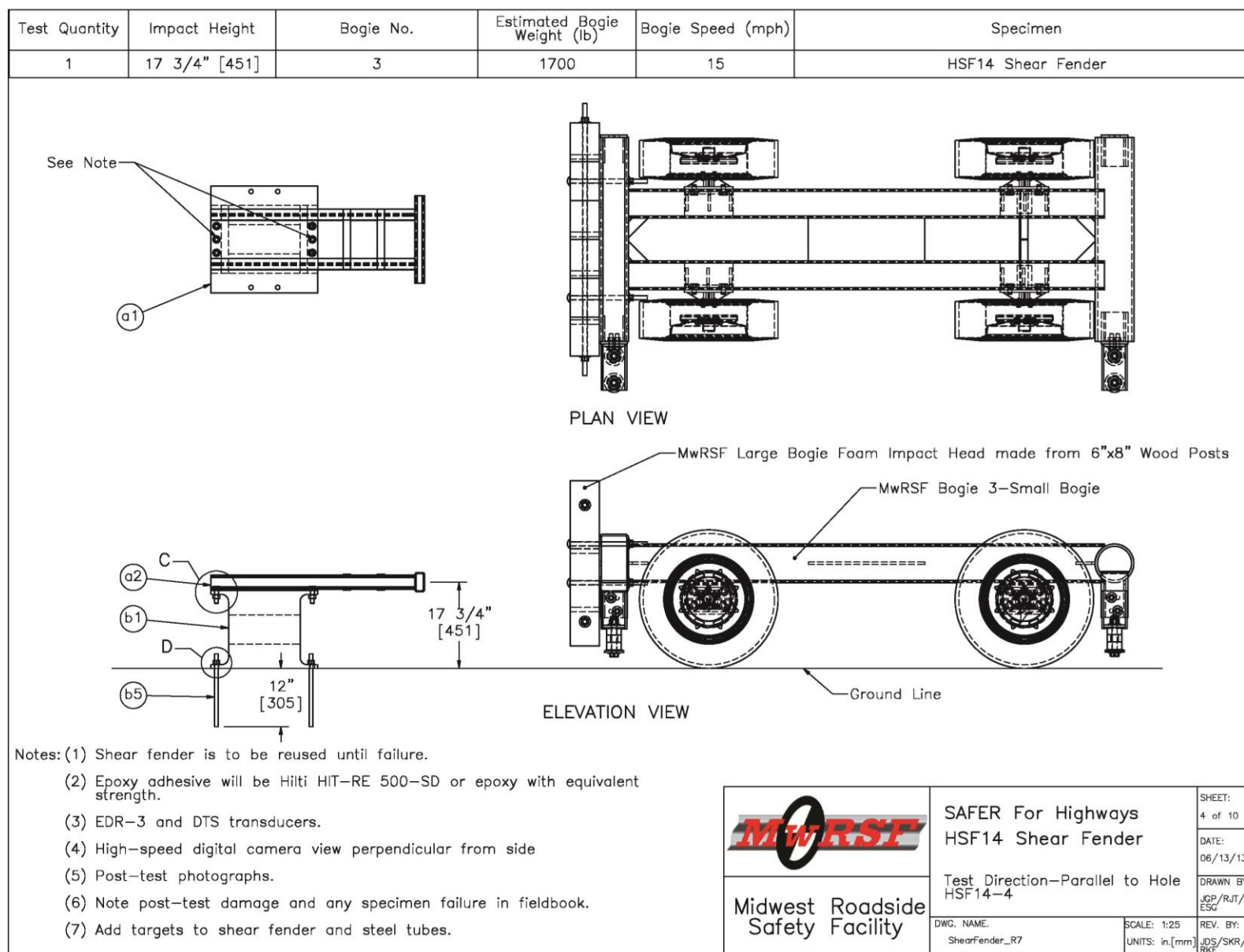


Figure 30. Bogie Testing Setup – Parallel to Hole, Test Nos. HSF14-4

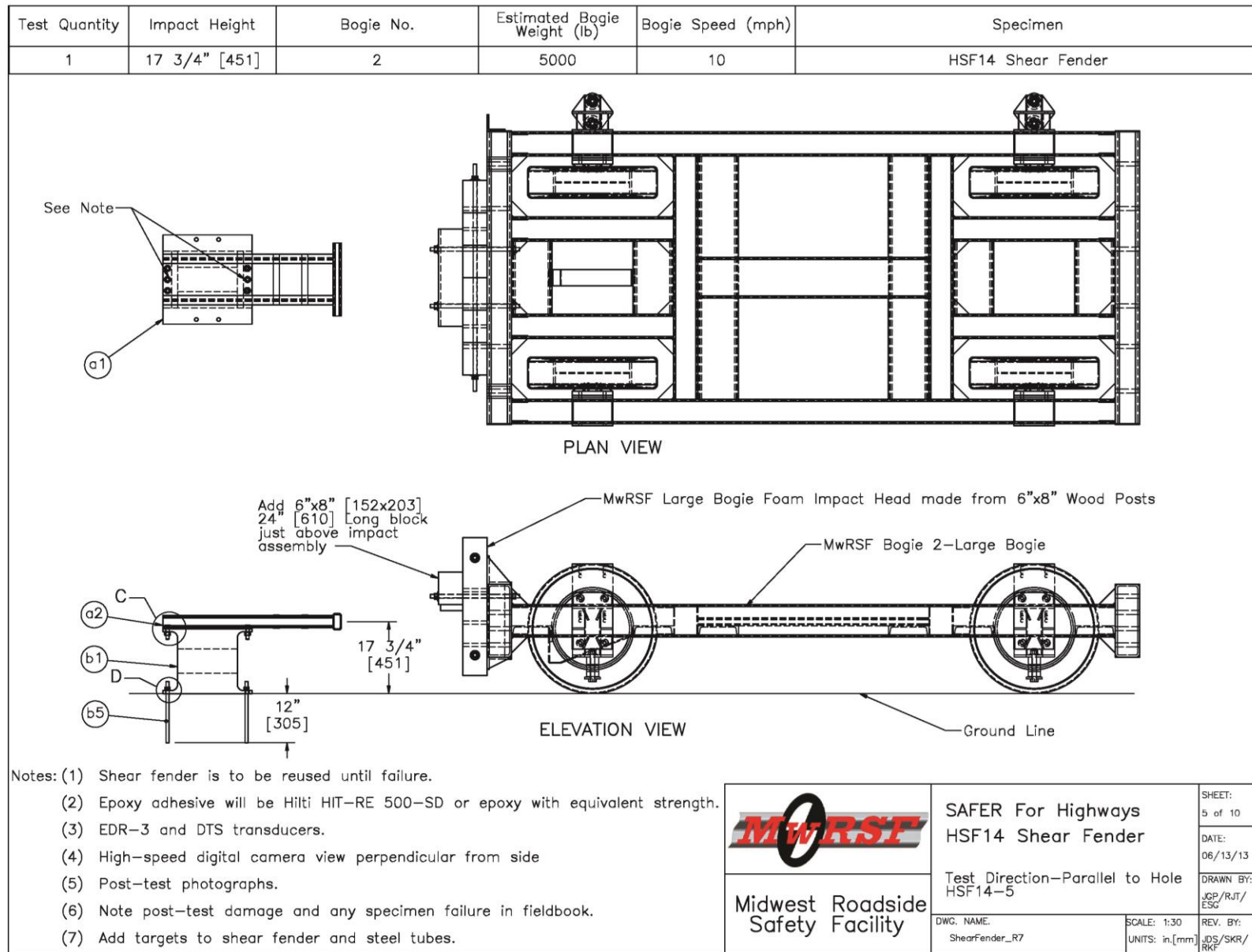


Figure 31. Bogie Testing Setup – Parallel to Hole, Test Nos. HSF14-5

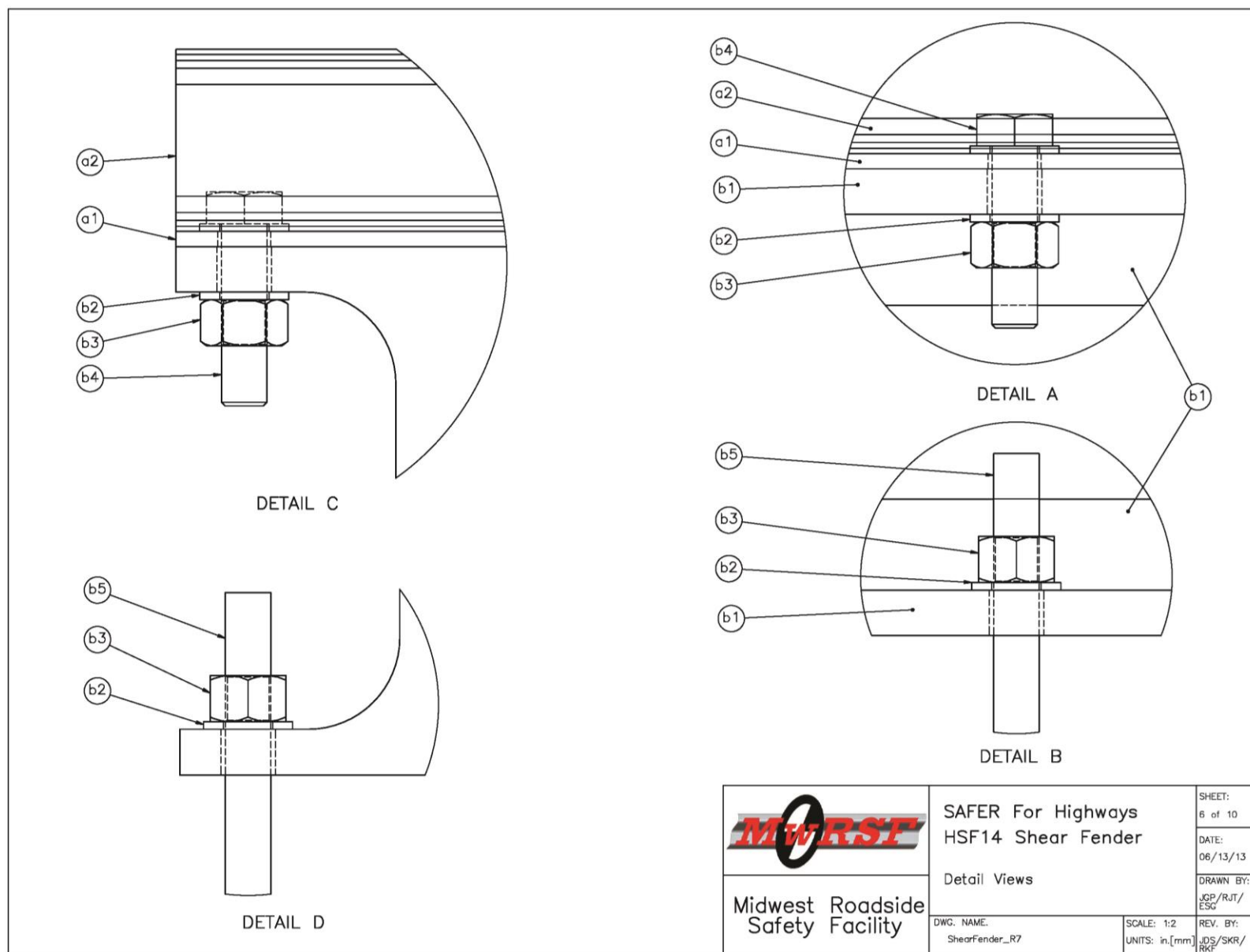


Figure 32. System Detail Views, Test Nos. HSF14-1 through HSF14-5

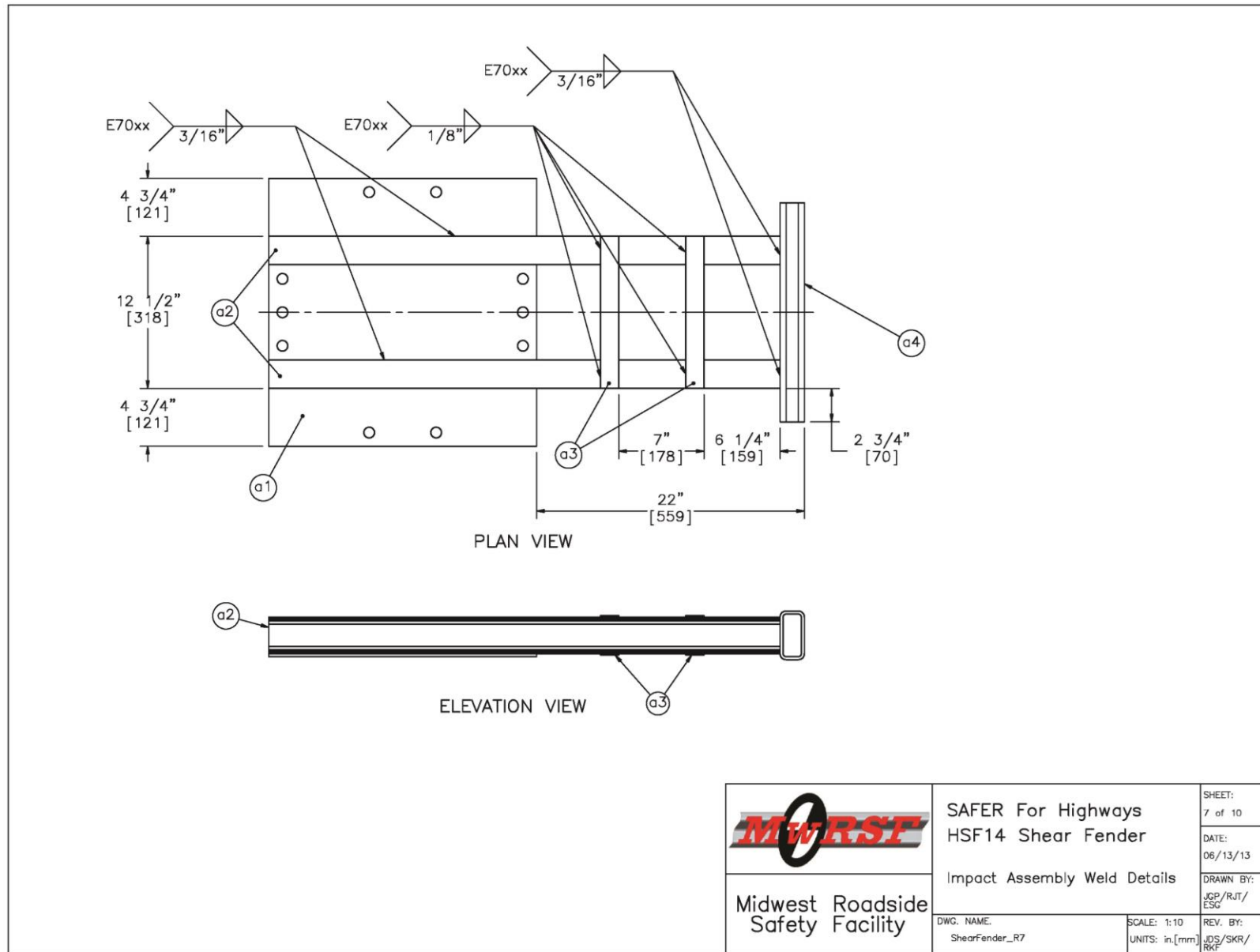


Figure 33. Impact Assembly Details, Test Nos. HSF14-1 through HSF14-5

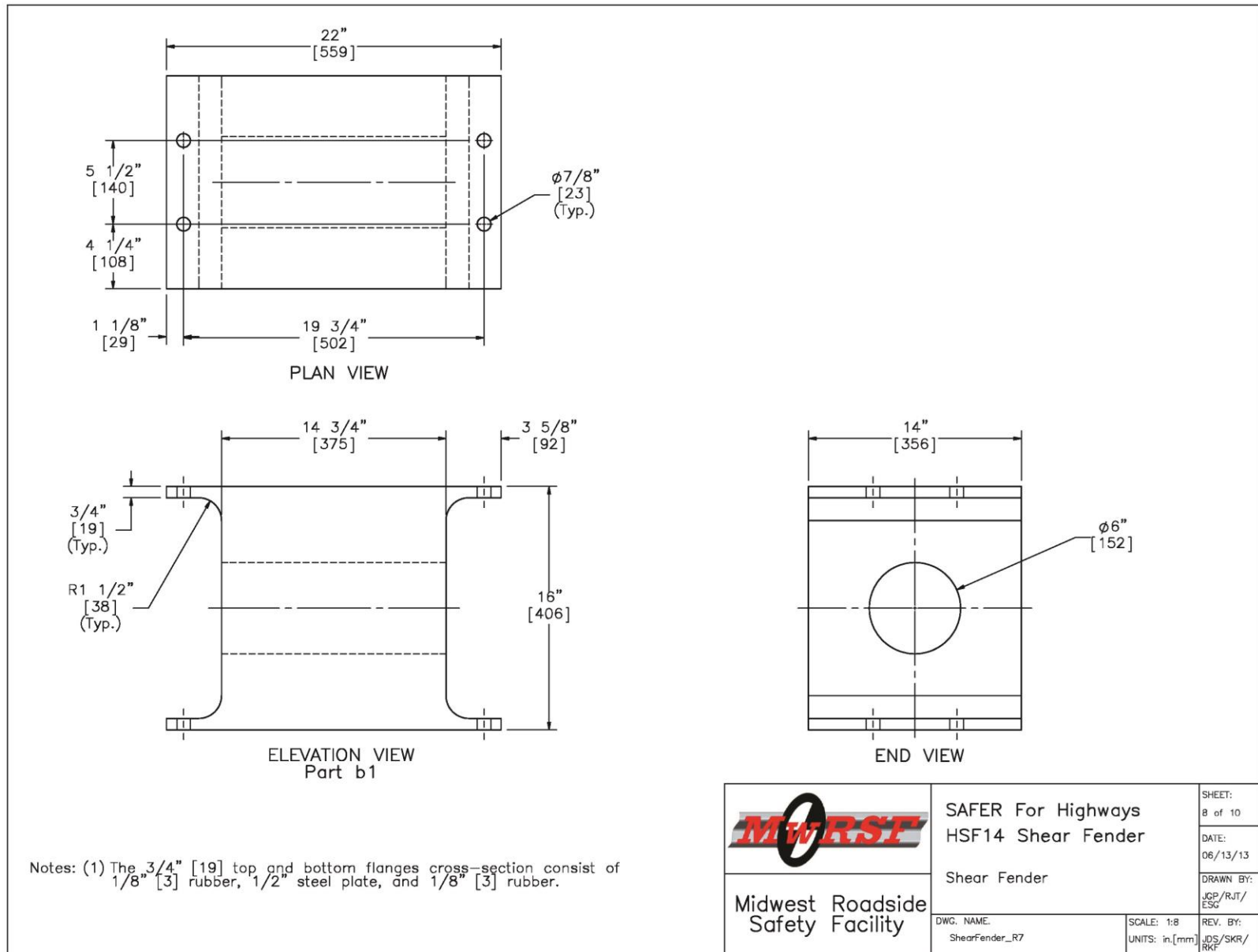


Figure 34. Shear Fender Details, Test Nos. HSF14-1 through HSF14-5

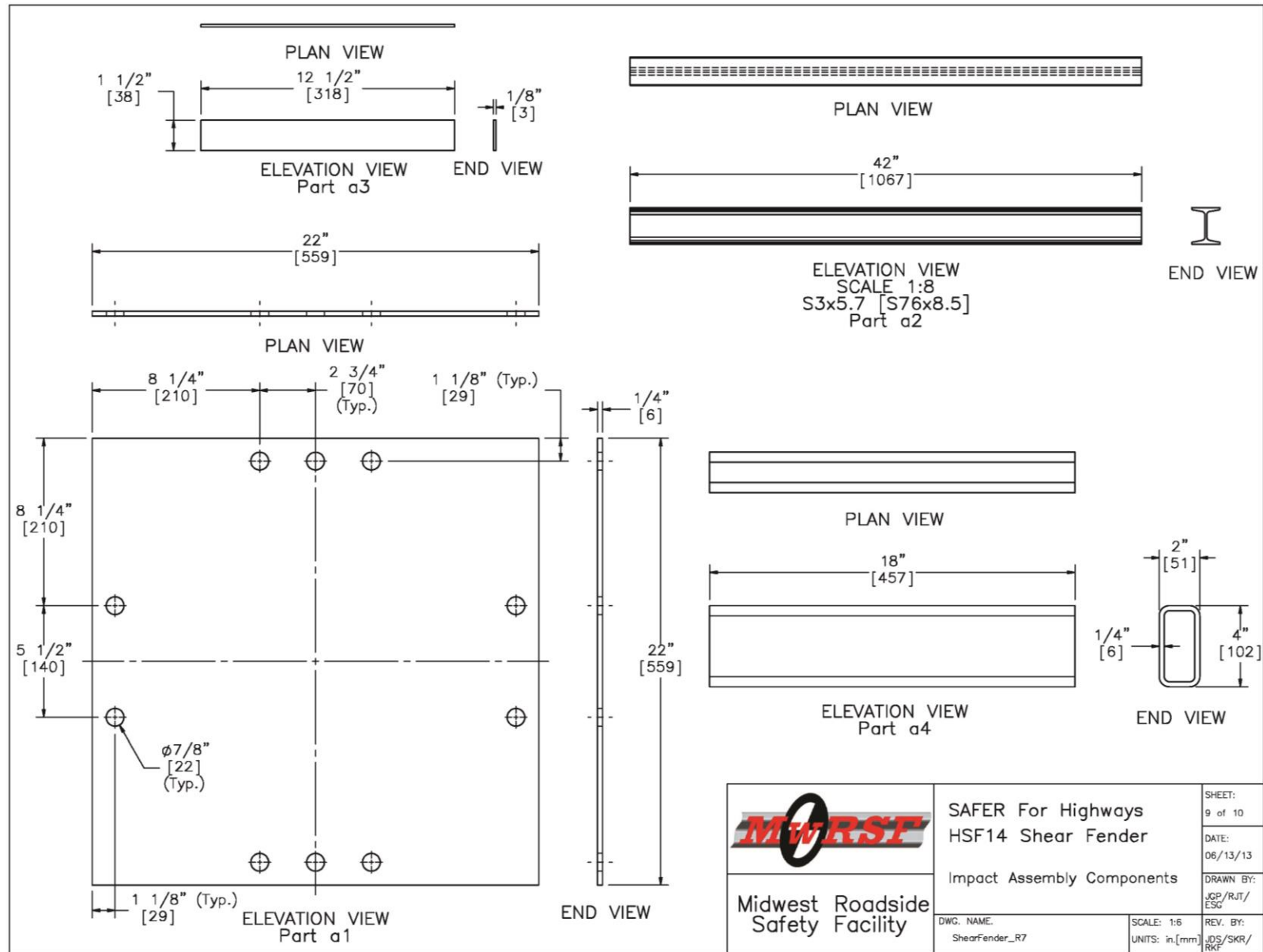


Figure 35. Impact Assembly Components, Test Nos. HSF14-1 through HSF14-5


Test Direction—Perpendicular to Hole			
Item No.	QTY.	Description	Material Specification
a1	1	22"x22"x1/4" [559x559x6] Steel Mounting Plate	ASTM A36
a2	2	42" [1067] Long S3x5.7 [S76x8.5] Steel Beam	ASTM A36/A992
a3	4	12 1/2" [318] Long 1/8"x1 1/2" [3x38] Strap	ASTM A36
a4	1	18" [457] Long 4"x2"x1/4" [102x51x6] Rectangular Tube	ASTM A500 Grade B
b1	1	Maritime HSF14 Shear Fender	ASTM D2000
b2	12	3/4" [19] Dia. Flat Washer	ASTM F436
b3	8	Dia. 3/4" [19] – 10 UNC Heavy Hex Nut	ASTM A563
b4	4	Dia. 3/4" [19] x 2" [51] Long – 10 UNC Heavy Hex Bolt	ASTM A325
b5	4	Dia. 3/4" [19] x 15" [381] Long – 10 UNC Threaded Rod	ASTM A193 type B7
Test Direction—Parallel to Hole			
Item No.	QTY.	Description	Material Specification
a1	1	22"x22"x1/4" [559x559x6] Steel Mounting Plate	ASTM A36
a2	2	42" [1067] Long S3x5.7 [S76x8.5] Steel Beam	ASTM A36/A992
a3	4	12 1/2" [318] Long 1/8"x1 1/2" [3x38] Strap	ASTM A36
a4	1	18" [457] Long 4"x2"x1/4" [102x51x6] Rectangular Tube	ASTM A500 Grade B
b4	6	Dia. 3/4" [19] x 2" [51] Long – 10 UNC Heavy Hex Bolt	ASTM A325
b1	1	Maritime HSF14 Shear Fender	ASTM D2000
b2	16	3/4" [19] Dia. Flat Washer	ASTM F436
b3	10	Dia. 3/4" [19] – 10 UNC Heavy Hex Nut	ASTM A563
b5	4	Dia. 3/4" [19] x 15" [381] Long – 10 UNC Threaded Rod	ASTM A193 type B7
		 SAFER For Highways HSF14 Shear Fender Bill of Materials	SHEET: 10 of 10 DATE: 06/13/13 DRAWN BY: JGP/RJT/ ESC
		DWG. NAME: ShearFender_R7	SCALE: 1:16 UNITS: in.[mm] REV. BY: JDS/SKR/ RKP
		Midwest Roadside Safety Facility	

Figure 36. Bill of Materials, Test Nos. HSF14-1 through HSF14-5



Figure 37. Bogie Setup, Test No. HSF14-1



Figure 38. Bogie Setup, Test Nos. HSF14-2 through HSF14-4

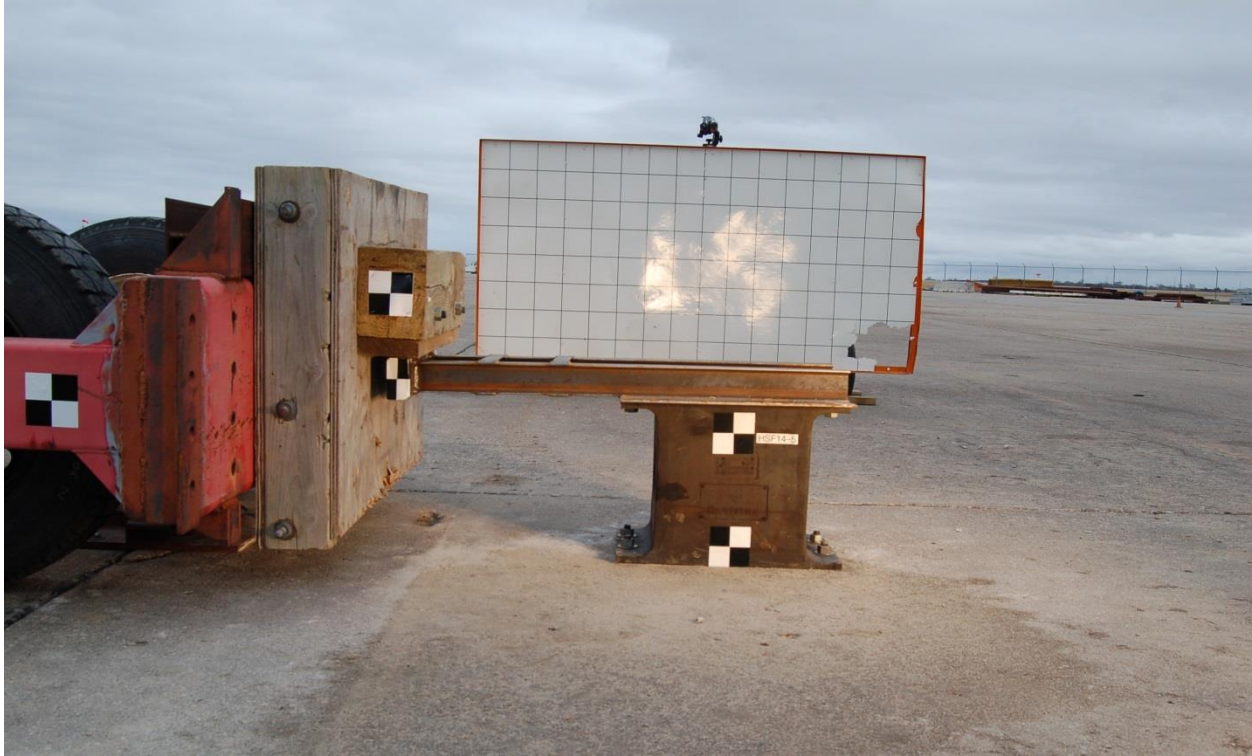


Figure 39. Bogie Setup Photograph, Test No. HSF14-5

4.3 Results

4.3.1 Test No. HSF14-1

The 1,818-lb (825-kg) bogie impacted the HSF14 shear fender laterally (perpendicular to hole) at 4.9 mph (7.9 km/h). The shear fender deflected in shear TO a maximum of 6.2 in. (158 mm) at 0.132 sec after impact. Upon post-test examination, the shear fender was not damaged and had no permanent set.

Force vs. deflection and energy vs. deflection curves created from the DTS accelerometer data are shown in Figure 40. Initially, inertial effects resulted in a high peak force over the first ½ in. (13 mm) of deflection. The force then returned to 0 kips through 2 in. (51 mm) of deflection due to the rebounding nature of rubber. From 2 in. to 6 in. (51 mm to 152 mm), the average force was approximately 4 kips (17.8 kN). At the maximum deflection of 6.2 in. (158

mm), the shear fender absorbed 17.8 k-in. (2.0 kJ) of energy. Sequential photographs are shown in Figure 41.

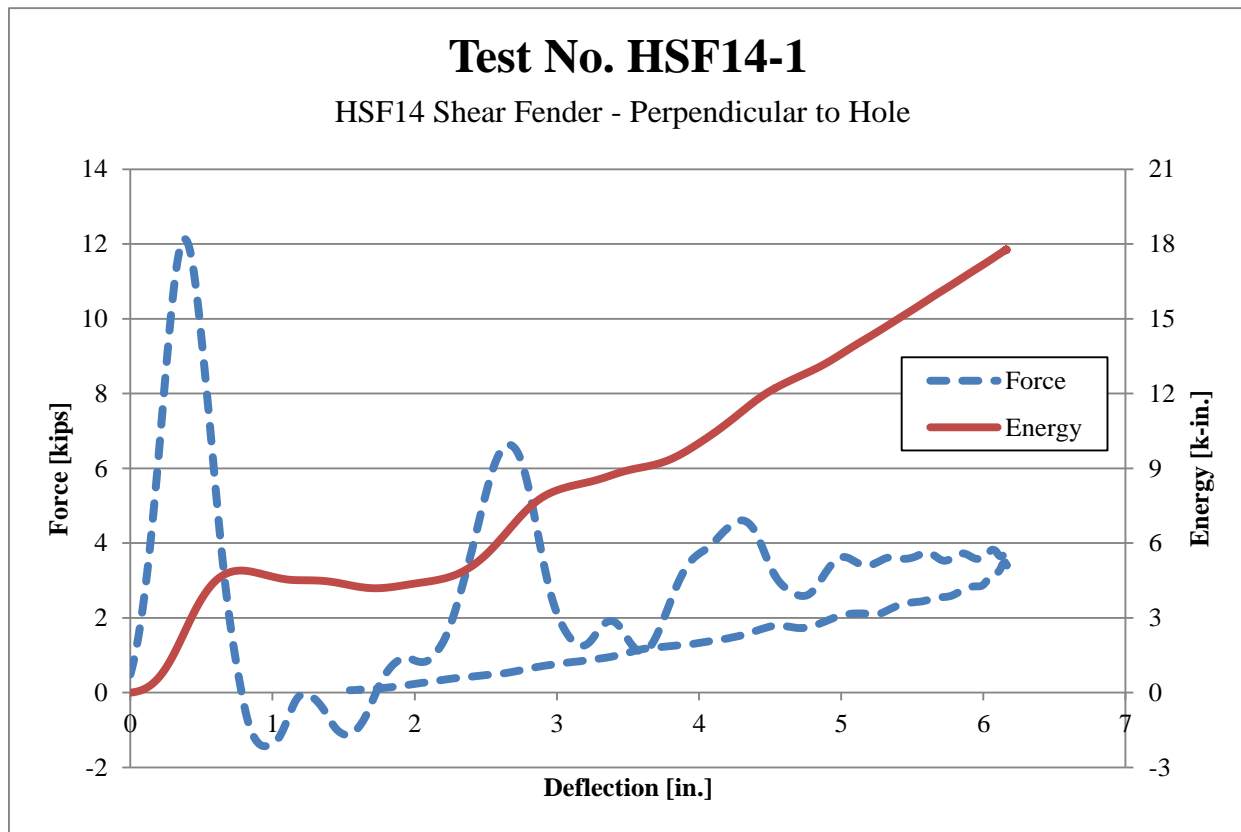
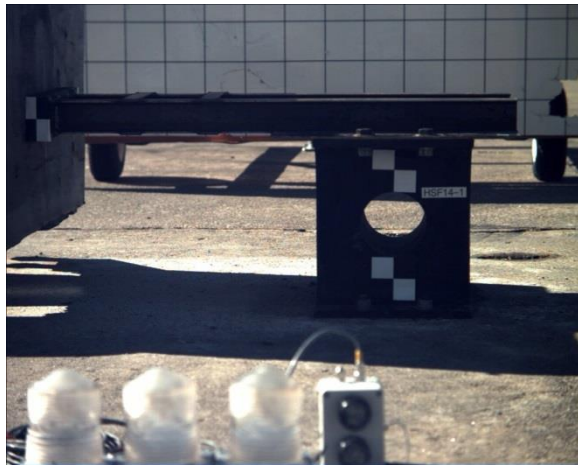


Figure 40. Force vs. Deflection and Energy vs. Deflection, Test No. HSF14-1



IMPACT



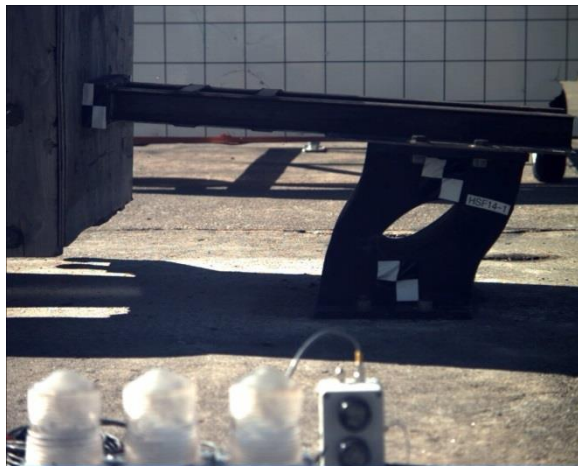
0.130 sec



0.040 sec



0.200 sec



0.080 sec



0.304 sec

Figure 41. Time-Sequential Photographs, Test No. HSF14-1

4.3.2 Test No. HSF14-2

The 1,818-lb (825-kg) bogie impacted a new HSF14 shear fender longitudinally (parallel to the hole) at 5.0 mph (8.0 km/h). The shear fender deflected in shear to a maximum of 5.3 in. (135 mm) at 0.110 sec after impact. Upon post-test examination, the shear fender was not damaged and had no permanent set.

Force vs. deflection and energy vs. deflection curves created from the DTS accelerometer data are shown in Figure 42. Initially, inertial effects resulted in a high peak force over the first 0.5 in. (13 mm) of deflection. The force then returned to 0 kips for the next 1 in. (25 mm) of deflection due to the rebounding nature of rubber. From 1.5 in. to 5.3 in. (38 mm to 135 mm), the average force was approximately 4 kips (17.8 kN). At the maximum deflection of 5.3 in. (135 mm), the shear fender had absorbed 18.2 k-in. (2.1 kJ) of energy. Sequential photographs are shown in Figure 43.

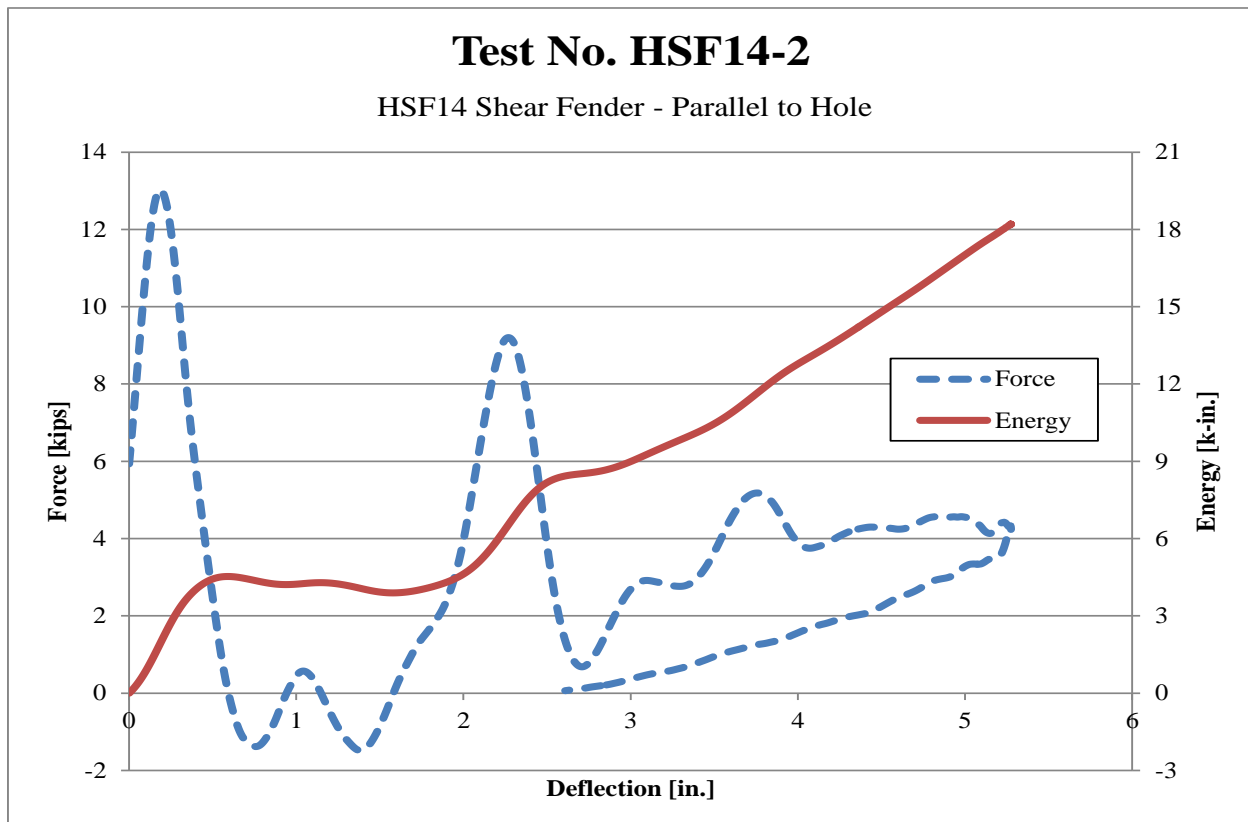


Figure 42. Force vs. Deflection and Energy vs. Deflection, Test No. HSF14-2

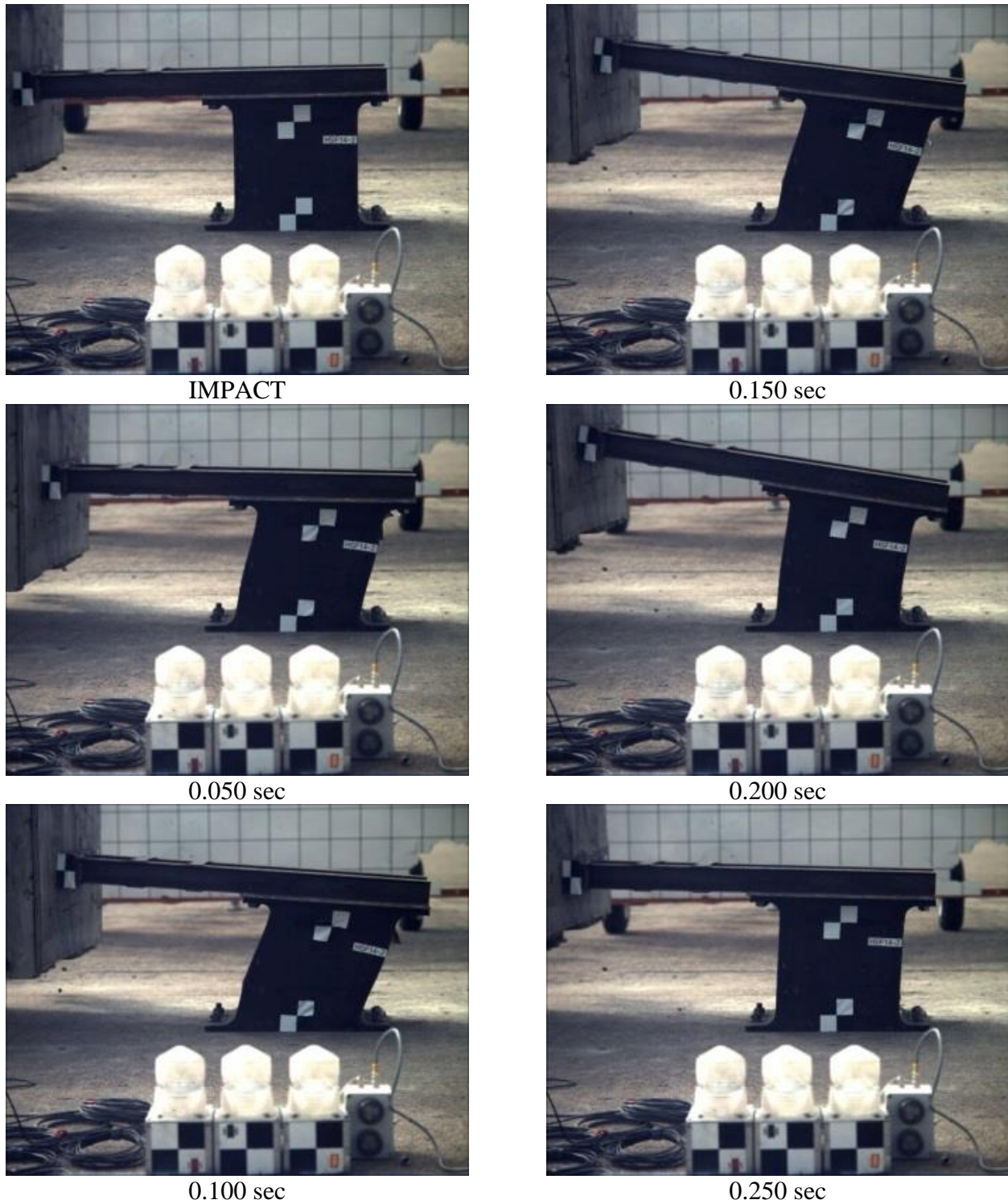


Figure 43. Time-Sequential Photographs, Test No. HSF14-2

4.3.3 Test No. HSF14-3

The 1,818-lb (825-kg) bogie impacted the HSF14 shear fender, which was used in HSF14-2, longitudinally (parallel to the hole) at 9.1 mph (14.6 km/h). The shear fender deflected in shear and reached a maximum deflection of 10.5 in. (267 mm) at 0.124 sec after impact. Upon post-test examination, the shear fender was not damaged and had no permanent set.

Force vs. deflection and energy vs. deflection curves created from the DTS accelerometer data are shown in Figure 44. Initially, inertial effects resulted in a high peak force over the first 1 in. (25 mm) of deflection. The force then returned to 0 kips for the next 2 in. (51 mm) of deflection due to the rebounding nature of rubber. From 3 in. to 10.5 in. (76 mm to 267 mm), the average force was approximately 6.5 kips (28.9 kN). At a maximum deflection of 10.5 in. (267 mm), the shear fender had absorbed 60.5 k-in. (6.8 kJ) of energy. Sequential photographs are shown in Figure 45.

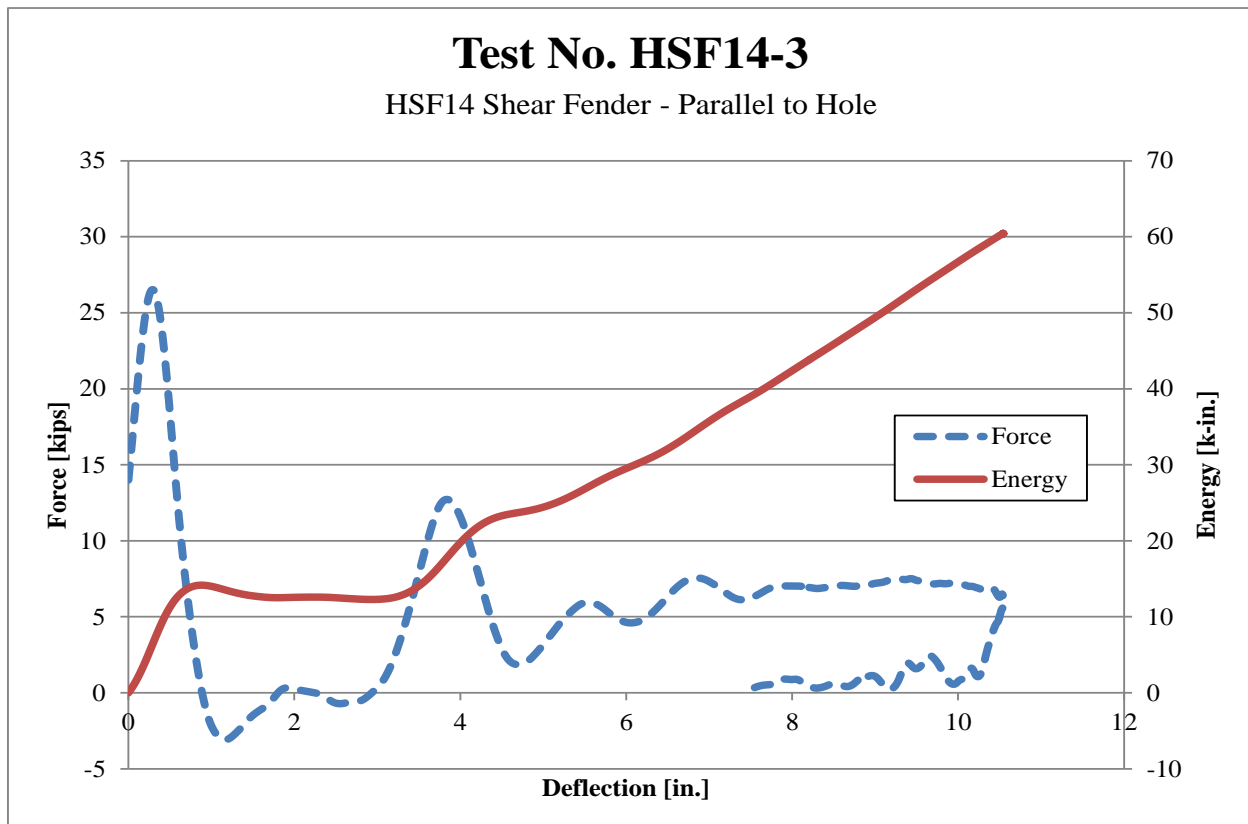


Figure 44. Force vs. Deflection and Energy vs. Deflection, Test No. HSF14-3

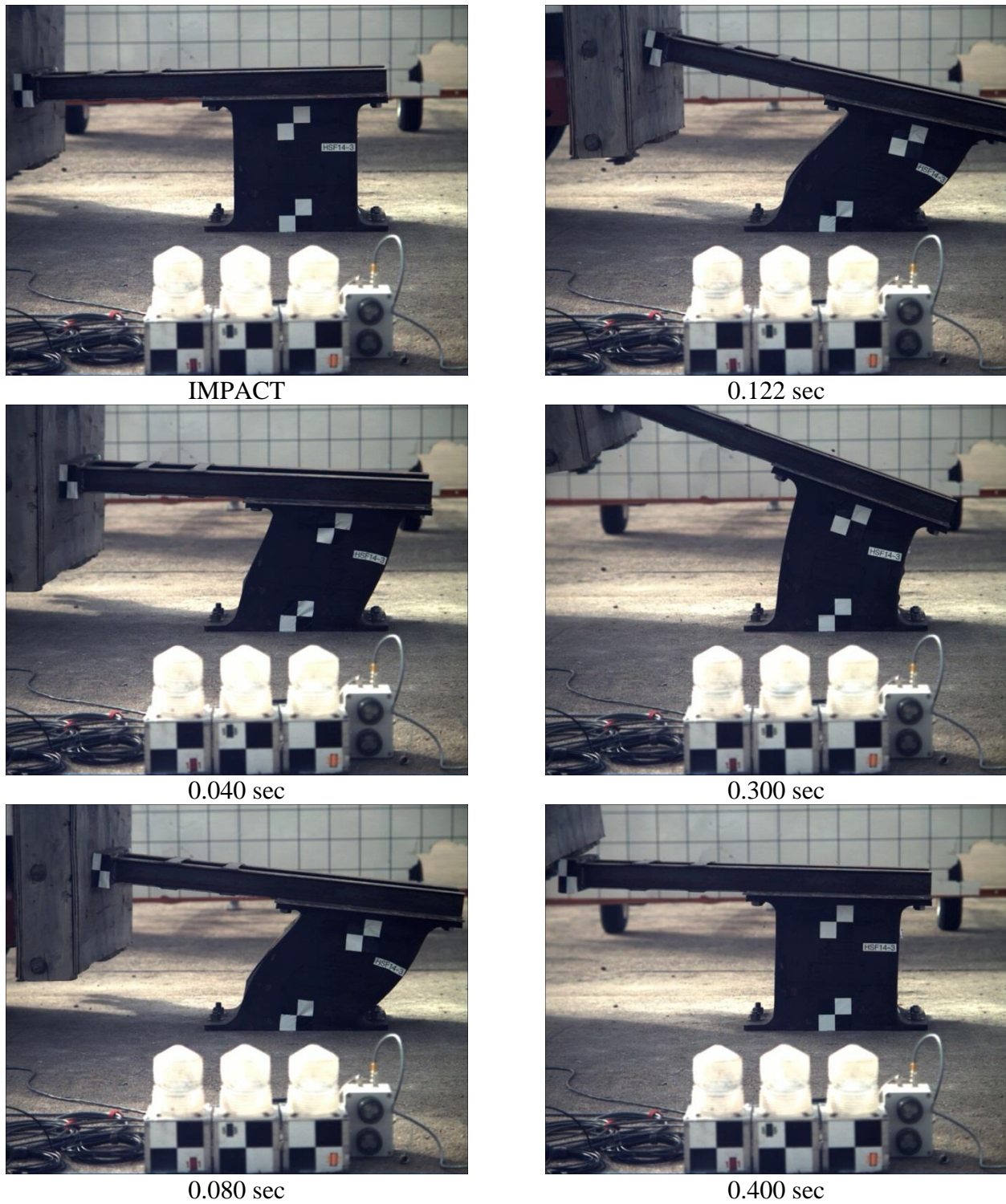


Figure 45. Time-Sequential Photographs, Test No. HSF14-3

4.3.4 Test No. HSF14-4

The 1,818-lb (825-kg) bogie impacted the HSF14 shear fender, which was used in test no. HSF14-3, longitudinally (parallel to the hole) at 14.3 mph (23.0 km/h). The maximum longitudinal displacement of the bogie was 37.3 in. (947 mm) at 0.274 sec after impact. However, the steel impact structure rotated and caught on top of the bogie head, and the maximum deflection of the shear fender was approximately 13 in. (330 mm), as determined from high-speed video. The shear fender was subjected to shear, torsional, and tensile loading. Upon post-test examination, the shear fender was not damaged and had no permanent set.

Force vs. deflection and energy vs. deflection curves created from the DTS accelerometer data are shown in Figure 46. Initially, inertial effects resulted in a high peak force over the first 1 in. (25 mm) of deflection. The force then returned to 0 kips for the next 3 in. (76 mm) of deflection due to the rebounding nature of rubber. From 4 in. to 13 in. (102 mm to 330 mm), the average force was approximately 7.0 kips (31.1 kN). At the shear fender's maximum deflection of 13 in. (330 mm), the shear fender had absorbed 90.2 k-in. (10.2 kJ) of energy. The steel impact structure slide up the face of the bogie head between 15 in. and 28 in. (381 mm to 711 mm) of deflection and the shear fender was mostly unloaded, so the force was approximately zero. From 28 in. to 37.3 in. (711 mm to 947 mm), the impact head contacted the face of the shear fender, and the average force was approximately 6.2 kips (27.6 kN). At the bogie's maximum deflection of 37.3 in. (947 mm), the shear fender had absorbed 149.7 k-in. (16.9 kJ) of energy. Sequential photographs are shown in Figure 43.

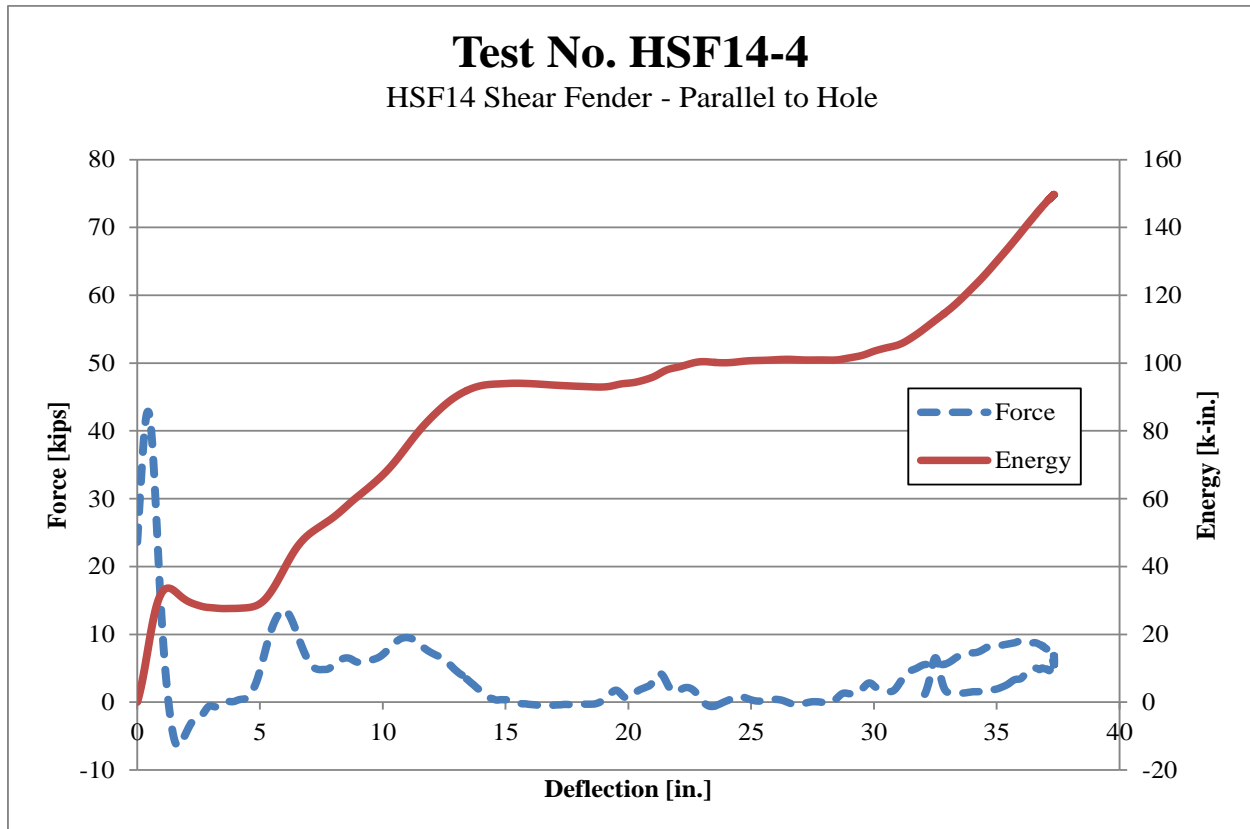


Figure 46. Force vs. Deflection and Energy vs. Deflection, Test No. HSF14-4

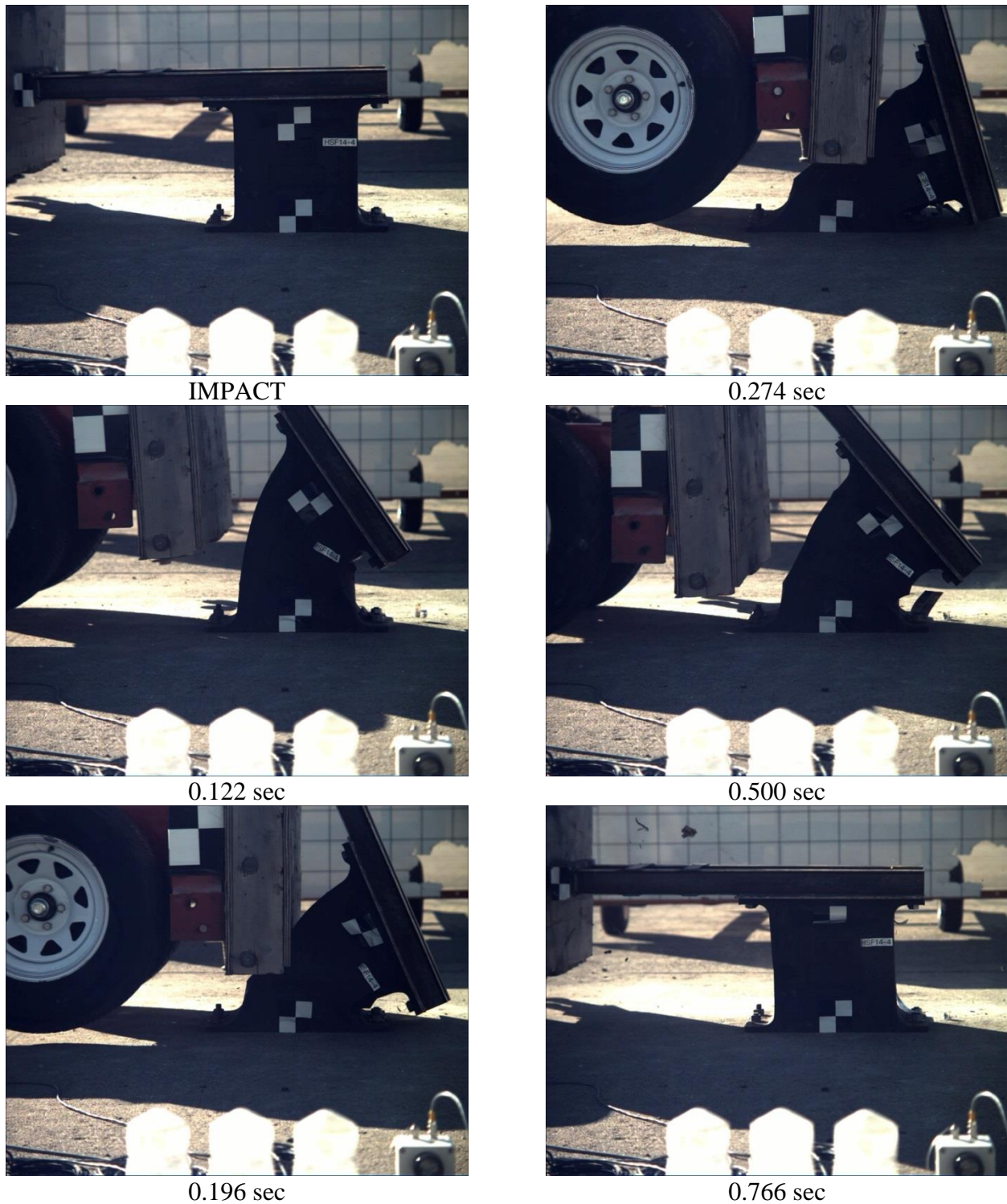


Figure 47. Time-Sequential Photographs, Test No. HSF14-4

4.3.5 Test No. HSF14-5

The 4,946-lb (2,243-kg) bogie impacted the HSF14 shear fender, which was used in test no. HSF14-4, longitudinally (parallel to the hole) at 11.9 mph (19.2 km/h). The maximum longitudinal displacement of the bogie was 28.5 in. (724 mm) at 0.236 sec after impact. The shear fender deflected approximately 20 in. (508 mm), as measured from digital video. Force vs. deflection and energy vs. deflection curves created from the DTS accelerometer data are shown in Figure 48. Initially, inertial effects resulted in a high peak force over the first 1 in. (25 mm) of deflection. The force then oscillated around zero over for the next 4 in. (102 mm) of deflection due to the rebounding nature of rubber. From 5 in. to 28.5 in. (127 mm to 724 mm), the average force was approximately 9.5 kips (42.3 kN). After approximately 20 in. (508 mm) of deflection, the steel impact structure slid up the face of the bogie, and the front of the bogie became airborne. Subsequently, the front of the bogie landed on top of the shear fender and steel-frame structure. At a maximum deflection of 28.5 in. (724 mm), the shear fender had absorbed 268.4 k-in. (30.3 kJ) of energy. Sequential photographs are shown in Figure 49. Post-impact photographs immediately after the test and after removal of the bogie are shown in Figure 50.

Upon post-test examination, slight permanent set was found. The impact-side height from the ground to the bottom of the impact plate was compressed $2\frac{1}{4}$ in. (57 mm), while the non-impact-side height was compressed $1\frac{5}{8}$ in. (41 mm) with the bogie resting on top of the shear fender. Upon removal of the bogie, the front of the shear fender was $\frac{1}{2}$ in. (13 mm) shorter and the back of the shear fender was $\frac{1}{8}$ in. (3 mm) taller. The shear fender later fully restored.

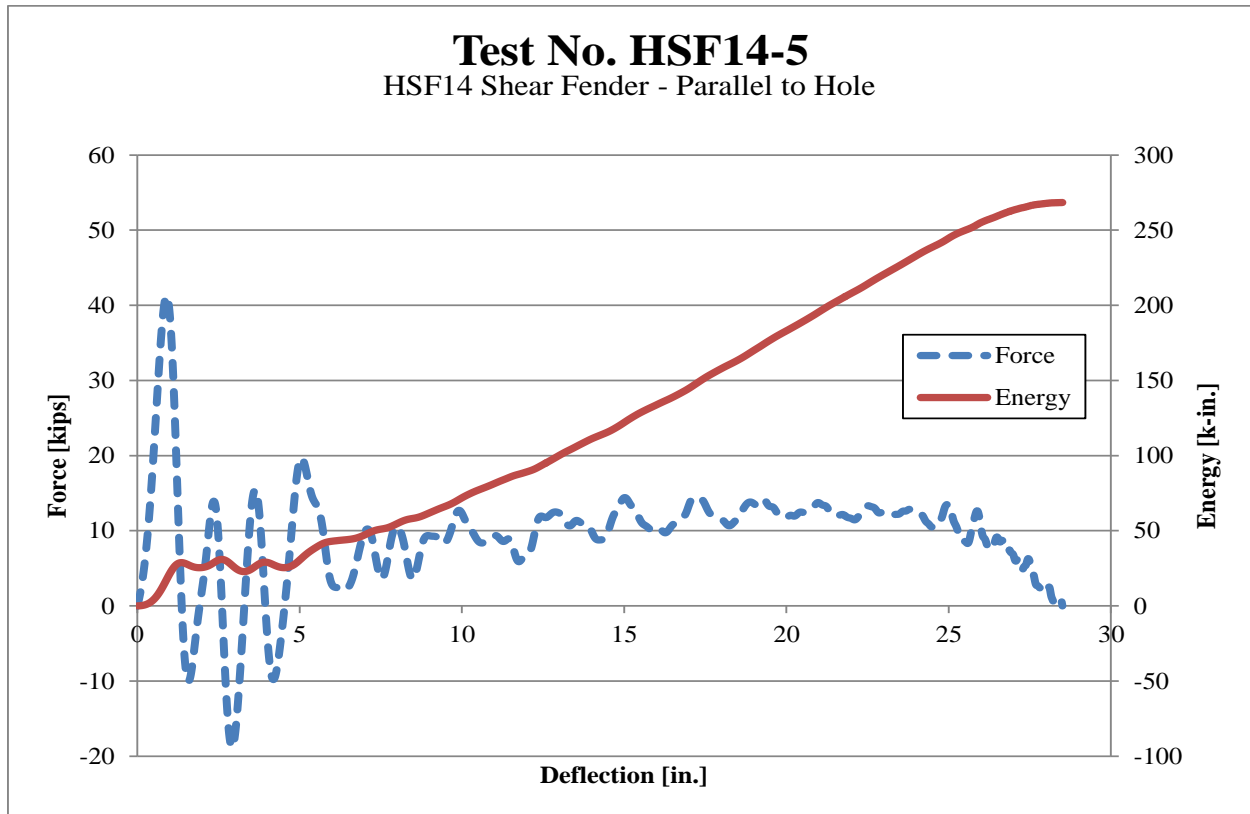


Figure 48. Force vs. Deflection and Energy vs. Deflection, Test No. HSF14-5



Figure 49. Time-Sequential Photographs, Test No. HSF14-5



Figure 50. Post-Impact Damage, Test No. HSF14-5

4.4 Discussion

Test nos. HSF14-1 through HSF14-5 were conducted on the HSF14 marine shear fender manufactured by Maritime International, Inc. The dynamic results from the bogie tests are summarized in Table 7. Force vs. deflection and energy vs. deflection plots from are shown in Figures 51 through 54. The bogie impact speed varied between 4.9 mph and 14.3 mph (7.9 km/h and 23.0 km/h). The peak energy absorbed by the shear fenders varied between 17.8 k-in. and 268.4 k-in. (2.0 kJ and 30.3 kJ).

Table 7. Dynamic Testing Results

Test No.	Bogie Weight lb (kg)	Impact Direction	Dimensions Height x Width x Length in. (mm)	Surface Temp. °F (°C)	Impact Velocity mph (km/h)	Max. Deflection in. (mm)	Peak Force kips (kN)	Total Energy k-in. (kJ)
HSF14-1	1,818 (825)	Lateral	16 x 14 x 22 (406 x 356 x 559)	84 (29)	4.9 (7.9)	6.2 (157)	12.1 (53.8)	17.8 (2.0)
HSF14-2	1,818 (825)	Longitudinal	16 x 14 x 22 (406 x 356 x 559)	73 (23)	5.0 (8.0)	5.3 (135)	13.0 (57.8)	18.2 (2.1)
HSF14-3	1,818 (825)	Longitudinal	16 x 14 x 22 (406 x 356 x 559)	66 (19)	9.1 (14.6)	10.5 (267)	26.5 (117.9)	60.5 (6.8)
HSF14-4	1,818 (825)	Longitudinal	16 x 14 x 22 (406 x 356 x 559)	75 (24)	14.3 (23.0)	37.3 (947)	42.9 (190.8)	149.7 (16.9)
HSF14-5	4,946 (2,243)	Longitudinal	16 x 14 x 22 (406 x 356 x 559)	138 (59)	11.9 (19.2)	28.5 (724)	41.2 (183.3)	268.4 (30.3)

Inertial effects at the beginning of each impact were observed during all five bogie tests. As illustrated in Figures 51 and 53, the recorded data from each of the tests showed a large force spike over the first 2 in. (51 mm) of deflection. These force spikes were all different in magnitude but extended over approximately the same duration.

Test nos. HSF14-1 and HSF14-2 had approximately the same impact velocity and surface temperature. The shear fender in test no. HSF14-1 was impacted laterally, and the shear fender in test no. HSF14-2 was impacted longitudinally. The force vs. deflection and energy vs. deflection curves are shown in Figures 51 and 52. The dynamic properties were very similar for the shear fenders in test nos. HSF14-1 and HSF14-2. However, the laterally-impacted shear fender deflected almost 1 in. (25 mm) farther than the longitudinally-impacted shear fender, but it did not absorb additional energy. Therefore, the longitudinal impact direction is more efficient than the lateral impact direction.

In test nos. HSF14-2 through HSF14-5, the shear fenders were impacted longitudinally. The force vs. deflection and energy vs. deflection curves are shown in Figures 53 and 54. The initial stiffness of the shear fenders were all approximately the same. Due to the rebounding nature of rubber, the rotation of the steel-frame structure, and the different impact speeds, the calculated forces varied between the tests. The average forces ranged from 4 kips (17.8 kN) in test no. HSF14-2 through 9.5 kips (42.3 kN) in test no. HSF14-5.

Schmidt, et al. estimated that each energy absorber would need to absorb 52.8 k-in. to 211.2 k-in. (6.0 kJ to 23.9 kJ) of kinetic energy when placed in a roadside/median barrier that was intended to provide a 30 percent reduction in lateral acceleration for 2270P crash events at a velocity of 62 mph (100 km/h) and at an angle of 25 degrees [1]. The shear fenders in test nos. HSF14-3, HSF14-4, and HSF14-5 all absorbed energies within the desired range. The deflection of the energy-absorbing roadside/median barrier was estimated to be 8 in. to 10 in. (203 mm to 254 mm). Approximately 54.0 k-in. (6.1 kJ) and 55.2 k-in. (6.2 kJ) of energy were absorbed at 8 in. (203 mm) of deflection in test nos. HSF14-4 and HSF14-5, respectively. Approximately 67.2 k-in. (7.6 kJ) and 72.0 k-in. (8.1 kJ) were absorbed at 10 in. (254 mm) of deflection in test nos. HSF14-4 and HSF14-5, respectively. Even more energy was absorbed beyond 10 in. (254 mm) of deflection, but greater deflections were not desired in the new barrier.

No conclusions could be drawn about the affect of temperature on the performance of the rubber shear fenders. In test nos. HSF14-1 through HSF14-4, the surface temperatures of the shear fender were similar. The surface temperature of the shear fender was significantly hotter in test no. HSF14-5, but a larger bogie was used and no temperature-specific changes in performance were discernible.

The shear fenders fully restored to their original dimensions after each impact. In test no. HSF14-5, the bogie landed on top of the shear fender, which applied a constant compression load

on it for several minutes. Upon removal of the bogie, a maximum deformation of ½ in. (13 mm) remained, but the shear fender later restored to its original dimensions. The shear fenders were not expected to have any long-term loads other than the weight of the beam. Therefore, the shear fenders should fully restore after an impact event.

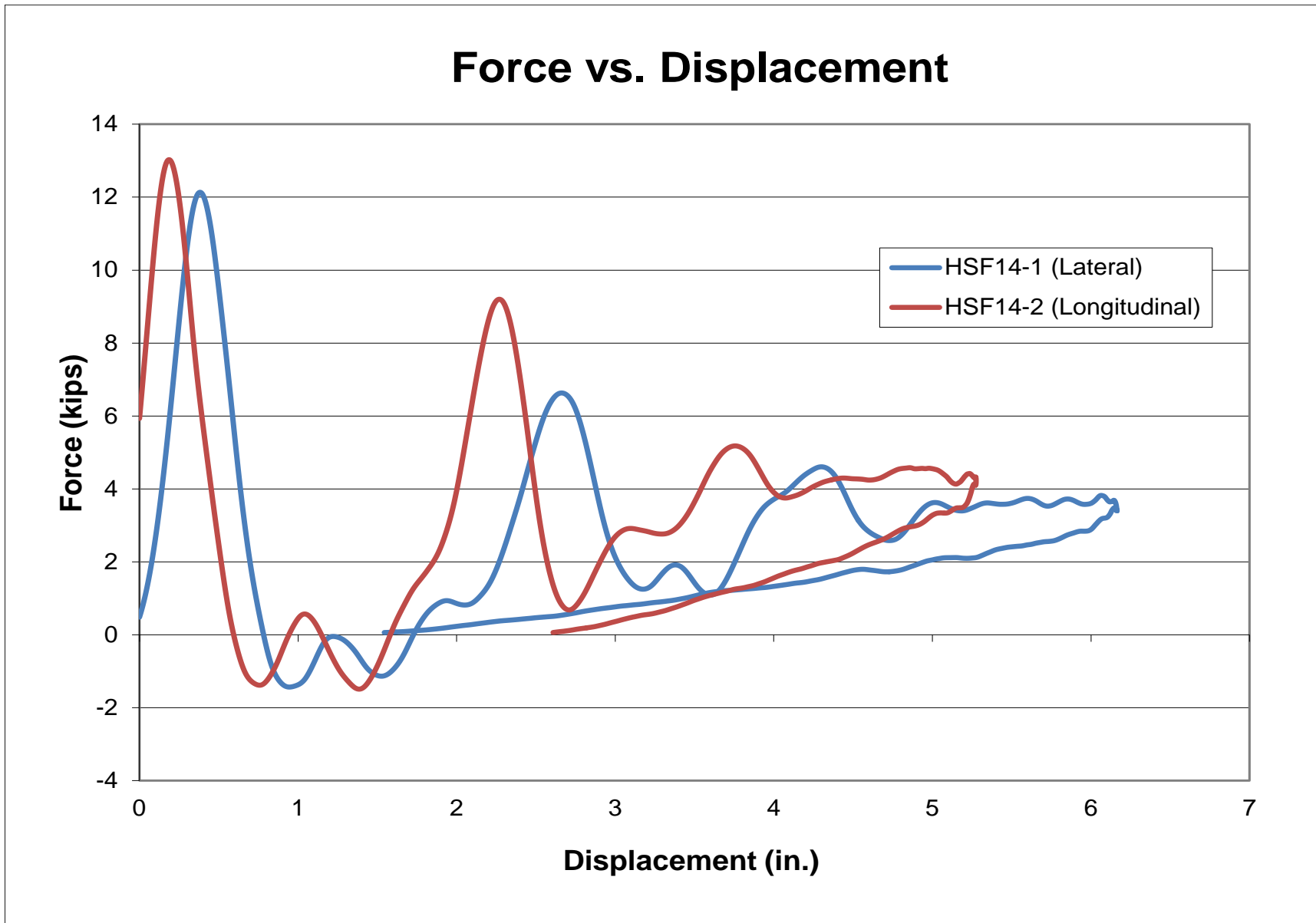


Figure 51. Force vs. Deflection, Test nos. HSF14-1 and HSF14-2

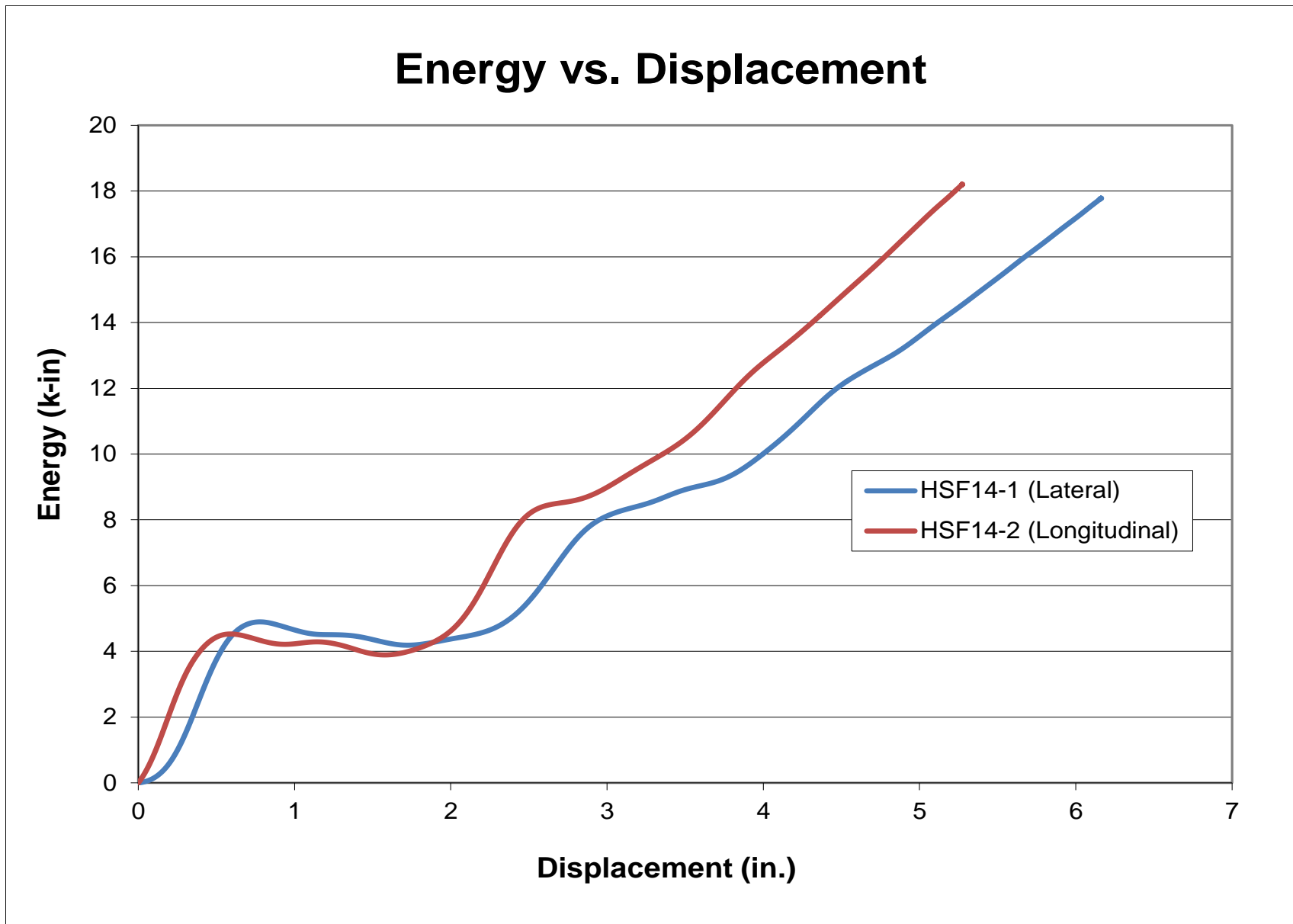


Figure 52. Energy vs. Deflection, Test Nos. HSF14-1 and HSF14-2

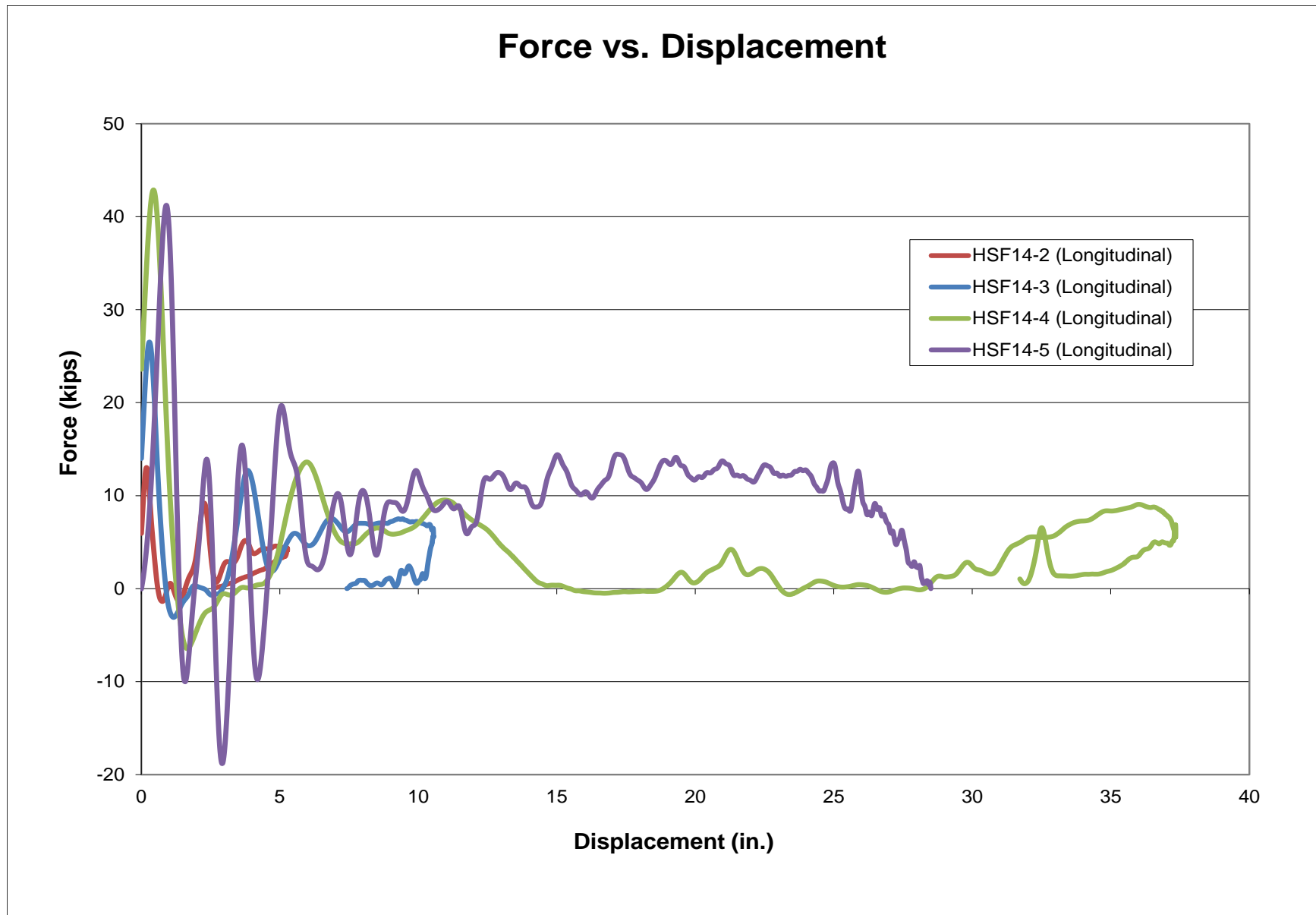


Figure 53. Force vs. Deflection, Test nos. HSF14-2 through HSF14-5

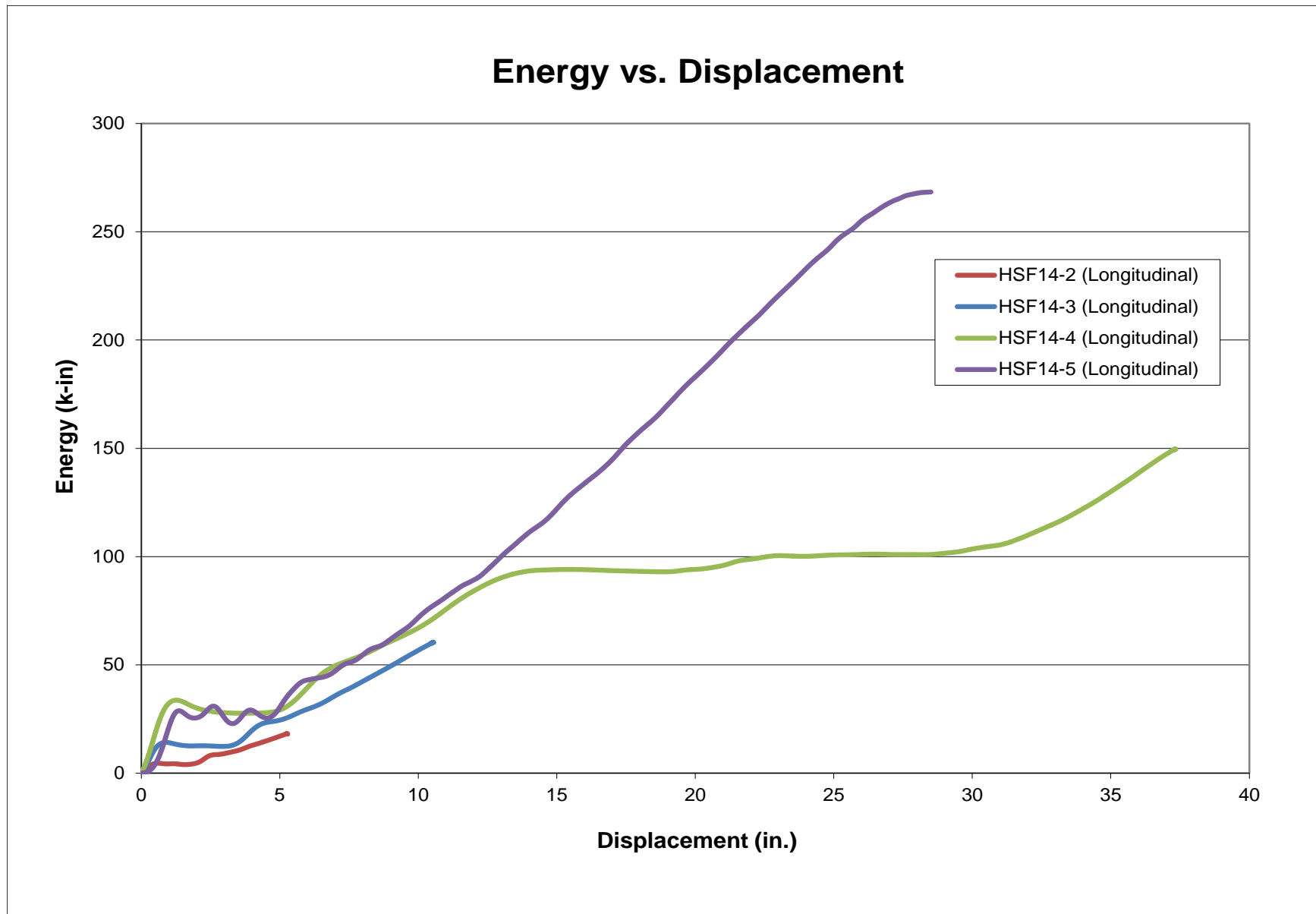


Figure 54. Energy vs. Deflection, Test nos. HSF14-2 through HSF14-5

5 RUBBER-CYLINDER RETROFIT SYSTEM - COMPONENT TESTING

5.1 Purpose

A dynamic bogie test was conducted on a prototype rubber-cylinder retrofit barrier system to determine load distribution, system deflection, and energy absorption for multiple cylinders.

5.2 Scope

A bogie test was conducted on a 27-ft (8.2-m) long prototype rubber-cylinder retrofit barrier system. The bogie impacted the system at a 90-degree angle with the target impact location at the midspan between the middle two rubber cylinders. The target impact speed was 18 mph (29.0 km/h). The impact height was 21½ in. (546 mm) above the ground line. Four 2-in. (51-mm) thick x 10-in. (254-mm) long rubber cylinders were spaced at 96 in. (2,438 mm) along a 32-in. (813-mm) tall New Jersey-shaped concrete barrier. Two ASTM A500 Grade B 6-in. x 6-in. x 3/16 in. thick (152-mm x 152-mm x 5-mm) steel tubes were placed on the front face of the cylinders. The tube hardware was selected from existing on-site remnants from prior research and development studies. The splice could not develop the full bending strength of the tube sections. However, it was deemed adequate for the concept evaluation test. The test matrix and test setup are shown in Figures 55 through 62. Testing setup photographs are shown in Figure 63.

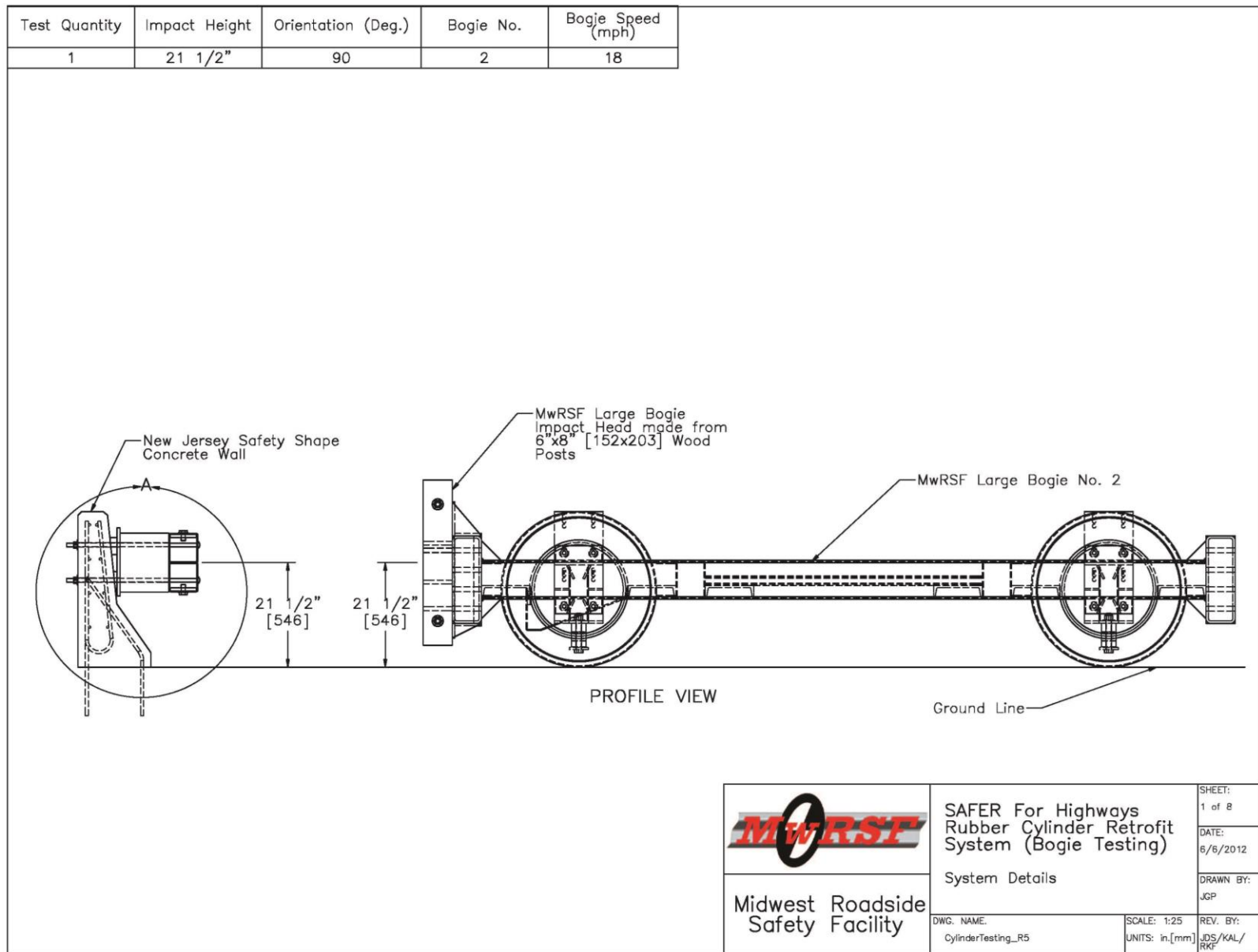


Figure 55. Bogie Testing Matrix and Setup, Test No. SFHC-1

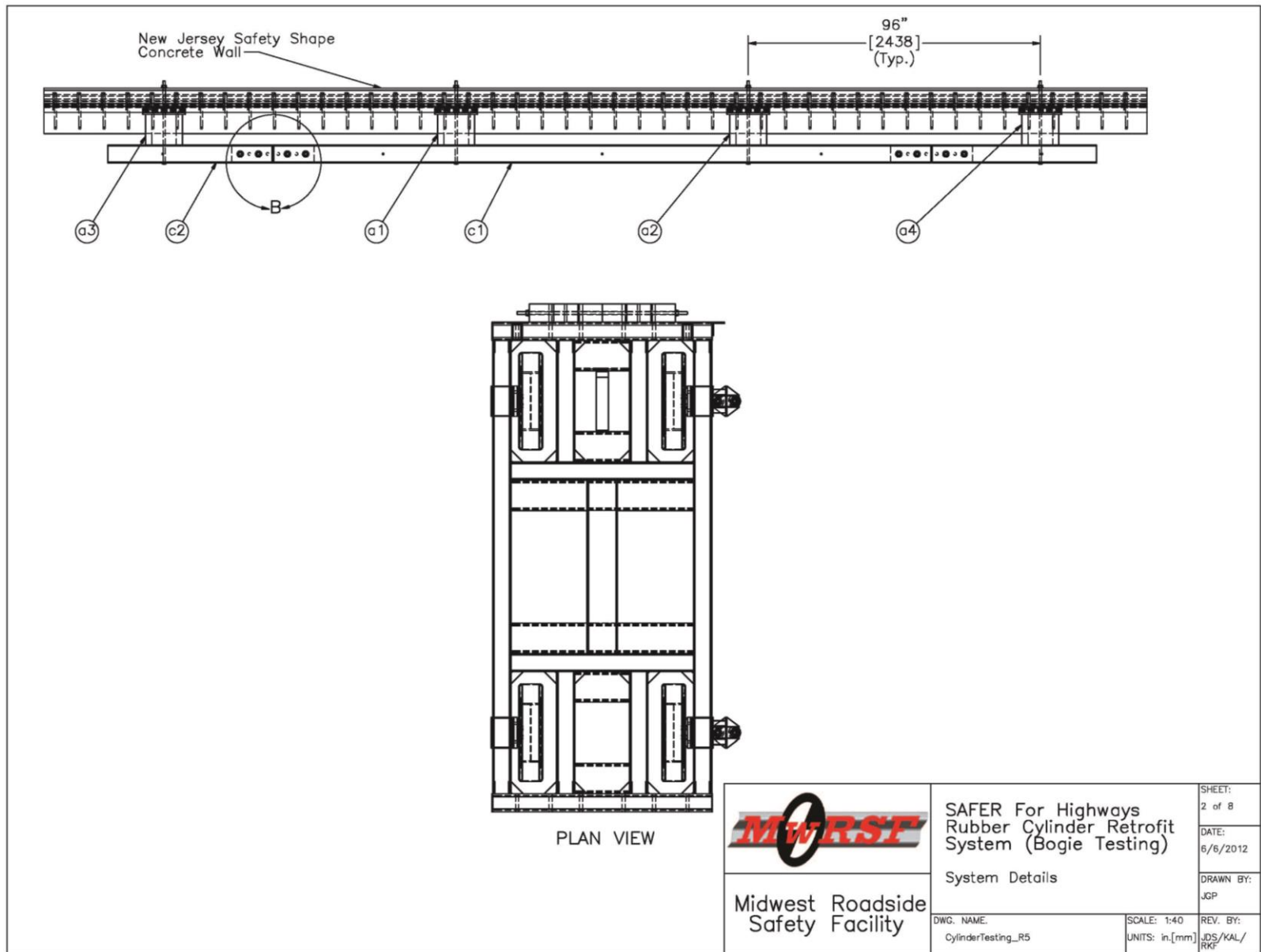


Figure 56. System Details, Test No. SFHC-1

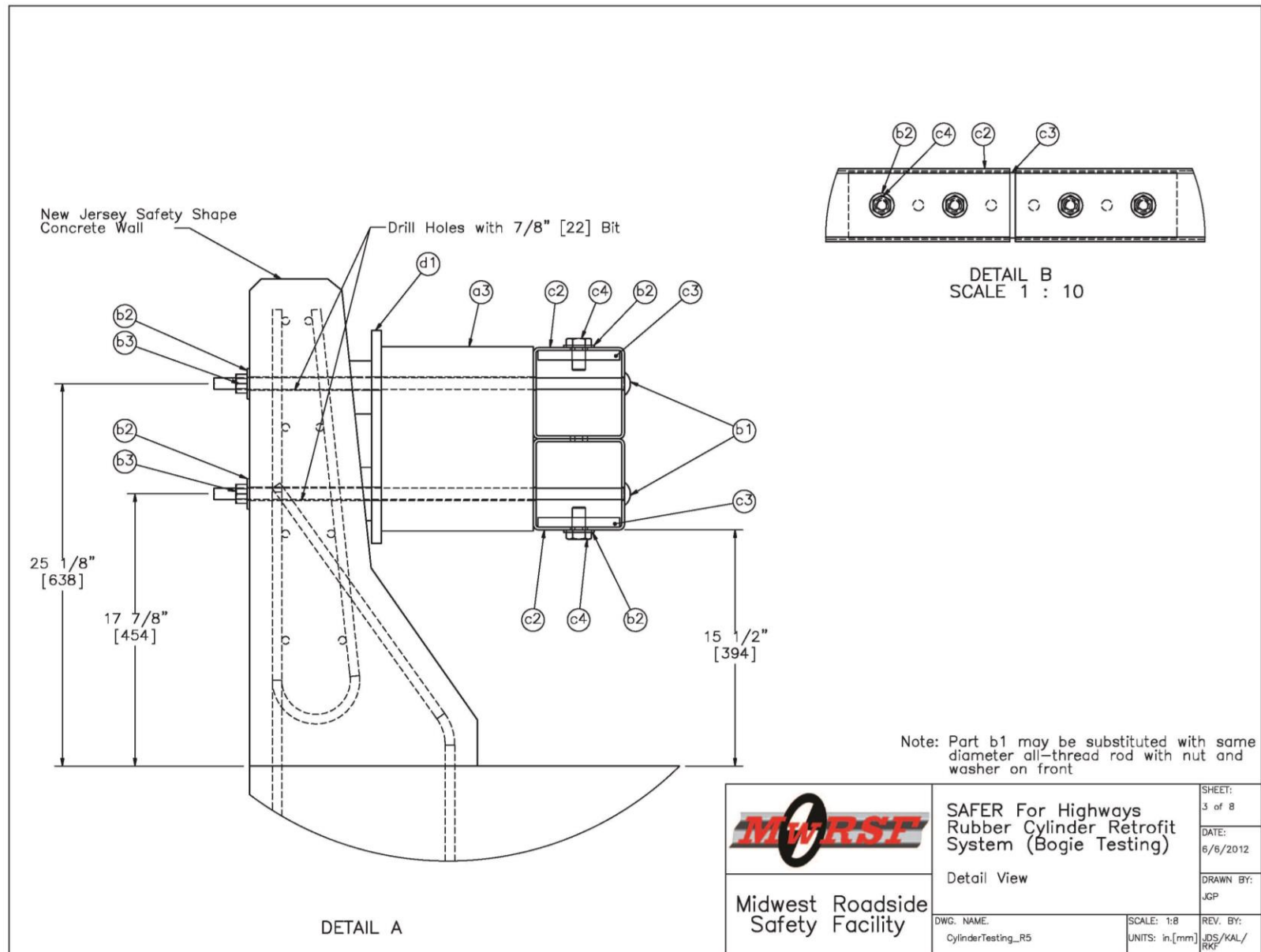


Figure 57. System Detail View, Test No. SFHC-1

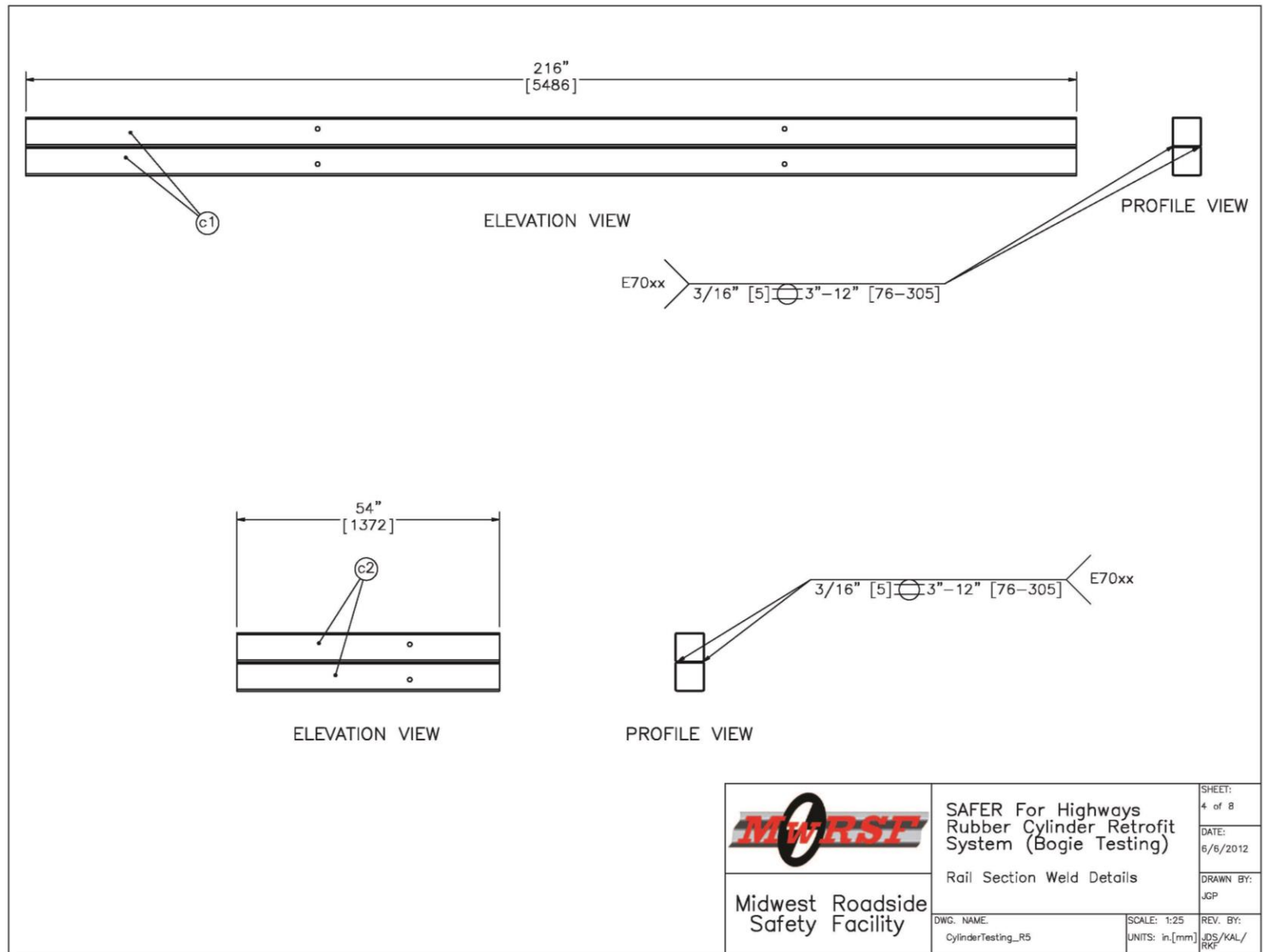


Figure 58. Rail Section Weld Details, Test No. SFHC-1

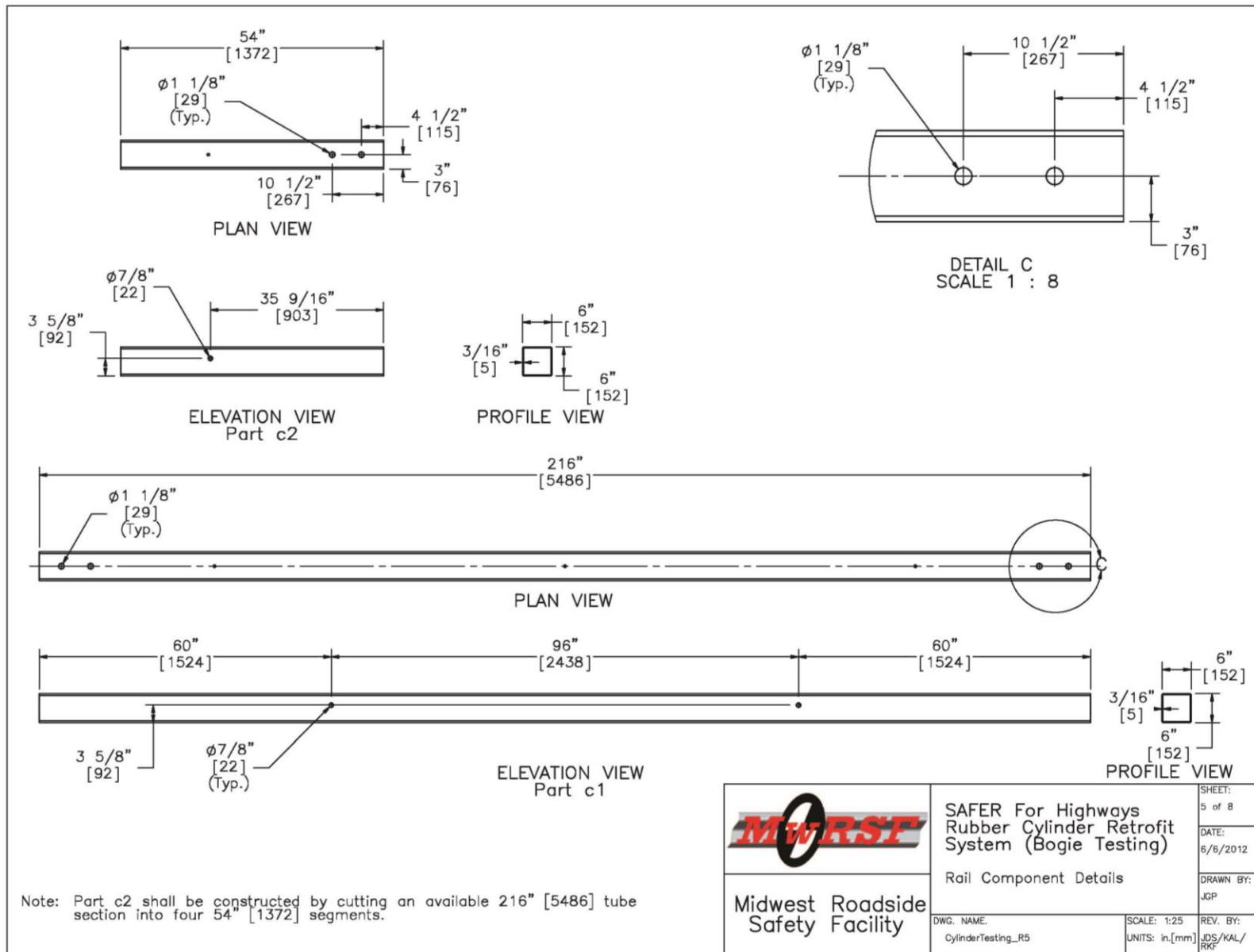


Figure 59. Rail Component Details, Test No. SFHC-1

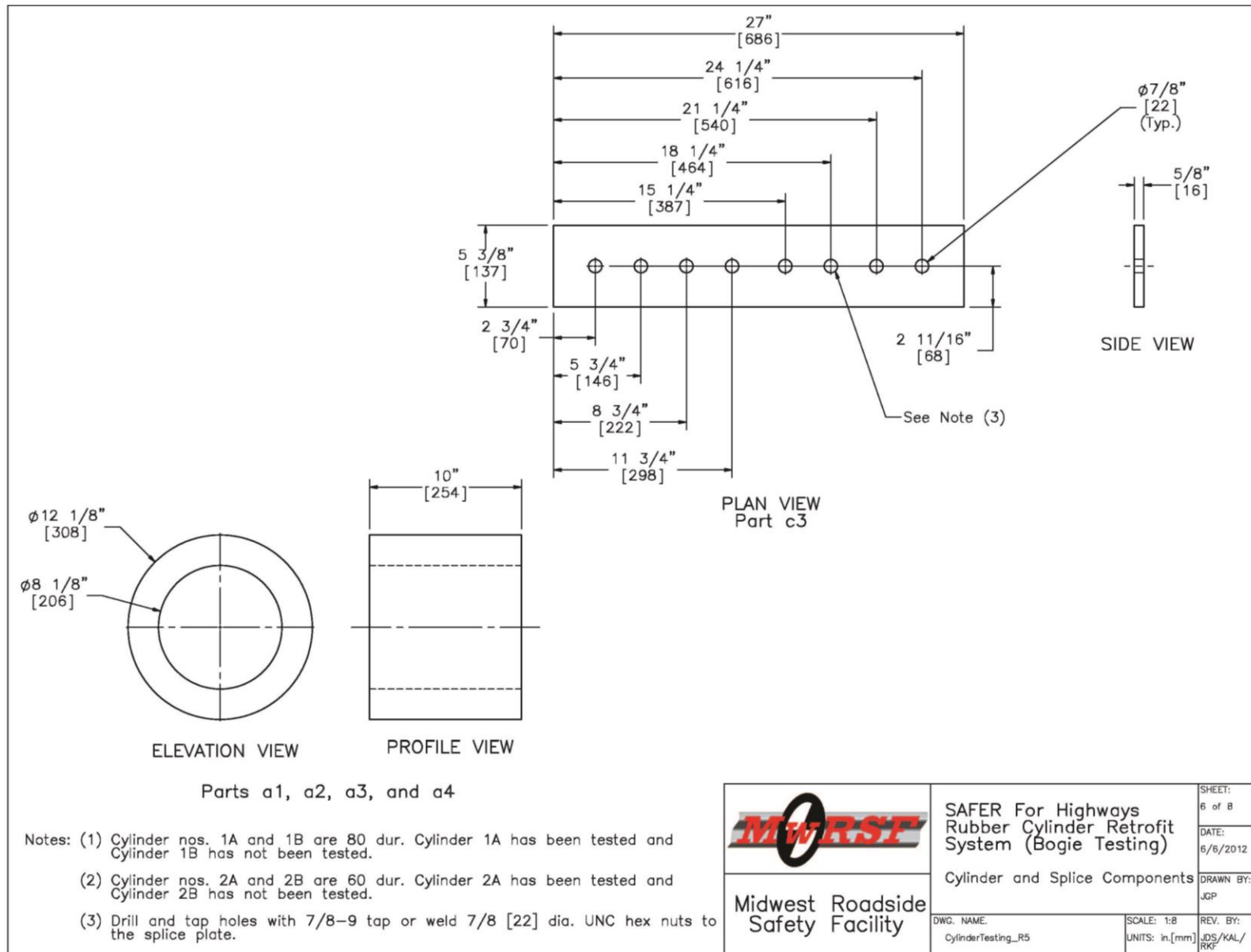


Figure 60. Cylinder and Splice Components, Test No. SFHC-1

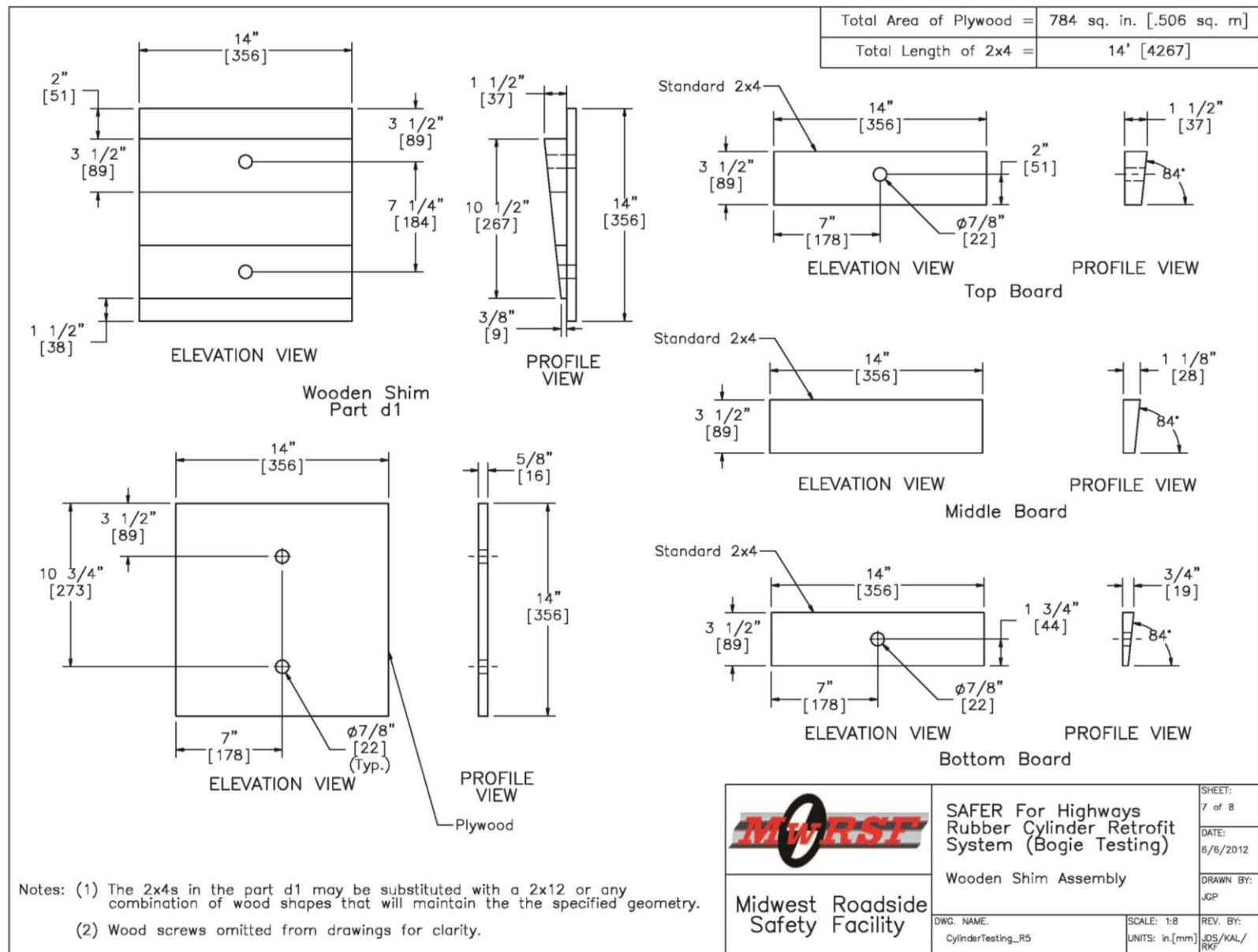


Figure 61. Wooden Shim Details, Test No. SFHC-1

Item No.	QTY.	Description	Material Specification
a1	1	Cylinder 1A (Previously Tested)	EPDM 80 dur. Shore A
a2	1	Cylinder 1B (Untested)	EPDM 80 dur. Shore A
a3	1	Cylinder 2A (Previously Tested)	EPDM 60 dur. Shore A
a4	1	Cylinder 2B (Untested)	EPDM 60 dur. Shore A
b1	8	3/4" [19] Dia. UNC, 27" [686] Long Dome (Round) Head Bolt or All-Thread Rod*	ASTM A307 Grade C/ASTM F1554 Grade 36/SAE Grade 2
b2	24**	3/4" [19] Dia. Plain Round Washer	ASTM F844
b3	8***	3/4" [19] Dia. UNC Heavy Hex Nut	ASTM A563A
c1	2	6"x6"x3/16" [152x152x5] by 216" [5,486] Long Square Steel Tube	ASTM A500 Grade B
c2	4	6"x6"x3/16" [152x152x5] by 54" [1,372] Long Square Steel Tube	ASTM A500 Grade B
c3	4	27"x5 3/8"x5/8" [686x137x16] Steel Splice Plate (Tapped Holes)	ASTM A36
c4	16	3/4" [19] Dia. UNC, 1 1/2" [38] Long Heavy Hex Bolt	ASTM A325
d1	4	Wooden Shirn	—

* Add 2" [51] to overall length if all-thread rod is used.
 ** 32 hardened round washers if all-thread rod is used.
 *** 16 heavy hex nuts if all-thread rod is used.


 Midwest Roadside Safety Facility	SAFER For Highways Rubber Cylinder Retrofit System (Bogie Testing)		SHEET: 8 of 8
	Bill of Materials		DATE: 6/6/2012
DWG. NAME: CylinderTesting_R5	SCALE: NONE UNITS: in.[mm]	REV. BY: JGP	DRAWN BY: JGP

Figure 62. Bill of Materials, Test No. SFHC-1

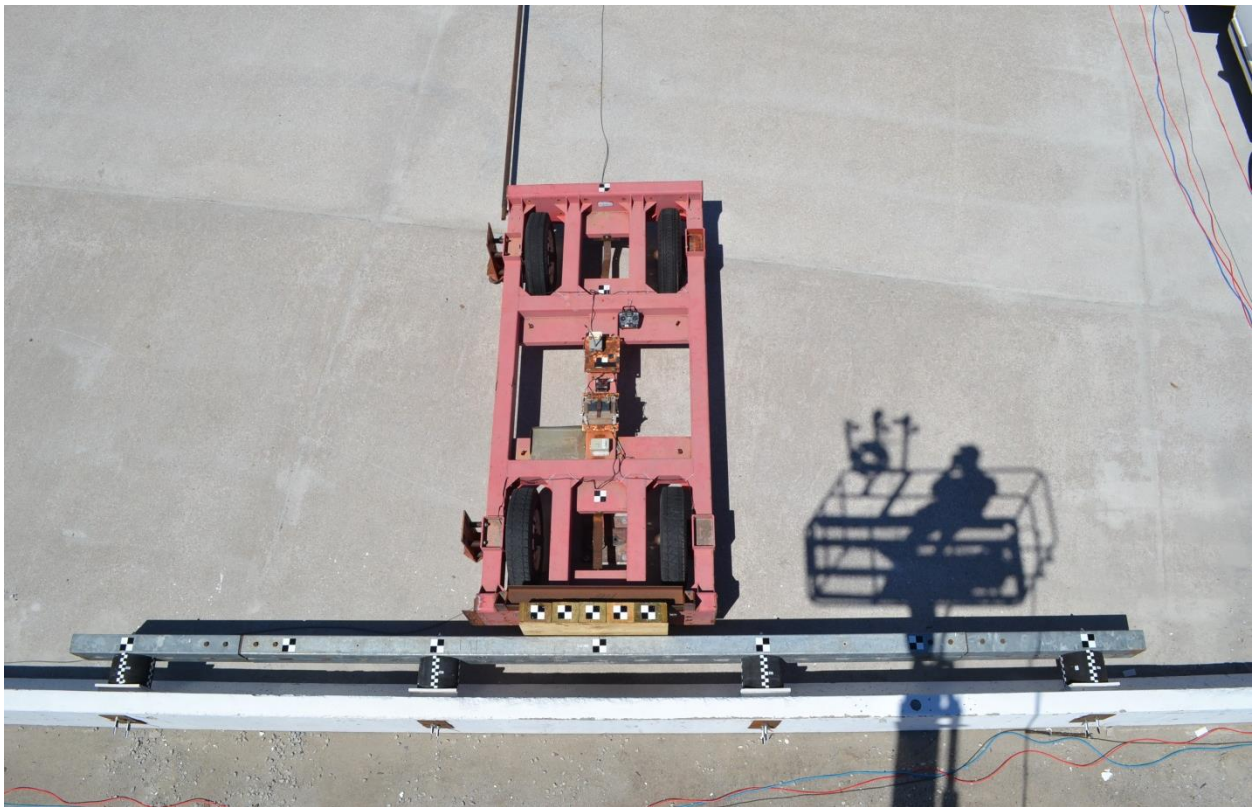


Figure 63. Bogie Test Setup, Test No. SFHC-1

5.3 Results

The 4,876-lb (2,212-kg) bogie impacted the prototype rubber-cylinder retrofit barrier system at 21.5 mph (34.6 km/h). The bogie impacted the steel tubes, and the rail deflected a maximum 11.6 in. (295 mm) at 0.051 sec after impact. The two inside rubber cylinders reached their maximum deflections quickly. However, the load was not well-distributed across the tube splices, and the two outer cylinders did not deflect as much as the inner cylinders. The steel tubes plastically deformed in the impact region, and the tubes splice deformed. The energy absorbers did not restore due the plastic deformations in the rail.

Force vs. deflection and energy vs. deflection curves created from the SLICE 6DX accelerometer data are shown in Figure 64. At the maximum deflection of 11.6 in. (295 mm), the rubber cylinder retrofit system had absorbed 904.8 k-in. (102.2 kJ) of energy. Sequential photographs are shown in Figure 65. Post-impact photographs are shown in Figures 66 and 67.

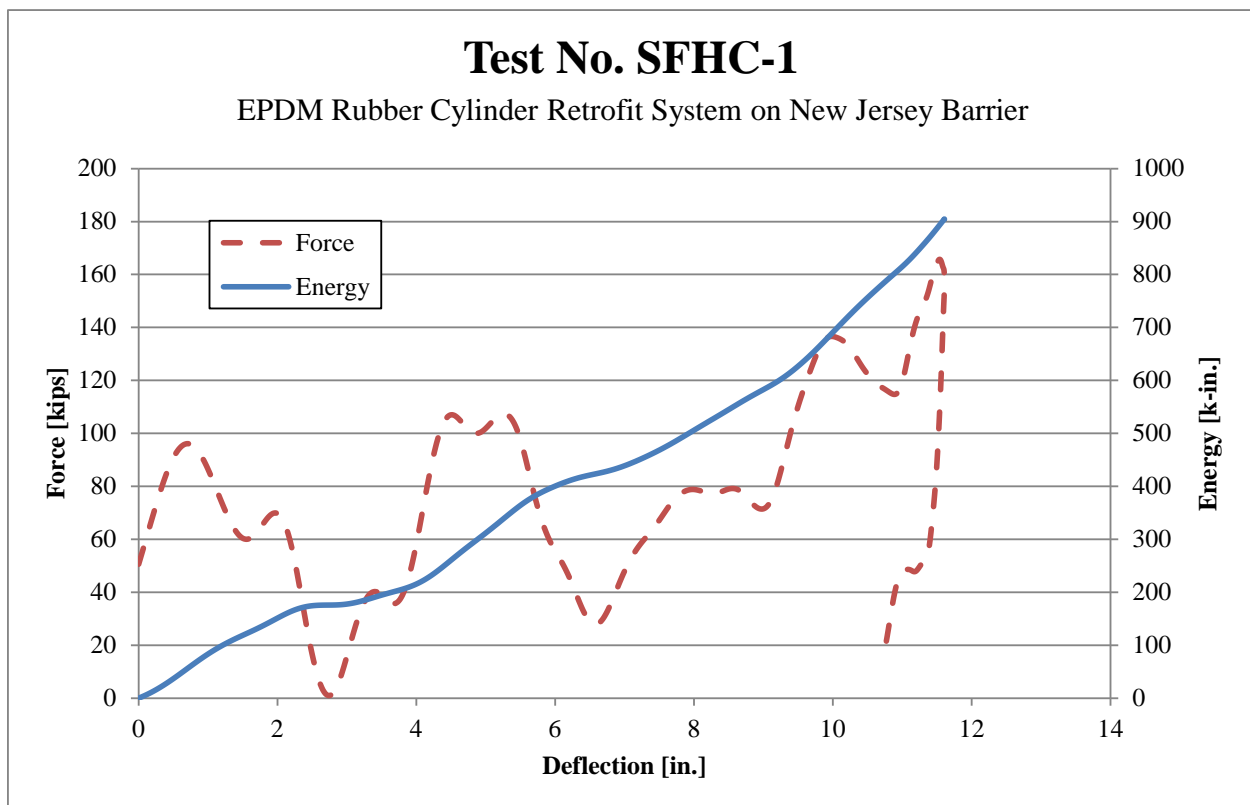


Figure 64. Force vs. Deflection and Energy vs. Deflection, Test No. SFHC-1

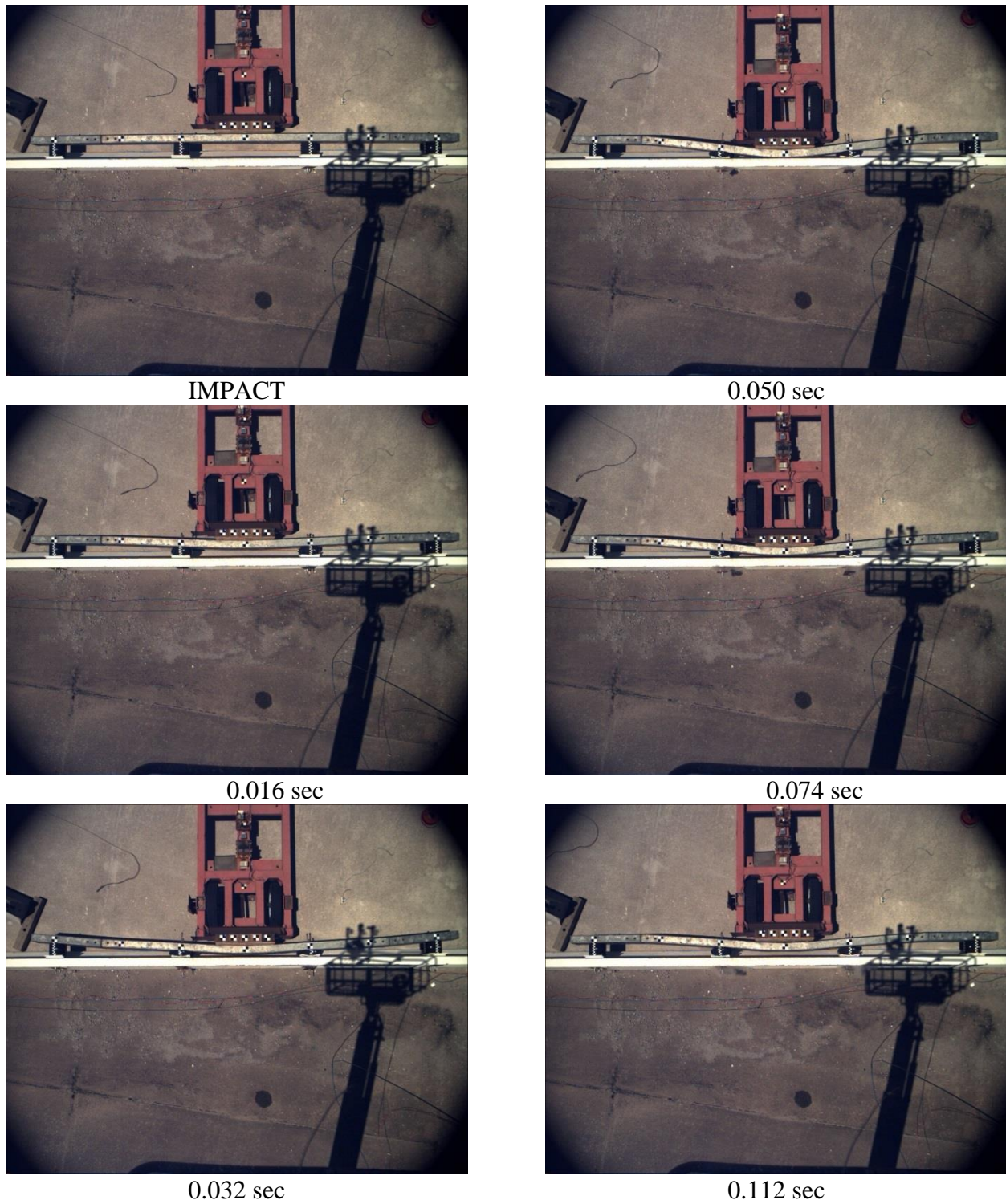


Figure 65. Time-Sequential Photographs, Test No. SFHC-1

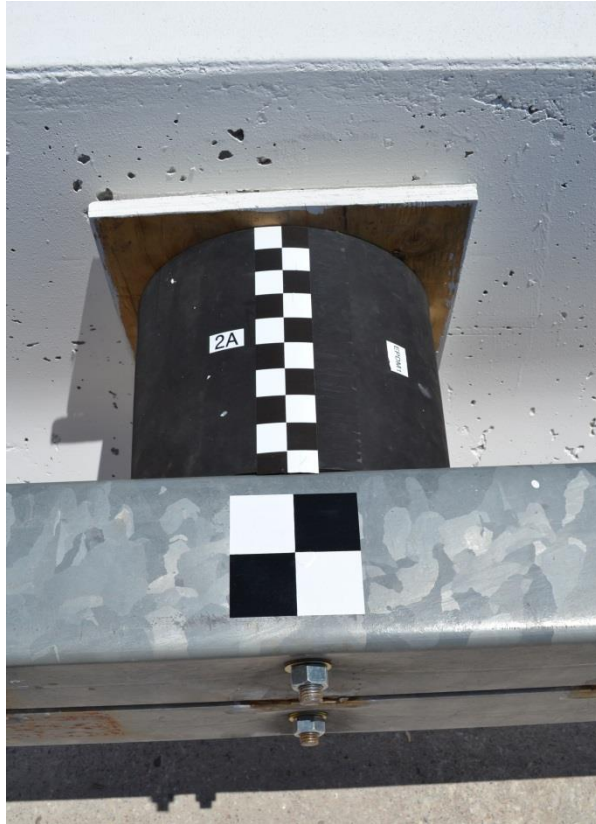


Figure 66. Cylinders Post-Impact Damage, Test No. SFHC-1



Figure 67. Post-Impact Damage, Test No. SFHC-1

5.4 Discussion

A bogie test was conducted on a 27-ft (8.2-m) long prototype rubber-cylinder retrofit barrier system to determine the deflection and energy absorption capabilities of a barrier segment. Four 2-in. (51-mm) thick x 10-in. (254-mm) long rubber cylinders were spaced at 96 in. (2,438 mm) along a 32-in. (813-mm) tall New Jersey-shaped concrete barrier. Two ASTM A500 Grade B 6-in. x 6-in. x 3/16 in. thick (152-mm x 152-mm x 5-mm) steel tubes were attached to the front face of the cylinders. The bogie impacted the steel tubular rail, and the two inside rubber cylinders quickly reached their maximum deflections. However, the load was not well-distributed across the tube splices, and the two outer cylinders did not deflect as much as the inner cylinders. The steel tubes plastically deformed around the edges of the wood impact head. Consequently, the cylinders did not restore due to the plastic rail deformations. However, the cylinders restored to their original dimensions once the rail was removed. Therefore, this barrier should be fully restorable and reusable after impact as long as the rail does not sustain permanent deformation.

The bogie's kinetic energy was absorbed by the barrier primarily through the deflection of the rubber cylinders, plastic deformation of the steel tubes, and fracturing of the wood supports behind the cylinders. The previous individual component tests of the 2-in. (51-mm) thick rubber cylinders had a maximum deflection of approximately 2 in. (51 mm). Therefore, the energy vs. deflection curves could not be used to estimate the energy absorbed by the rubber cylinders at greater deflections. However, force vs. deflection and energy vs. deflection curves were created for the 80-durometer, 2-in. (51-mm) thick rubber cylinder from undocumented simulations related to the project, as shown in Figures 68 and 69. While the full force vs. deflection curve from the simulation could not be validated. The force and energy response were similar to component test no. EPDM-1 over the first 1.9 in. (48 mm) of deflection. Therefore, the

full energy vs. deflection curve from the simulation was used to estimate energy absorption of the barrier system. Each cylinder, from the left side to the right side of the barrier, the deflections, and corresponding energy dissipated is shown in Table 8. The deflections were measured from the overhead high-speed digital video.

An estimated total of 130 k-in. (14.7 kJ) of energy was absorbed specifically through the deflection of the rubber cylinders. Approximately 15 percent of the initial kinetic energy of the bogie was absorbed by the two middle rubber cylinders. The rail splices and the steel tubular system did not sufficiently transfer the load to the outer cylinders. If the impact load can be distributed to multiple energy absorbers, then there exists a potential for this barrier concept to reduce lateral accelerations by 30 percent as compared to impact events into a rigid concrete barrier.

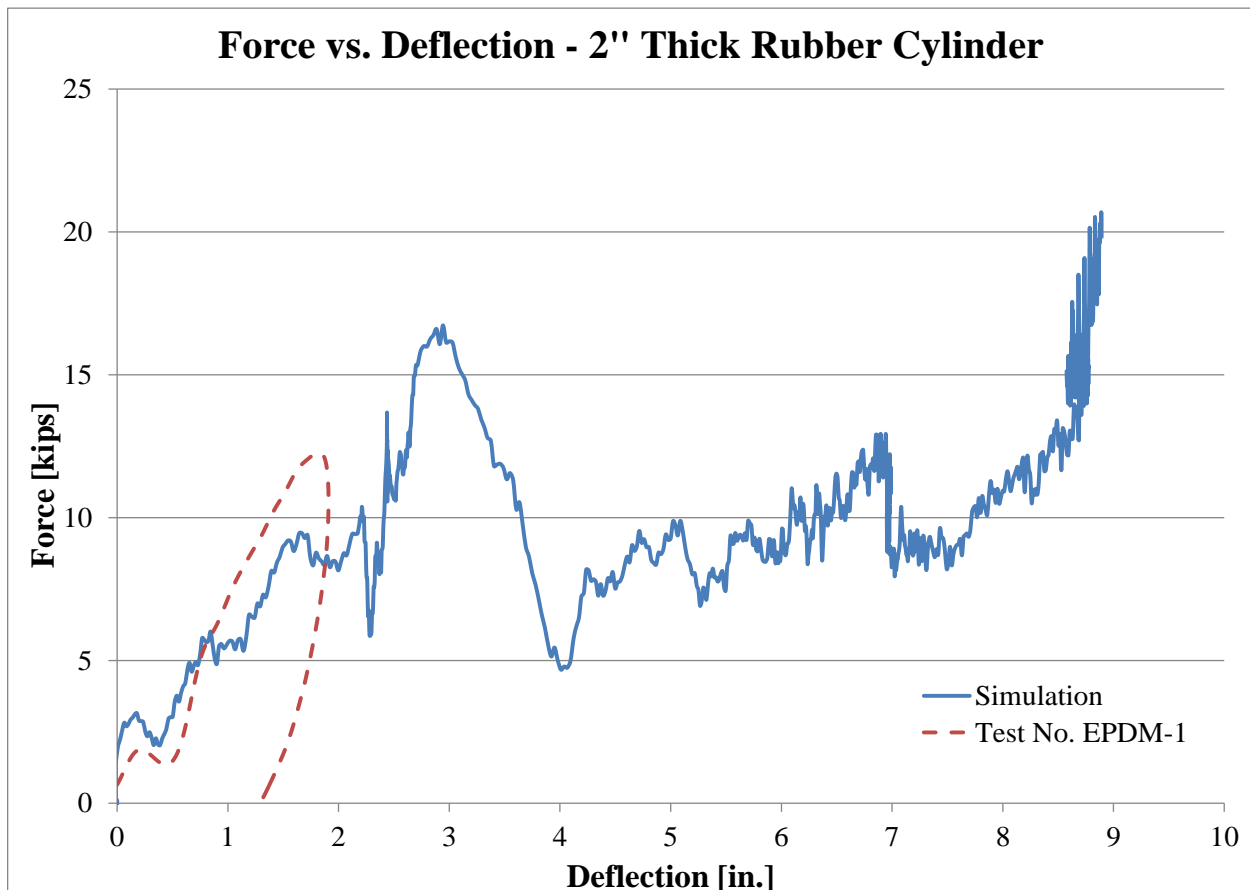


Figure 68. Force vs. Deflection – 2-in. (51-mm) Thick Rubber Cylinder

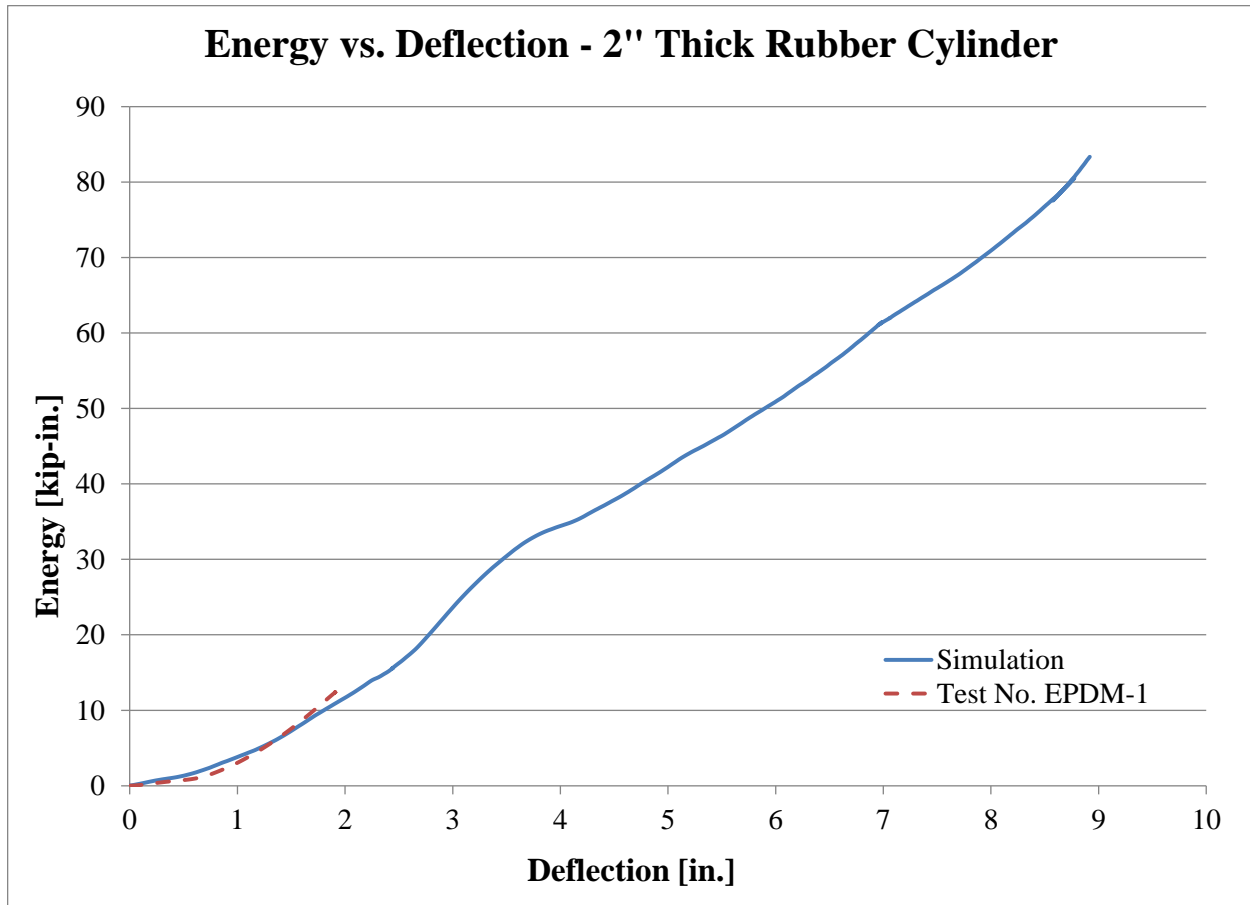


Figure 69. Energy vs. Deflection – 2-in. (51-mm) Thick Rubber Cylinder

Table 8. Cylinder Deflection and Energy, Test No. SFHC-1

Part No.	Cylinder No.	Deflection in. (mm)	Energy k-in. (kJ)
a3	2A	NA*	0
a1	1A	6.9 (175)	60 (6.8)
a2	1B	8.0 (203)	70 (7.9)
a4	2B	NA*	0

*Deflections were minimal and were not measured from overhead video.

6 SHEAR FENDER POST AND BEAM SYSTEM - COMPONENT TESTING

6.1 Purpose

A dynamic bogie test was conducted on a prototype rubber shear fender post and beam system to determine load distribution, system deflection, and energy absorption for multiple shear fenders.

6.2 Scope

A bogie test was conducted on a 28-ft (8.5-m) long prototype shear fender post and beam system. The bogie impacted the system at a 90-degree angle with the target impact location at the midspan between the middle posts. The target speed was 15 mph (24.1 km/h). The impact height was 15 in. (381 mm) above the ground line. Four 10-in. (254-mm) wide x 11 $\frac{5}{8}$ -in. (295-mm) tall x 15 $\frac{3}{4}$ -in. (400-mm) long shear fender posts were spaced at 96 in. (2,438 mm) on center. A glue-laminated timber rail was selected from existing on-site remnants from prior research and development studies. A splice was necessary along the beam length, which was used to transfer the load along the timber section. The test matrix and test setup are shown in Figures 70 through 80.

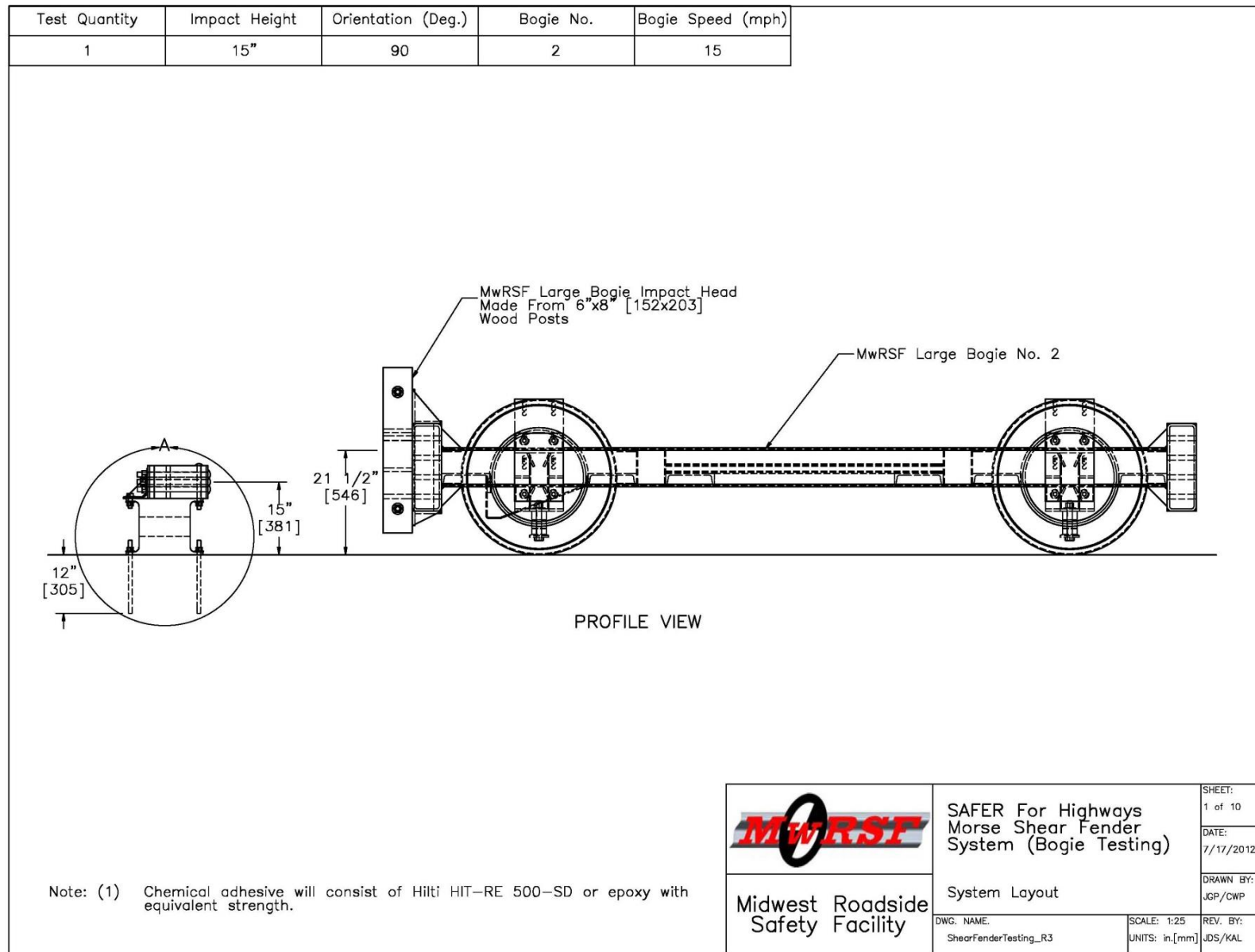


Figure 70. Bogie Testing Matrix and System Layout, Test No. SFHT-1

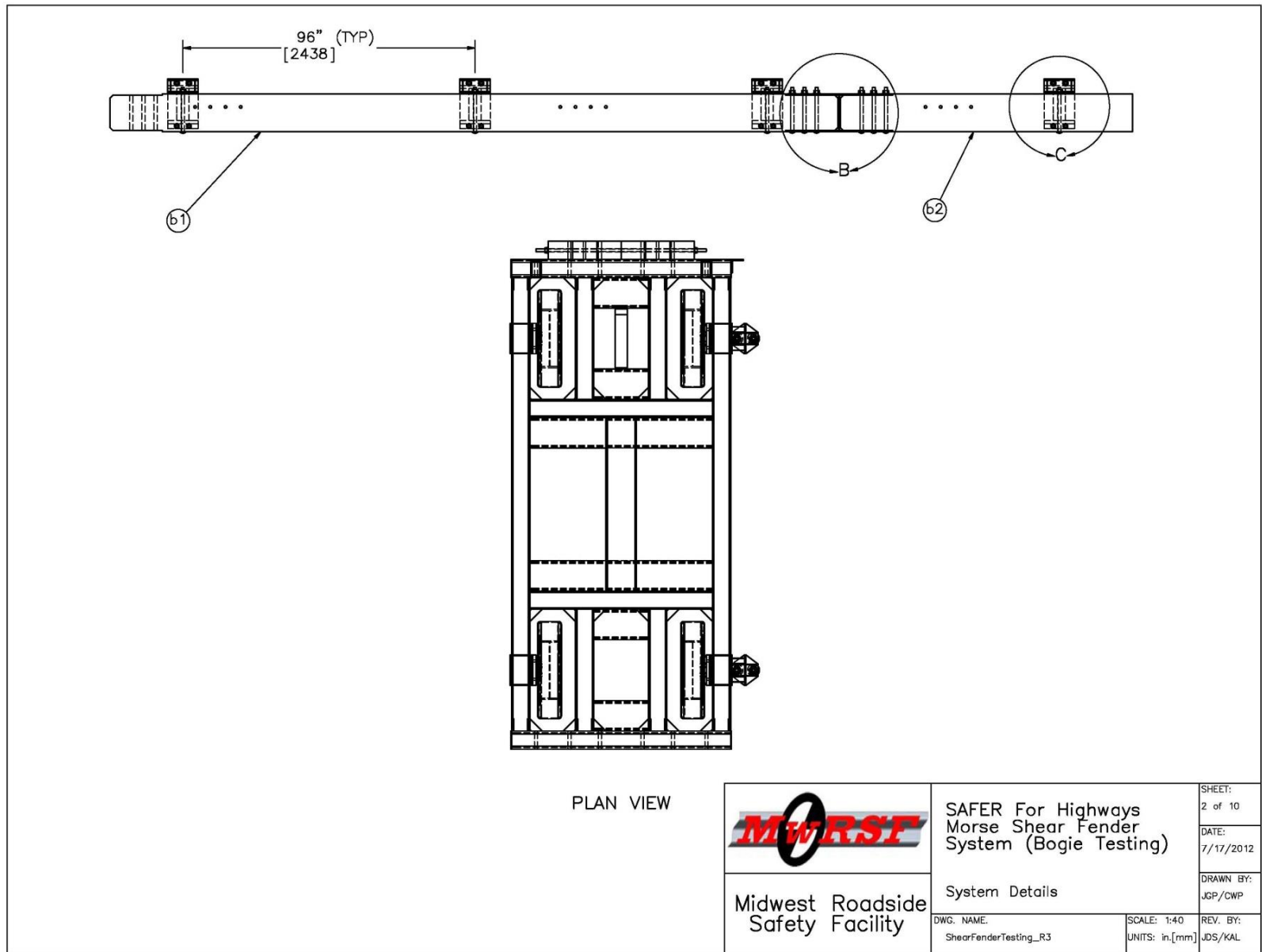


Figure 71. System Details, Test No. SFHT-1

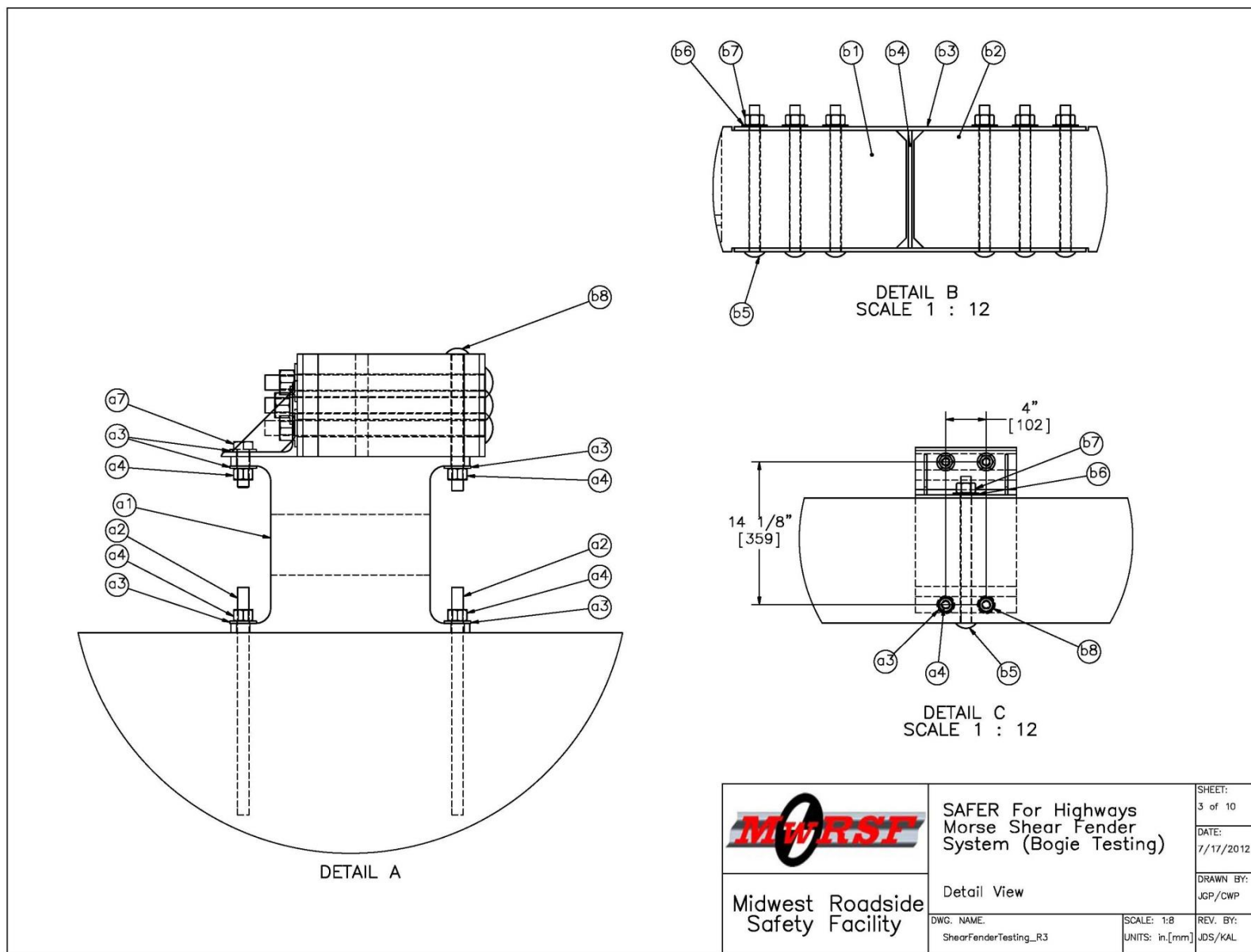
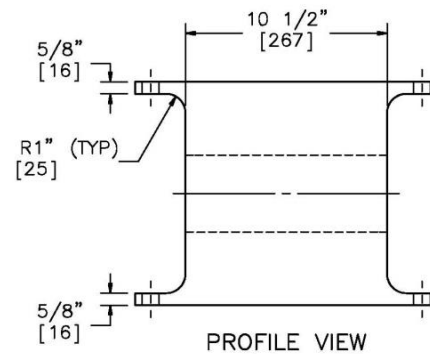
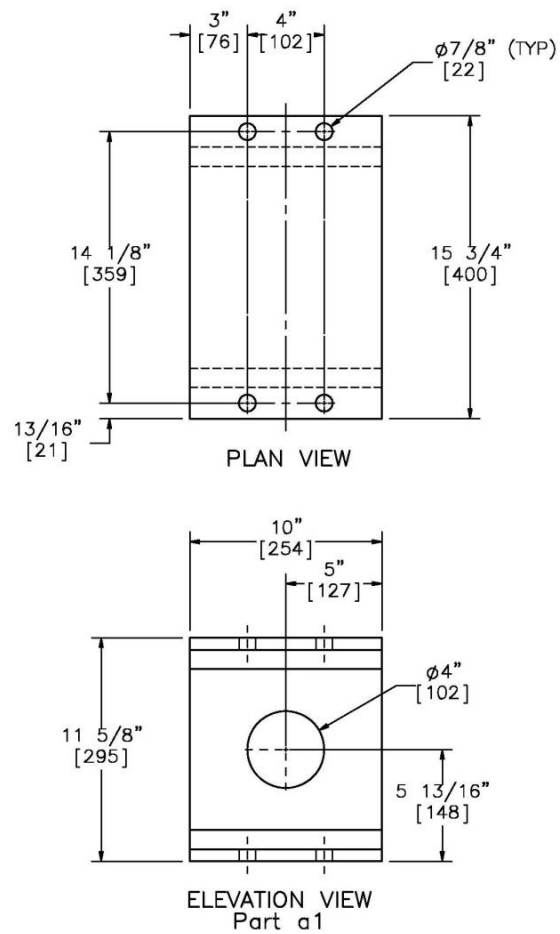


Figure 72. System Detail Views, Test No. SFHT-1



 Midwest Roadside Safety Facility	SAFER For Highways Morse Shear Fender System (Bogie Testing)		SHEET: 4 of 10
	Shear Fender Details		DATE: 7/17/2012
DWG. NAME: ShearFenderTesting_R3	SCALE: 1:8 UNITS: in./mm	REV. BY: JDS/KAL	DRAWN BY: JGP/CWP

Figure 73. Shear Fender Details, Test No. SFHT-1

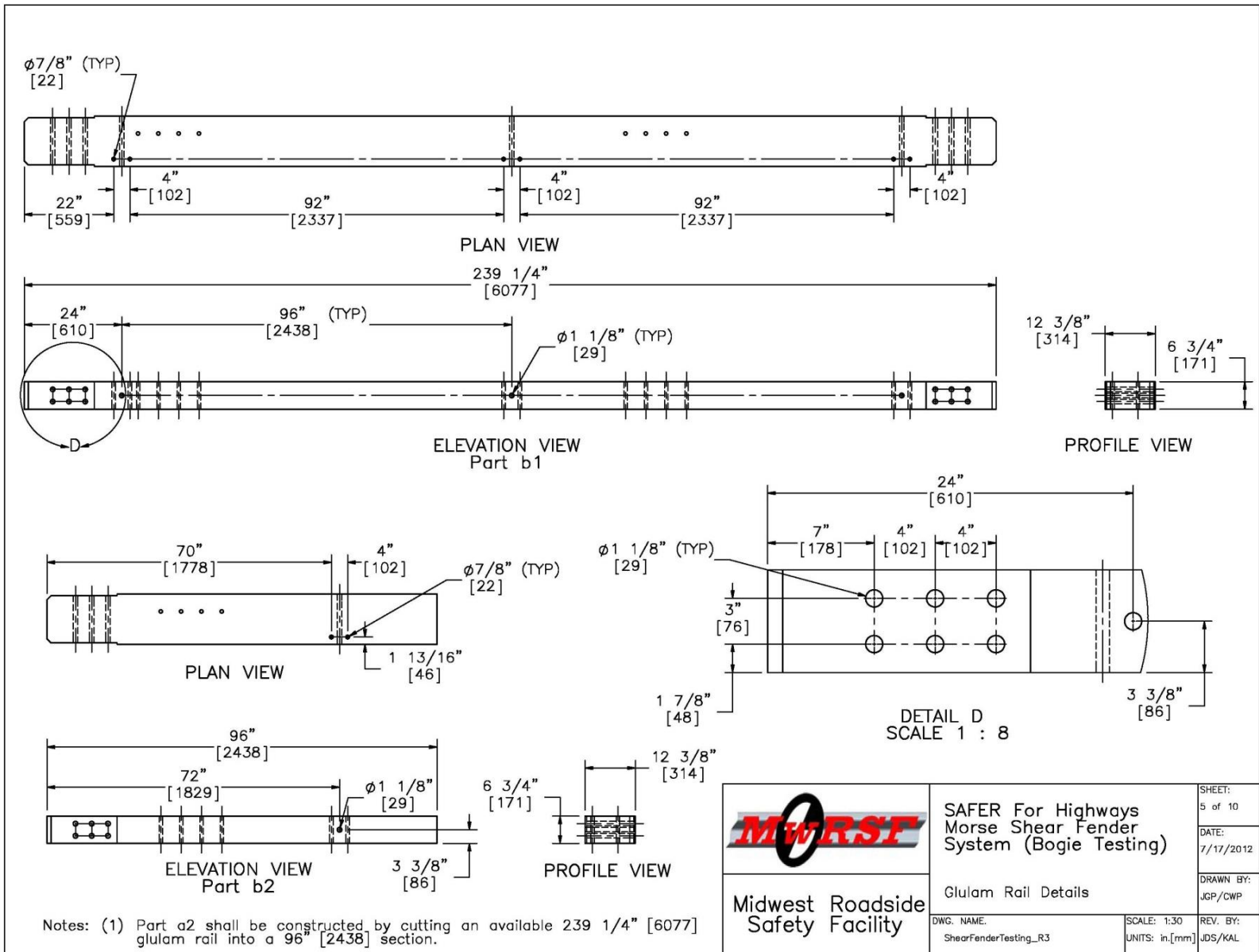


Figure 74. Rail Details, Test No. SFHT-1

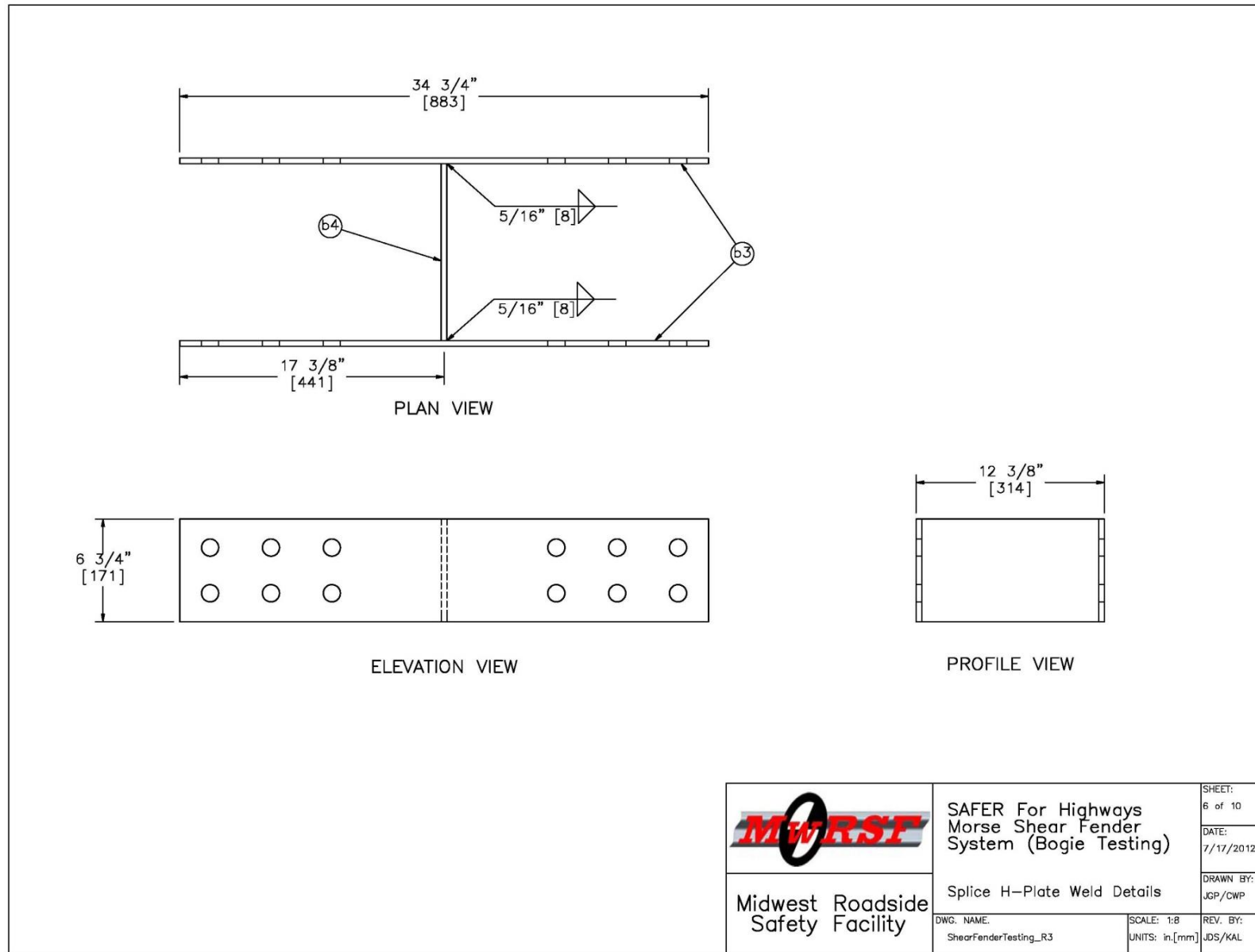


Figure 75. Splice Component Details, Test No. SFHT-1

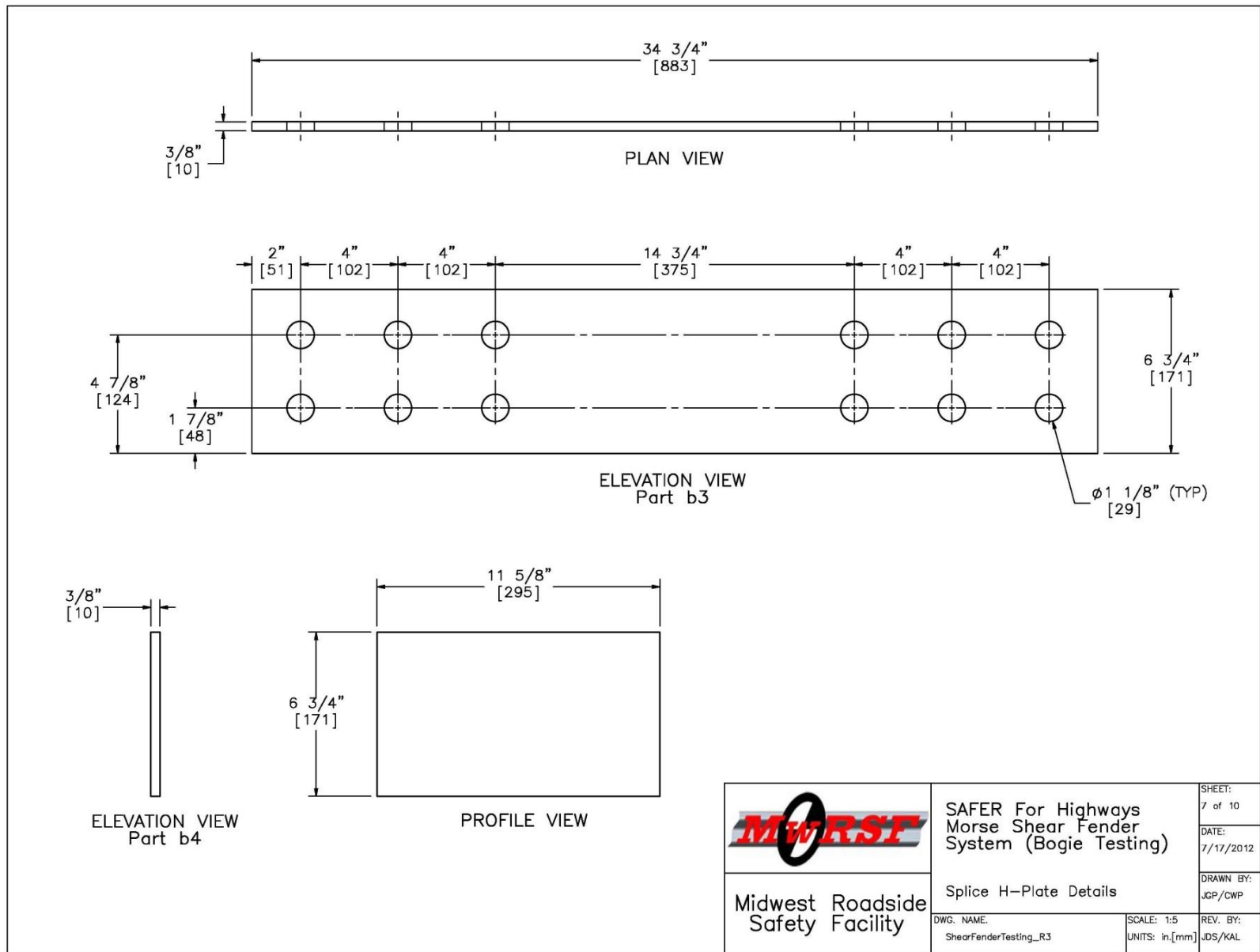


Figure 76. Splice Details, Test No. SFHT-1

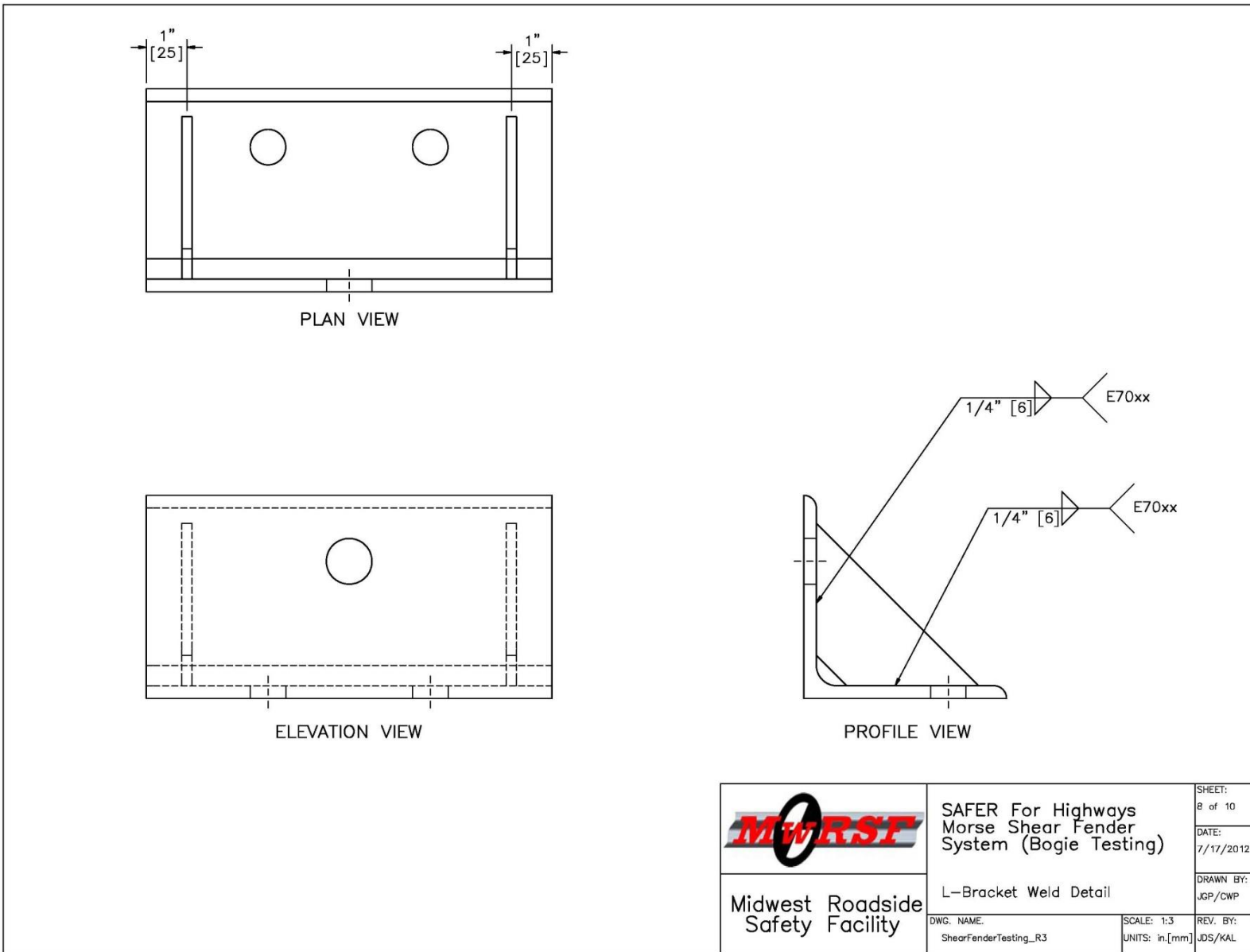


Figure 77. L-Bracket Details, Test No. SFHT-1

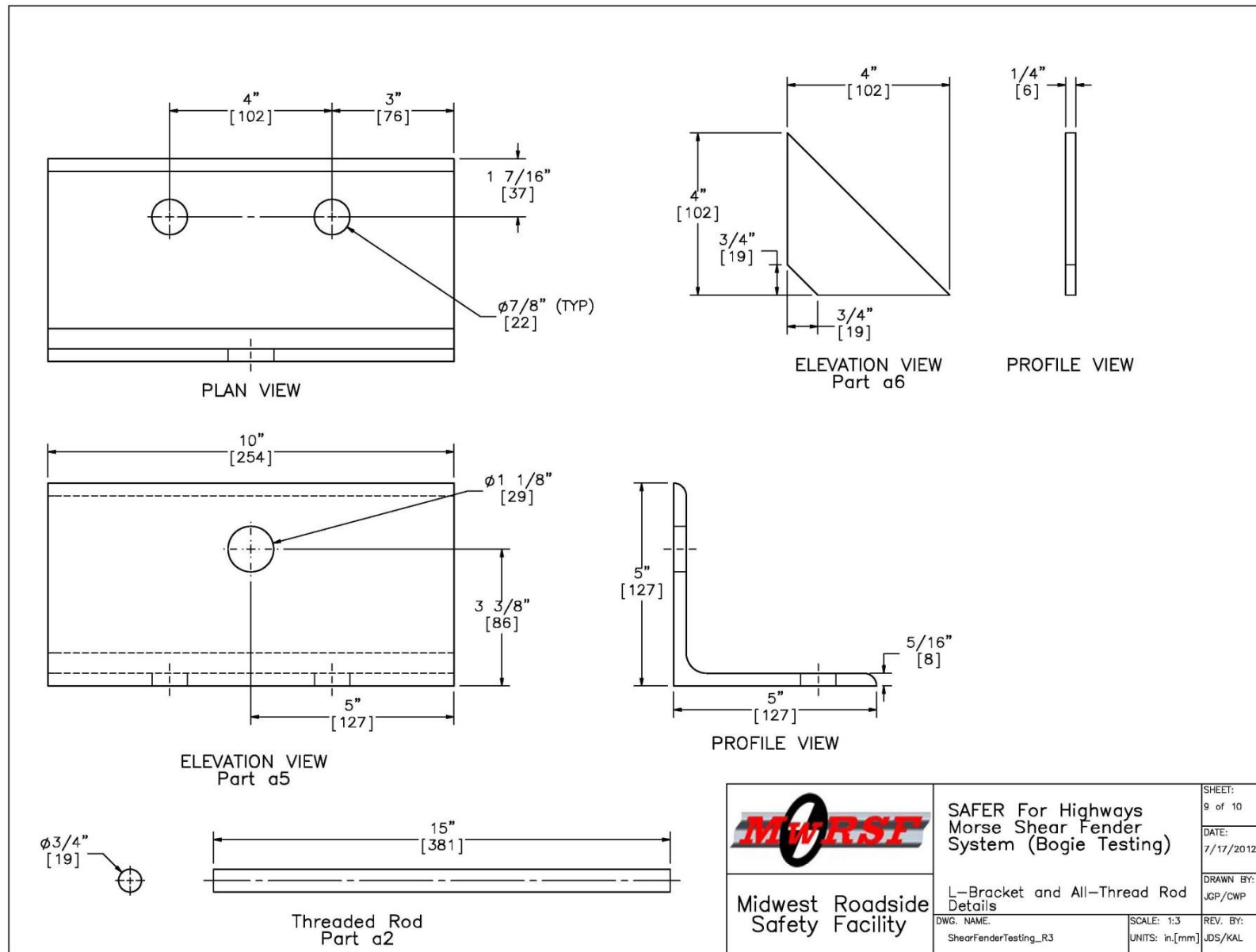


Figure 78. L-Bracket and Threaded Rod Details, Test No. SFHT-1

Item No.	Qty.	Description	Material Specification
a1	4	Morse E46496 Shear Fender	ASTM D2000
a2	16	3/4" [19] Dia. UNC, 15" [381] Long Threaded Rod	ASTM A193 Gr. B7/ASTM F1554 Gr. 105
a3	40	3/4" [19] Dia. Narrow Round Washer	ASTM F436 Type 1
a4	32	3/4" [19] Dia. UNC Heavy Hex Nut	ASTM A194 Gr. 2H
a5	4	5"x5"x5/16" [127x127x8], 10" [254] Long L-Shaped Beam	ASTM A36
a6	8	4"x4"x1/4" [102x102x6] Gusset	ASTM A36
a7	8	3/4" [19] Dia. UNC, 2 1/2" [64] Long Heavy Hex Bolt	ASTM A325 Type 1/ASTM A449 Type 1/SAE J429 Gr. 5
b1	1	12 3/8"x6 3/4" [314x171], 239 1/2" [6083] Long Glulam Rail Section	Southern Yellow Pine Combination No. 48
b2	1	12 3/8"x6 3/4" [314x171], 96" [2438] Long Glulam Rail Section	Southern Yellow Pine Combination No. 48
b3	2	14 3/4"x6 3/4"x3/8" [375x171x10] Straight Splice Plate	ASTM A572 Gr. 42
b4	1	11 5/8"x6 3/4"x3/8" [295x171x10] Splice Gusset	ASTM A572 Gr. 42
b5	16	1" [25] Dia. UNC, 14 1/2" [368] Long Dome (Round) Head Bolt	ASTM A307 Gr. A/ASTM F1554 Gr. 36/SAE J429 Gr. 2
b6	16	1" [25] Dia. Hardened Round Washer	ASTM F844
b7	16	1" [25] Dia. UNC Heavy Hex Nut	ASTM A563 Gr. A
b8	8	3/4" [19] Dia. UNC, 9" [229] Long Dome (Round) Head Bolt	ASTM A307 Gr. A/ASTM F1554 Gr. 36/SAE J429 Gr. 2
<div> <div>  <div> Midwest Roadside Safety Facility </div> </div> <div> <div> SAFER For Highways Morse Shear Fender System (Bogie Testing) </div> <div> Bill of Materials </div> </div> <div> <div> DWG. NAME: ShearFenderTesting_R3 </div> <div> SCALE: NONE UNITS: in,[mm] </div> <div> REV. BY: JDS/KAL </div> </div> </div> <div> <div> SHEET: 10 of 10 </div> <div> DATE: 7/17/2012 </div> <div> DRAWN BY: JGP/CWP </div> </div>			

Figure 79. Bill of Materials, Test No. SFHT-1



Figure 80. Bogie Test Setup, Test No. SFHT-1

6.3 Results

The 4,871-lb (2,209-kg) bogie impacted the prototype shear fender post and beam system at 15.2 mph (24.5 km/h). The timber rail displaced a maximum of 35 in. (889 mm). The timber rail rotated backward and completely fractured near the bogie's maximum displacement of 35 in. (889 mm). Each shear fender, as labeled from left to right of the barrier (nos. 1-4), rotated and deflected differently during the impact event. Shear fender no. 1 rotated for almost the entire impact to a maximum lateral deflection of 13.5 in. (343 mm). Shear fender no. 2 deflected 8 in. (203 mm) in shear and then began rotating until a maximum lateral deflection of 21.8 in. (554 mm). Shear fender no. 3 deflected 7.1 in. (180 mm) in shear and then began rotating until a maximum lateral deflection of 23 in. (584 mm). Shear fender no. 4 deflected 3.4 in. (86 mm) in shear and then began rotating until a maximum lateral deflection of 16.3 in. (414 mm).

The bogie's kinetic energy was absorbed by the barrier primarily through the deflection of the rubber shear fenders and bending and fracture of the timber rail. Shear fender no. 1 rotated during almost the entire impact. Shear fender nos. 2, 3, and 4 deflected in almost pure shear for 8 in. (203 mm), 7.1 in. (180 mm), and 3.4 in. (86 mm), respectively.

Force vs. deflection and energy vs. deflection curves created from the SLICE 6DX accelerometer data are shown in Figure 81. Initially, inertial effects resulted in an initial maximum jump in the force to 53.5 kips (238 kN). At a maximum deflection of 35 in. (889 mm), the shear fender system absorbed 452.2 k-in. (51.1 kJ) of energy. Sequential and post-impact photographs are shown in Figures 82 and 86.

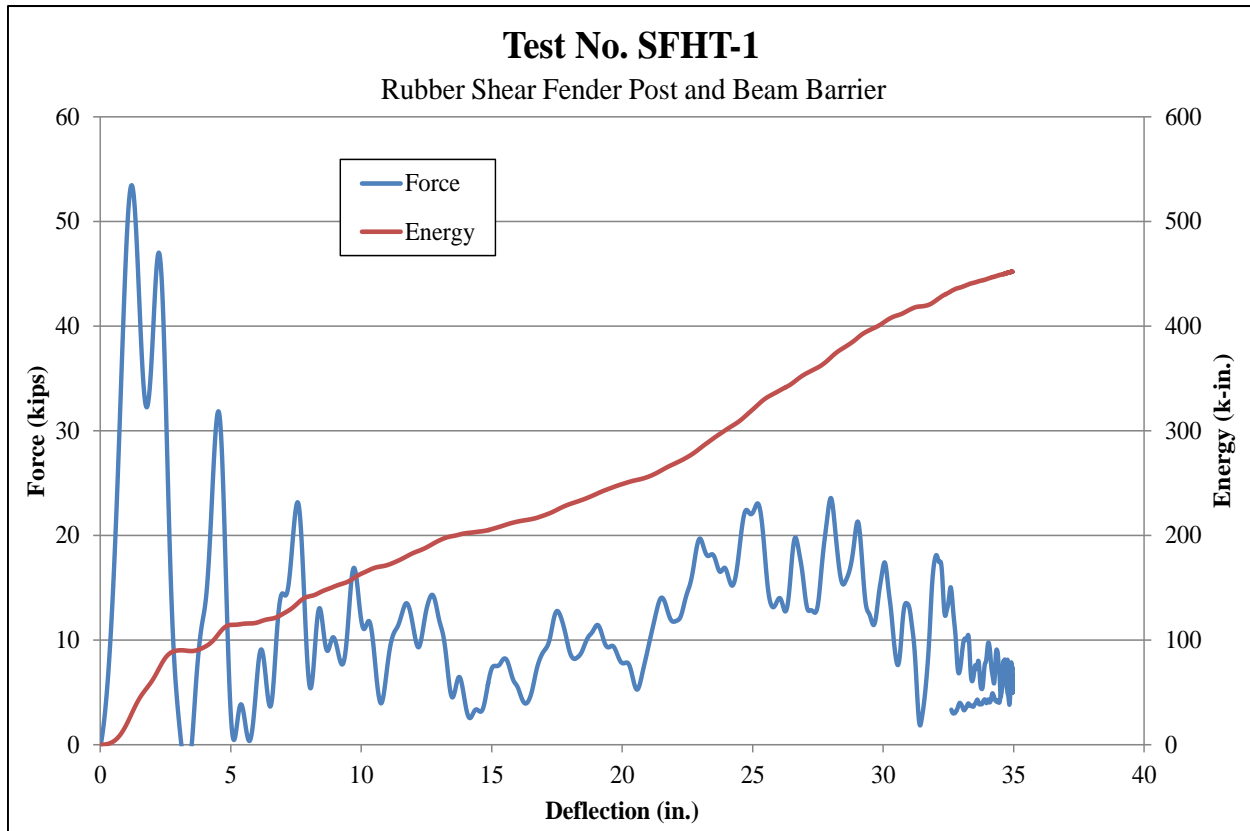


Figure 81. Force vs. Deflection and Energy vs. Deflection, Test No. SFHT-1

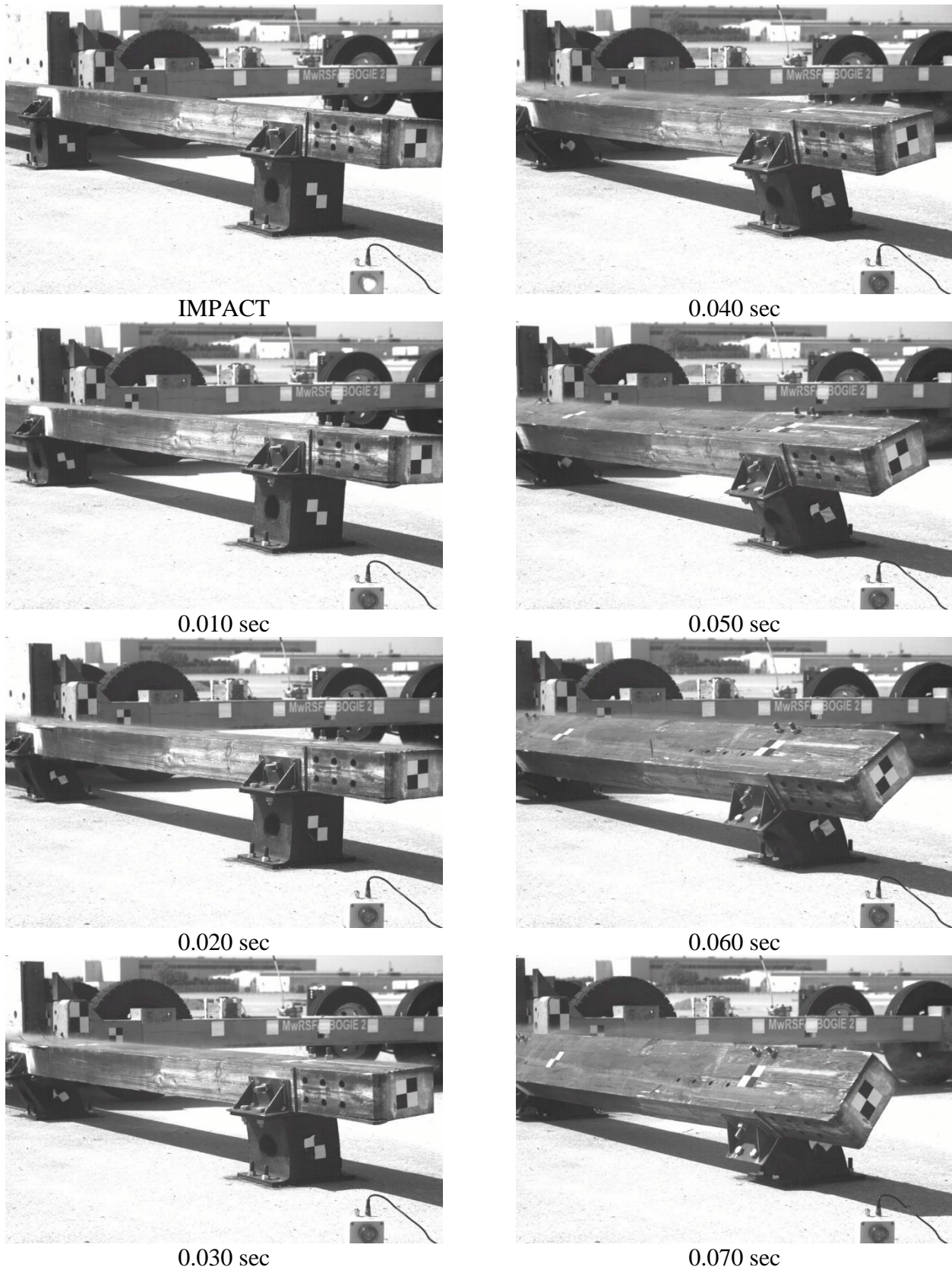


Figure 82. Time-Sequential Photographs, Test No. SFHT-1



IMPACT



0.040 sec



0.010 sec



0.050 sec



0.020 sec



0.060 sec



0.030 sec



0.070 sec

Figure 83. Time-Sequential Photographs, Test No. SFHT-1



Figure 84. Time-Sequential Photographs, Test No. SFHT-1

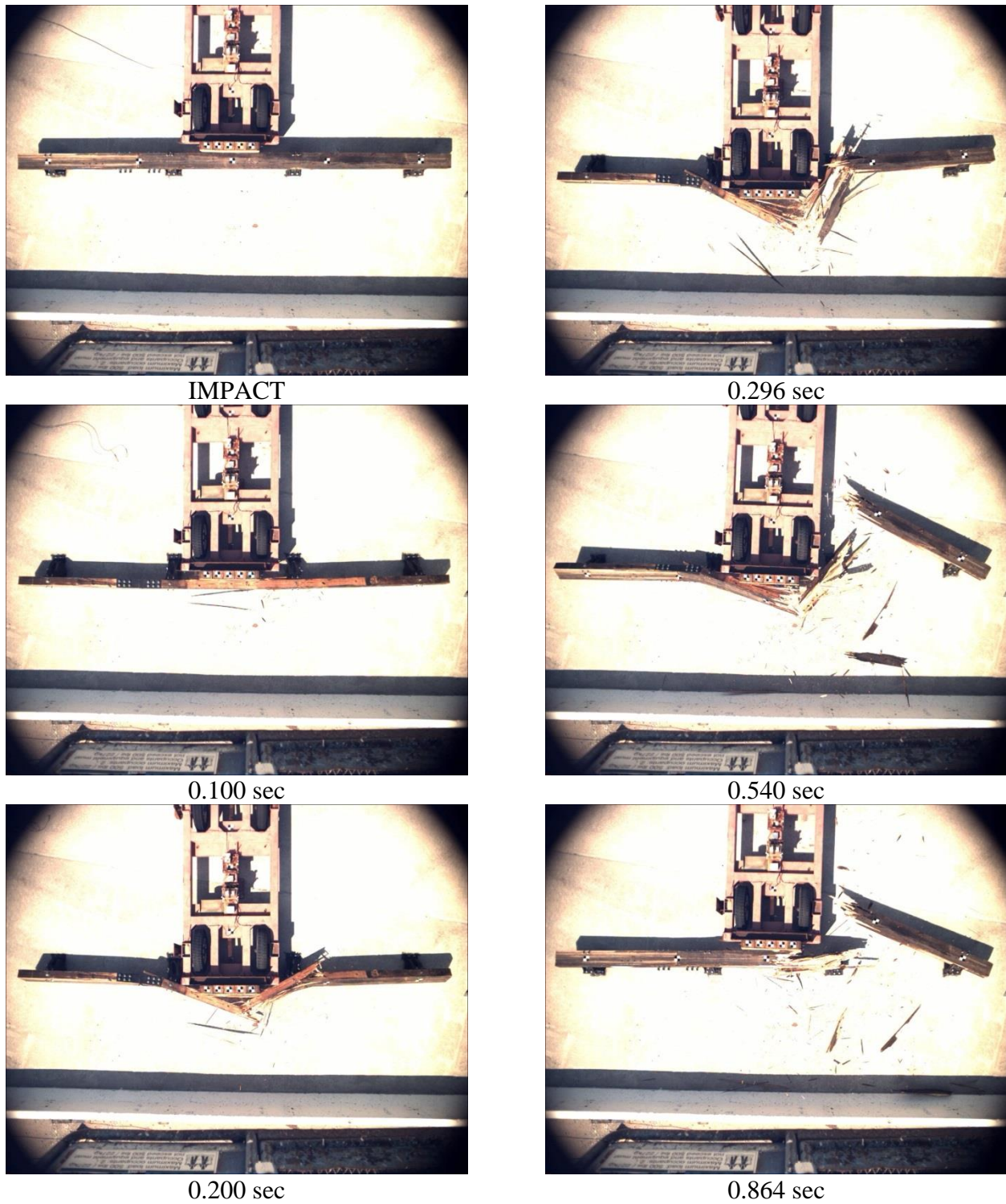


Figure 85. Time-Sequential Photographs, Test No. SFHT-1



Figure 86. Post-Impact Damage, Test No. SFHT-1

6.4 Discussion

A bogie test was conducted on a 28-ft (8.5-m) long prototype shear fender post and beam system to determine the deflection and energy absorption of the barrier system. Four 10-in. (254-mm) wide x 11 $\frac{5}{8}$ -in. (295-mm) tall x 15 $\frac{3}{4}$ -in. (400-mm) long shear fender posts were spaced at 96 in. (2,438 mm) on center. The center of gravity of the bogie was about 6 in. (152 mm) higher than the impact height on the timber rail. Therefore, the barrier was loaded eccentrically and the shear fenders rotated more than deforming in shear. The timber rail rotated backward and completely fractured near the bogie's maximum displacement.

The bogie's kinetic energy was absorbed by the barrier primarily through the deflection of the rubber shear fenders and bending and fracture of the timber rail. No individual dynamic component tests had been conducted on the 10-in. (254-mm) wide x 11 $\frac{5}{8}$ -in. (295-mm) tall x 15 $\frac{3}{4}$ in. (400-mm) long shear fenders prior to test no. SFHT-1. Therefore, the static force vs. deflection and energy vs. deflection curves, which were provided by the manufacturer, were used to evaluate the energy absorption of the barrier system [6].

From test no. HSF14-5, the dynamic component test had an energy vs. deflection curve that followed the same trend as the static curve, except that it was about 30 k-in. (3.4 kJ) higher due to inertia, as shown in Figure 87. When a shear fender bends and rotates rather than deflecting in pure shear, less energy is absorbed, which is evident in Figure 87. It should be noted that the energy from the dynamic test does not increase as quickly as the static test after 20 in. (508 mm) of deflection. Considering that the dynamic energy dissipation was greater than the static energy dissipation and a rotating shear fender absorbs less energy than when deforming in shear, the energy absorbed by each shear fender during the dynamic test would be approximately the same as the static energy.

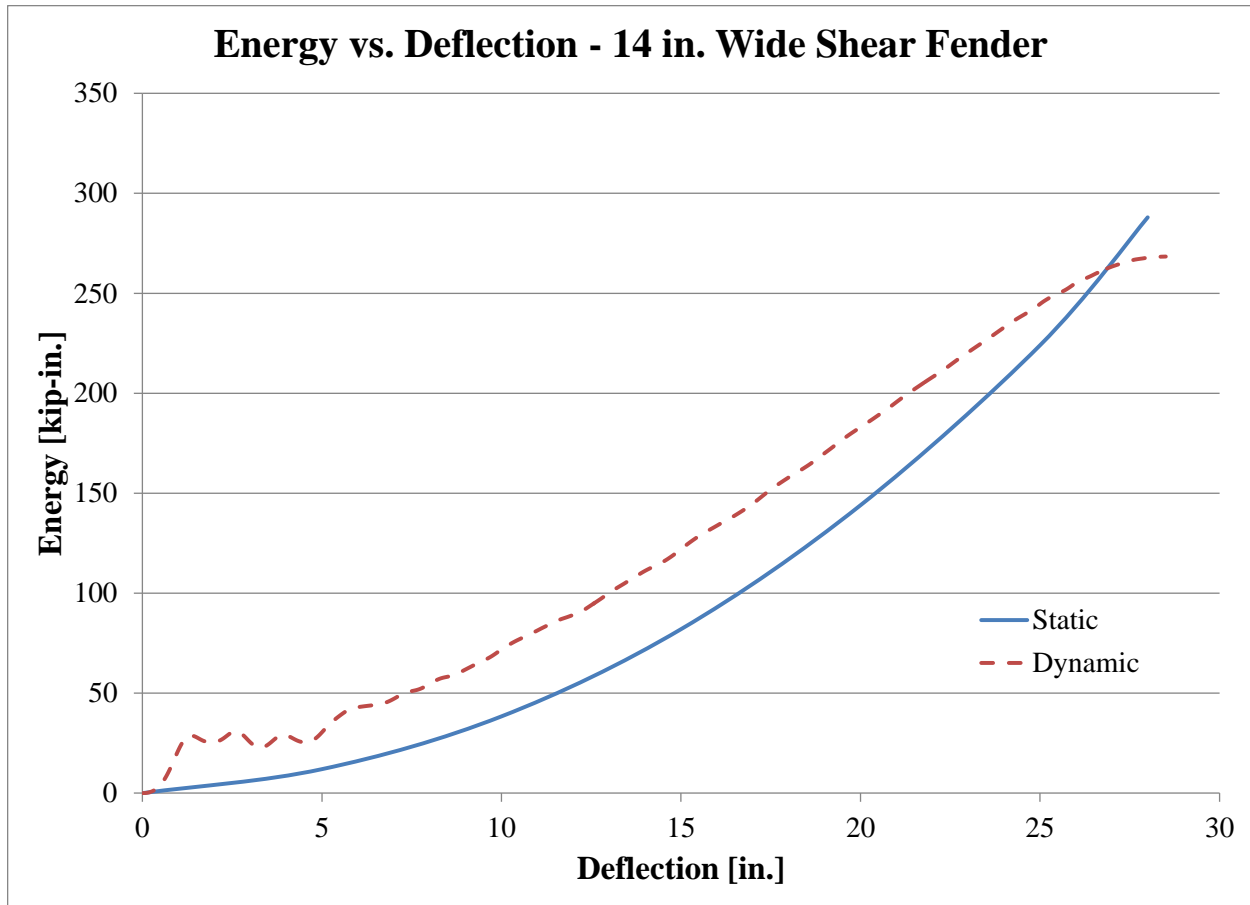


Figure 87. Static and Dynamic Energy vs. Deflection – 14-in. (356-mm) Wide Shear Fender

The static force vs. deflection and energy vs. deflection curves are shown in Figure 88 [7]. The deflection and energy of each shear fender, as labeled from left to right of the barrier (nos. 1-4), is shown in Table 9. Shear fender no. 1 rotated during almost the entire impact. Shear fender nos. 2, 3, and 4 deflected in almost pure shear for 8 in. (203 mm), 7.1 in. (180 mm), and 3.4 in. (86 mm), respectively, before beginning to rotate to the total deflections shown in Table 9. For the shear fenders that deflected more than 20 in. (508 mm), which is the maximum, the shear fenders were assumed to absorb the maximum of 115 k-in. (13.0 kJ), as shown in Figure 88. The estimated total energy absorbed by the shear fenders alone was 345 k-in. (39.0 kJ). When compared to the total energy absorbed by the barrier, 76 percent was specifically by the shear fenders. This value may be artificially high, considering that the shear fenders rotated

significantly. However, it is still believed to be a reasonable estimate of the energy-absorbing capacity of the shear fenders. If an optimal rail and splice were designed to distribute the impact load to multiple shear fenders, then there exists a potential for this barrier concept to reduce lateral accelerations 30 percent as compared to impact events into a rigid concrete barrier. Optimizing the barrier deformation in shear, rather than rotation, would also increase energy absorption.

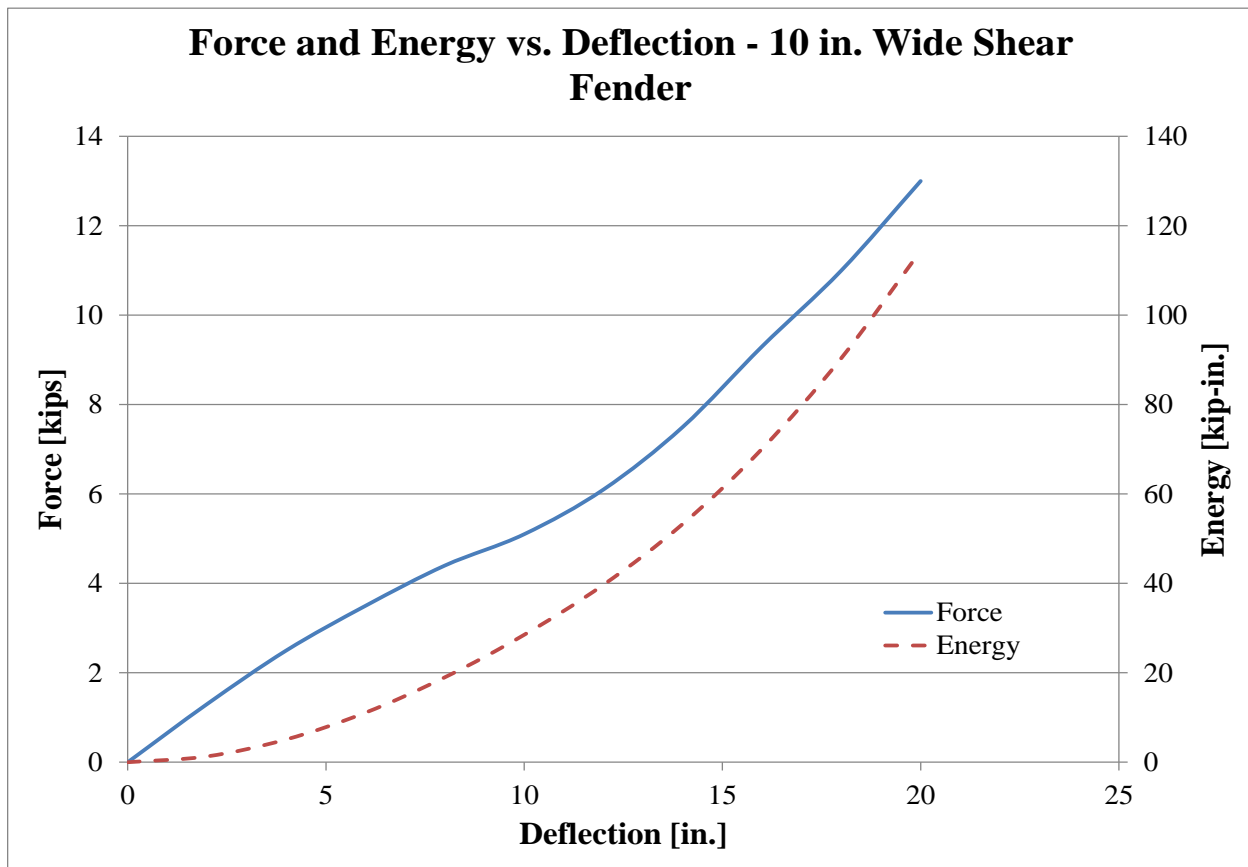


Figure 88. Static Force and Energy vs. Deflection – 10-in. (254-mm) Wide Shear Fender

Table 9. Cylinder Deflection and Energy Absorption, Test No. SFHT-1

Shear Fender No.	Deflection in. (mm)	Energy Absorption k-in. (kJ)
1	13.5 (343)	45 (5.1)
2	21.8 (554)	115 (13.0)
3	23 (584)	115 (13.0)
4	16.3 (414)	70 (7.9)

7 SHEAR FENDER STATIC LOAD TESTING

7.1 Purpose

The shear fenders were statically loaded in compression to determine the rail weight which could be supported at cold, room, and hot temperatures. The optimal post spacing and rail weight were explored. The vertical deflection of the shear fenders under the static rail weight were needed to determine the overall barrier height after the shear fenders settled. The preliminary concrete beam in the design concept had 14-in. (356-mm) wide shear fender posts supporting a weight of 4,600 lb (2,087 kg) each, or a 460 lb/ft (685 kg/m) uniform load [1].

7.2 Scope

A total of ten static tests, as shown in Table 10, were conducted on the 14-in. (356-mm) wide x 16-in. (406-mm) high x 22-in. (559-mm) long and the 10-in. (254-mm) wide x 11⁵/₈-in. (295-mm) tall x 15³/₄-in. (400-mm) long shear fenders previously explored through dynamic component testing. In test nos. SFHS-1 through SFHS-3, a 4,934-lb (2,238-kg) safety-shaped concrete barrier was lowered incrementally onto a 14-in. (356-mm) wide shear fender at temperatures of 16°F (-9°C), 67°F (19°C), and 130°F (54°C), respectively. In test no. SFHS-4, a safety-shaped concrete barrier was lowered incrementally onto two 14-in. (356-mm) wide shear fenders spaced at approximately 16 ft (4.9 m).

In test nos. SFHS-5 and SFHS-6, an 18-in. (457-mm) wide x 12-in. (305-mm) high x 16-ft (4.9-m) long concrete beam was lowered incrementally onto four 10-in. (254-mm) wide shear fenders spaced at 4 ft (1.2 m) on center, as shown in Figures 89 and 90. The lateral faces of the shear fenders were offset 4 in. (102 mm) and alternated. Test nos. SFHS-5 and SFHS-6 were conducted at 58°F (14°C) and 111°F (44°C), respectively. In test no. SFHS-7, an 18-in. (457-mm) wide x 12-in. (305-mm) high x 16-ft (4.9-m) long concrete beam was lowered incrementally onto four 10-in. (254-mm) wide shear fenders spaced at 5 ft (1.5 m) on center. In

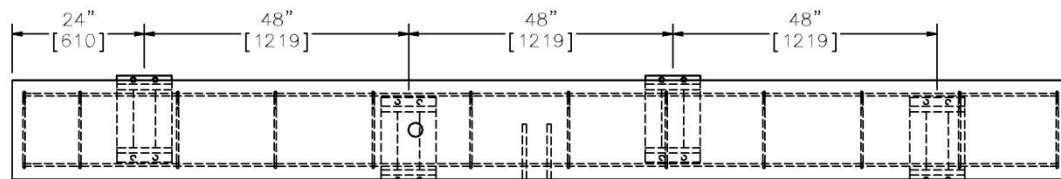
test no. SFHS-8, an 18-in. (457-mm) wide x 12-in. (305-mm) high x 16-ft (4.9-m) long concrete beam was lowered incrementally onto four 10-in. (254-mm) wide shear fenders spaced at 5 ft (1.5 m) on center on a 14 percent grade. In test no. SFHS-9, an 18-in. (457-mm) wide x 12-in. (305-mm) high x 16-ft (4.9-m) long concrete beam was lowered incrementally onto four 10-in. (254-mm) wide shear fenders spaced at 5 ft (1.5 m) on center with the alternating 4-in. (152-mm) offset on a 14 percent grade. In test no. SFHS-10, an 18-in. (457-mm) wide x 12-in. (305-mm) high x 16-ft (4.9-m) long concrete beam was lowered incrementally onto three 10-in. (254-mm) wide shear fenders spaced at 7 ft (2.1 m) on center. An additional 18-in. (457-mm) wide x 12-in. (305-mm) high x 16-ft (4.9-m) long concrete beam was incrementally added in test nos. SFHS-5 through SFHS-10 when a larger load was desired.

The surface temperature of the rubber shear fenders was documented prior to each test when available. Test nos. SFHS-4 and SFHS-7 through SFHS-10 were conducted at an ambient indoor air temperature, or approximately 65°F (18°C).

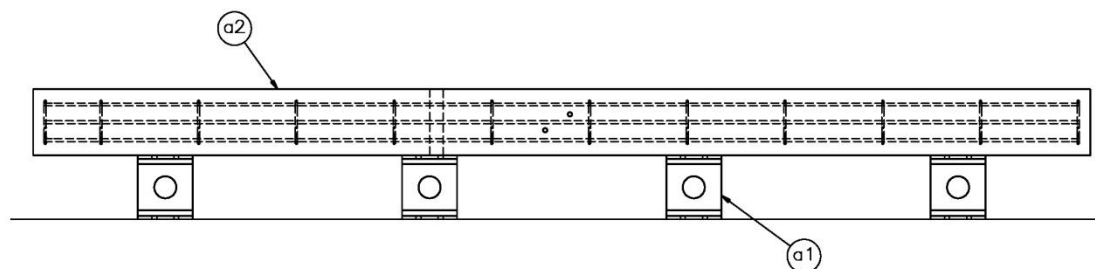
Table 10. Static Shear Fender Testing Summary

Test No.	Shear Fender Width in. (mm)	No. of Fenders	Temp °F (°C)	Spacing ft (m)	Special Conditions
SFHS-1	14 (356)	1	16 (-9)	NA	no
SFHS-2	14 (356)	1	67 (19)	NA	no
SFHS-3	14 (356)	1	130 (54)	NA	no
SFHS-4	14 (356)	2	65 (18)	16 (4.9)	no
SFHS-5	10 (254)	4	58 (14)	4 (1.2)	4" lat offset
SFHS-6	10 (254)	4	111 (44)	4 (1.2)	4" lat offset
SFHS-7	10 (254)	4	65 (18)	5 (1.5)	no
SFHS-8	10 (254)	4	65 (18)	5 (1.5)	on 14% slope
SFHS-9	10 (254)	4	65 (18)	5 (1.5)	on 14% slope, 4" lat offset
SFHS-10	10 (254)	3	65 (18)	7 (2.1)	no

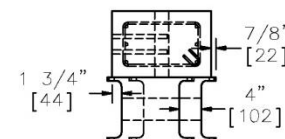
Item No.	QTY.	Description	Material Specification
a1	4	Morse E46496 Shear Fender	ASTM D2000
a2	1	12"x18"x16' [305x457x4877] Concrete Post	f'c=4000ksi



PLAN VIEW



ELEVATION VIEW



PROFILE VIEW

- Notes: (1) Scales not necessary.
 (2) Document vertical displacement at full load.
 (3) If stable, add more weight. No definite increase in weight (recommend 15–40 lb/ft) per trial. If unstable, do nothing more.
 (4) Jennifer must be present for testing.

 Midwest Roadside Safety Facility	SAFER Rub Rail with Offset Shear Fenders		SHEET: 1 of 2
	System Details		DATE: 2/13/2013
DWG. NAME: SAFER-offset_v1	SCALE: 1:28 UNITS: in./mm	REV. BY:	DRAWN BY: CWP

Figure 89. Test Setup, Test Nos. SFHS-5 and SFHS-6

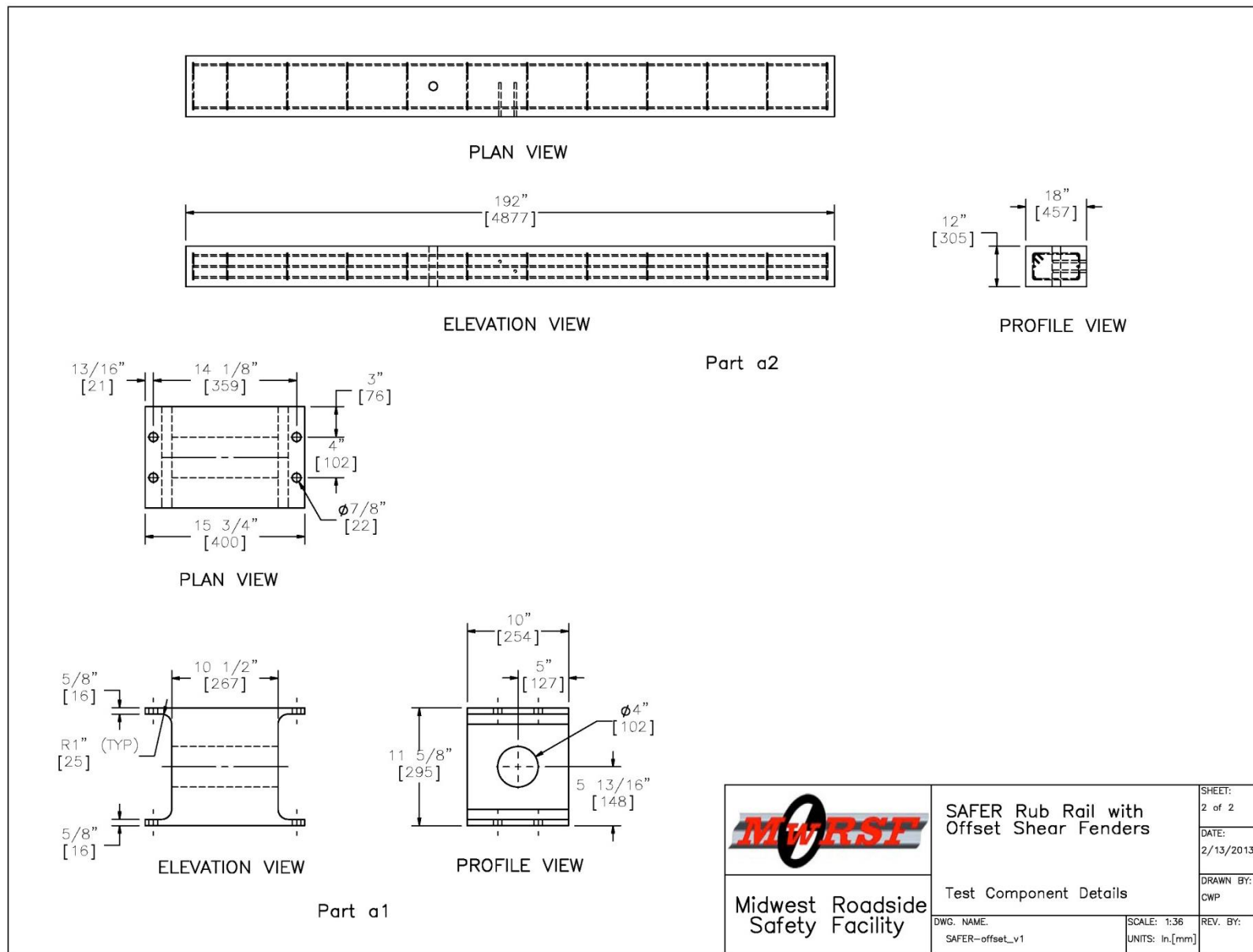


Figure 90. Component Details, Test Nos. SFHS-5 and SFHS-6

7.3 Results

The information desired from the static tests was the relation between the applied load and the vertical deflection of the shear fender at various temperatures. In some of the tests, the system began to lean and/or twist with larger loads. When this occurred, the load was recorded as the approximate unstable load. However, this point was somewhat subjective because there was not one definitive point where the system was unstable, but rather, a large range of loads where the beam was leaning. The stable load was the last recorded applied load before the unstable load occurred. The average deflection of the system with a 5,000-lb (2,268-kg) applied load was also determined. The results of the ten static tests are shown in Table 11.

Table 11. Static Shear Fender Testing Results

Test No.	Shear Fender Width in. (mm)	No. of Fenders	Temp °F (°C)	Spacing ft (m)	Special Conditions	Stable Load lb (kg)	Unstable Load lb (kg)	5,000 lb (2,268 kg) Deflection in. (mm)
SFHS-1	14 (356)	1	16 (-9)	NA	no	-	4,000 (1,814)	1.4 (36)
SFHS-2	14 (356)	1	67 (19)	NA	no	-	3,000 (1,361)	1.4 (36)
SFHS-3	14 (356)	1	130 (54)	NA	no	-	500 (227)	1.5 (38)
SFHS-4	14 (356)	2	65 (18)	16 (4.9)	no	2,977 (1,350)	3,760 (1,705)	NA
SFHS-5	10 (254)	4	58 (14)	4 (1.2)	4" lat offset	5,088 (2,308)	6,360 (2,885)	0.28 (7)
SFHS-6	10 (254)	4	111 (44)	4 (1.2)	4" lat offset	5,122 (2,323)	6,970 (3,162)	0.41 (10)
SFHS-7	10 (254)	4	65 (18)	5 (1.5)	no	4,994 (2,265)	over 7,000 (3,175)	0.41 (10)
SFHS-8	10 (254)	4	65 (18)	5 (1.5)	on 14% slope	3,500 (1,588)	over 3,500 (1,588)	NA
SFHS-9	10 (254)	4	65 (18)	5 (1.5)	on 14% slope, 4" lat offset	3,970 (1,801)	4,500 (2,041)	NA
SFHS-10	10 (254)	3	65 (18)	7 (2.1)	no	4,994 (2,265)	6,500 (2,948)	0.53 (13)

7.3.1 Test Nos. SFHS-1 through SFHS-3

A 4,934-lb (2,238-kg) safety-shaped concrete barrier was lowered incrementally onto a 14-in. (356-mm) wide shear fender. The concrete barrier was suspended from a chain that was attached to an overhead crane. It was difficult to center the barrier weight, so a skid-steer loader was used to stabilize the barrier to prevent lateral movement. A floor scale was placed under the shear fender and then zeroed so that the scale reading would be equal to the load applied to the

shear fender. The shear fender was loaded incrementally and deflections were measured at each known load. The test setup is shown in Figure 91.



Figure 91. Testing Apparatus, Test Nos. SFHS-1 through SFHS-3

The shear fender was tested at three temperatures: 16°F (-9°C) (subfreezing), 67°F (19°C) (room temperature), and 130°F (54°C) (hot). These three temperatures were used to simulate the extreme boundaries and the ideal conditions for the shear fender. Since a surface thermometer was used to measure the temperature of the shear fender, it was important that the temperature throughout the shear fender be uniform. To attain this, the shear fender was placed in an environment for at least an hour, and it was assumed that the surface temperatures of the shear fender represented the overall temperature of the shear fender.

Heights were measured at six points on the outside top face of the shear fender. These six points were average to find the compressed height of one shear fender. Deflection was calculated relative to the undeformed shear fender height at room temperature. The deflection of the shear

fender at approximately 500-lb (227-kg) load increments for test nos. SFHS-1 through SFHS-3 are shown in Tables 12 through 14, respectively.

The shear fender was loaded as uniformly as possible. However, the barrier began to lean and/or twist at higher loads and temperatures, which caused the system to be unstable, as shown in Figure 92. Therefore, the barrier was supported laterally when needed so that deflections could be measured at each load.

Table 12. Shear Fender Loads and Deflections at Subfreezing Temperature, Test No. SFHS-1

Load lb (kg)	Deflection in. (mm)
550 (249)	0.26 (7)
1,160 (526)	0.34 (9)
1,603 (727)	0.43 (11)
2,470 (1,120)	0.66 (17)
3,560 (1,615)	1.01 (26)
4,020 (1,823)	1.20 (30)
4,650 (2,109)	1.32 (34)
4,920 (2,232)	1.44 (37)

Table 13. Shear Fender Loads and Deflections at Room Temperature, Test No. SFHS-2

Load lb (kg)	Deflection in. (mm)
550 (249)	0.18 (5)
1,034 (469)	0.27 (7)
1,550 (703)	0.43 (11)
2,000 (907)	0.54 (14)
2,520 (1,143)	0.68 (17)
3,020 (1,370)	0.85 (22)
3,550 (1,610)	0.99 (25)
4,090 (1,855)	1.18 (30)
4,670 (2,118)	1.34 (34)
4,910 (2,227)	1.43 (36)

Table 14. Shear Fender Loads and Deflections at Hot Temperature, Test No. SFHS-3

Load lb (kg)	Deflection in. (mm)
492 (223)	0.09 (2)
1,060 (481)	0.25 (6)
1,586 (719)	0.45 (11)
2,000 (907)	0.57 (14)
2,580 (1,170)	0.74 (19)
3,010 (1,365)	0.90 (23)
3,520 (1,597)	1.02 (26)
4,050 (1,837)	1.20 (30)
4,520 (2,050)	1.35 (34)
4,840 (2,195)	1.50 (38)



Figure 92. Example of System Instabilities, Test Nos. SFHS-1 through SFHS-3

The system appeared to be more unstable when the shear fender was warmer. For the subfreezing temperature measurement, the shear fender was relatively stiff, and instability was not seen until loads of 4,000 to 4,500 lb (1,814 to 2,041 kg). At room temperature, instability was seen at loads of 3,000 to 3,500 lb (1,361 to 1,588 kg). For the hot temperature measurement, instability was seen at loads as low as 500 lb (227 kg). This observation may be attributed to non-uniform or unsymmetrical loading on the shear fender as well as a decrease in the modulus of rubber at warmer temperatures. Nonetheless, the shear fender showed similar load versus deflection curves over all temperature ranges, as shown in Figure 93. Vertical deflections at each point were averaged to obtain an average shear fender deflection.

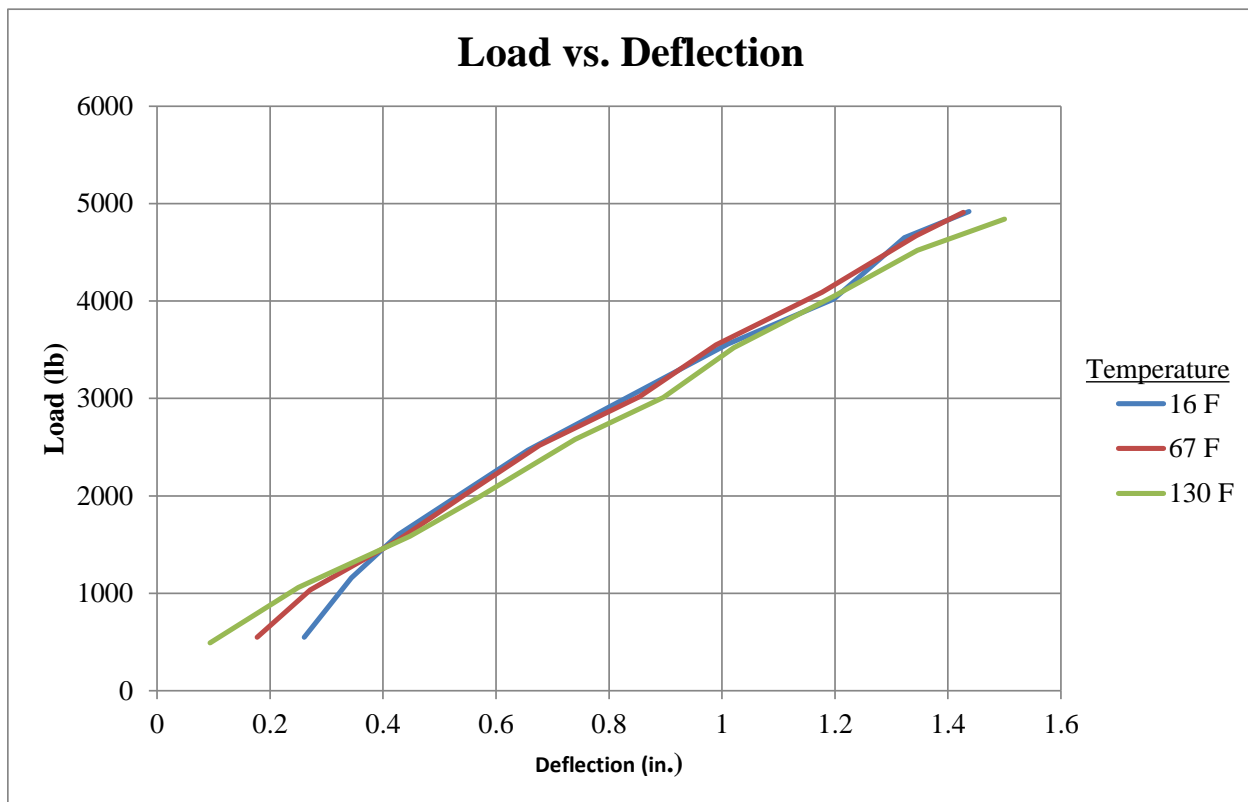


Figure 93. Load vs. Deflection at Subfreezing, Room, and Hot Temperatures

Initial conclusions from test nos. SFHS-1 through SFHS-3 include:

- 1) Temperature does not affect the vertical deflection significantly;
- 2) The vertical deflection for a barrier system with 14-in. (356-mm) wide shear fender posts could be estimated based on the weight applied to each post;
- 3) The 14-in. (356-mm) wide shear fender may not be able to support a large static rail weight; and
- 4) The post-and-rail system may become unstable if the load is not applied symmetrically and uniformly to the posts.

7.3.2 Test No. SFHS-4

In test no. SFHS-4, a safety-shaped concrete barrier was lowered incrementally onto two 14-in. (356-mm) wide shear fenders spaced at approximately 16 ft (4.9 m) at room temperature, as shown in Figure 94. Since the weight of the barrier was more evenly distributed over two shear fender post faces, it was believed that the system would be more stable.



Figure 94. Test Setup, Test No. SFHS-4

When the total applied load on top of the shear fenders was 2,977 lb (1,350 kg), the system was stable. However, when the total applied load reached 3,760 lb (1,706 kg), the barrier began leaning toward one side, as shown in Figure 95. Additional load was not applied and deflection measurements were not taken.



Figure 95. System Instabilities, Test No. SFHS-4

Initial conclusions from test no. SFHS-4 include:

- 1) The 14-in. (356-mm) wide shear fender may not be able to support a large static rail weight;
- 2) The post-and-rail system may become unstable if the load is not applied symmetrically and uniformly to the posts; and
- 3) A safety-shaped barrier with a high center of gravity and non-flat bottom may not be the best shape to load shear fenders spaced uniformly and symmetrically apart.

7.3.3 Test Nos. SFHS-5 and SFHS-6

To mitigate the lateral system instabilities observed in the previous static tests, it was believed that laterally offsetting alternate shear fenders from the centerline of the beam would improve stability. In test nos. SFHS-5 and SFHS-6, an 18-in. (457-mm) wide x 12-in. (305-mm) high x 16-ft (4.9-m) long concrete beam was lowered incrementally onto four 10-in. (254-mm) wide shear fenders spaced at 4 ft (1.2 m) on center. The lateral faces of the shear fenders were alternating offset 4 in. (102 mm), as shown in Figures 89 and 90. The 10-in. (254-mm) wide shear fenders were selected because a larger quantity was available and they could be loaded uniformly with an 18-in. (457-mm) wide x 12-in. (305-mm) high x 16-ft (4.9-m) long concrete beam. The rectangular beam was desired for a more symmetric and uniform load.

In test no. SFHS-5, 6,360 lb (2,885 kg) was applied to the four shear fenders at 58°F (14°C) before the system leaned slightly toward one side. Load and average deflection measurements are shown in Table 15. When the system started leaning, the differential between the highest and lowest sides of the shear fender was 9/16 in. (14 mm). While this was not large enough for the beam to fall off, it was more than what would be desired for a barrier system.

Table 15. Test No. SFHS-5 Results

Total Load Applied lb (kg)	Average Deflection in. (mm)
0	0.00
3,496 (1,586)	0.08 (2)
4,210 (1,910)	0.25 (6)
5,088 (2,308)	0.28 (7)
6,360 (2,885)	0.38 (10)
0	-0.03 (-1)

In test no. SFHS-6, 6,970 lb (3,162 kg) was applied to the four shear fenders at 111°F (44°C) before the system leaned toward one side. Load and average deflection measurements are shown in Table 16. The largest differential between the highest and lowest sides of the shear fender was 1⅛ in. (29 mm). However, all deflections at the final state were not measured because the system was unstable.

Table 16. Test No. SFHS-6 Results

Total Load Applied lb (kg)	Average Deflection in. (mm)
0	0.00
3,492 (1,584)	0.33 (8)
5,112 (2,319)	0.41 (10)
6,970 (3,162)	0.70 (18)

Initial conclusions from test nos. SFHS-5 and SFHS-6 include:

- 1) The 10-in. (254-mm) wide shear fenders spaced at 4 ft (1.2 m) on center and with a 4-in. (102-mm) lateral offset were stable through at least a 5,112-lb (2,319-kg) load, or 320 lb/ft (476 kg/m); and
- 2) The rectangular beam shape seemed to contribute to improved stability and was easier to align.

7.3.4 Test No. SFHS-7

The 10-in. wide shear fenders were investigated to see if they were stable with no lateral offset. In test no. SFHS-7, an 18-in. (457-mm) wide x 12-in. (305-mm) high x 16-ft (4.9-m) long rectangular concrete beam was lowered incrementally onto four 10-in. (254-mm) wide shear fenders spaced at 5 ft (1.5 m) on center, as shown in Figure 96. An additional 18-in. (457-mm) wide x 12-in. (305-mm) high x 16-ft (4.9-m) long concrete beam was lowered incrementally on top of the other concrete beam. The system was loaded up to 7,000 lb (3,175 kg), and the system

did not present any instabilities. Load and average deflection measurements up to 4,994 lb (2,265 kg) are shown in Table 17. The deflection of one of the shear fender at the 7,000 lb (3,175-kg) load is shown in Figure 97.



Figure 96. Test Setup, Test No. SFHS-7

Table 17. Test No. SFHS-7 Results

Total Applied Load lb (kg)	Average Deflection in. (mm)
3,490 (1,583)	0.23
3,970 (1,801)	0.33
4,494 (2,038)	0.36
4,994 (2,265)	0.41



Figure 97. System Deflection at 7,000-lb (3,175-kg) Load, Test No. SFHS-7

Initial conclusions from test no. SFHS-7 include:

- 1) The 10-in. (254-mm) wide shear fenders spaced at 5 ft (1.2 m) on center were stable through at least a 7,000-lb (3,175-kg) load, or 438 lb/ft (651 kg/m);
- 2) The minimum spacing for 10-in. (254-mm) wide shear fender posts in a full system would be 5 ft (1.2 m) on center; and
- 3) The 4-in. (102-mm) lateral front-face offset of alternating shear fenders is not necessary for the system to be stable.

7.3.5 Test Nos. SFHS-8 and SFHS-9

The stability of the barrier on a 8 percent superelevated roadway was to be investigated. The 8 percent was chosen as the maximum superelevation that would be used for a high-speed, urban median roadway. However, ramps with a 14 percent grade were available and used during

test nos. SFHS-8 and SFHS-9. In test no. SFHS-8, an 18-in. (457-mm) wide x 12-in. (305-mm) high x 16-ft (4.9-m) long rectangular concrete beam was lowered incrementally onto four 10-in. (254-mm) wide shear fenders spaced at 5 ft (1.5 m) on center on a 14 percent grade, as shown in Figure 98. This setup appeared to be more unstable, so only 3,490 lb (1,583 kg) was applied to the four shear fenders. The system deflected an average of 0.30 in. (8 mm) under this load.

In test no. SFHS-9, an 18-in. (457-mm) wide x 12-in. (305-mm) high x 16-ft (4.9-m) long rectangular concrete beam was lowered incrementally onto four 10-in. (254-mm) wide shear fenders spaced at 5 ft (1.5 m) on center with the alternating 4-in. (102-mm) offset on a 14 percent grade, as shown in Figure 99. Load and average deflection measurements up to 4,994 lb (2,265 kg) are shown in Table 18. The system was stable up to a 3,970-lb (1,801-kg) load. The unstable load was approximately 4,500 lb (2,041 kg).

Table 18. Test No. SFHS-9 Results

Total Applied Load lb (kg)	Average Deflection in. (mm)
3,490 (1,583)	0.31 (8)
3,970 (1,801)	0.36 (9)

Initial conclusions from test nos. SFHS-8 and SFHS-9 include:

- 1) The 10-in. (254-mm) wide shear fenders spaced at 5 ft (1.5 m) on center on a 14 percent grade were stable through at least a 3,490-lb (1,583-kg) load, or 218 lb/ft (325 kg/m);
- 2) At an 8 percent grade, which is the maximum grade expected for an urban median roadway, the stable load is expected to be much higher; and
- 3) The 4-in. (102-mm) lateral front-face offset of alternating shear fenders increased the stability of the system when placed on a slope.



Figure 98. Test Setup, Test No. SFHS-8



Figure 99. Test Setup, Test No. SFHS-9

7.3.6 Test No. SFHS-10

In test no. SFHS-10, an 18-in. (457-mm) wide x 12-in. (305-mm) high x 16-ft (4.9-m) long rectangular concrete beam was lowered incrementally onto three 10-in. (254-mm) wide shear fenders spaced at 7 ft (2.1 m) on center, as shown in Figure 100. An additional 18-in. (457-mm) wide x 12-in. (305-mm) high x 16-ft (4.9-m) long concrete beam was lowered incrementally on top of the other concrete beam. The system became unstable at approximately a 6,500-lb (2,948-kg) load. Load and average deflection measurements up to 4,994 lb (2,265 kg) are shown in Table 19. The deflection of one of the shear fenders at the 4,994-lb (2,265-kg) load is shown in Figure 101.



Figure 100. Test Setup, Test No. SFHS-10

Table 19. Test No. SFHS-10 Results

Total Applied Load lb (kg)	Average Deflection in. (mm)
3,490 (1,583)	0.37 (9)
3,970 (1,801)	0.44 (11)
4,494 (2,038)	0.47 (12)
4,994 (2,265)	0.53 (13)



Figure 101. System Deflection at 4,994-lb (2,265-kg) Load, Test No. SFHS-10

Initial conclusions from test no. SFHS-10 include:

- 1) The 10-in. (254-mm) wide shear fenders spaced at 7 ft (2.1 m) on center were stable through approximately a 6,500-lb (2,948-kg) load, or 406 lb/ft (604 kg/m).

7.4 Discussion

A total of ten static tests were conducted on the 14-in. (356-mm) wide x 16-in. (406-mm) high x 22-in. (559-mm) long and the 10-in. (254-mm) wide x 11⁵/₈-in. (295-mm) tall x 15³/₄-in. (400-mm) long shear fenders previously explored through dynamic component testing. The shear fenders were statically loaded in compression to determine the rail weight which could be supported at cold, room, and hot temperatures. The optimal post spacing and rail weight were explored. The vertical deflection of the shear fenders under the static rail weight were needed to determine the overall barrier height after the shear fenders had settled.

The preliminary concrete beam in the design concept had 14-in. (356-mm) wide shear fender posts supporting a weight of 4,600 lb (2,086 kg) each, or a 460 lb/ft (684 kg/m) uniform load [1]. Several of the static tests showed that this static load would be too great for the system to be stable. Based on the performance of the system in test nos. SFHS-5, SFHS-6, SFHS-7, and SFHS-10, the targeted weight for a new rail is under approximately 320 lb/ft (476 kg/m) when the 10-in. (254-mm) shear fender posts are spaced at 5 ft (1.5 m). A maximum of 1/2 in. (13 mm) vertical deflection from the static weight of a beam is anticipated for a hot temperature condition. The spacing of the 10-in. (254-mm) wide shear fender posts may be increased up to 7 ft (2.1 m) if further evaluation shows favorable results.

At the targeted beam weight, stability problems are not anticipated at a maximum 8 percent superelevated road. However, this configuration was not explicitly tested and will be evaluated once the barrier design is finalized. While the alternating shear fenders with a lateral offset provided a more stable configuration on a 14 percent grade, it may not be necessary for the targeted beam weight in a full barrier system. Alternating shear fenders with a lateral offset also provided little, if any, advantage when the shear fenders were placed on flat ground.

8 SUMMARY, CONCLUSIONS, AND RECOMMENDATIONS

The dynamic properties of EPDM rubber cylinders and rubber marine shear fenders, including energy, force, and deflection, were determined through dynamic bogie tests. Schmidt, et al. estimated that 52.8 k-in. to 211.2 k-in. (6.0 kJ to 23.9 kJ) of energy, depending on the spacing, needs to be absorbed by each energy absorber in a new roadside/median barrier for a 30 percent reduction in lateral acceleration as compared to a rigid concrete barrier for a 2270P impact event [1]. Barrier concepts with both cylinders and shear fenders were evaluated with a short system installation and dynamic testing. Static testing was used to determine optimal rail weight and post spacing for the shear fender post design concept. The change in rubber properties as a function of temperature was also explored. A summary of the test results with rubber cylinders and shear fenders and discussion on their implementation into barrier designs are provided in the following sections.

8.1 Rubber Cylinders

Test nos. EPDM-1 through EPDM-3 were conducted on three EPDM rubber cylinders: (1) 8 $\frac{1}{8}$ -in. (206-mm) inner diameter x 2-in. (51-mm) thick x 10-in. (254-mm) long, 80-durometer cylinder; (2) 8 $\frac{1}{8}$ -in. (206-mm) inner diameter x 2-in. (51-mm) thick x 10-in. (254-mm) long, 60-durometer cylinder; and (3) 9 $\frac{5}{8}$ -in. (244-mm) inner diameter x 1-in. (25-mm) thick x 10-in. (254-mm) long, 80-durometer cylinder. The results from the bogie testing matrix are summarized in Table 6.

Only a slight difference was observed between the 60 and 80 durometer rubber cylinders (test nos. EPDM-1 and EPDM-2). The 1-in. (25-mm) thick cylinder (test no. EPDM-3) had one-half of the peak force, 2.5 times the total energy, and deflected 3 times as much as the 2-in. (51-mm) thick cylinder (test no. EPDM-1). However, the velocity of test no. EPDM-3 was also 1.5 times greater than test no. EPDM-1. Test nos. EPDM-4 through EPDM-12 did not show much

variation in the energy absorption of the 1-in. (25-mm) diameter EPDM cylinders with repeated impact events. A relationship between the change in temperature and energy absorption could not be determined.

All of the rubber cylinders absorbed less energy than what was desired. In test no. EPDM-3, the cylinder was loaded very close to its maximum deflection, and it did not absorb adequate energy for the new barrier. Thus, it is not recommended for use in its current configuration. The 2-in. (51-mm) rubber cylinders were not loaded to their maximum deflection, and they are expected to absorb significantly more energy if impacted with a larger load. The 2-in. (51-mm) thick EPDM rubber cylinders was recommended for further evaluation.

A bogie test was conducted on a 27-ft (8.2-m) long prototype rubber-cylinder retrofit barrier system to determine the deflection and energy absorption of a barrier configuration with rubber cylinders. Four 2-in. (51-mm) thick x 10-in. (254-mm) long rubber cylinders were spaced at 96 in. (2,438 mm) along a 32-in. (813-mm) tall New Jersey-shaped concrete barrier. Two ASTM A500 Grade B 6-in. x 6-in. x 3/16 in. thick (152-mm x 152-mm x 5-mm) steel tubes were placed on the front face of the cylinders. The bogie impacted the steel tube rail, and the two middle rubber cylinders reached their maximum deflections of 6.9 in. (175 mm) and 8.0 in. (203 mm) quickly. However, the load was not transferred across the tube splices, and the two outer cylinders did not deflect as much as the inner cylinders. The steel tubes plastically deformed around the edges of the wood impact head. The cylinders did not restore due to the plastic deformation in the rail. However, the cylinders did restore to their original dimensions once the rail was removed. Therefore, this barrier should be fully restorable and reusable after impact as long as the rail does not sustain permanent deformation.

The bogie's kinetic energy was absorbed by the barrier primarily through the deflection of the rubber cylinders, plastic deformation of the steel tubes, and fracturing of the wood

supports behind the cylinders. An estimated total energy of 130 k-in. (14.7 kJ) was absorbed through the deflection of the rubber cylinders. Approximately 15 percent of the initial kinetic energy of the bogie was absorbed by the two middle rubber cylinders. The splices in the steel tubular rail did not transfer the load to the outer cylinders. If the impact load can be distributed to multiple energy absorbers, then there exists a potential for this barrier concept to reduce lateral accelerations by 30 percent as compared to impact events into a rigid concrete barrier.

8.2 Rubber Shear Fenders

Several dynamic bogie tests were conducted to determine the energy absorption capabilities of rubber shear fenders. Test nos. HSF14-1 through HSF14-5 were conducted on HSF14 marine shear fender manufactured by Maritime International, Inc. The dynamic results from the bogie testing matrix are summarized in Table 7. The peak energy absorbed by the shear fenders varied between 17.8 k-in. and 268.4 k-in. (2.0 kJ and 30.3 kJ), which was highly dependent on the impact speed.

The laterally-impacted shear fender (test no. HSF14-1) deflected almost 1 in. (25 mm) farther than the longitudinally-impacted shear fender (test no. HSF14-2), but it did not absorb additional energy. Therefore, the longitudinal impact direction is more efficient than the lateral impact direction.

The shear fenders in test nos. HSF14-4 and HSF14-5 both absorbed energies within the desired range. Approximately 54.0 k-in. (6.1 kJ) and 55.2 k-in. (6.2 kJ) of energy were absorbed at 8 in. (203 mm) of deflection in test nos. HSF14-4 and HSF14-5, respectively. Approximately 67.2 k-in. (7.6 kJ) and 72.0 k-in. (8.1 kJ) were absorbed at 10 in. (254 mm) of deflection in test nos. HSF14-4 and HSF14-5, respectively. Even more energy was absorbed beyond 10 in. (254 mm) of deflection, but greater deflections were not desired in the new barrier.

The shear fenders fully restored to their original dimensions after each impact event. In test no. HSF14-5, the bogie landed on top of the shear fender, which applied a constant compression load for several minutes. Upon removal of the bogie, a maximum deformation of ½ in. (13 mm) remained, but the shear fender later restored to its original dimensions. The shear fenders are not expected to have any long-term loads other than the weight of the beam. Therefore, the shear fenders should restore after an impact event.

A bogie test was conducted on a 28-ft (8.5-m) long prototype shear fender post and beam system to determine the deflection and energy absorption of the barrier system. Four 10-in. (254-mm) wide x 11⅝-in. (295-mm) tall x 15¾-in. (400-mm) long shear fender posts were spaced at 96 in. (2,438 mm) on center. The center of gravity of the bogie was about 6 in. (152 mm) higher than the impact height on the timber rail. Therefore, the barrier was loaded eccentrically, and the shear fenders rotated more than deforming in shear. The timber rail rotated backward and completely fractured near the bogie's maximum displacement of 35 in. (889 mm). The bogie's kinetic energy was absorbed by the barrier primarily through the deflection of the rubber shear fenders and bending and fracture of the timber rail.

Shear fender no. 1 rotated during almost the entire impact. Shear fender nos. 2, 3, and 4 deflected in almost pure shear for 8 in. (203 mm), 7.1 in. (180 mm), and 3.4 in. (86 mm), respectively, before beginning to rotate to the total deflection shown in Table 9. The estimated total energy absorbed by the shear fenders was 345 k-in. (39.0 kJ). When compared to the total energy absorbed by the barrier, 76 percent was absorbed by the shear fenders. This value may be artificially high, considering that the shear fenders rotated significantly. However, it is still believed to be a reasonable estimate of the energy-absorbing capacity of the shear fenders. If an optimal rail and splice were designed to distribute the impact load to multiple shear fenders, then there exists a potential for this barrier concept to reduce lateral accelerations by 30 percent as

compared to impact events into a rigid concrete barrier. Optimizing the barrier to deform in shear, rather than rotating, would also increase energy absorption.

A total of ten static tests were conducted on the 14-in. (356-mm) wide x 16-in. (406-mm) high x 22-in. (559-mm) long and the 10-in. (254-mm) wide x 11⁵/₈-in. (295-mm) tall x 15³/₄-in. (400-mm) long shear fenders previously explored through dynamic component testing. The shear fenders were statically loaded in compression to determine the rail weight they could support at cold, room, and hot temperatures. The optimal post spacing and rail weight were explored. The vertical deflections of the shear fenders under the static rail weights were determined to evaluate the overall barrier height when settled.

The preliminary concrete beam in the design concept had 14-in. (356-mm) wide shear fender posts supporting a weight of 4,600 lb (2,086 kg) each, or a 460 lb/ft (684 kg/m) uniform load. Several of the static tests showed that this static load would be too great for the shear fender post system to be stable. Based on the system performance in test nos. SFHS-5, SFHS-6, SFHS-7, and SFHS-10, the targeted weight for a new rail is under approximately 320 lb/ft (476 kg/m) when the 10-in. (254-mm) shear fender posts are spaced at 5 ft (1.5 m). A maximum of 1/2 in. (13 mm) vertical deflection from the static weight of a beam is anticipated for a hot temperature condition. The spacing of the 10-in. (254-mm) wide shear fender posts may be increased up to 7 ft (2.1 m) if further evaluation shows favorable results.

At the targeted beam weight, stability problems are not anticipated at a maximum 8 percent superelevated road. However, this configuration was not explicitly tested and will be evaluated once the barrier design is finalized. While the alternating shear fenders with a lateral offset provided a more stable configuration on a 14 percent grade, it may not be necessary for the targeted beam weight in a full barrier system. Alternating shear fenders with a lateral offset also provided little, if any, advantage when the shear fenders were placed on flat ground.

9 REFERENCES

1. Schmidt, J.D., Faller, R.K., Sicking, D.L., Reid, J.D., Lechtenberg, K.A., Bielenberg, R.W., Rosenbaugh, S.K., and Holloway, J.C., *Development of a New Energy-Absorbing Roadside/Median Barrier System with Restorable Elastomer Cartridges*, Final Report to the Nebraska Department of Roads and the Federal Highway Administration, MwRSF Research Report No. TRP-03-281-13, Midwest Roadside Safety Facility, University of Nebraska-Lincoln, Lincoln, Nebraska, July 16, 2013.
2. *Manual for Assessing Safety Hardware (MASH)*, American Association of State Highway and Transportation Officials (AASHTO), Washington, D.C., 2009.
3. Society of Automotive Engineers (SAE), *Instrumentation for Impact Test – Part 1 – Electronic Instrumentation*, SAE J211/1 MAR95, New York City, NY, July, 2007.
4. CLA-VAL, *Selection Guide for Chemical Resistance of Elastomer*, www.claval.com/pdfs/N-Elastomer_Selection_Guide.pdf, 2003.
5. MSC Software, *Whitepaper – Nonlinear Finite Element Analysis of Elastomers*, www.axelproducts.com/downloads/WP_Nonlinear_FEA-Elastomers.pdf
6. Maritime International, Inc., “HSF14 Shear Fender Load and Energy Vs. Deflection”.
7. Morse Rubber Products Co., *Morse Dock Fenders*, MRP 001-84, July 1, 1984.

10 APPENDICES

Appendix A. Bogie Test Results

The results of the recorded data from each accelerometer on every dynamic bogie test are provided in the summary sheets found in this appendix. Summary sheets include acceleration, velocity, and displacement versus time plots as well as force and energy versus displacement plots.

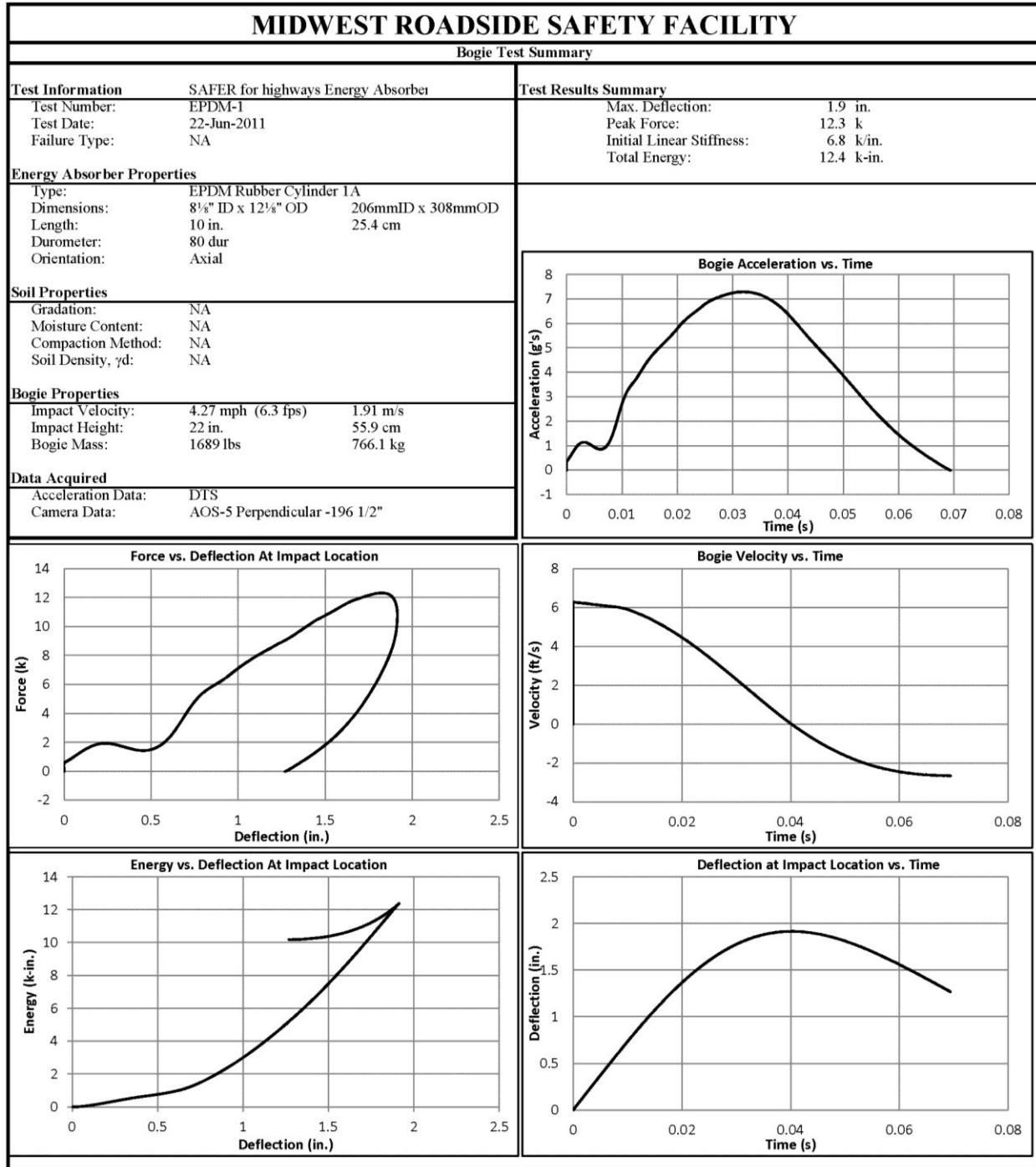


Figure A-1. Results of Test No. EPDM-1 (DTS)

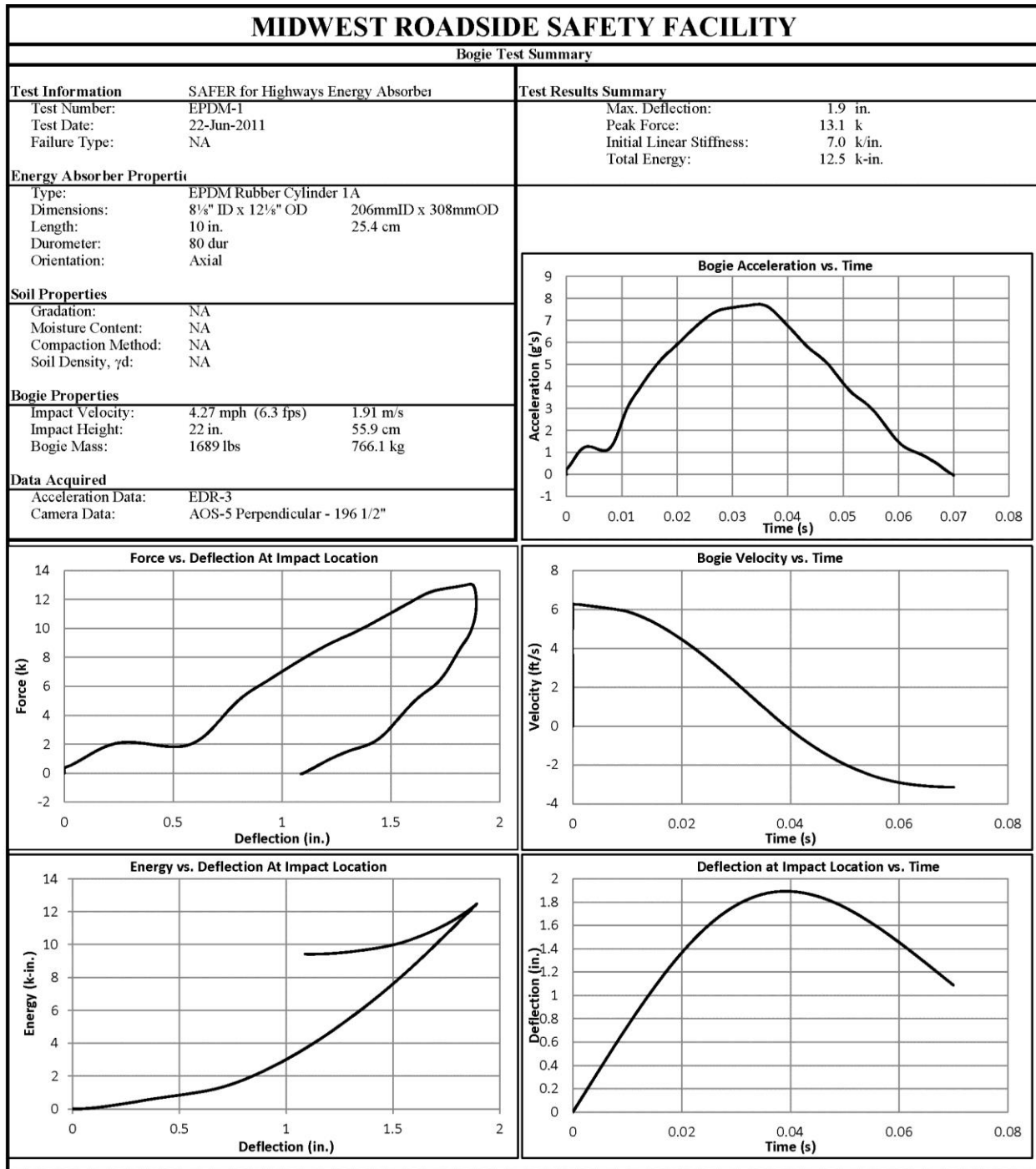


Figure A-2. Results of Test No. EPDM-1 (EDR-3)

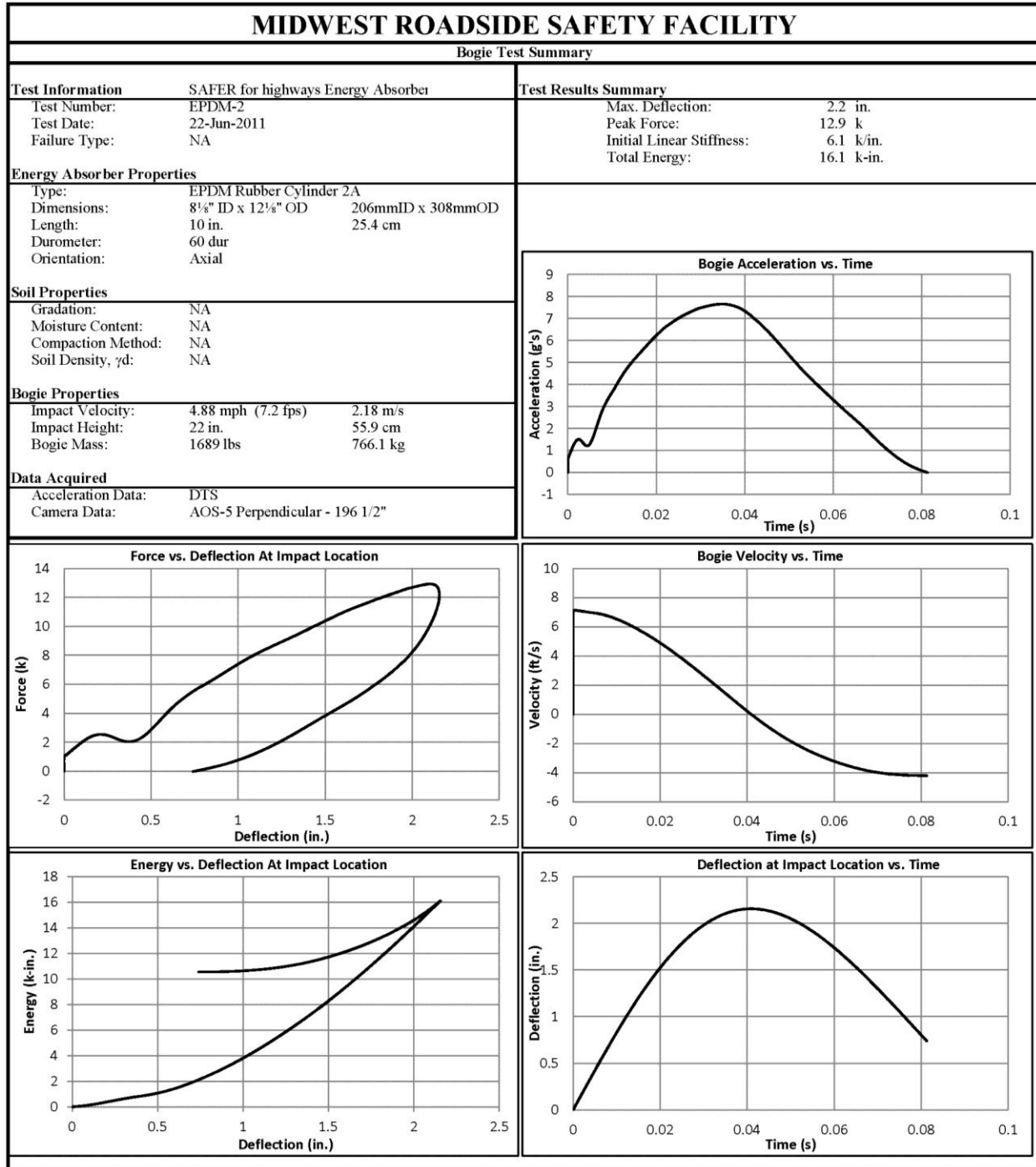


Figure A-3. Results of Test No. EPDM-2 (DTS)

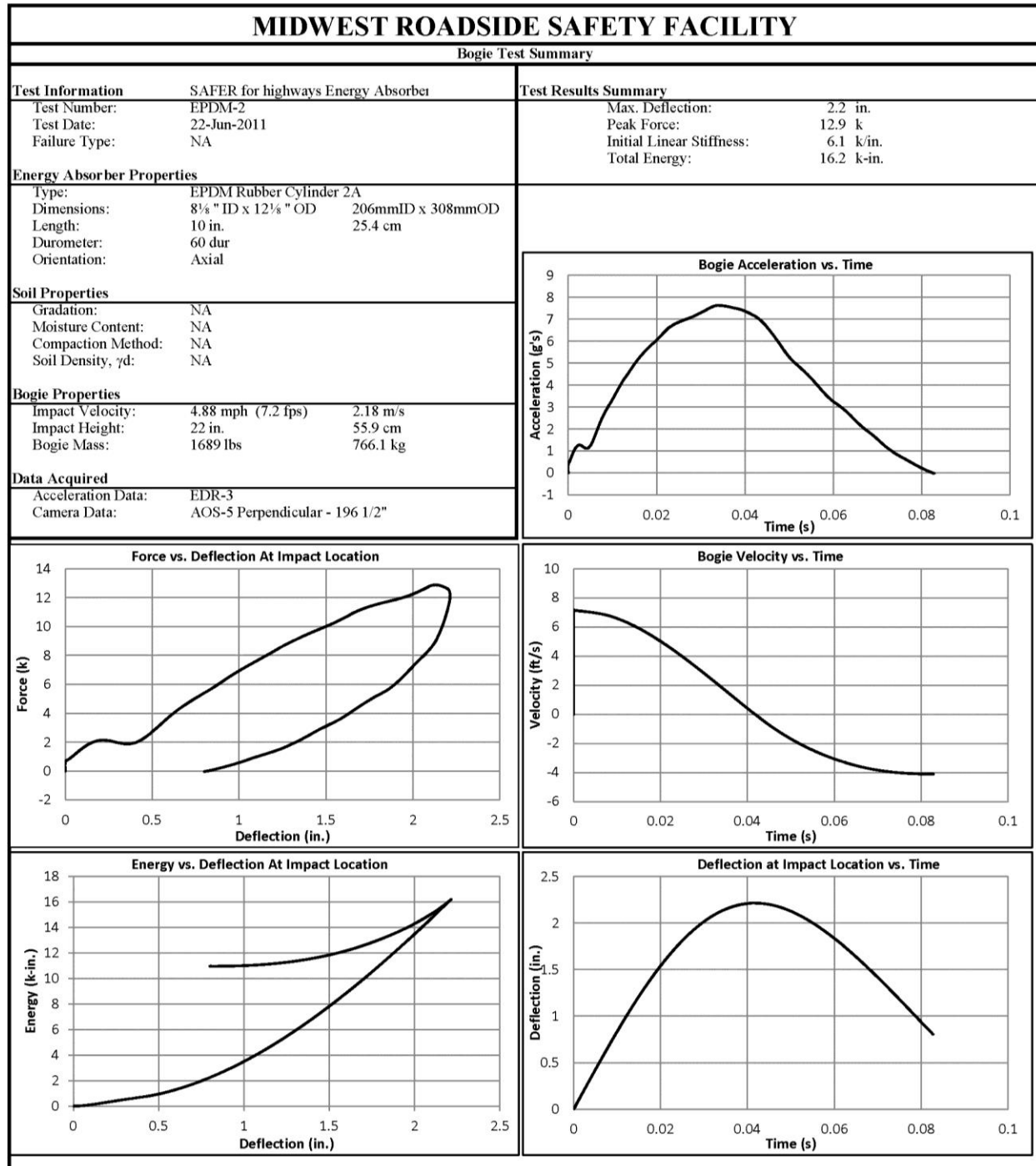


Figure A-4. Results of Test No. EPDM-2 (EDR-3)

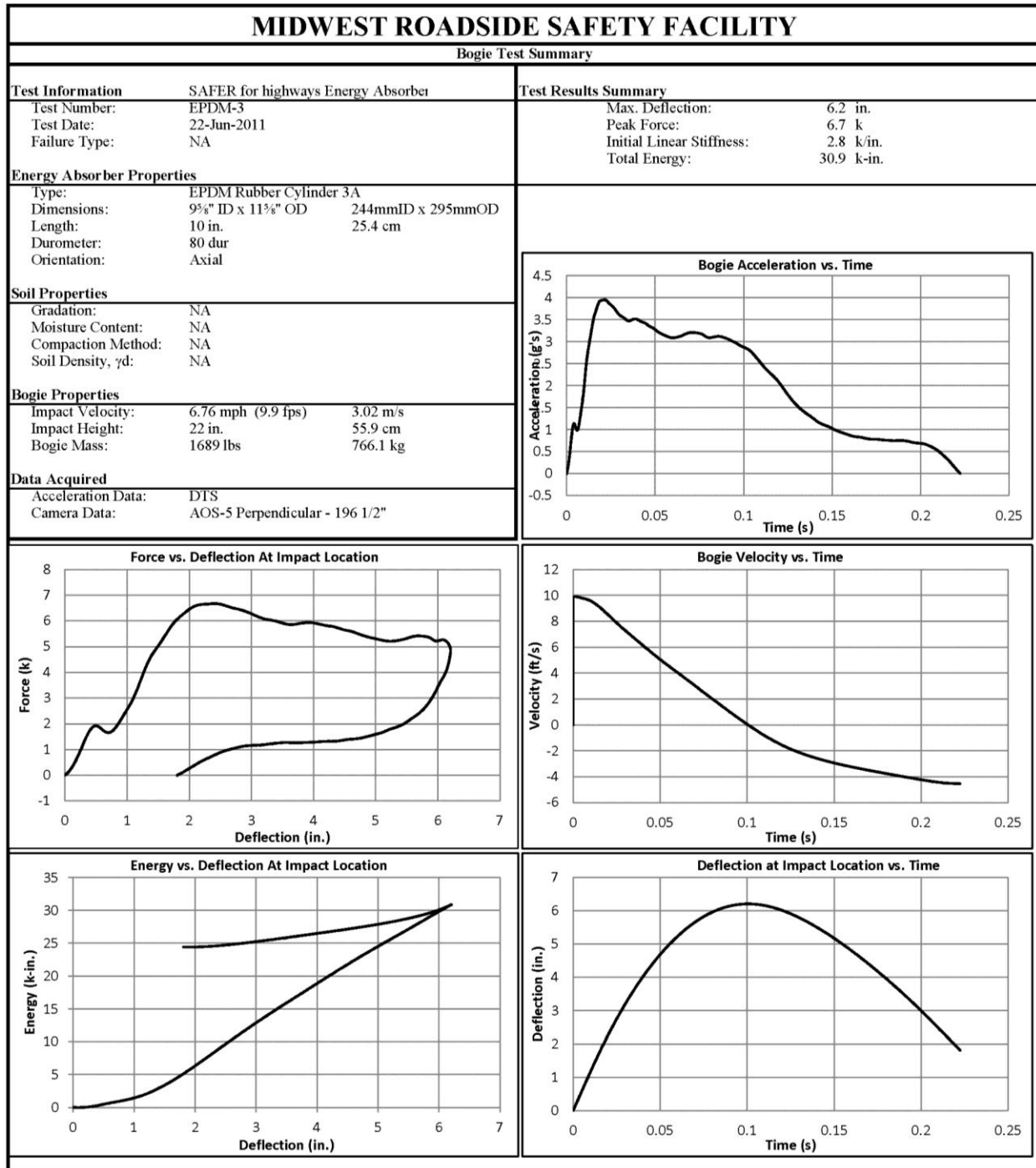


Figure A-5. Results of Test No. EPDM-3 (DTS)

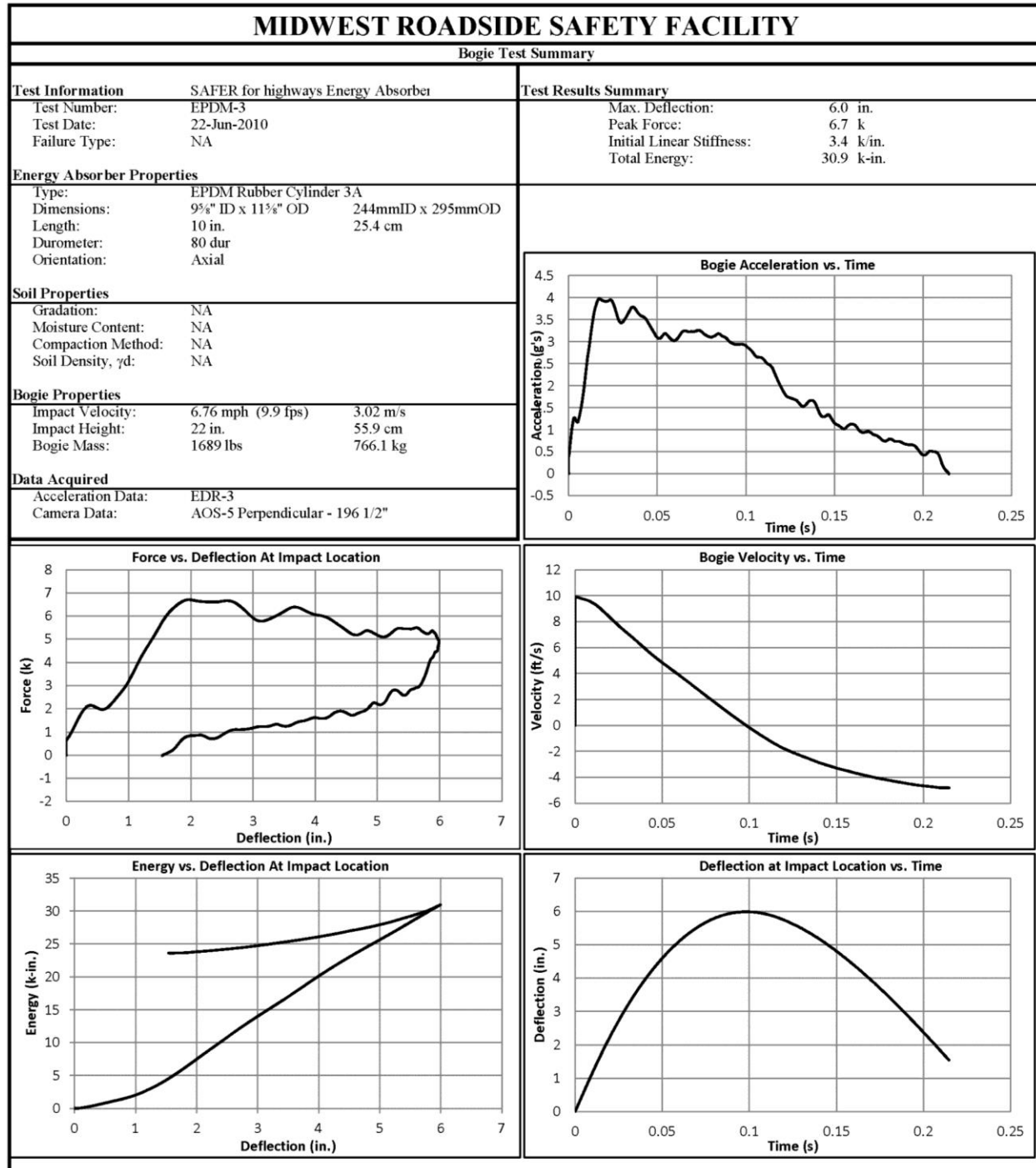


Figure A-6. Results of Test No. EPDM-3 (EDR-3)

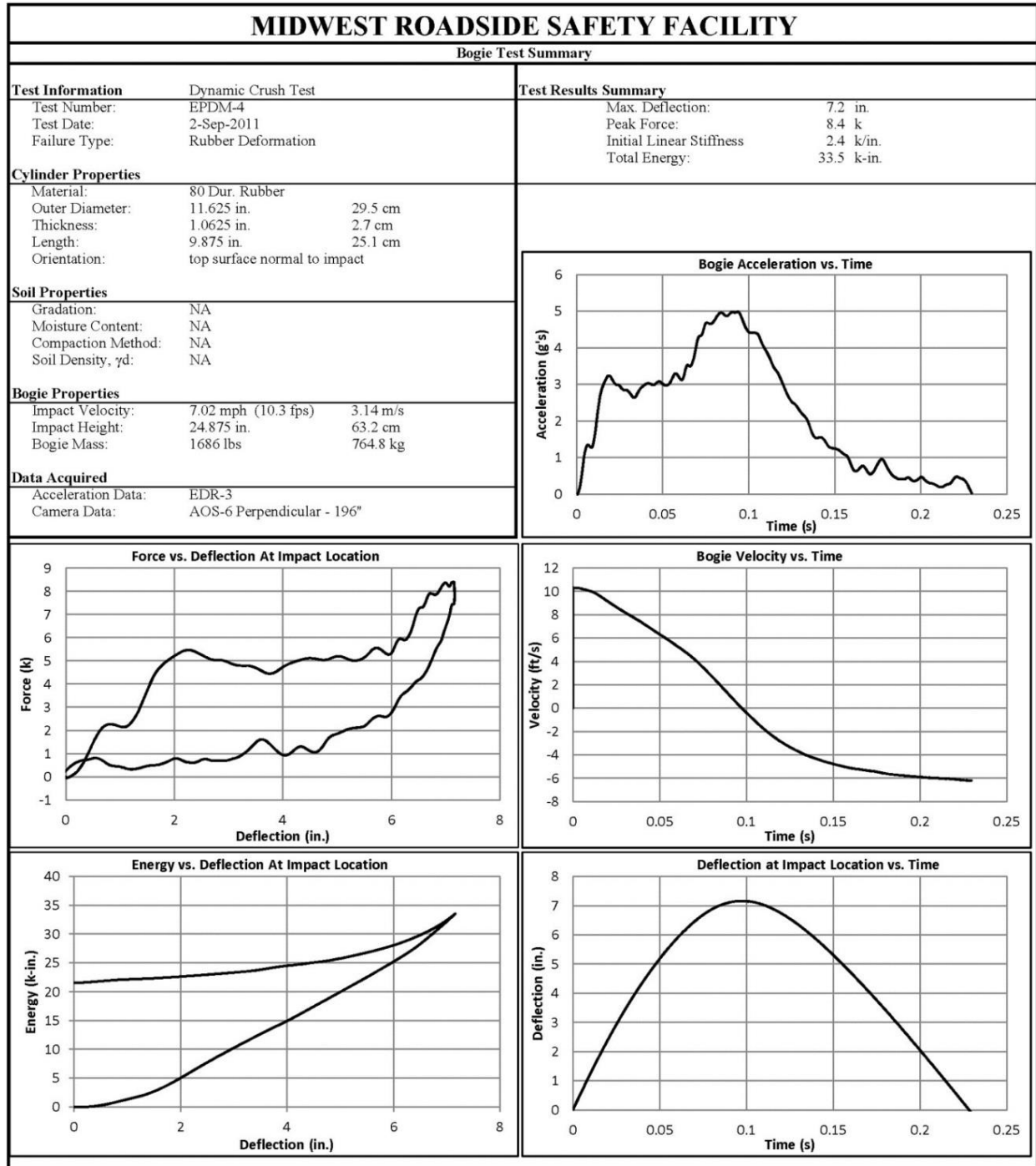


Figure A-7. Results of Test No. EPDM-4 (EDR-3)

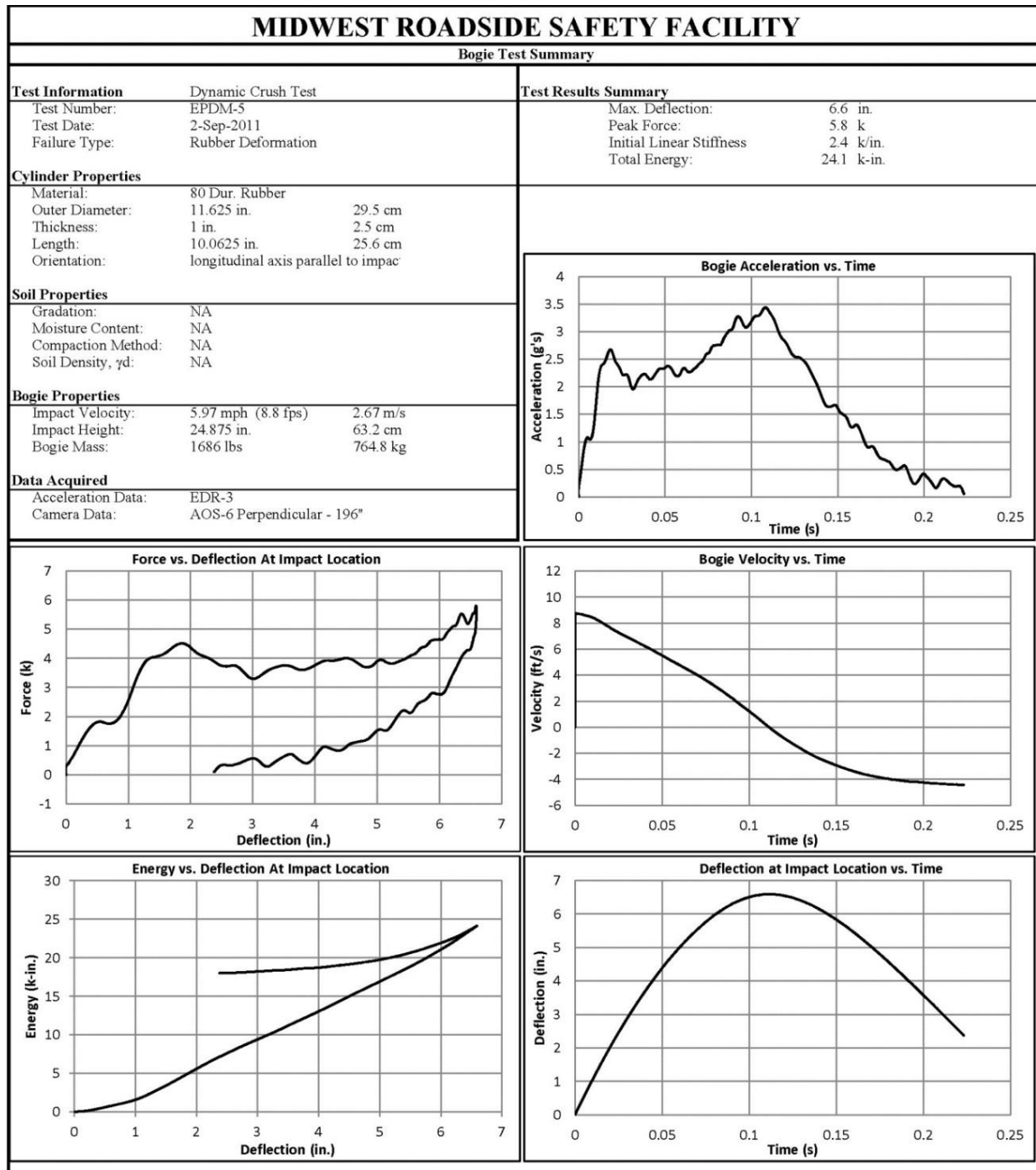


Figure A-8. Results of Test No. EPDM-5 (EDR-3)

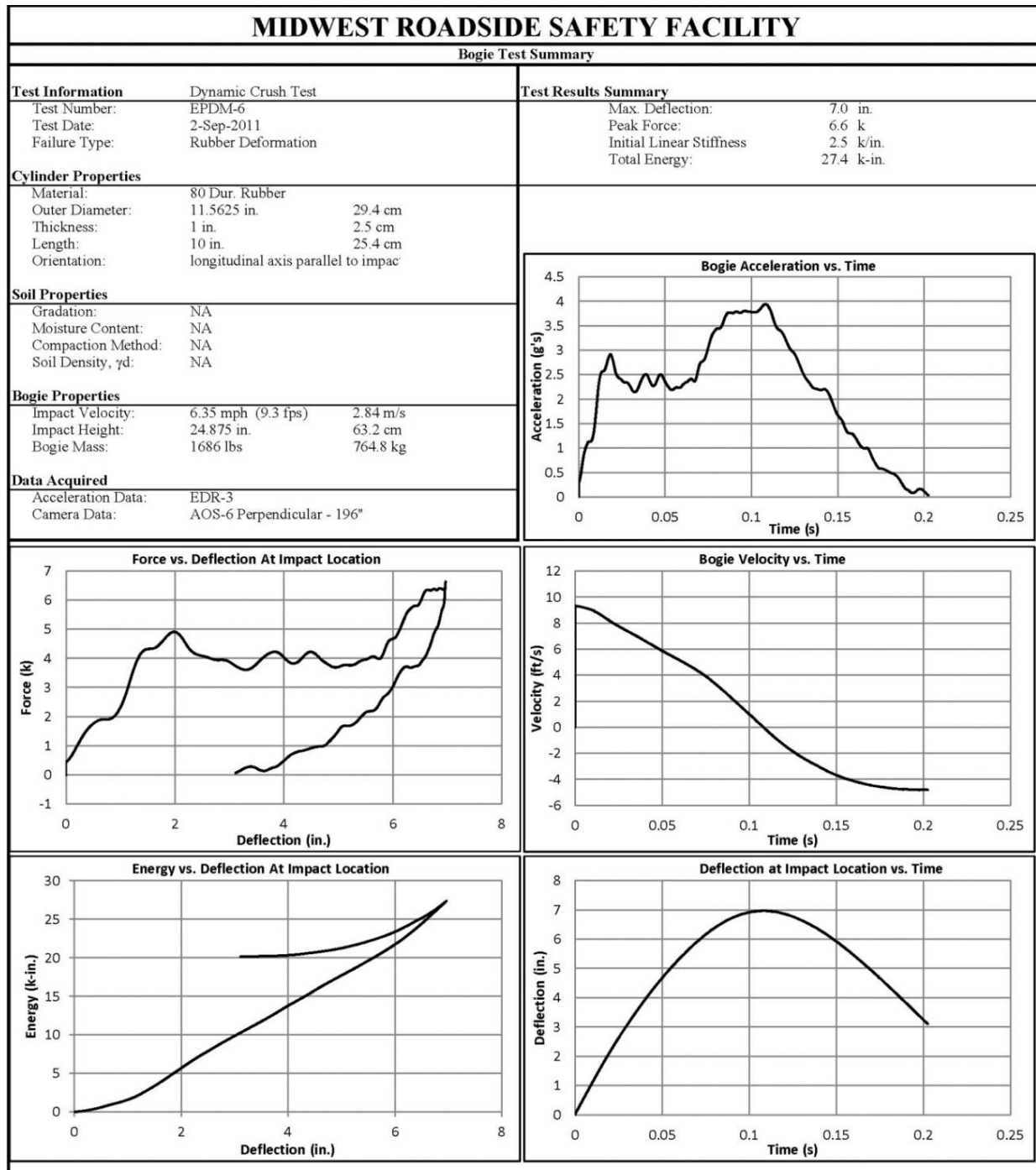


Figure A-9. Results of Test No. EPDM-6 (EDR-3)

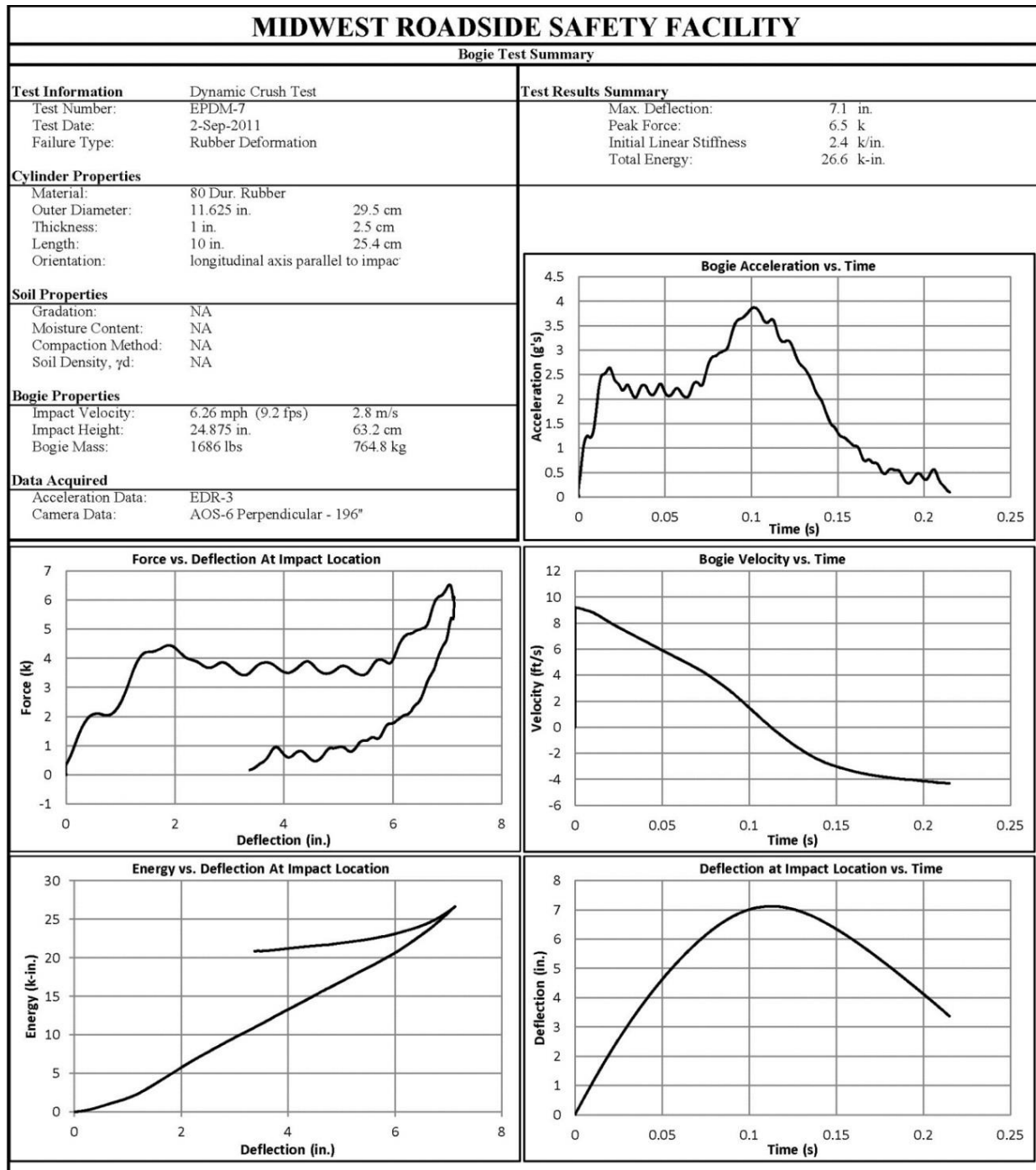


Figure A-10. Results of Test No. EPDM-7 (EDR-3)

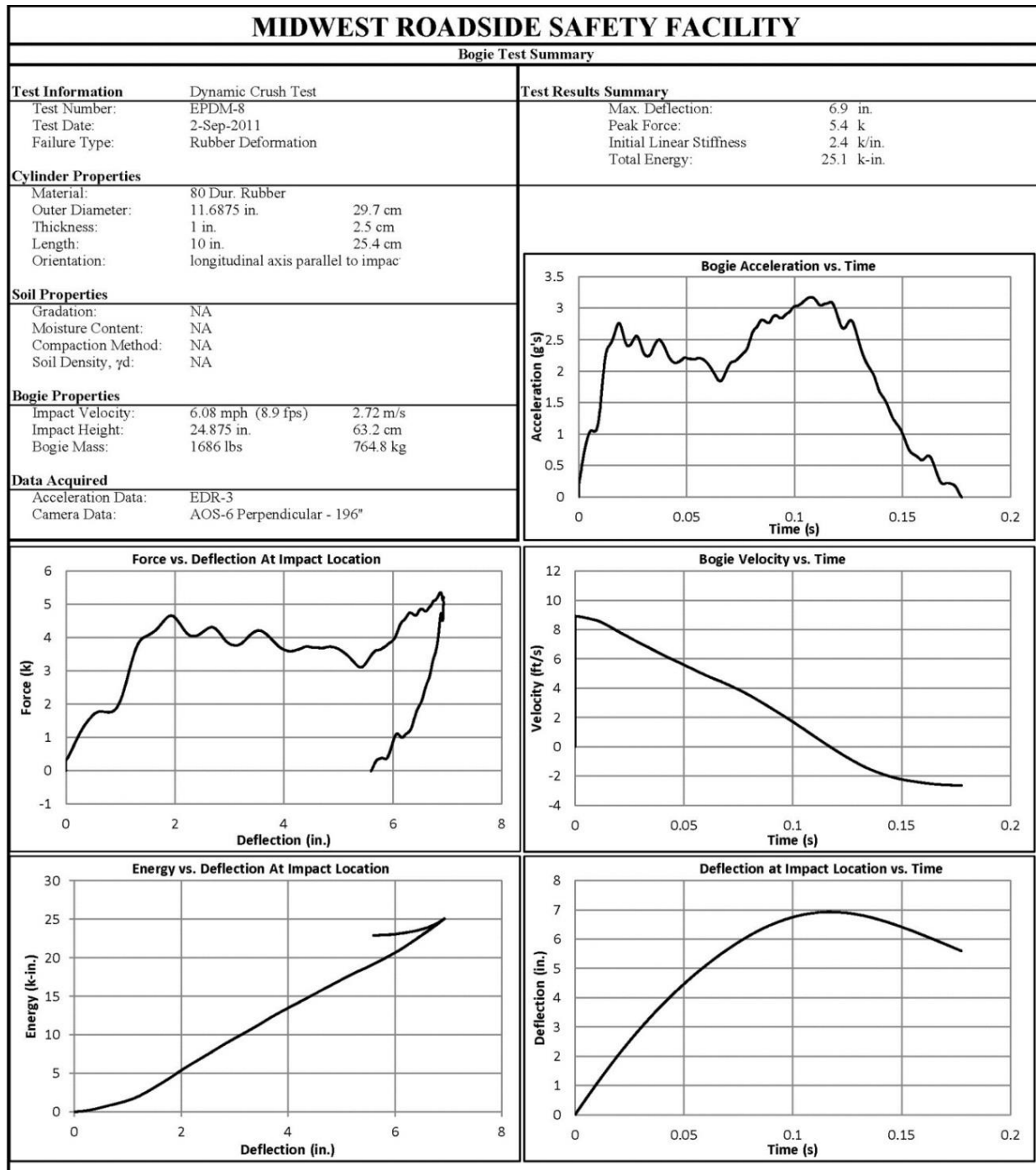


Figure A-11. Results of Test No. EPDM-8 (EDR-3)

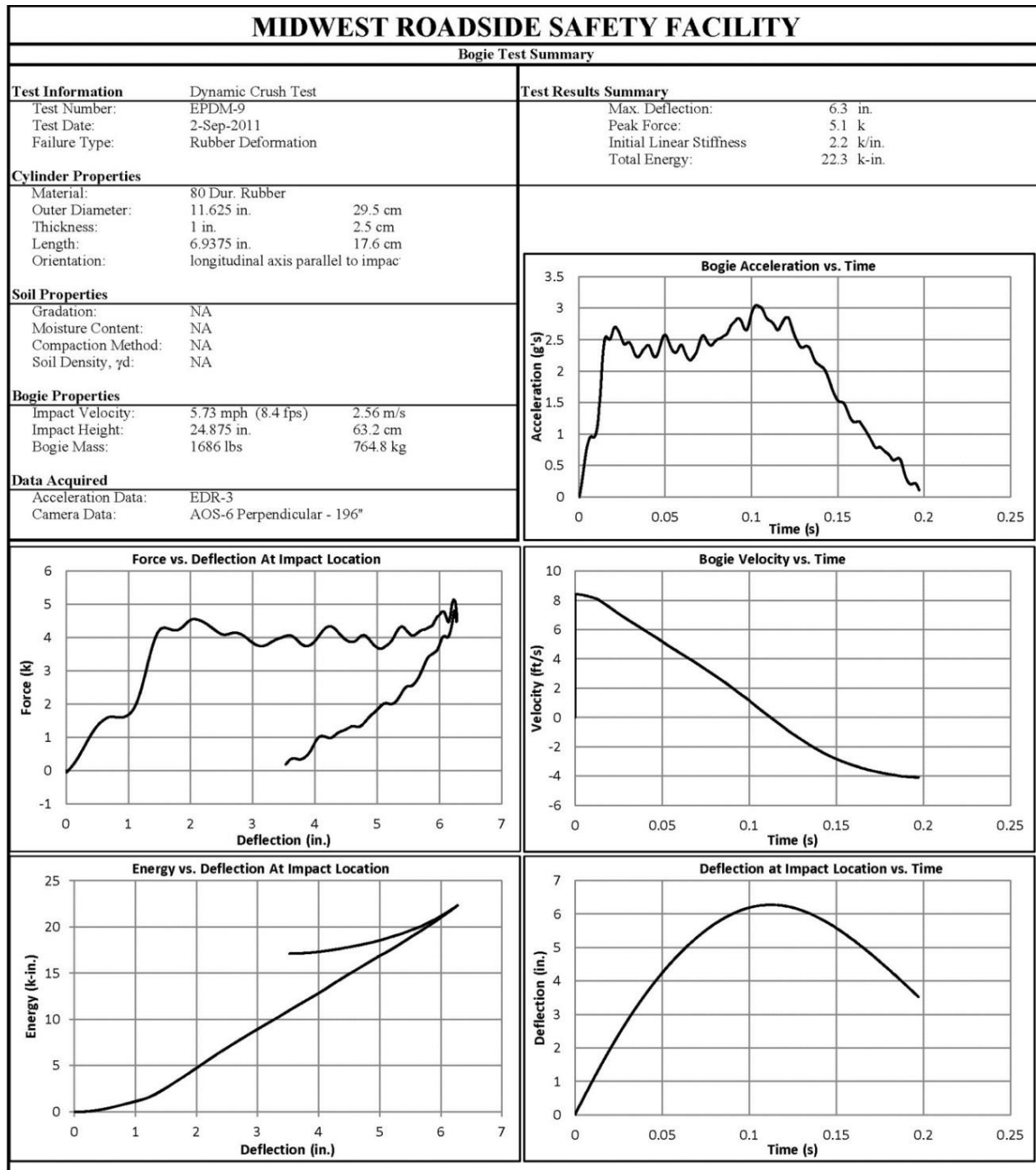


Figure A-12. Results of Test No. EPDM-9 (EDR-3)

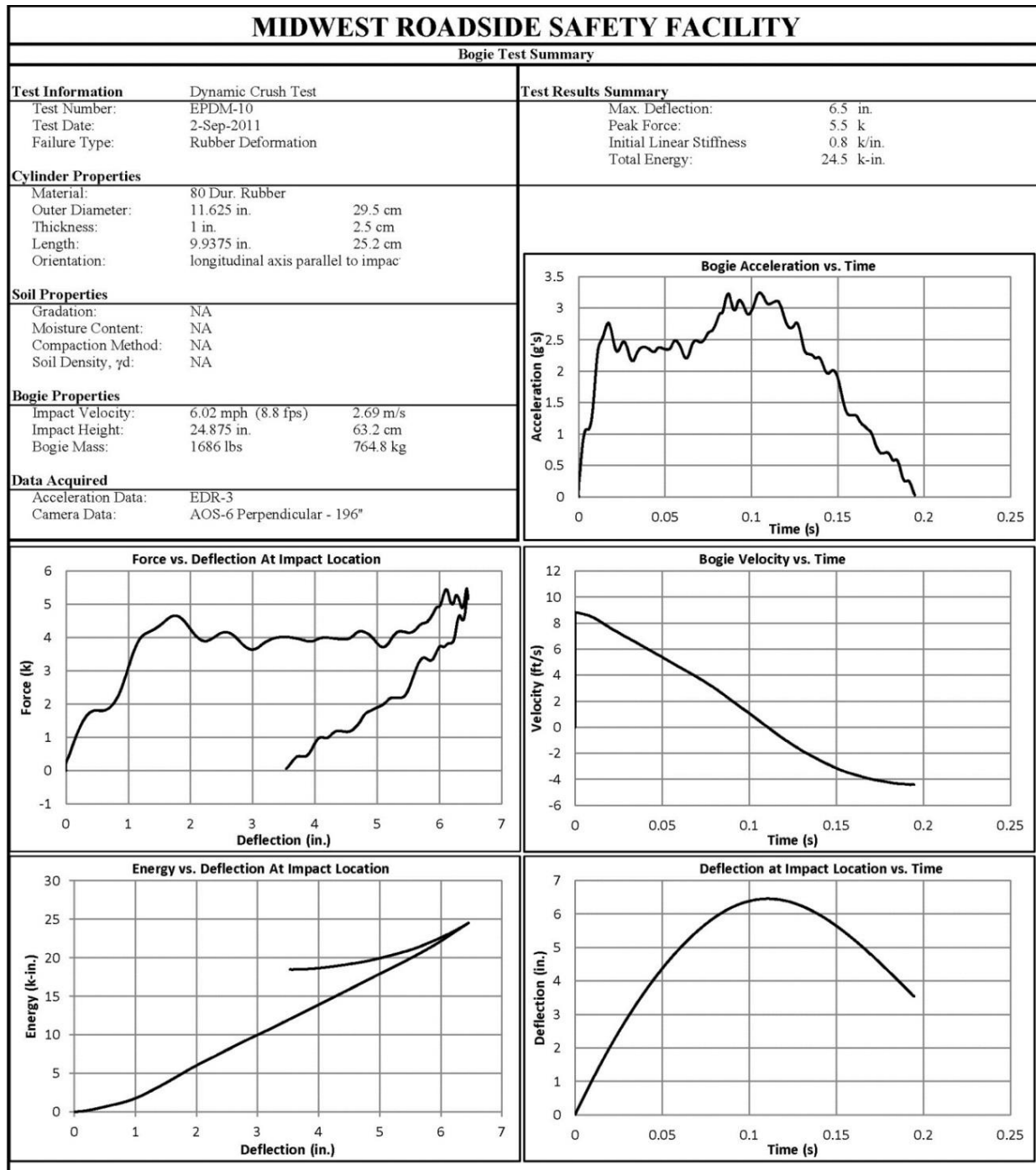


Figure A-13. Results of Test No. EPDM-10 (EDR-3)

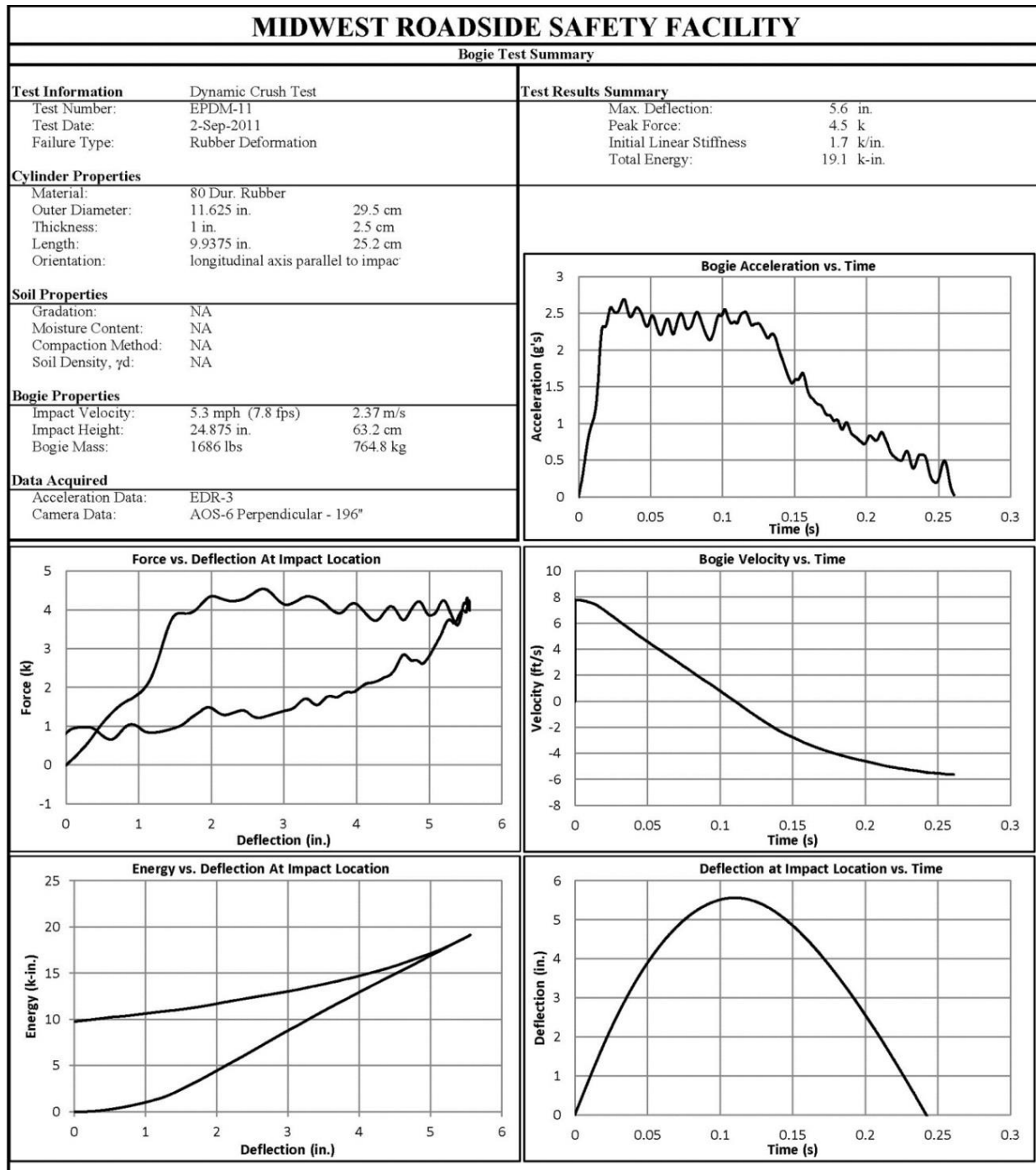


Figure A-14. Results of Test No. EPDM-11 (EDR-3)

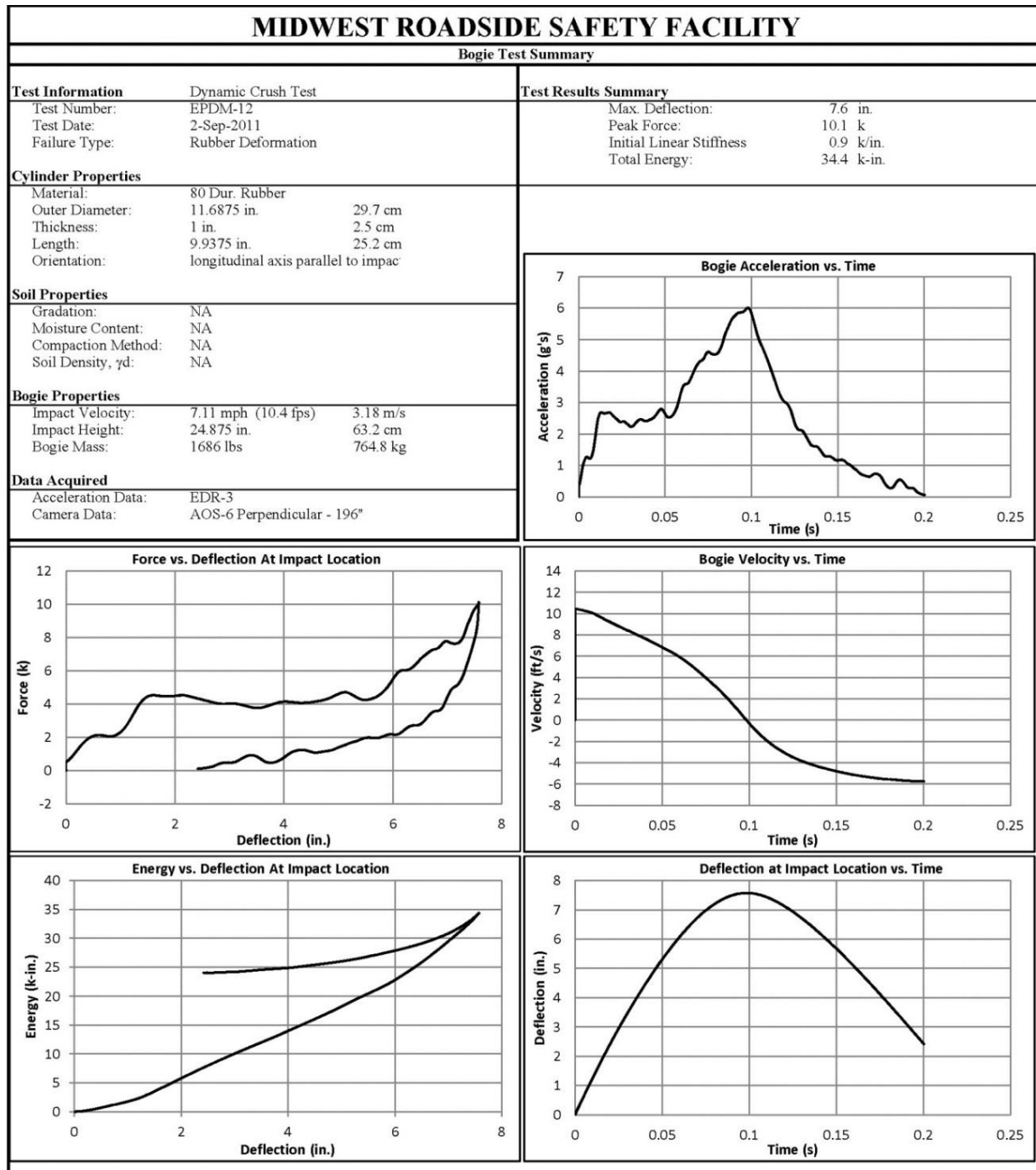


Figure A-15. Results of Test No. EPDM-12 (EDR-3)

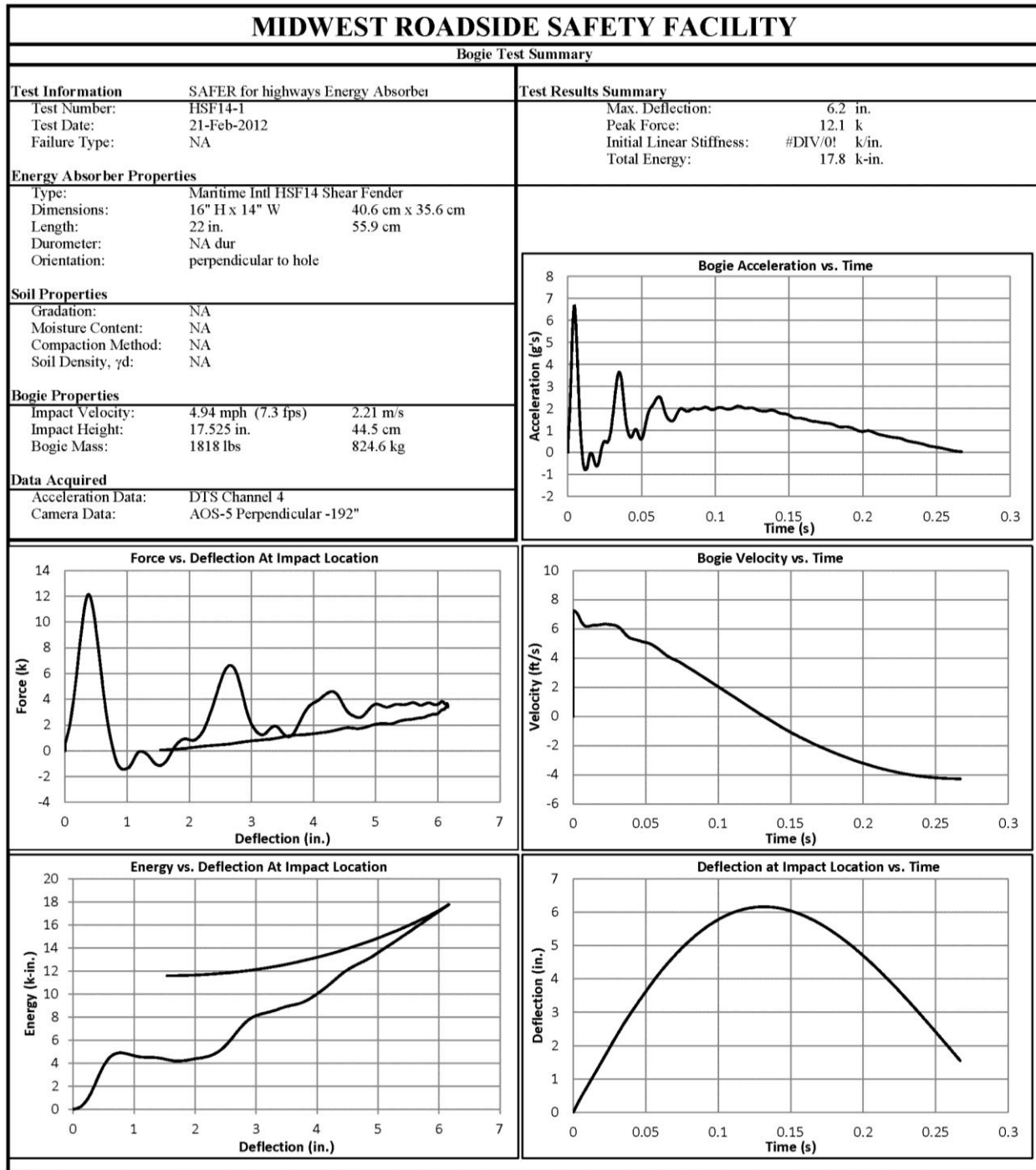


Figure A-16. Results of Test No. HSF14-1 (DTS)

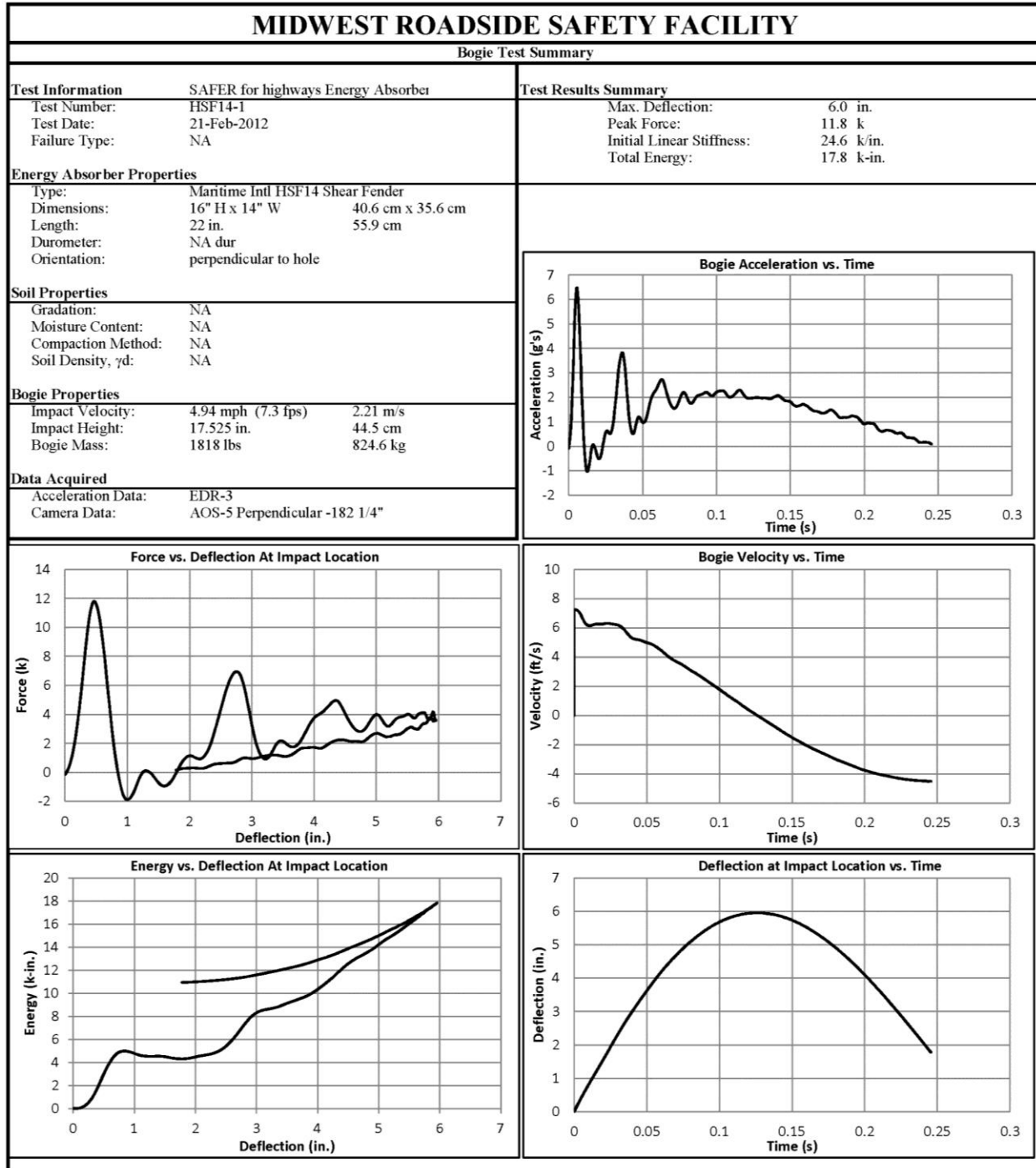


Figure A-17. Results of Test No. HSF14-1 (EDR-3)

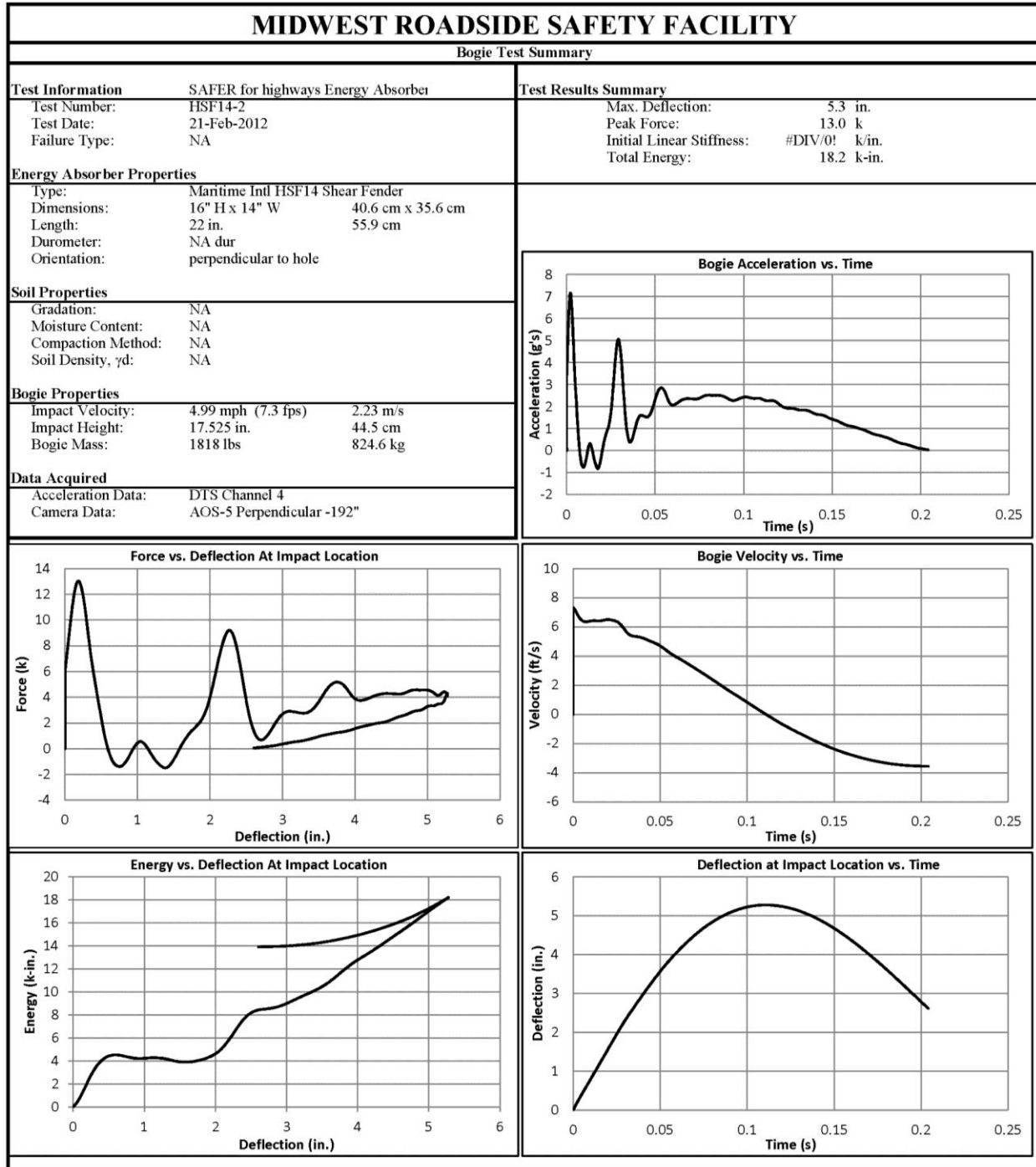


Figure A-18. Results of Test No. HSF14-2 (DTS)

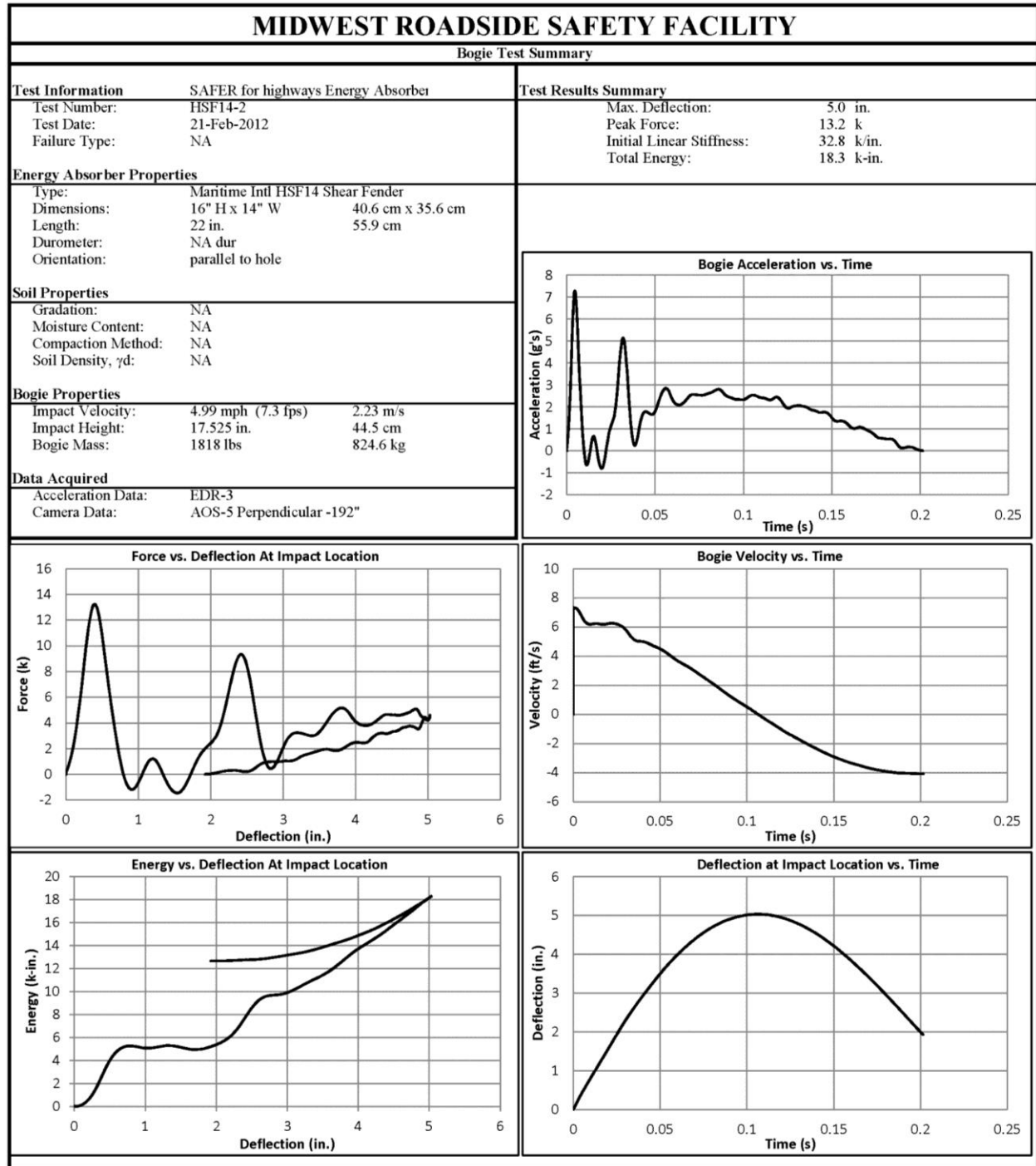


Figure A-19. Results of Test No. HSF14-2 (EDR-3)

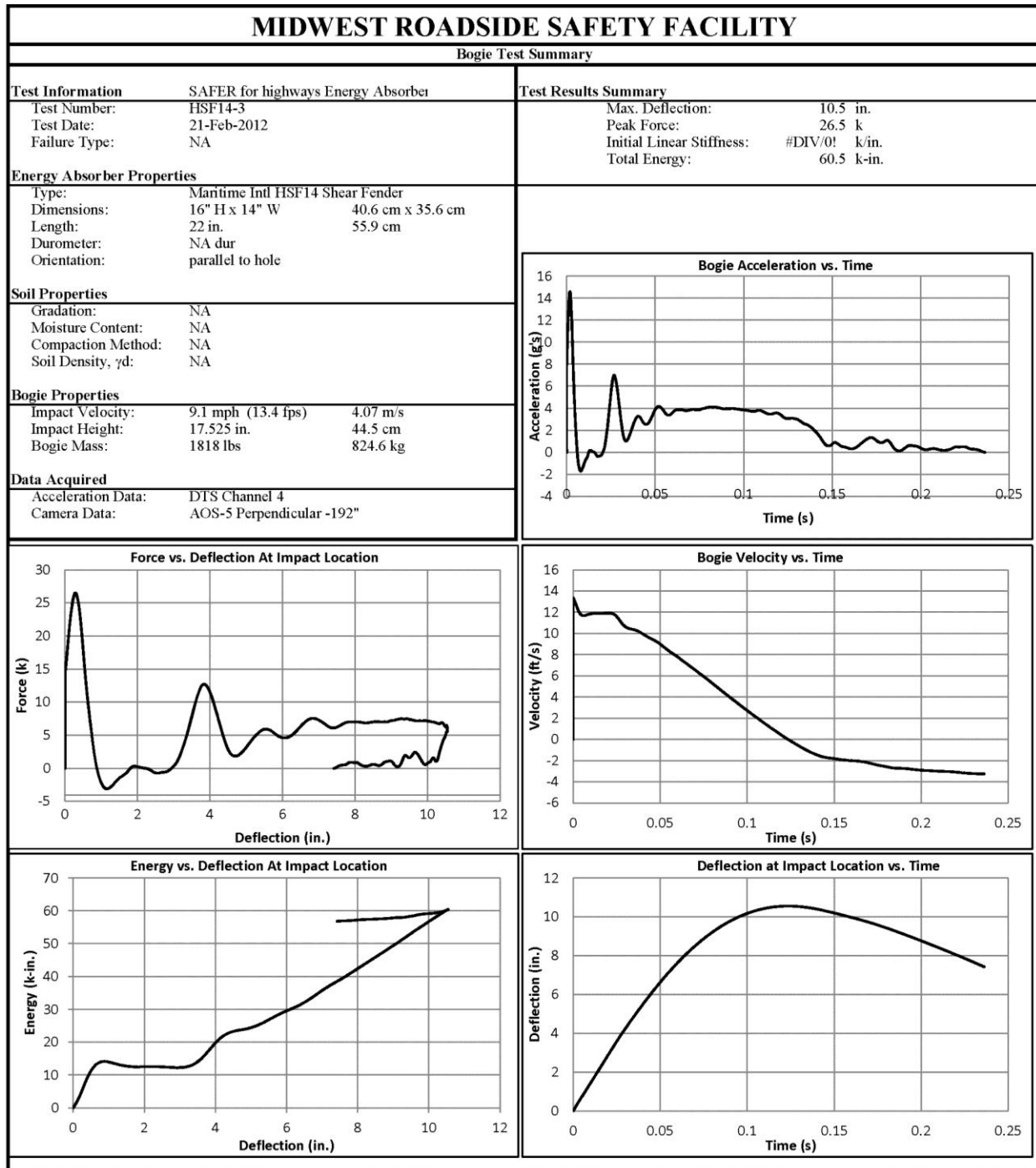


Figure A-20. Results of Test No. HSF14-3 (DTS)

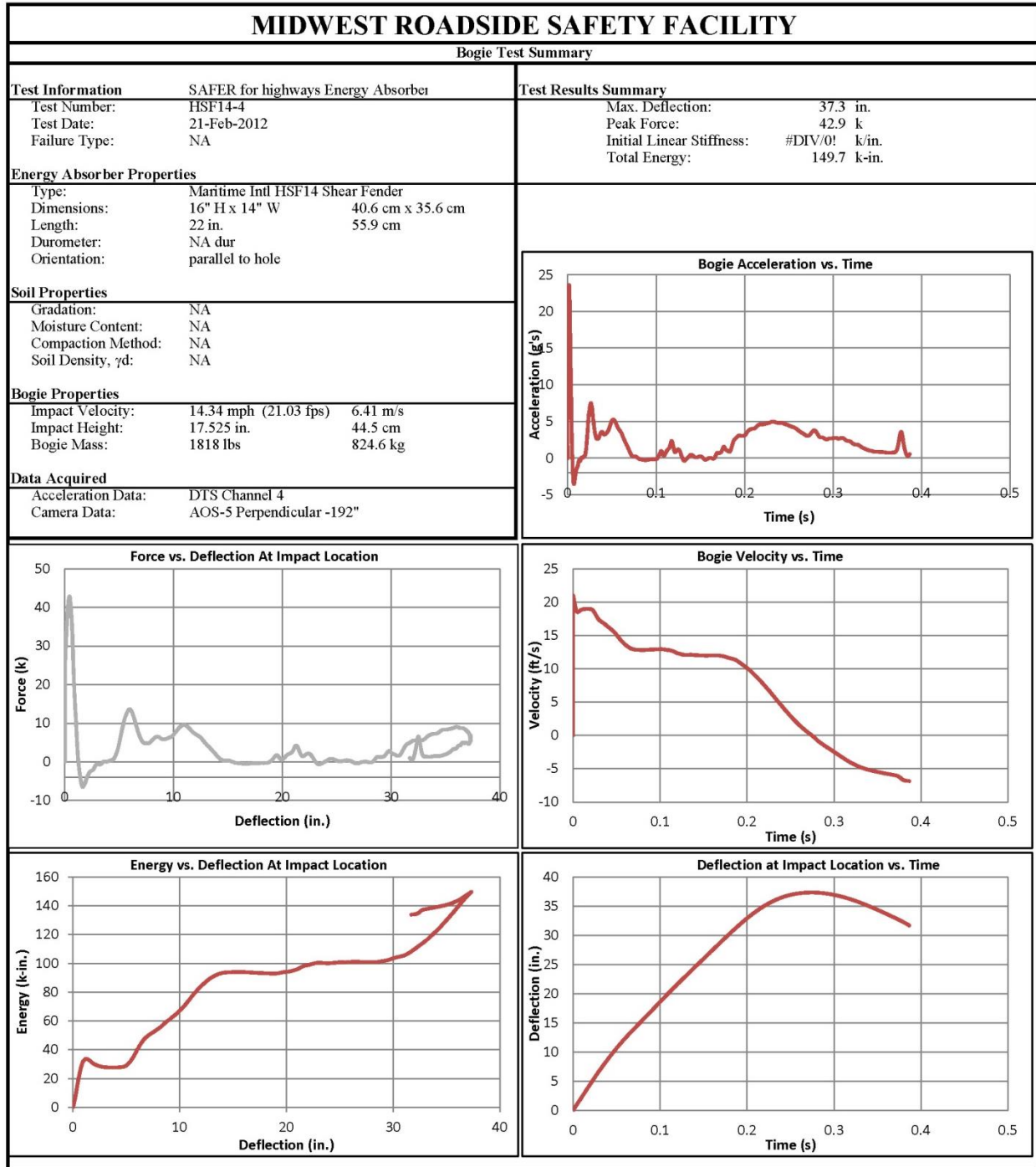


Figure A-21. Results of Test No. HSF14-4 (DTS)

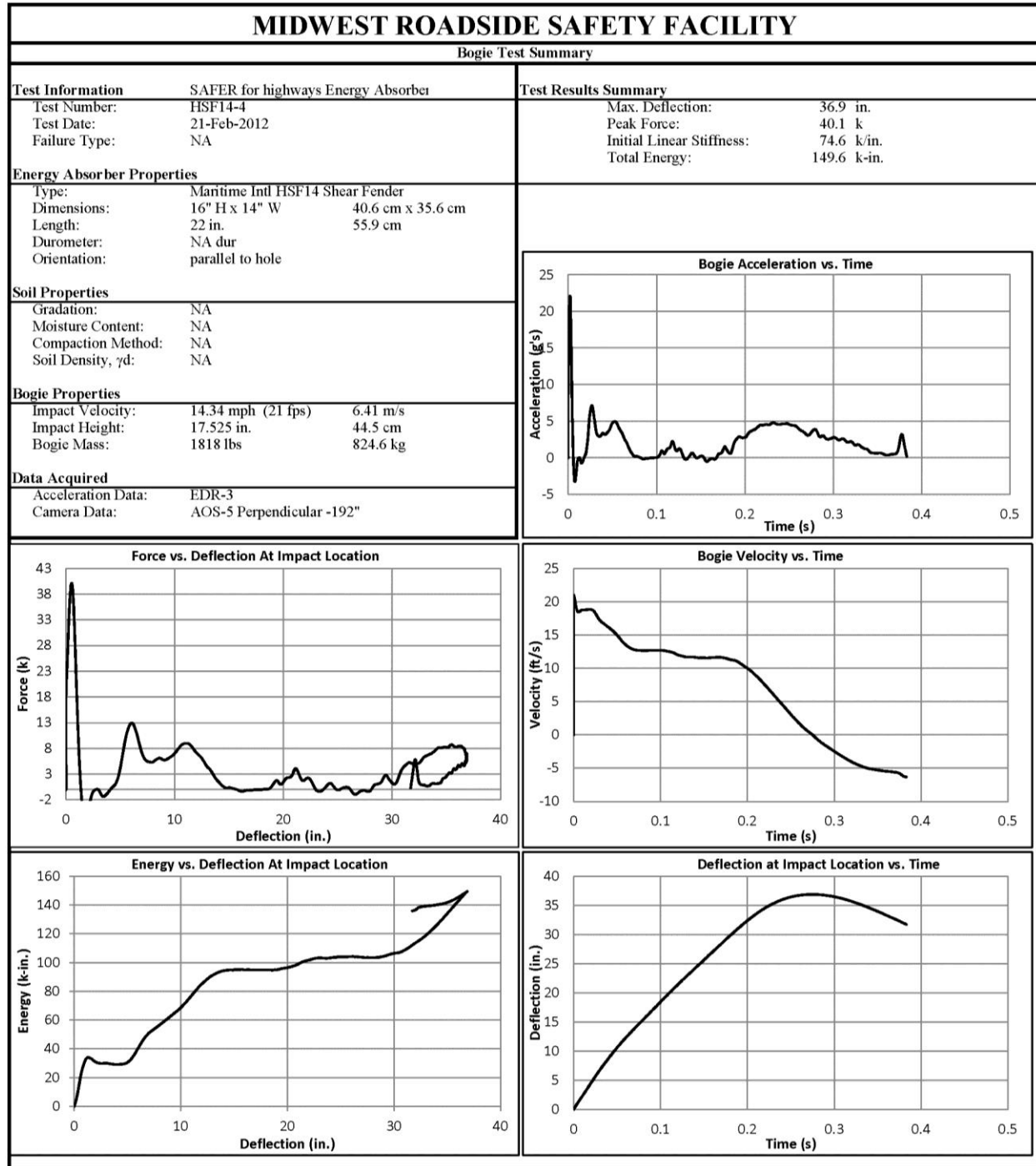


Figure A-22. Results of Test No. HSF14-4 (EDR-3)

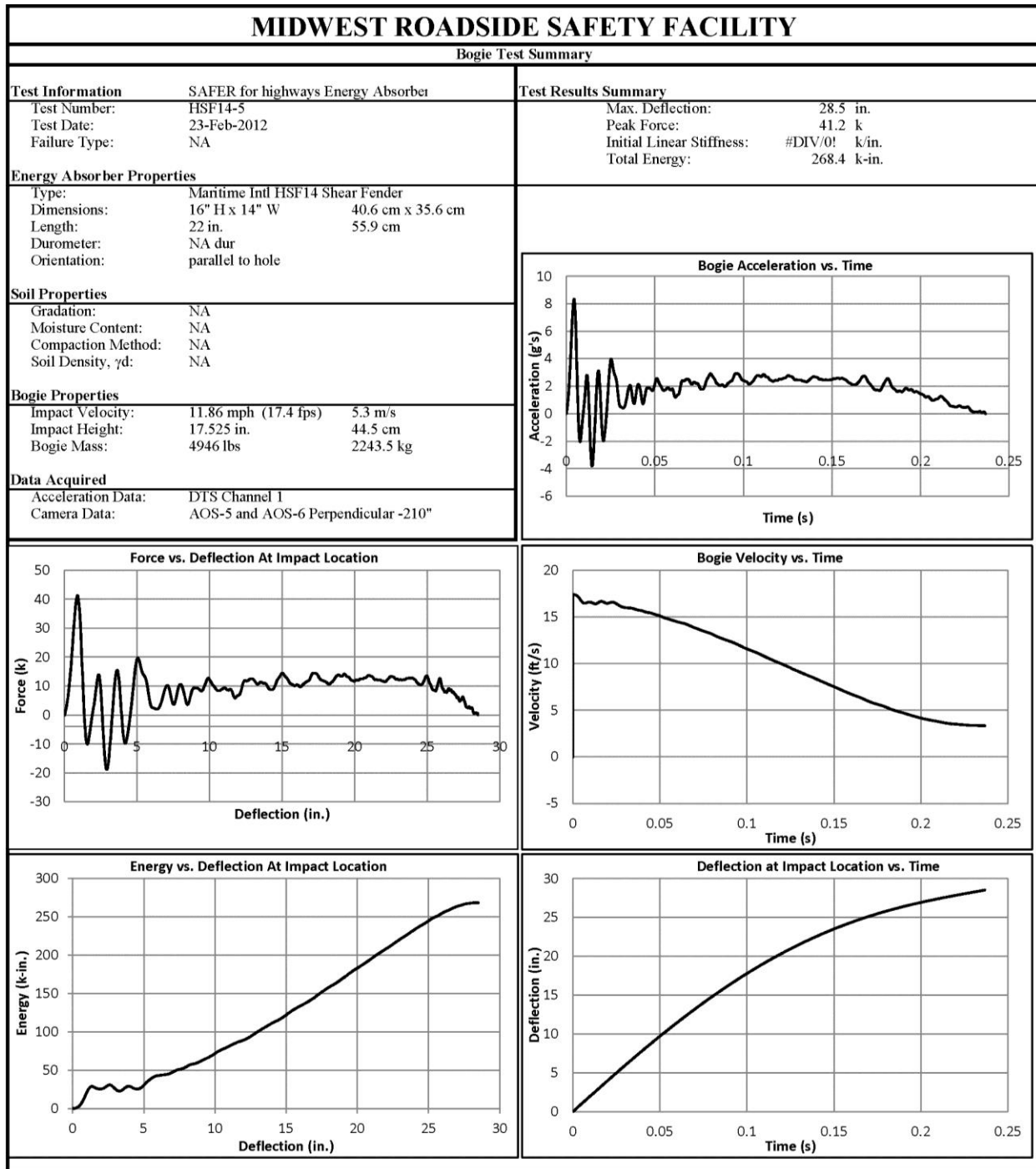


Figure A-23. Results of Test No. HSF14-5 (DTS)

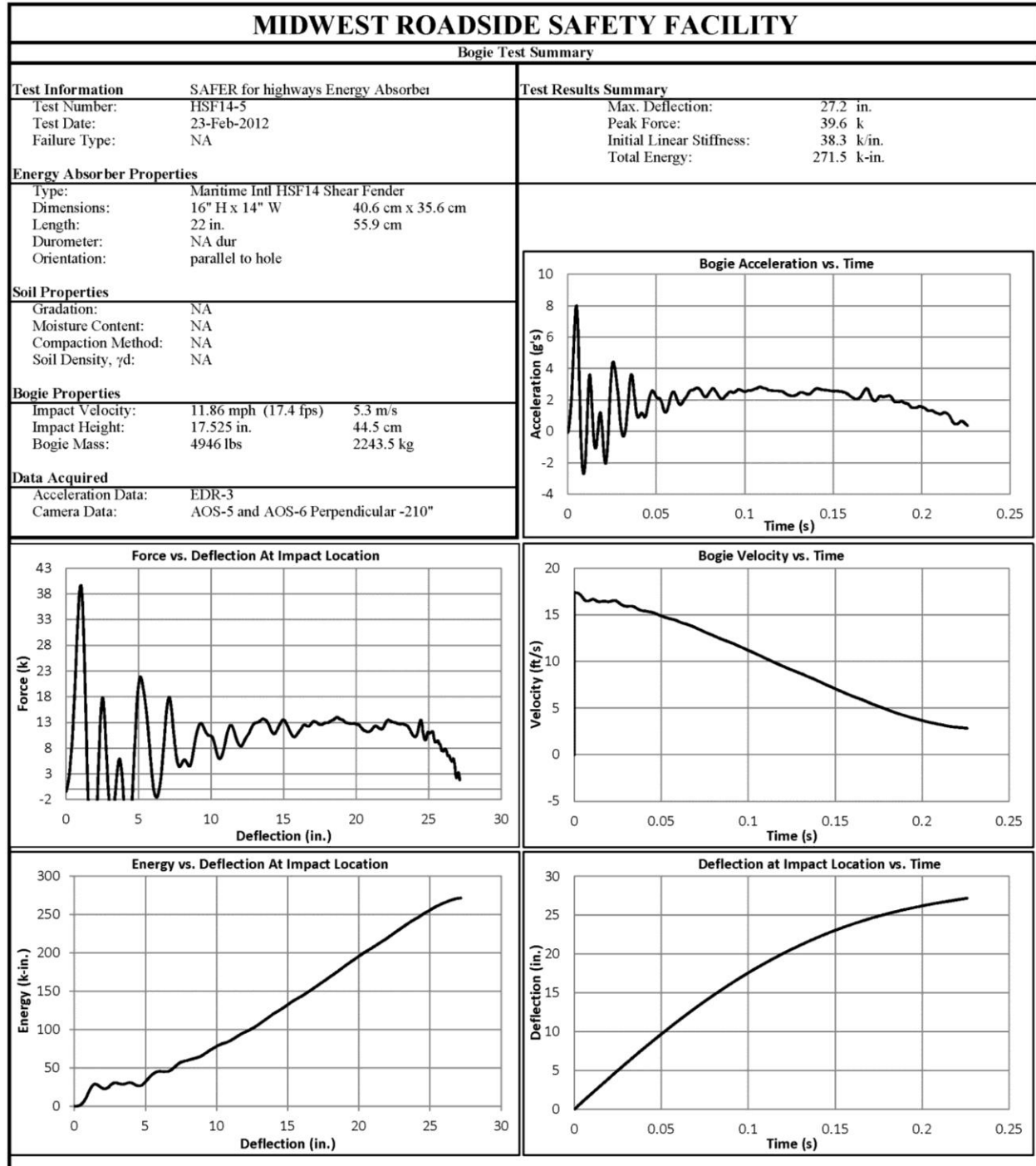


Figure A-24. Results of Test No. HSF14-5 (EDR-3)

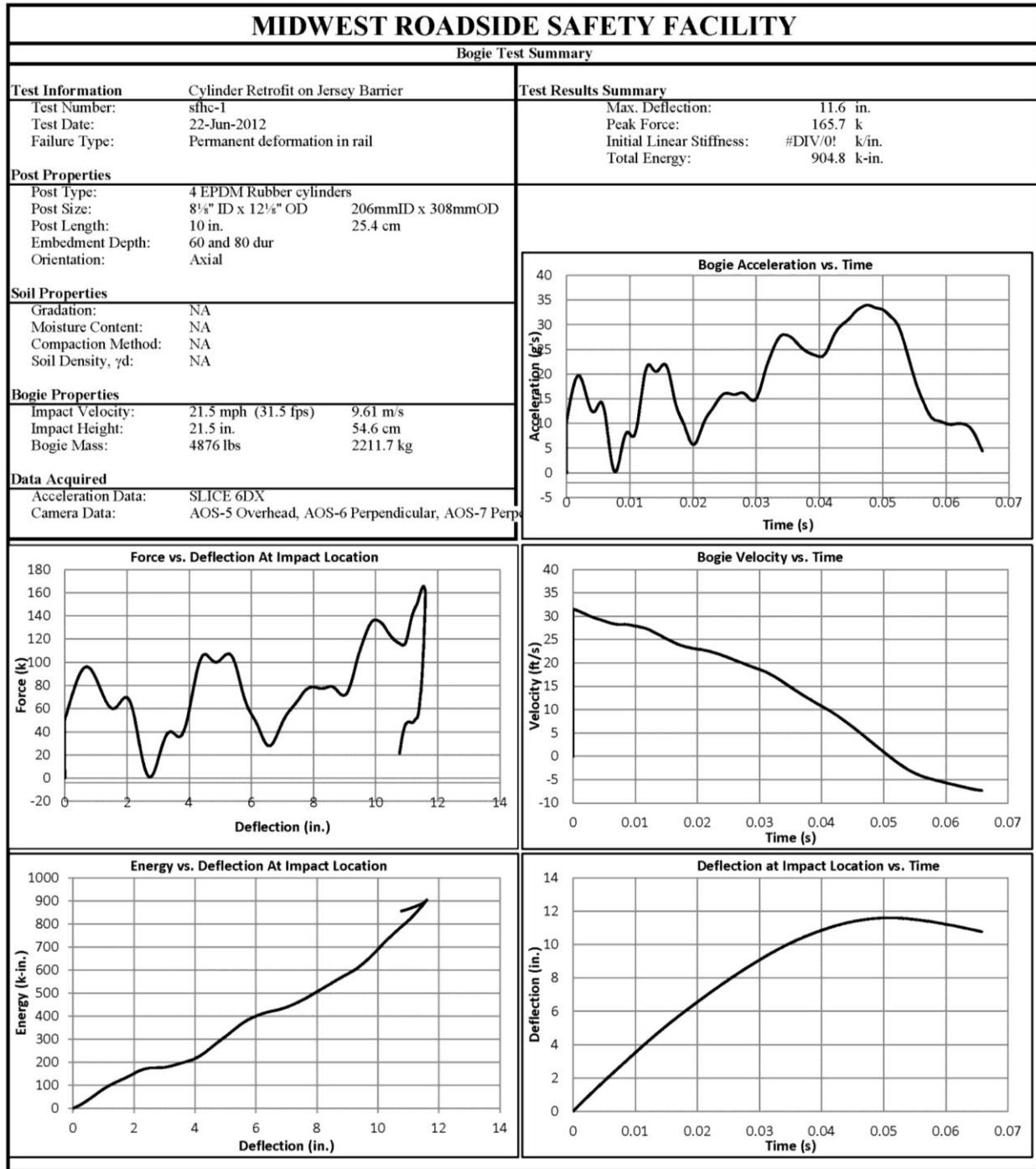


Figure A-25. Results of Test No. SFHC-1 (SLICE 6DX)

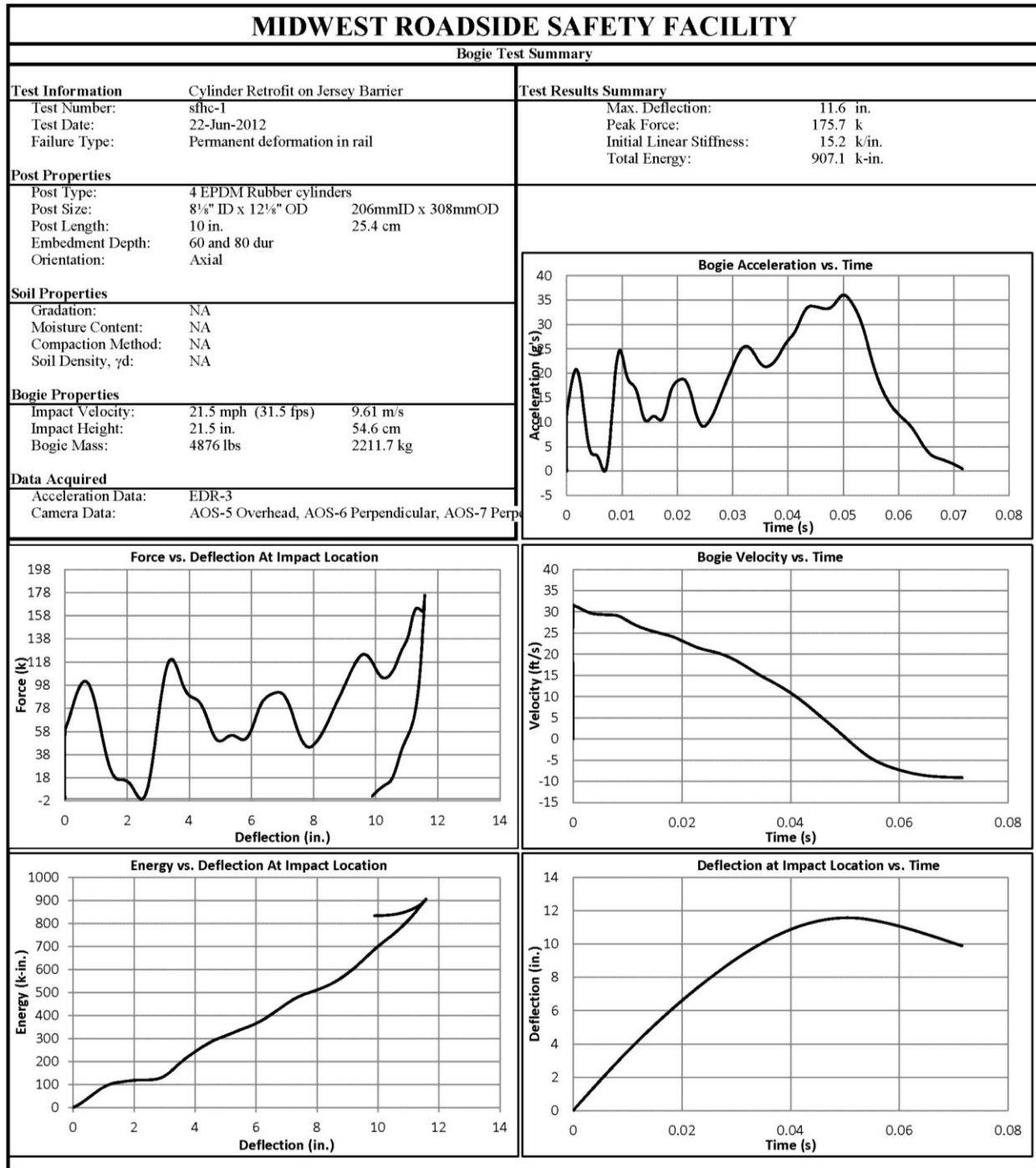


Figure A-26. Results of Test No. SFHC-1 (EDR-3)

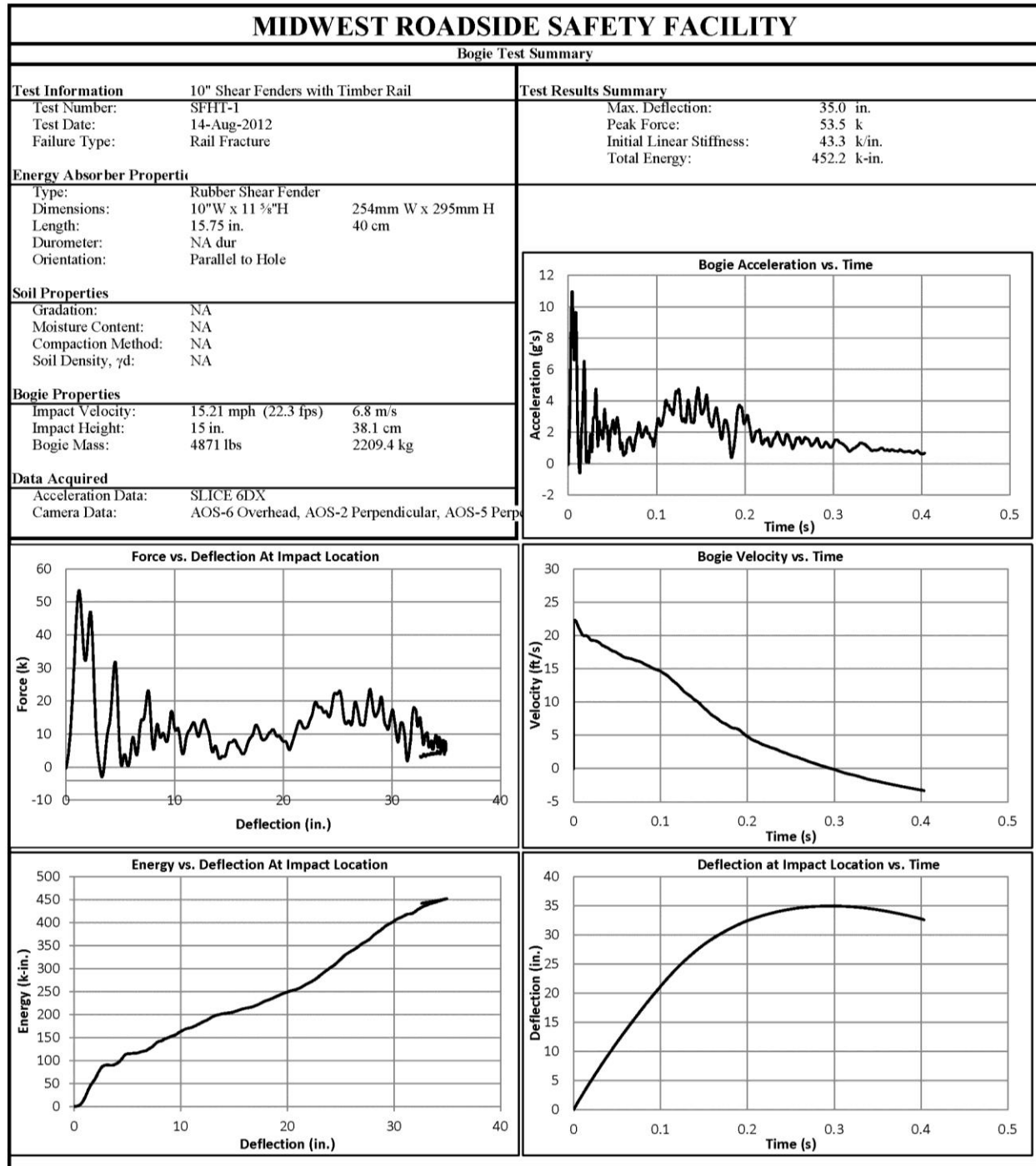


Figure A-27. Results of Test No. SFHT-1 (SLICE 6DX)

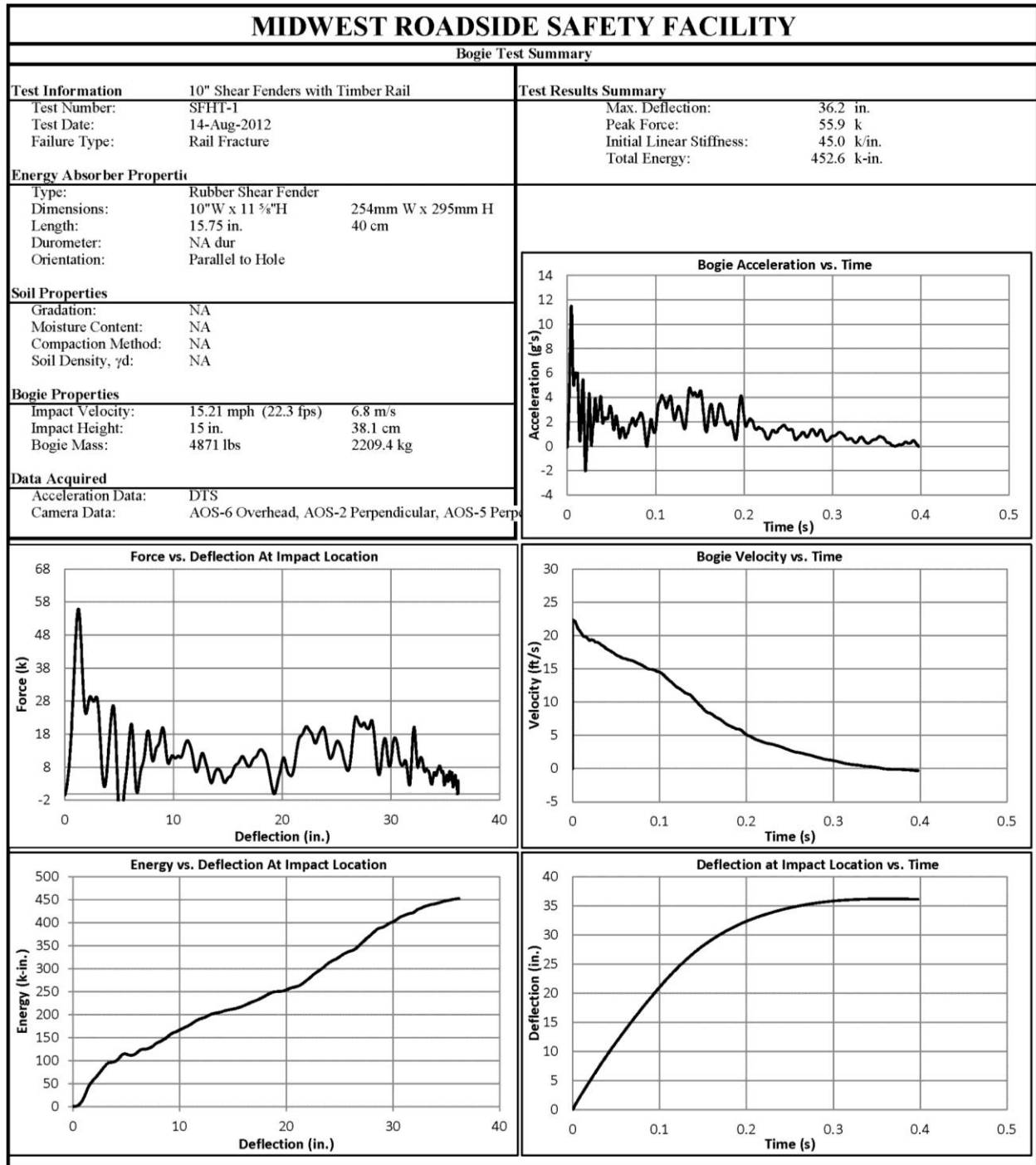


Figure A-28. Results of Test No. SFHT-1 (EDR-3)

Appendix B. Material Specifications



**EUTSLER TECHNICAL PRODUCTS, INC.
CERTIFICATION OF
CONFORMANCE
(CERTS)**

**WE CERTIFY THE PARTS LISTED BELOW
HAVE BEEN MANUFACTURED WITH THE
SPECIFIED ELASTOMER; AND FOUND
TO MEET SPECIFIED REQUIREMENTS:**

CUSTOMER: UNIVERSITY OF NEBRASKA LINCOLN

PURCHASE ORDER: 4500236631

<u>QUANTITY</u>	<u>PART No.</u>	<u>PART NOMENCLATURE</u>
2	12.12" x 8.12" ID	EPDM RUBBER SLEEVES
2	11-5/8" x 9-5/8" ID	EPDM RUBBER SLEEVES

COMPOUND No.: 414

BATCH No.: 4140511556 & 4140211120

CURE DATE: 2 ND QTR. 2011

MATERIAL: EPDM 80 +-5 SHORE A

DUROMETER: 80 +-5

EUTSLER INVOICE No.: 59496 **DATE:** 6/1/2011

**I HEREBY CERTIFY THE ABOVE TO BE
TRUE AND CORRECT.**


SIGNATURE: *Douglas Loukanis*

TITLE: QUALITY ASSURANCE MANAGER

**EUTSLER TECHNICAL PRODUCTS, INC.
QC 8 REV. 0**

P.O. Box 920818 Houston, TX 77292-0818 • 3718 Creekmont • Houston, TX 77091
Phone: 713-686-8209 • Fax: 713-686-0613 • ISO 9001:2000 Certified
Web: www.eutsler-rubber.com • E-mail: sales@eutsler-rubber.com

Figure B-1. 80-durometer EPDM Rubber Cylinders



EUTSLER

PHYSICAL TEST RECORD

QC 10 REV 0

EUTSLER TECHNICAL PRODUCTS, INC.

COMPOUND	414	MAT'L TYPE	EPDM	DATE:	8/27/03
HARDNESS S	70 / 80	BUTTONS	77	TESTED BY:	DS
BATCH NO.	0503357				

MODULUS					
SPECIMEN	100%	200%	300%	400%	500%
1	567.41	1096	1612.7		
2	631.28	1283.6	1855.2		
3					
AVE.	599.34	1189.8	1733.9		

SPECIMEN	THICKNESS	ELONGATION	TENSILE	COMMENTS	
1	.080	406.20	1983.4		
2	.082	364.96	2080.6		
3	.082	Broke out off mark			
AVE.	.081	385.58%	2032		
				CURE CONDITION @ 330 DEG F	
				SLAB - 20 MIN	
				BUTTONS - 30 MIN	

DIE C	THICKNESS	TEAR LBS/PULL	LBS PER IN.
1	.081	16.72	206.4
2	.080	14.91	186.4
AVE.	.0805	15.81	196.4

COMPRESSION SET - METHOD B			
25% COMPRESSION - DRY AIR OVER 22 HR 212 F			
SPECIMEN	THICKNESS AS MOLDED	THICKNESS AFTER OVEN AGING	% SET
1	.512	.471	29.93%
2	.513	.467	33.33%
AVE.	.5125	.469	31.63%
VITON SPEC 22 HRS @ 350 F (AFTER POST CURED 16 HR AT 350 F)			
SPECIMEN	THICKNESS AS MOLDED	THICKNESS AFTER OVEN AGING	% SET
1			
2			
AVE.			

SPECIFIC GRAVITY (DENSITY)	SAMPLE NO.	NO 1	NO 2
DRY WEIGHT	A	10.01	
BEAKER + WATER + SAMPLE	B	792.39	
BEAKER + WATER	C	784.09	
(B) MINUS (C) =	D	8.30	
(A) DIV BY (D) = SPECIFIC GRAVITY		1.21	

Figure B-2. 80-durometer EPDM Rubber Cylinders



**EUTSLER TECHNICAL PRODUCTS, INC.
CERTIFICATION OF
CONFORMANCE
(CERTS)**

**WE CERTIFY THE PARTS LISTED BELOW
HAVE BEEN MANUFACTURED WITH THE
SPECIFIED ELASTOMER; AND FOUND
TO MEET SPECIFIED REQUIREMENTS:**

CUSTOMER: UNIVERSITY OF NEBRASKA LINCOLN

PURCHASE ORDER: 4500236631

<u>QUANTITY</u>	<u>PART No.</u>	<u>PART NOMENCLATURE</u>
2	12.12" x 8.12" ID	EPDM RUBBER SLEEVES

COMPOUND No.: 421

BATCH No.: 4210511571

CURE DATE: 2 ND QTR. 2011

MATERIAL: EPDM

DUROMETER: 60 +/- 5 SHORE A

EUTSLER INVOICE No.: 59496 **DATE:** 6/1/2011

**I HEREBY CERTIFY THE ABOVE TO BE
TRUE AND CORRECT.**


SIGNATURE: *Douglas Loukanis*

TITLE: QUALITY ASSURANCE MANAGER

**EUTSLER TECHNICAL PRODUCTS, INC.
QC 8 REV. 0**

P.O. Box 920818 Houston, TX 77292-0818 • 3718 Creekmont • Houston, TX 77091
Phone: 713-686-8209 • Fax: 713-686-0613 • ISO 9001:2000 Certified
Web: www.eutsler-rubber.com • E-mail: sales@eutsler-rubber.com

Figure B-3. 60-durometer EPDM Rubber Cylinders


PHYSICAL TEST RECORD

EUTSLE TECHNICAL PRODUCTS, INC.

COMPOUND	421	MAT'L TYPE	epdm	DATE:	10/28/2005
HARDNESS S	60 - 70	BUTTONS	65	TESTED BY:	DS
BATCH NO.	421404303				

MODULUS					
SPECIMEN	100%	200%	300%	400%	500%
1	296	475	685	889	1074
2	285	455	646	835	1017
AVE	291	465	666	862	1046
SPECIMEN	THICKNESS	ELONGATION	TENSILE	COMMENTS	
1	.076	979%	1993		
2	.079	957%	1902		
AVE.	.078	968%	1948		
DIE C	THICKNESS	TEAR LBS/PULL	LBS PER IN.		
1	0.078	19.56	251		
2	0.079	18.19	230		
AVE.	0.078	18.88	241		

COMPRESSION SET - METHOD B			
25% COMPRESSION - DRY AIR OVER 22 HR 212 F			orig - test spec
			orig - .375 bar
SPECIMEN	THICKNESS AS MOLDED	THICKNESS AFTER OVEN AGING	% SET
1	.510	.531	58.5%
2	.511	.532	58.1%
AVE.	.5105	.5315	58.3%
VITON SPEC 22 HRS @ 350 F (AFTER POST CURED 16 HR AT 350 F)			
SPECIMEN	THICKNESS AS MOLDED	THICKNESS AFTER OVEN AGING	% SET
1			
2			
AVE.			

SPECIFIC GRAVITY (DENSITY)	SAMPLE NO.	NO 1	NO 2
DRY WEIGHT	A	9.69	
BEAKER + WATER + SAMPLE	B	805.15	
BEAKER + WATER	C	796.84	
(B) MINUS (C) =	D	8.31	
(A) DIV BY (D) = SPECIFIC GRAVITY		1.17	

Figure B-4. 60-durometer EPDM Rubber Cylinders



1186 Petroleum Pkwy
Broussard, LA 70518
USA
Ph: 337.321.4240
Fx: 337.321.4241

Date: January 11, 2012

Attention: Jennifer D. Schmidt

Re: Maritime shear fender material specification

Jennifer,

The Maritime HSF shear fender we have supplied you is manufactured according to the following ASTM material specification. This ASTM callout fully defines the material properties.

ASTM D2000 5AA425 A₁₃ B₁₃ C₂₀ F₁₇ K₁₁ L₁₄

Please let me know if you need anything else.

Regards,

A handwritten signature in black ink that reads "Donald E. Nassar Jr.".

Donald E. Nassar Jr.
VP Engineering
Maritime International



Figure B-5. 14-in. (356-mm) Wide Shear Fender

Morse Rubber

CERTIFICATE OF CONFORMANCE

University of Nebraska-Lincoln 8/8/12 EF6496
Company Date Part Number

We hereby certify that all items shipped on our Order No. 52730 &
Shipper No. 0157, against your Purchase Order No. 4500256306
comply with all published requirements and specifications.

John E. Rector

John E. Rector
Name

Vice President
Title

Morse Rubber L.L.C.
3588 Main Street, Keokuk, IA 52632
Telephone (319) 524-8430 Telefax (319) 524-7290

Figure B-6. 10-in. (254-mm) Wide Shear Fender

END OF DOCUMENT